Characterizing mitochondrial signaling networks by quantitative proteomics

Zur Erlangung des akademischen Grades eines
Dr.rer.nat
von der Fakultät Bio- und Chemieingenieurwesen
der Technischen Universität Dortmund

Dissertation
vorgelegt von
M.Sc. Humberto Gonczarowska Jorge
aus
Brasília, DF, Brazil

Tag der mündlichen Prüfung: 14.06.2019
1. Gutachter: Prof. Dr. Albert Sickmann
2. Gutachter: Prof. Dr. Oliver Kayser

Dortmund, 2020

Summary

Summary

1 Publications, Oral and Poster presentations

1.1 Publications

1. Mutations in glycyl-tRNA-synthetase impair mitochondrial metabolism in neurons. Boczonadi V, Meyer K, **Gonczarowska-Jorge H**, Griffin H, Roos A, Bartsakoulia M, Bansagi B, Ricci G, Palinkas F, Zahedi RP, Bruni F, Kaspar B, Lochmüller H, Boycott KM, Müller JS, Horvath R. Hum Mol Genet. 2018 Apr 10. doi: 10.1093/hmg/ddy127
2. Advanced tools for the analysis of protein phosphorylation in yeast mitochondria. Walter C, Gonczarowska-Jorge H, Sickmann A, Zahedi RP, Meisinger C, Schmidt O. Anal Biochem. 2018 Aug 1;554:23-27. doi: 10.1016/j.ab.2018.05.022
3. PKA-RII subunit phosphorylation precedes activation by cAMP and regulates activity termination. Isensee J, Kaufholz M, Knape MJ, Hasenauer J, Hammerich H, **Gonczarowska-Jorge H**, Zahedi RP, Schwede F, Herberg FW, Hucho T. J Cell Biol. 2018 Apr 3. pii: jcb.201708053. doi: 10.1083/jcb.201708053
4. Quantifying Missing (Phospho)Proteome Regions with the Broad-Specificity Protease Subtilisin. **Gonczarowska-Jorge H**, Loroch S, Dell'Aica M, Sickmann A, Roos A, Zahedi RP. Anal Chem. 2017 Dec 19;89(24):13137-13145. doi: 10.1021/acs.analchem.7b02395
5. Landscape of submitochondrial protein distribution. Vögtle FN, Burkhart JM, **Gonczarowska-Jorge H**, Kücükköse C, Taskin AA, Kopczynski D, Ahrends R, Mossmann D, Sickmann A, Zahedi RP, Meisinger C. Nat Commun. 2017 Aug 18;8(1):290. doi: 10.1038/s41467-017-00359-0.
6. The proteome of baker's yeast mitochondria. **Gonczarowska-Jorge H**, Zahedi RP, Sickmann A. Mitochondrion. 2017 Mar;33:15-21. doi: 10.1016/j.mito.2016.08.007
7. Variable Digestion Strategies for Phosphoproteomics Analysis. **Gonczarowska-Jorge H**, Dell'Aica M, Dickhut C, Zahedi RP. Methods Mol Biol. 2016;1355:225-39. doi: 10.1007/978-1-4939-3049-4_15

1.2 Oral presentations

Subtilisin for large scale (phospho)proteomics – the beginning of a wonderful love story?
Gonczarowska-Jorge H, Loroch S, Dell'Aica M, Zahedi RZ. 15th Human Proteome Organization World Congress, Taipei, Taiwan, 2016

1.3 Poster presentations

1. Dissecting the inhibitory cAMP/PKA and cGMP/PKG signalling networks in human platelets to identify novel targets for antiplatelet treatment. Pagel O, Walter E, Gonczarowska-Jorge H, U. Walter2 , K. Jurk2 , R. Zahedi RP. Proteomics Forum, Potsdam, Germany, 2017
2. Subtilisin for large scale (phospho)proteomics – the beginning of a wonderful love story? Gonczarowska-Jorge H, Loroch S, Dell'Aica M, Zahedi RZ. Proteomics Forum, Potsdam, Germany, 2017
3. Comprehensive phosphoproteome analysis of activated and inhibited hedgehog signaling in human medulloblastoma cells. Scheidt T, Gonczarowska-Jorge H, Gruber W, Dell'Aica M, Zahedi RP, Aberger F, Huber CG. Proteomics Forum, Potsdam, Germany, 2017
4. Subtilisin for large scale (phospho)proteomics – the beginning of a wonderful love story? Gonczarowska-Jorge H, Loroch S, Dell'Aica M, Zahedi RZ. 15th Human Proteome Organization World Congress, Taipei, Taiwan, 2016

2 Zusammenfassung

Die Mitochondrien der Hefe besitzen über 1000 Proteine, von denen mehr als 99% durch nukleäre DNA und nur der Rest durch mitochondriale DNA kodiert wird. Um das Mitochondrium erreichen zu können, ist eine effiziente Protein-Zell-Signalweiterleitung notwendig, um die Moleküle nicht nur an das Organell selbst, sondern auch an eines der vier Subkompartimente des Mitochondriums korrekt zu adressieren. Mitochondriale Protein-Fehlzuordnung ist mit verschiedenen Krankheiten wie Alzheimer und Parkinson assoziiert. Um den Proteintransport in die Mitochondrien besser zu verstehen, wurde ein wichtiger Komplex namens Mitochondrial Processing Peptidase (MPP) gestört, um die proteomische Dynamik unter diesen Bedingungen zu untersuchen. Die MPP ist notwendig, um Proteine fertig zu stellen, die nukleär codiert sind und die innere Membran oder die Matrix der Mitochondrien als Ziel haben. Mit einem funktional eingeschränktem MPP war es möglich, Proteine, die diesem Weg folgen, sicher zuzuordnen und die Lokalisierung dieser Proteine in einem Subkompartiment zu bestimmen. Da auch Phosphorylierungen eine wichtige Rolle bei der zellulären Signalübertragung spielen, wurde das Phosphoproteom untersucht, was mögliche Phosphorylierungsstellen, die am zellulären Wachstum von Hefe beteiligt sind, offenbarte. Mit dem Ziel die (Phospho-)Proteomabdeckung der mitochondrialen Proben [HG-1] zu erhöhen, wurde eine neue Methode der Bottom-up Proteomik entwickelt, da die klassische Methode durch Lücken in der Proteomabdeckung die Möglichkeit reduzierte, dynamische biologische Systeme zu verstehen. Subtilisin wurde aufgrund seiner breiten Schnittstellen-Spezifität als proteolytisches Enzym ausgewählt, was die Wahrscheinlichkeit erhöhte, verborgene Bereiche des (Phospho-)Proteoms zu enthüllen. In der Tat war es mit Subtilisin möglich, die Proteomabdeckung zu erhöhen und Phosphorylierungsstellen zu erreichen, die noch nicht mit herkömmlichen proteolytischen Enzymen abgedeckt waren. Subtilisin wurde weiter untersucht und die Kompatibilität mit Label-Techniken (TMT, iTRAQ und label-free) und In-depth Proteomik-Untersuchungen wurde bestätigt, wobei Subtilisin sich als ein leistungsfähiges Werkzeug erwies, um dynamische Systeme in Mitochondrien und zelluläre Signalweiterleitung besser zu verstehen.

3 Abstract

Yeast mitochondria possess over 1000 protein, in which over 99% are nuclear DNA encoded and the rest are encoded by the mitochondrial DNA. In order to correctly reach the mitochondrion, an efficient protein cell signaling is necessary to address the molecules not only to the organelle, but to one of the 4 subcompartments. Mitochondrial protein miss-assignment is related to several diseases, such as Alzheimer and Parkinson. To better understand protein transport in the mitochondrion, a vital complex called mitochondrial processing peptidase (MPP) was impaired to evaluate the proteomic dynamics under that condition. The MPP is necessary to mature proteins nuclear encoded that are directed to the inner membrane or matrix of the mitochondrion. With a less functional MPP, it was possible to confidently assign proteins that follow this pathway and assign subcomparment localization of such proteins. Since phosphorylations also take an important part on cellular signaling, the phosphoproteome was assessed, reveling possible phosphorylation sites involved in yeast cellular growth. A new method for bottom-up proteomics was developed with the objective to increase (phospho)proteome coverage of mitochondrial samples, because the traditional method left coverage gaps that reduced possibility to be better understand dynamic biological systems. Subtilisin was selected as proteolytic enzyme because of its broad cleavage site specificity, increasing chance of unrevealing hidden areas of the (phospho)proteome. Indeed, with subtilisin was possible to increase proteome coverage and achieve phosphorylation sites not yet covered by the traditional proteolytic enzymes. Subtilisin was further evaluated and confirmed compatibility with quantification techniques (TMT, iTRAQ and label free) and in depth proteomic studies, revealing as a powerful tool be better understand dynamic systems in mitochondria and cellular signaling.

4 Abbreviation list

ABC – ammonium bicarbonate buffer

TFA – trifluoroacetic acid

FA – formic acid

LC – liquid chromatography

MS – mass spectrometry

LC/MS – liquid chromatography coupled to mass spectrometry

TOMM – translocase of the outer mitochondrial membrane

TIMM – translocase of the inner mitochondrial membrane

MPP – mitochondrial processing peptidase

SCX – strong cationic exchange

RP-HPLC – reversed phase high performance liquid chromatography

HpH – high pH reversed phase fractionation

HILIC -hydrophilic interaction liquid chromatography

COFRADIC – combined fractional diagonal chromatography

ChaFRADIC - charge-based fractional diagonal chromatography

d3-NHS - N-hydroxysuccinimide esters of D_3-acetate

iTRAQ – isobaric tags for relative and absolute quantification

TMT – tandem mass tag

CID – collision induced dissociation

HCD – higher collisional induced dissociation

4| Abbreviation list

ETD – electron transfer dissociation

TiO_2 – titanium dioxide

PTM – post-translational modification

ACN – acetonitrile

EtOH – etanol

DTT – dithiothreitol

GuHCl – guanidine hydrochloride

IAA – iodoacetamide

SDS – sodium dodecyl sulfate

DNA – Deoxyribonucleic acid

mtDNA – mitochondrial DNA

OM – outer membrane (mitochondrial)

IMS – intermembrane space (mitochondrial)

IM – inner membrane (mitochondrial)

ATP – adenosine triphosphate

5 Introduction

5.1 Mitochodrion: general role

Throughout a wide range of collaborations, the *Saccharomyces cerevisiae*'s genome has already been fully sequenced, whereas the 16 chromosomes of this yeast had its nucleotide map and potential protein-encoding genes defined. Also, due to the possibility of controlled media growth and sufficient life span of this unicellular organism, yeast became a model for experimental studies of eukaryote organism[1], especially because many proteins sets participate in biological processes which equivalent exists in other eukaryote organism, as humans[2].

No different, yeast mitochondria have shown to be an important model to study diverse mitochondrial processes and disorders. It has being used to understand mitochondrial function, to describe different mechanisms, regulatory processes, physical compartments and the interaction with other cellular compartments[3]. Due to the possibility of efficiently switch between respiration and fermentation, the yeast can survive studies in which the complete mitochondrial genome is deleted, the oxidative phosphorylation (respiration) is totally impaired, besides being manageable to many different mutations, both at the nuclear and mitochondrial DNA[4]. Also, the circular mitochondrial DNA (mtDNA) of the *Saccharomyces cerevisiae* (*S. cerevisiae*) has been fully sequenced, composed by 85,779 base pairs and encodes strictly 8 mitochondrial proteins: subunits of the respiratory chain complex III (Cob), complex IV (Cox1, Cox2 and Cox3), complex V (Atp6, Atp8 and Atp9) and a ribosome-associated protein (Var1)[5,6].

Yeast mitochondria are mostly known by the duty of energy production in form of adenosine triphosphate (ATP) to the cell by oxidative phosphorylation (respiration) or alcoholic fermentation, i.e. yeast is a facultative anaerobic organism[7]. Less known but still vital, it is the role mitochondria in lipid and steroid synthesis[8], biosynthesis of iron-sulfur cluster[9] and heme[10,11], ubiquinone biosynthesis [12], amino acids metabolism [13], cell signaling[14] and apoptosis[15].

Due to the amount of vital functions, many diseases are involved with improper mitochondrial function, whether source of problem could be related to mutations either in the mtDNA or nuclear DNA. Diabetes mellitus, cardiomyopathy, liver and renal dysfunctions, dementia, optical and hearing impairments are a few examples of clinical deficiencies mitochondrial related[16,17]. The neurodegenerative diseases Parkinson, Alzheimer and Huntington are also mitochondrial related

and could be a loss of functionality due to time-aging[18]. In summary, over 150 mitochondrial dysfunction syndromes have been reported, whereas affects 1 in 5000 births and so far no medical treatments have been proved efficient[17,19,20].

As the proteome mitochondrion is composed by estimated 1000 proteins, over 99% of the proteins are nuclear-encoded and must be imported to the four different compartments of mitochondria: the outer membrane (OM), intermembrane space (IMS), inner membrane (IM) and the matrix [21]. To properly understand the mitochondria physiology in health and disease, it is necessary to comprehend the proteome composition of each subcompartment[22].

5.2 Mitochondrial proteome and subproteomes

Over the last decades, the mitochondrial proteome have been better elucidated, whereas mitochondrial proteins could be categorized by function (Figure 1).

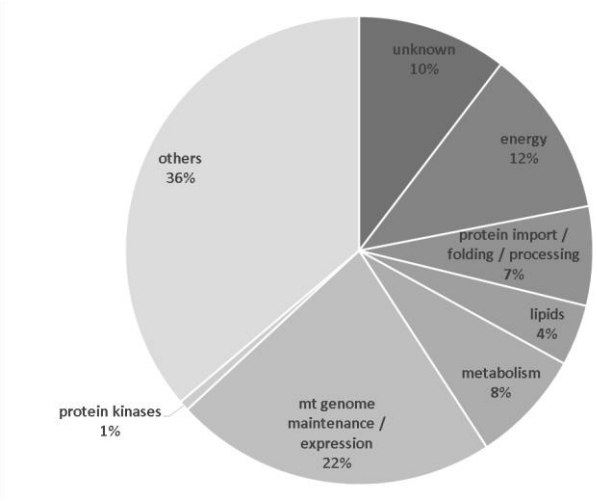

Figure 1. Categorization of the mitochondrial proteome. The Saccharomyces Genome Database (SGD, http://www.yeastgenome.org)[23], in May 2016, assigned 1187 proteins as part of the mitochondrial proteome. Compared to the first large mitochondrial proteome study where Sickmann et al[24] identified 749 proteins, which share of proteins related to expression and maintenance of the mtDNA is unexpectedly high (22% compared to 25% from the previous study), while the share of proteins with unknown function decreased from 25% to 10%.

Since over 99% of the mitochondrial proteome is generated by the nuclear DNA, an efficient protein import mechanism is recruited to direct precursor proteins to their final destination in one of the 4 different compartments from the organelle[21,25]. In a brief description of the protein import system, most of the (precursor) proteins encoded by the nuclear DNA possess a cleavable positively charged

amphipathic α helix presequence that are recognized by the translocase of the outer mitochondrial membrane (TOMM complex) that directs the precursor proteins into the inner membrane compartment, being later on driven to the translocase of the inner mitochondrial membrane (TIMM 23 complex). The different electrochemical potential ($\Delta\psi$)[20,26] generated by the expel of protons by the ATP synthase from the matrix to the inner membrane space exerts an electrophoretic effect on the positively charged sequence of the precursor proteins, since the matrix compartment is now less positively charged, driving the proteins into the direction of the inner membrane. With the demand of ATP, the precursor proteins are laterally inserted by the TIMM 23 complex in the inner membrane or driven into the matrix with the assistance of the presequence translocase-associated motor (PAM) with the ATP-dependent heat-shock protein 70 (mtHsp70). The precursor proteins are then maturated by mitochondrial processing peptidase (MPP) that cleaves off the presequence (Figure 2a). The MPP is composed by two subunits, MAS1 and MAS2, and is an essential complex, vital to cell survival. A few proteins are alternatively inserted in the inner membrane after partially being imported into the matrix by the OXA complex. A few hydrophobic proteins contain, instead of a positively cleavable presequence, some transmembrane segments with internal targeting signals. Those proteins are imported from the cytosol into to the inner membrane starting the translocase through the TOMM complex, being then directed to the TIMM 22 complex by small chaperones in the inter membrane space. At last, they are inserted laterally into the inner membrane driven by the $\Delta\psi$. This pathway is called the carrier pathway[27-30] (Figure 2b).

Another known pathway is the oxidative folding pathway of the inter membrane space, wherein unfolded proteins with rich reduced cysteine motifs (that typically are either twin CX9C or twin CX3C motifs) are translocated into the inter membrane space through the TOMM complex, being later a few cysteines oxidized to disulfide bonds by the MIA complex, turning into a folded conformation that preclude the proteins to return to the cytosol[27-30].

β-barrel proteins destined to the outer membrane are imported into the inter membrane space through the TOMM complex. In the inner membrane space, small Tim chaperones drive the proteins to the sort and assembly machinery (SAM) complex, which is already located in the outer membrane. The SAM complex then inserts the β-barrel proteins into the outer membrane of the mitochondria[27-30].

The protein import machinery have been quite well study during the past two decades, but little is known about the regulatory mechanisms of the protein import. Using *S. cerevisiae* as a model, the

Tim8 chaperone, responsible to target proteins across the intermembrane space, for instance, was correlated to cause the deafness dystonia syndrome in human when the protein Tim8 has some kind of defect [31].

Other human diseases related to the mitochondrial protein import and processing machinery are the dilated cardiomyopathy with ataxia [32], mitochondrial disease related to multisystem failure with unknown cause but related to decreased levels of the mitochondrial matrix chaperone Hsp60 [33,34], spastic paraplegia-13 (also associated to dysfunctional Hsp60) [35,36].

Pyruvate dehydrogenase deficiency [37], primary hyperoxaluria type 1 [38-40] and severe alcoholic liver disease [41] are diseases related to incorrect targeting of proteins even in wrong regions of the mitochondria. In the severe alcoholic liver disease, a mutation in the targeting sequence of the precursor manganese superoxide dismutase (MnSOD) do not avoid the protein to be directed to the mitochondria, but avoid it to reached the matrix of the organelle, being actually arrested in the inner membrane.

The inter membrane space (IMS) is the smallest subcompartment of the mitochondria, but represents a fundamental region of the organelle, because it takes part in many process, such as (1) translocation of proteins, lipids, metal ions and other metabolites, (2) redox activity of cysteine residues, (3) assembly of complexes from the respiratory chain, (4) the apoptotic pathway [42-44].

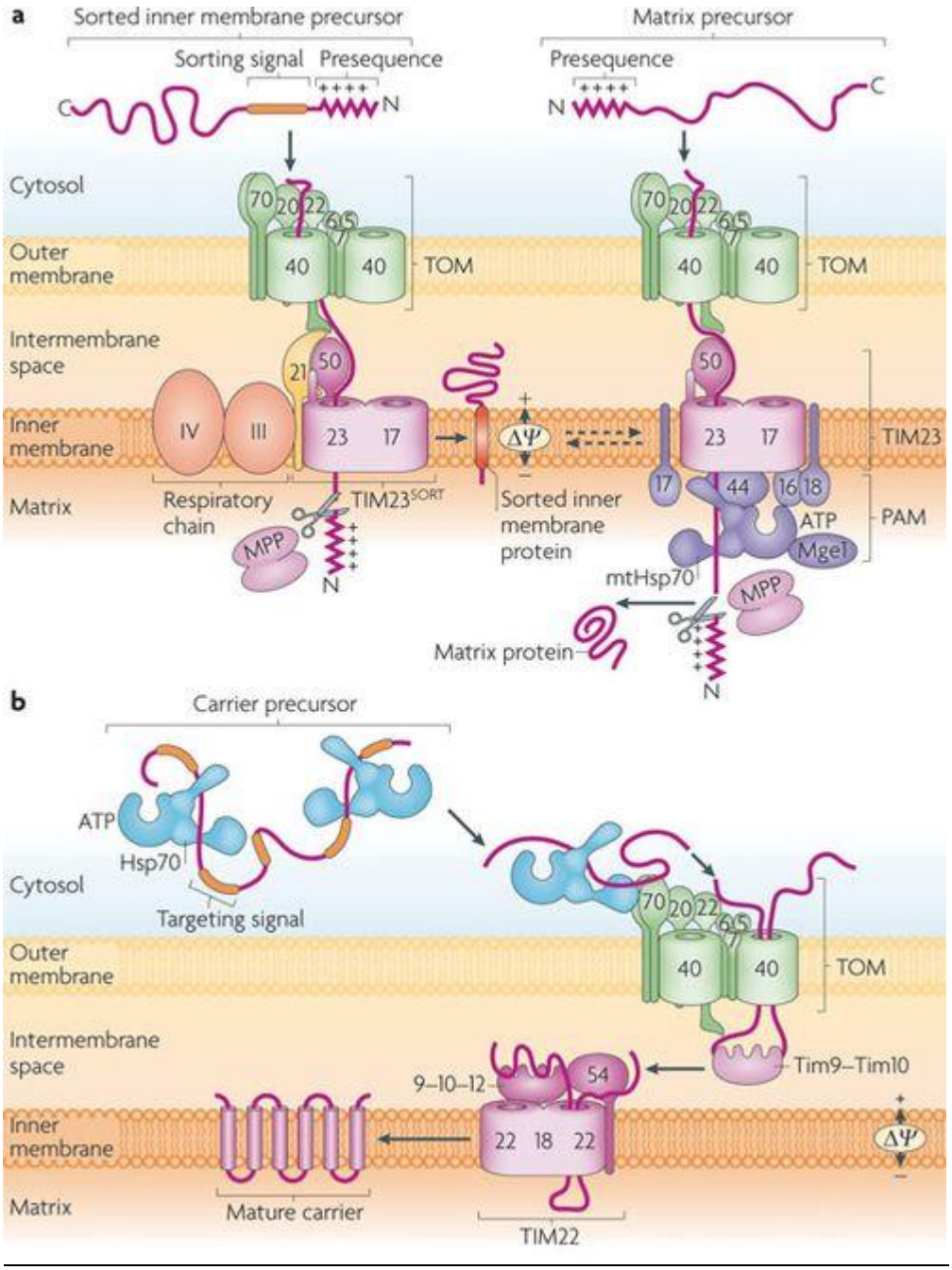

Figure 2. Mitochondrial protein import pathways. Summary of proteins nuclear enconded imported into the mitochondrion, following the (a) presequence pathway or the (b) carrier precursor pathway. Imagine obtained from Schmidt et al [28] (2010).

Over the years, our basic knowledge about mitochondria has been reshaped by (quantitative) large-scale and focused studies with methods using mass spectrometry (MS). Geissler et al[45], in 2002, using high-affinity tags to purify protein complexes, identified the protein Tim50, a fundamental subunit of the TIMM 23 complex responsible to direct precursor proteins to the IM. Moreover,

systematic analysis of yeast mutants focusing on purification of protein complexes using blue native gel electrophoresis followed by MS analysis allowed the identification of novel protein complexes, such as the SAM complex, and unrevealed new stages of precursor protein import to the mitochondria[46-50].

Large-scale mitochondrial proteome studies only became possible of the development of optimized protocols to highly purify the organelle and its membrane vesicles[51,52]. In 2002, Kumar et al[53], by immunolocalization of tagged gene products and estimation of the subcellular proteins, identified 332 mitochondrial proteins of and estimated around 800 proteins as part of the organelle. One year later, Sickmann et al[54], using purified mitochondria, accounted 749 proteins identified by mass spectrometry. Surprisingly, it was observed that 25% of the total proteome was related to expression and maintenance of the mtDNA that encodes less than 10 stable proteins, while only 14% counted for energy metabolism. This study was able to identify proteins that later on revealed important functions for cell home. With the advance of LC and LC-MS methods and technology, Reinders et al[55] identified plus 102 mitochondrial proteins, leading to a total of 851 mitochondrial proteins, reaching what would be expected of 84% of the organelle's total protein composition as listed in the MITOP yeast database[56]. To the date of May 2015, the SGD, based on the Gene Ontology Terms, has over 1180 genes assigned to the mitochondrion.

Since high throughput proteomics studies enable the identification of hundreds of proteins, only possible due to highly pure mitochondria and advances in mass spectrometry, newest studies emphasizes now protein function and protein-protein interaction, making use of already well established methods (e.g. 1D/2D-BN/SDS PAGE and gene silencing or deletion), as well of non-complicated approaches with, as well, already established protocols as stable isotope labeling by amino acids in cell culture (SILAC) in conjunction with mass spectrometry [57]. With an approach based in SILAC labeling, yeast temperature-sensitive mutants and interest His-tagged proteins, Böttinger et al [58] described the importance of the mtHsp70-Mge1-Cox4 complex for the assembly of the complex IV from the respiratory chain, and also Böttinger et al [59] described the interaction between mtHsp70 with Hsp10 for the biogenesis of the Hsp60 complex, responsible for protein assembly in the mitochondrial matrix [60]. Further, an approach using SILAC and gene deletion enabled the identification of two inner membrane proteins (Ina17 and Ina22) that together promote assembly and stability of the F1F0-ATP synthase [61].

Indeed, diverse genome wide studies focused in the gene deletion revealed protein function. Especially in yeast, an facultative anaerobic organism, gene deletion of protein components involved in ATP production via respiration was possible without causing cell death [62]. Also, transfection of human genes into the yeast DNA is certainly an effective way to study conserved protein and pathways between yeast and human mitochondrial proteins [63].

Proteins of the outer membrane (OM) are synthetized as precursors by the nuclear DNA of the yeast cell. The OM is the interface between the cytosol and mitochondria, harboring also connections between other organelles, such as endoplasmic reticulum, peroxisomes and vacuoles. Process as mitophagy, apoptosis, mitochondrial fusion and fission were described to be mediated by the outer membrane. As well, the outer membrane is the main precursor protein entry gate into the mitochondria[64,65]. To evaluate the proteome of the outer membrane, a very crucial and important step is to have highly purified mitochondria, since this organelle associate with other components from the cell, such as the endoplasmic reticulum and cytoskeletal proteins [66]. Zahedi et al [64] developed a protocol to isolate the mitochondrial outer membrane proteins applying firstly a series of centrifugation steps to remove cytosolic proteins. Later on, with two successive sucrose gradients, the highly pure mitochondria were free of proteins from the endoplasmic reticulum, peroxisomes and vacuoles. In order to obtain purified OM, using gentle mechanical forces, the outer membrane was sheared off and, after successive sedimentation and flotation steps, the OM were devoid of proteins from the IMS, inner membrane and matrix. Also, domains of proteins (mainly receptors) of the OM exposed to the cytosol were “shaved” off by intact highly pure mitochondrial treatment with trypsin or proteinase K, technique that does not disrupt the membrane. From protein identification, the purified OM was subjected to an extensive trypsin treatment, followed by strong cationic exchange chromatography and reversed phase chromatography. Peptides were subjected to ESI nano-LC/MS^2 and a total of 112 OM proteins (~85%) were able to be identified, including 27 additional proteins if comparing to the studies done by Sickmann et al [54,64].

The inter membrane space (IMS) is the smallest subcompartment of the mitochondria, but represents a fundamental region of the organelle, because it takes part in many process, such as (1) translocation of proteins, lipids, metal ions and other metabolites, (2) redox activity of cysteine residues, (3) assembly of complexes from the respiratory chain, (4) the apoptotic pathway [43,44,56]. The proteins from the IMS are encoded by the nuclear DNA and must be imported into the mitochondria. There two known pathways of the proteins of the IMS to be imported: (1) through

the oxidative folding pathway, as already described, or (2) precursor proteins that contains two signaling regions, one consisting in a matrix targeting signal and another in a hydrophobic sorting signal. Those two signaling regions together arrest the protein in the TIMM 23 complex, that laterally inserts the precursor protein into the inner membrane. The inner membrane protease releases the mature protein in to the IMS [56]. Most of the proteins of the IMS are described as soluble proteins, a few with enzymatic characteristics and a few described to be superficially attached to the inner membrane [43]. In summary, from the 51 proteins known as located in the IMS, 31 proteins were described as soluble or only loosely attached to the inner membrane [56].

The mitochondrial inner membrane (IM) harbors 228 integral or loosely associated proteins according to the *Saccharomyces* genome database [67]. Between those proteins, it can the found in the inner membrane the proteins that take part into the respiratory electron transporter chain and ATP synthase [68-72], iron-sulfur metabolism [9], heme biosynthesis [10,11], ubiquinone biosynthesis [12], amino acids metabolism [13]. Interestingly, differently from the mammalian mitochondria, the yeast respiratory chain does not contain a complex I, instead there are present three NADH dehydrogenase associated to the inner membrane[73-75]. As well, the IM acts an barrier enabling the existence of the ΔΨ potential, which is mandatory for protein import to the matrix or laterally insertion via TIMM 23[26] and TIMM 22[49] complexes. The IM also harbors the i-AAA and m-AAA (ATPases associated with a variety of cellular activities and vital for mitochondrial homeostasis [76]), besides the already well-studied protein import complexes TIMM 23 and TIMM 22 [10,14,16].

Even though divided in four, the different subcompartments of the mitochondria are strictly interconnected to each other, especially when it refers to protein import. As a few examples, nuclear precursor proteins targeted to the mitochondria are generally imported by the TOMM complex, located in the outer membrane. Tim chaperones from the IMS drive the precursor protein to the TIMM 23 complex in the IM. Precursor protein release from the TOMM to the TIMM 23 complex relies on direct interaction between TOMM and TIMM 23 complex. In the IM and the matrix, proteases and chaperones mature the precursor protein and possibly direct the proteins to final destinations. As well, direct interaction between the OM and IM, in order to maintain vital mitochondrial architecture, is possible due to direct binding between the SAM complex and the mitochondrial contact site and cristae organizing system (MICOS) [77-79]. As a last example, the important membrane potential ΔΨ for energy production and protein import is possible only due the proton gradient through the IM generated by the respiratory chain complex. By that, it is

possible to visualize the mitochondrial proteome highly interconnecting all subcompartments of the mitochondria.

5.3 Alternative proteolysis

In mass spectrometry (MS), a technique named bottom-up proteomics is the most common approach to analyze proteins or the full proteome of tissues of cells [80,81]. It is based in the enzymatic cleavage of proteins into peptides prior liquid chromatography (LC) and mass spectrometry measurement [82]. Trypsin became the enzyme-of-choice in bottom-up proteomics, due mainly to amino acid cleavage site predictability and generation of peptides well suitable for separation by LC and detection by MS [83,84]. In MS data repositories, such as PRIDE [85], Peptide Atlas [86] and ProteomeXchange [87], it becomes evident the vast use of trypsin as the main enzyme used by the majority of scientific groups for their studies. Still, when analyzing the human proteome, less than 50% of coverage has been identified by bottom-up mass spectrometry. This low identification might be due to lack or excess of amino acid cleavage sites, difficult peptide ionization, low abundance proteins and non-unique sequences. Trypsin, for instance, depending on the position of cleavage sites (arginine and lysine), if too close or too distance, will generate too long or too short peptides for confident identification by mass spectrometry. Also, proline, phosphorylations, glutamate or aspartate near the cleavage site will reduce trypsin cleavage efficiency [88-92]. In that sense, the use of solely trypsin may prevent identification of certain parts of proteome and possibly miss identification of the whole protein [83,93]. Consequently, if a part of the proteome is never identified, the PTM information attached to this missed region will definitely be lost. To uneven this situation, further enzymes have been applied to dig proteome identification, as GluC, ArgC, LysN, AspN [93-96] and LysArginase [97], for instance, in which they all have in common is cleavage site specificity.

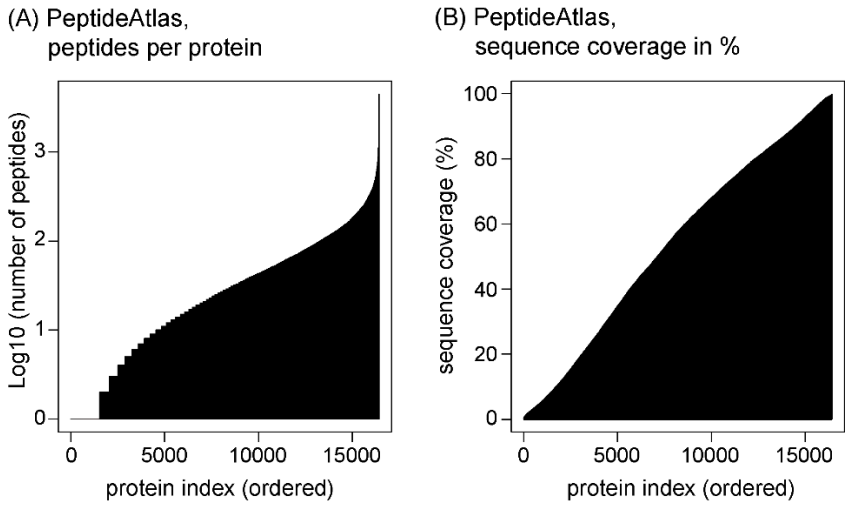

Figure 3. Actual human proteome coverage. Over 1,200,000 peptide sequences were retrieved from PeptideAtlas [86] (October, 2017) were compared to the human Uniprot [98] database to calculate (a) amount of identified non-overlapping peptides per protein and (b) total sequence coverage per protein ever measured by mass spectrometry.

The current mass spectrometers with high mass accuracy detectors, combined with developed false discovery rate (FDR) algorithms, allowed the use of broad specificity enzymes in for bottom-up proteomics experiments without the constrains of large database search spaces when using unspecific searches. This gave the possibility to use enzymes such as subtilisin [99-101], proteinase K [102-104] an elastase [105,106] for qualitative experiments to increase specific proteins or the full proteome coverage. Since they lack clear specific motif consensus or specific amino acid to perform proteolysis, this gives the possibility of identifying missing regions of the proteome that were, for some reason, not identifiable using limited specificity enzymes. To illustrate it, Engel et al [107] intended to identify the specific amino acid site on which a novel EGFR inhibitor was bound. Even after trypsin and GluC digestion using different MS fragmentation techniques (CID, HCD, ETD and EThcD), only after subtilisin digestion a peptide containing a cysteine amino acid residue was identified as the binding site of the inhibitor.

Taking into consideration the possible benefits of subtilisin to increase (phospho)proteome coverage of yeast mitochondrial samples, allowing to better understand the signaling pathways of protein import into the mitochondrion, this broad specificity enzyme was first evaluated to check compatibility with bottom-up mass spectrometry studies, including sample digestion

reproducibility, best digestion conditions, compatibility with quantitative techniques as label free and chemical labelling (iTRAQ and TMT) and in-depth (phospho)proteomics studies.

The name "subtilisin" was specifically mentioned since 1956 by M. Ottesen[108], but first description was done by K. Linderstrøm-Lang and M. Ottesen from the Carlsberg Laboratory (Copenhagen, Denmark) in 1947[109], and defined as subtilisin of Carlsberg to differentiate from other subtilisins[110,111]. Subtilisin is classified as serine protease[112,113] of broad specificity[114,115]. Other groups have previously used subtilisin in the past for proteomics studies, but a ready to use protocol, as already described for trypsin and other highly specific enzymes, was still due. This enzyme has been studied, usage protocol described and the potential use to unveil protein import signaling pathways into the mitochondrial by means of bottom-up proteomics techniques confirmed. Subtilisin was chosen in spite many other broad specificity enzymes because it has not been characterized so far in aspects approached here, it has similar digestion conditions to trypsin regarding buffer and pH and our group has used it in the past[24], indicating a strong candidate in between other enzymes.

5.4 From top to bottom – following the ion until measurement

Protein measurement is a straightforward pathway when adopting bottom-up proteomics for protein measurement and identification. In summary, pre prepared samples containing proteins are first enzymatically digested into peptides, peptides are then separated by liquid chromatography (LC) and later measured by a mass spectrometer for further protein identification [82].

Samples obtained from tissues or cell cultures, for instance, are processed to remove other molecules (cell membrane, DNA) than protein to facilitate further steps of peptide measurement (Figure 4a,b). There are a few methods already described for protein purification[116-118], and all proceed before digestion. Proteins are then reduced to peptides by proteolytic cleavage by a selected enzyme or group of enzymes (Figure 4c). The preference for peptide measurement than protein comes from the fact that peptides have more similar physico-chemical characteristics than proteins, are better ionizable and more sensitive for the mass spectrometer. In that sense, it is easier to handle peptides once they have similar properties, but it comes with the expense of incomplete protein sequence coverage, since not all peptides from a complex mixture are identified, losing as well side information as post-translational modifications (PTM) [115,119].

5| Introduction

After the proteins are digested, usually peptides are injected in a high performance liquid chromatography (HPLC) system (Figure 4d), or, depending on the experiment objective, extra steps are performed, as peptide labeling, PTM enrichment (Figure 4e), sample fractionation (Figure 4f) and/or other procedures. The peptides injected in the HPLC pass through a capillary with solid material (stationary phase) that binds the majority of peptides. Peptides are slowly eluted (depending on peptide hydrophobicity/hydrophilicity) by gradient increase of the solvent (mobile phase) [120]. The eluted peptides reach the end of the column and pass through a needle that is positioned in front of the entrance of the mass spectrometer, setup called "on-line". The droplet containing peptides formed at the end of the needle is vaporized and peptides are positively ionized by a strong electrical potential in a process named electrospray ionization [121,122]. In this process, peptides become protonated, with a positive charge at the N-terminal and extra positive charges for each basic amino acid, histidine, lysine or arginine, present in the peptide backbone [119]. In a QExactive HF mass spectrometer (Thermo Scientific, Germany), the peptide ions enter the instrument by a transfer capillary and are guided through a sequence of electric fields until the ion mass detector, called Orbitrap [123]. First, the Orbitrap do a survey scan (MS survey scan), in which define the masses of all analytes present in the spectrum. The masses are given as mass over charge (m/z), in which is calculated the mass of a peptide summed with the number of protons, divided by the charge (M+xH)/x+, "M" standing for the mass in Da and "x" the number of protons (H). To exemplify, a peptide with a mass of 998 Da and 2 protonations woud be seen as (998 + (2 x 1))/2 = 500 m/z in the spectrum. To determine the charge state, it is necessary to observe the isotope peaks generated by this specific peptide. Each peptide containing a ^{13}C atom instead of a common ^{12}C atom with generate another peak with 1 Da difference. In the mass spectrum, they would be seen as 500 and 500.5 m/z, in which the 0.5 m/z difference refers to the 1 Da difference [119]. Triple charged and quadruple charged peptides would have mass difference between isotopes of ~0.33 and 0.25 m/z, respectively, in the mass spectrum. After identifying masses in the MS survey scan, usually the most intense ions follow a second measurement step on the Orbitrap after isolated peptide fragmentation with inert gases (nitrogen, helium or argon), called MS/MS or MS^2. The MS^2 fragmentation gives the opportunity to identify the amino acid composition of the peptide, including possible PTMs. In the Q Exactive HF, the higher collision induced dissociation (HCD) fragmentation occurs in the HCD cell, in which one of the inert gases is accelerated to collide with the many copies of a specific isolated peptide, fragmenting it at the amino acid bond, generating many fragments of the peptide that are acquired the Orbitrap in a new spectrum (Figure 5) [119]. Other MS instruments

possess different fragmentation techniques, such as collision induced dissociation (CID), electron transfer dissociation (ETD) and a combined HCD with ETD (EThcD), in which all have similar principle of peptide fragmentation and further peptide identification.

Peptide structural composition is obtained with the MS^2 spectrum. Once the MS survey scan determines the peptide mass, the MS^2 masses can be determined by the peptide mass minus the mass of one of the existing 20 amino acid residues, in which probably exists a fragment that is the composition of all the amino acids minus the N-terminal. In the example peptide MDELLHGK with 2 positive charges, the MS survey scan would show an average mass of 471.74 m/z or 941.48 Da (without 2 protons). The MS^2 spectrum would have, between many other peaks, one with a mass of 810.44 Da (DELLHGK), indicating that a methionine, with a mass of 131.04 Da, has been lost (941.48 – 810.44 = 131.04 Da). Later, the MS^2 spectrum would have a peak with 695.40 Da (ELLHGK), indicating that the following amino acid residue, an aspartic acid, has been lost (810.44 – 695.40 = 115.04 Da). PTMs as phosphorylation increase in ~79 Da the mass of the attached amino acid residue, in which any variation between two peptide fragments with a mass shift of a specific amino acid residue plus 79 Da indicate the presence of a phosphorylation. Peptide search algorithms, such as Mascot [124], MS Amanda [125] and SEQUEST [126], use protein amino residue sequence to create theoretical MS2 spectrum of peptides, speeding up peptide identification. Digestions using enzymes with specific amino acid or consensus motif cleavage usually give faster and more confident results than broad specificity enzymes, once there is a known C-terminal peptide and facilitates for the search algorithms to create theoretical MS^2 spectra [127].

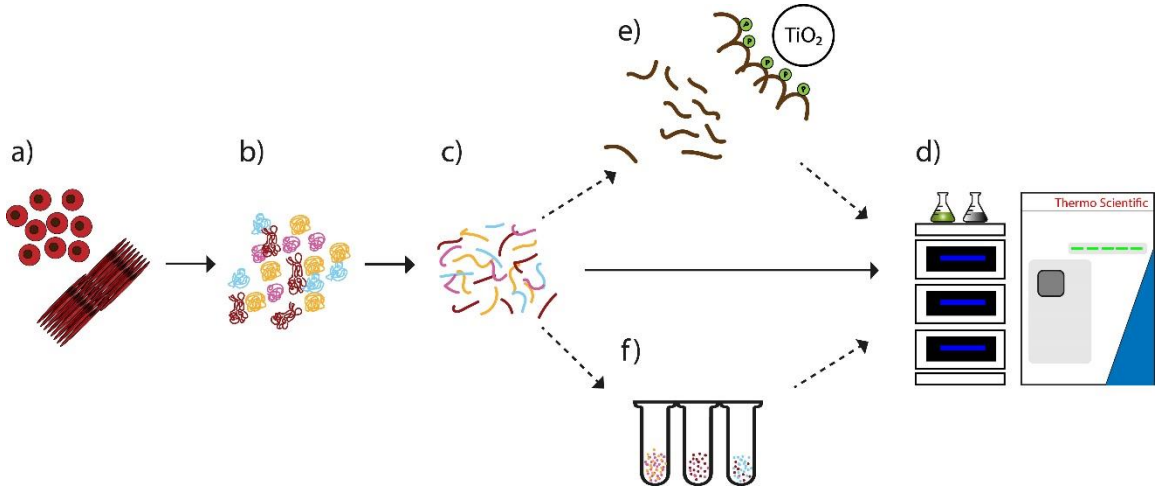

Figure 4. Sample preparation workflow. a) Cell cultures or tissues are lysed and processed to remove cell debris and DNA until achieving (b) purified proteins. Proteins are digested into (c) peptides using a selected

proteolytic enzyme. (d) Peptides are injected in a HPLC system, separated during the liquid chromatography, electrospray ionized and measured by a mass spectrometer. Extra steps as (e) post-translational modification enrichment or (f) sample fractionation to reduce sample complexity may be applied if necessary.

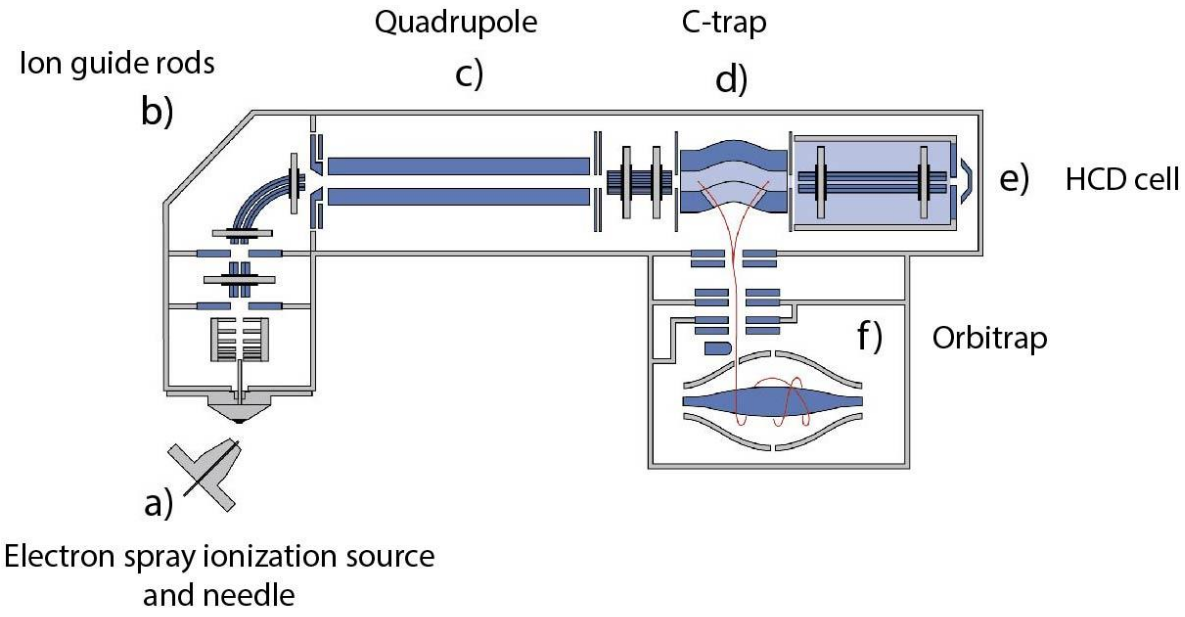

Figure 5. Schematic of a ThermoFischer Q Exactive mass spectrometer. a) Needle at the end of the liquid chromatography electrospray positively charged peptides ions inside the mass spectrometer. b) A set of rods with electric fields guide the ions through the instrument. c) A quadruple set of rods can additionally filter peptide ions by mass, necessary for peptide isolation prior fragmentation. d) A C-trap chamber temporarily accumulate ions injection in the Orbitrap chamber. e) HCD cell, in which isolated peptide ions are fragmented by a technique called higher collisional induced dissociation (HCD). f) The Orbitrap is the mass detector of the instrument. During a MS survey scan acquisition, peptide ions pass through a, b, c, d and f steps. After the Orbitrap performs a mass detection of the peptides, the most N intense ions are isolated in the quadrupole (c), HCD fragmented and measured on the Orbitrap, a process called MS^2. The MS survey scan and MS^2 sprectra are generated in the orbitrap chamber. Figure downloaded from the Planet Orbitrap website [128] (2018).

5.5 Phosphorylation

A simple post-translational modification may have a wide range of consequences to the protein. It can alter protein conformation and activity, it can impair protein binding to a substrate, and it can signalize protein for turnover or correct location assignment. Regulating so many proteins,

phosphorylation takes a vital role in cell homeostasis, growth, proliferation, specification, apoptosis and cellular communication. Wrong dynamic regulation of phosphorylations by kinases and phosphatases, or the lack of one of them, may cause severe diseases, as cancers, neurodegenerative disorders and diabetes [115,129,130]. In yeast mitochondria, for instance, a phosphorylation in the residual serine 62 of the subunit of Atp20 inhibited dimerization of the ATP synthase complex, indicating that this PTM could regulate whole cell bioenergetics, as oligomerization of the ATP synthase complex is necessary for complete bioenergetics activity [68].

Phosphorylation (and dephosphorylation) regulation activity dates to the 1950s, when first was described an enzyme from the liver that catalyzed casein phosphorylation. Later, an interconversion between two forms of glycogen phosphorylase (a and b), an enzyme involved in the glycogenolysis, was observed when form b turned into the a form in the presence of Mg-ATP and an enzyme that was named phosphorylase kinase. Also, the a form could be reconverted into the b form in the presence of another enzyme named at the time phosphate-releasing, today named as protein phosphatase 1. It was observed as well that glycogenolysis in liver tissue would be stimulated in the presence of the hormones glucagon or adrenalin. Those hormones also increased activity of phosphorylase a. When the tissue was homogenized, activity of the hormones were lost, but the addition of Mg-ATP restored response of the hormones in a cell-free system. This led to series of discoveries, including the generation of cyclic AMP (cAMP) by adrenalin, that activated cAMP-dependent protein kinase (PKA), that activated phosphorylase kinase and, by its turn, converted phosphorylase b into the a form and it could stimulate the glycogenolysis. Later, PKA was observed in many other tissues and organisms, revealing the importance of this enzyme in many other cascade events of cell signaling [131].

Studying how phosphorylations mediate cell signaling is necessary to understand the dynamics of proteome that is subject to the different situations may occur. Many scientific groups are focus to characterize the regular work of a cell proteome in order to have a standard model before to better comprehend differences from the proteome of diseases. Since one third of the proteins are estimated to be phosphorylated at least once in their lifetime, becoming the most common PTM, the characterization of the phosphoproteome significantly increase knowledge on how proteins act and interact [132].

Phosphorylation, spite being the most common PTM, is a low abundant modification, in which proteins might be present at a given period in both phosphorylated and not phosphorylated forms.

In mass spectrometry, usually phosphopeptide enrichment methods are applied before MS measurement for higher detection, improved identification and better quantification. With the advances in mass spectrometry sensitiveness and improved enrichment methods, one single experiment allowed to identify thousands of phosphorylation sites in comparison to a few dozen before existing these techniques [133].

Between the different methods published [134], a phosphopeptide enrichment protocol with high selectivity is based on titanium dioxide (TiO_2). In acid pH solutions, an electrostatic attractive force between the negatively charged phosphate group and the positively charged surface of the TiO_2 induce biding (Figure 6). To avoid high unspecific interaction between the TiO_2 and others than phosphate groups, there is the presence in the solution of competitive binders, as dihydroxybenzoic acid (DHB) and glycolic acid, which it is enough to displace only acid non-phosphorylated peptides from the TiO_2 beads[127,135].

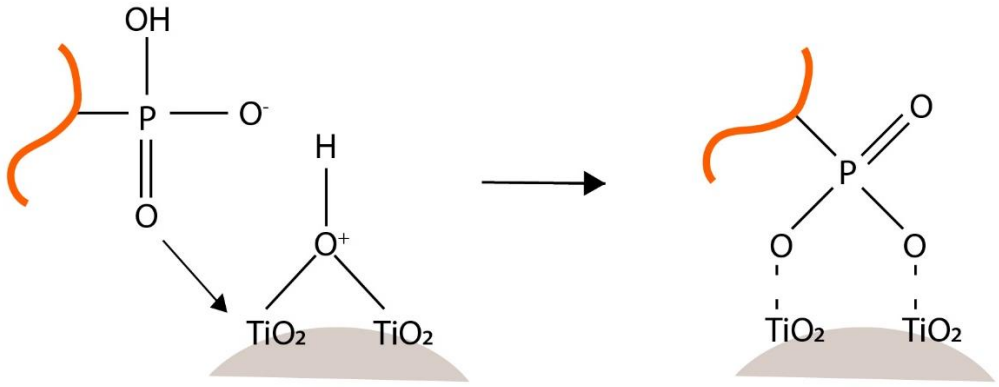

Figure 6. Interaction between the phosphate group and the TiO_2 surface.

5.6 HILIC

Hydrophilic interaction chromatography (HILIC) is a variation of the normal phase chromatography, in which the interaction between the hydrophilic stationary phase and the analytes happens by partitioning. One mobile phase contains high percentage of an organic compound, e.g. acetonitrile, mixed with a small percentage of water. The surface of the HILIC stationary phase is polar, e.g. bare

silica, often derivatized with polar or polymer-based functional groups [136]. The polar surface attract the water, forming a water-rich layer over the stationary phase. Higher the organic content, stronger is the interaction between the water and the stationary phase. The injected analyte is then retained in the water-rich layer, and partitioning separation occurs increasing the amount of water in the mobile phase (Figure 7). Since the stationary phase is polar, when there is an increase in the organic solvent (e.g. acetonitrile), the present water in the solvent interacts stronger with the stationary phase. The residual silanols present on the solid phase and the acetonitrile do not interact, making room for the water to interact with those silanol groups. It was actually observed that, when the mobile phase contains approximately 20% of water and 80% of acetonitrile, it reaches the maximum surface area of the stationary phase covered with water. But higher the amount of the organic in the mobile phase, higher is the adsorption of the water to the stationary phase[136]. Higher is the hydrophilicity of the analyte, more it is retained in the immobilized water-rich layer. In other words, the more hydrophilic the analyte is, more the partitioning equilibrium is pushed in the direction of the water-rich layer on the stationary phase, causing the analyte to be more retained. Alpert et al[137] suggested that hydrogen bond and dipole-dipole interactions between analyte and the stationary phase and immobilized water-rich layer could also play an effect to partitioning during HILIC. Alpert noted that basic groups appeared to turn the analyte more hydrophilic, leading to increased retention, thus affecting separation by other type of interactions. The analyte separation during HILIC is strongly influenced by the eluent pH. Yoshida[138] summarizes that also dipole-dipole interactions made an effect on analyte retention, but also considered that hydrogen bonds could also make an influence. Depending on the analyte p*Ka*, the higher or lower solution pH determines its charge state, by its turn affecting the hydrophilicity. Acidic analytes, for instance, at mobile phases containing trifluoroacetic acid (TFA), had greater retentions on a silica based stationary phase, once the repulsion of the ionized silanol groups towards the solute anions was suppressed by the low pH due to the presence of the TFA[136] .

During studies using two different type of stationary phase, one neutral and other for cation-exchange, Alpert[137] realized that not only HILIC (hydrophilic based interaction) retention was occurring, but also ion-exchange (electrostatic) retention as well, since he could observe a retention of basic molecules happing in the absence of organic compounds in the mobile phase. He also observed that the retention capacity factor of the molecule increased when the concentration of the organic solvent increased as well, probably due to hydrophilic interactions. When the organic compound was above 50% concentration in the mobile phase, Alpert could see the hydrophilic

interactions more noticeable than the electrostatic interactions, suggesting a "mixed-mode" retention with a lower participation of the second mechanism (Figure 7a).

This opened the possibility of new molecule separation using HILIC mode based. While HILIC is the separation by hydrophilic interaction, it was introduced on the market the zwitterionic ZIC®-HILIC (Merck), in which involved ion-exchange retention in combination with HILIC retention, possible due to the combined presence of the positive and negative charge on the mandatory hydrophilic stationary phase. The ZIC®-HILIC has a permanently functional zwitterionic sulfobetaine type group bounded to a wide-pore silica stationary phase. The sulfobetaine group strongly binds water by hydrogen bonds. This water now makes part of the stationary phase, being the main component on the retention mechanism. As explained above, the water-rich layer and the sulfobetaine groups make a "mixed-mode" retention mechanism in this HILIC like chromatography[136].

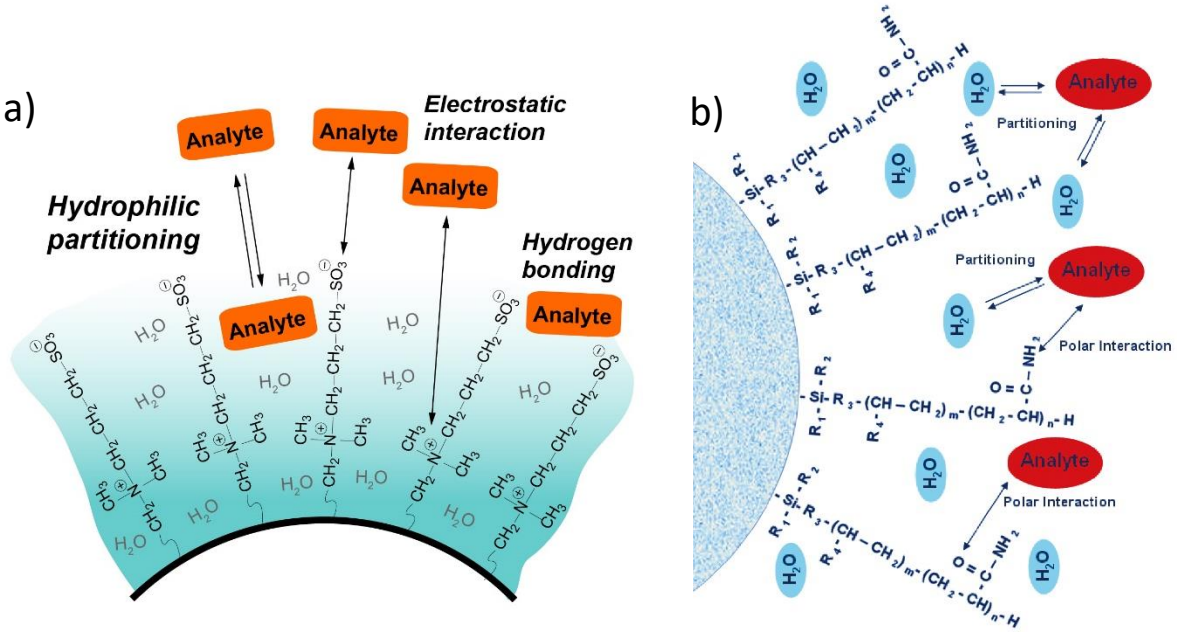

Figure 7. Schematic of HILIC. a) A stationary water-rich layer is formed over the silica stationary phase bounded to a polar group. The analyte is retained in the water-rich layer due to high concentration of organic compound, e.g. acetonitrile, in the mobile phase. When the water content increases in the mobile phase, the analyte is partitioned to the mobile phase, occurring the partitioning type separation. Also, hydrogen bond, dipole-dipole and electrostatic interaction retention can occur (based on MERCK figure[139]). b) HILIC separation using TSK® Amide-80 (Tosoh) particle used in this project. The separation of analytes is based on a combination of hydrophilicity and polarity (obtained from Tosoh online flyer[140]).

In this present work, HILIC was performed using a stationary phase composed by spherical silica particles covalently bonded with non-ionic carbamoyl groups, named TSK® Amide-80 (Tosoh, Japan). This stationary phase has a considerable good separation/retention of analytes due to partitioning, or polar interaction or a mix-mode of both types, i.e. using HILIC separation supported by analyte

polar interaction to the bead, which could explorer a better separation of those analytes based on a combination of hydrophilicity and polarity (Figure 7b).

The HILIC demonstrated to be a great technique for the separation of phosphopeptide enriched samples. Enrichment of high amount of starting material generate a too concentrated and complex phosphoproteomic sample for mass spectrometry. A single shot MS measurement would result in an undersampling of phosphorylations due the high amount of phosphopeptides eluting at the same time. Also, no phosphopeptide enrichment is totally effective due to unselective binding of non-acidic phosphorylated peptides as well, probably to an heterogeneity of the TiO_2 surface or an induced-like dipole effect[141], what could obfuscate low abundant phosphopeptides during the LC separation and MS measurement. HILIC would serve as a sample fractionation system, diving the phosphopeptide enriched sample into many different fractions, and also would separate non-phosphopeptide from phosphopeptides. This occurs due the polarity aggregated to the peptide by the phosphate group, increasing general hydrophilicity of the phosphopeptide. Non-phosphorylated peptides would elute first during HILIC fractionation due to a lower hydrophilicity, increasing purity of the phosphopeptides in later fractions and decreasing the chance of obfuscation during MS measurement [142].

5.7 Reversed phase liquid chromatography

Reversed phase (high performance) liquid chromatography (RP-HPLC) is usually the chosen method to drive peptides into the mass spectrometer in an “on-line” configuration, since that is no other procedural step after injecting the sample in the HPLC. In other words, the HPLC is coupled with the mass spectrometer. Other liquid chromatography techniques, as HILIC or strong cationic exchange (SCX), since they not coupled with the mass spectrometer, are called “off-line” chromatography [115,119].

The RP-HPLC principle is based in a hydrophobic stationary phase with peptides loaded in a hydrophilic solution. Peptides less polar would interact stronger with the stationary phase than polar peptides. With a gradient increase of high organic in the mobile phase, the more polar peptide would elute earlier than less polar peptides, separating the peptides prior MS measurement, reducing complexity and increasing identification of peptides [143]. The signal intensity of the peptide observed in the spectrum generated after MS measurement is directly proportional to the

concentration of the analyte. Higher the signal, better changes of MS^2 fragmentation and identification. To achieve a higher peak (signal intensities), it is necessary to elute the peptide in the smallest volume as possible. To achieve it, chromatography columns should be uniformly packed as small as possible, between 50 and 150 µm inner diameter. Interestingly, these columns usually support only µg of peptides and run in small flow rates, at the order of 100 nl/min, for instance. This setup is sufficient for an efficient sample identification [119].

Another variant of the RP-HPLC is the high pH reversed phase chromatography (HpH) used to sample fractionation[144]. While the RP-HPLC is run in an acidic mobile phase, the HpH runs in pHs close to 7.5. HpH is as well based on hydrophobic interactions with high resolving power, but it is highly orthogonal to the low pH RP-HPLC [145], since basic peptides are more retained at high pH and acidic peptide at low pH, and also due to peptide net charge be affected by the pH, varying retention time[144]. HpH may be also combined with a concatenation strategy, based on pooling fractions from different parts of the gradient in one single fraction, reducing MS measurement time while increasing a better dispersion of peptides in the RP-HPLC run when on-line with the mass spectrometer. Usually early, middle and later fractions of the HpH are combined in a single fraction prior LC/MS. The HpH objective is to reduce sample complexity and increase peptide identification and protein coverage [146].

5.8 Strong cationic exchange and ChaFRADIC

SCX was previously used as a peptide separation method “on-line” with the mass spectrometer, in which the chromatography follow after the SCX separation column was directly connected to the electron spray ionization source of the MS[147], but has been mainly replaced by RP-HPLC due to a higher buffer compatibility between the LC and mass spectrometer interface. Still, SCX remained as an alternative off-line fractionation method, but it has other useful advantages. The SCX is based on net surface charge separation of peptides. At low pHs, peptides possess positive net surface charge. Tryptic peptides comes usually with at least 2 positive charges, one from the N-terminal and other from the lysine or arginine side chain that contains a nitrogen, which pKa is high enough to bind a proton in acid conditions. The side chain of histidine as well increase one positive charge if present in the peptide backbone at low pHs following the same principle as lysine and arginine. Peptides are

loaded with a non-competing mobile phase in order to bind the negatively charged stationary phase. Later, ionic strength of the mobile phase is gradiently increased competing with the peptides to the stationary phase. In that way, less strong linked peptides will elute first, and usually weaker binding is due to a lower net surface charge [148].

The SCX became a powerful tool to enrich protein N-termini peptides using charge-based fractional diagonal chromatography (ChaFRADIC)[149]. ChaFRADIC is a technique based in COFRADIC (combined fractional diagonal chromatography), which is based on diagonal chromatography: first peptides are separated by reversed phase chromatography into distinct fractions, followed by a chemical derivatization that modifies a selected class of peptides, changing retention time on the chromatographic column. Later, fractions are reinjected into the same chromatography conditions, separating that way modified and non-modified peptides [150].

Protein N-terminal might pay a crucial role in protein signaling, as described previously for proteins nuclear encoded that have the mitochondria as final destination [27].The complex ChaFRADIC technique elucidated the function of the yeast mitochondrial protein Icp55, once this protein acts in the protein N-termini of recently imported proteins into the mitochondrion [149].

In bottom-up experiments, proteins are digested into many peptides. After digestion, the original protein N-terminal could not be distinguished from the newly generated peptides. To solve this issue, prior the digestion, primary amines (original free protein N termini and side chain of lysine residues) were labelled with a chemical label called iTRAQ (chapter 5.9). After labeling, samples were enzymatically digested, e.g. trypsin, followed by a SCX fractionation by charge state (+1, +2, +3, +4 and >+4). Each fraction passed through an acetylation step, with a molecule named N-hydroxysuccinimide esters of D_3-acetate (d3-NHS). Only free N-terminal peptides were acetylated, i.e. newly generated N-terminal after digestion. The original protein N-terminal iTRAQ remained unaltered, while all recently acetylated peptides reduce charge state by at least 1 charge. Since the physico-chemical properties of iTRAQ labeled peptides remained unaltered, a second SCX chromatography is applied for each fraction individually. At the same chromatography conditions, iTRAQ labeled peptides elute at the same retention time, while non-original N-terminal peptides, now acetylated, elute earlier in the gradient, being now possible to separate original and non-original protein N-terminal peptides. Another advantage of this technique is the possibility of combining samples after iTRAQ labeling, allowing to perform proteomic and PTM comparison between different conditions [149,151].

5.9 Proteome relative quantification techniques

Bottom-up proteomics progressed in many different fronts to highly increase organism proteome coverage. It has advance in faster, more sensitive and accurate mass spectrometers, created different peptide fractionation methods to increase sample coverage and developed methods to enrich sensitive information hidden in the proteome. Nowadays, having a depth proteome coverage using bottom-up proteomics is not sufficient to understand the dynamics of several biological processes, including diseases. Since protein abundances are oscillating depending on the condition that the organism is subjected, such as heat shock proteins that increase in abundance when the organism undergo a stress situation[152], a remarkably successful technique to discoverer protein function, biological pathways and diseases alterations is protein comparison between two different states, i.e protein quantification. Different protein levels might give hints of possible drug targets, indicate possible biomarkers to diagnose diseases, even in early stages of development. For those reasons, protein quantification passed to be an integral part of proteomics studies.

Two common approaches using chemical labels for quantification on the MS2 level are isobaric tags for relative and absolute quantification (iTRAQ)[153] and tandem mass tags (TMT)[154]. Both have a similar working principle. These labels consist of 3 elements, an amine-reactive group (to bind a label to the peptide at any free primary amine), a cleavable linker (to balance the mass of the different labels, mass normalizer) and a unique mass reporter (to differentiate between samples) (Figure 8). The isobaric tags (or channels) have different masses for the mass reporter (or reporter ion) and a mass normalizer that gives equalize the overall mass of the tag, and once the peptides are labeled with the different tags, they keep same final mass, even with different mass tags. This is necessary to do not alter peptide properties, and with the same properties, the peptides with the different channels elute all together and are MS survey and MS^2 measured, allowing further quantification. The mass reporters have different masses, and a variation of the amount of ^{13}C and ^{15}N in the mass normalizer allows the overall equal mass between channels. For instance, meanwhile mass tag of one channel is 131 Da with a ^{14}N in the mass normalizer, the mass tag of another channel is 130 Da with a ^{15}N in the mass normalizer, equalizing the overall mass between channels.

A downside of isobaric labeling might occur as ratio compression, when reporter ions are forced by mistake to a 1:1 ratio. It occurs due to the MS parameter called isolation window, in which the peptide m/z selected for MS2 fragmentation is isolated in a range comprising 2 to 3 m/z more or less of the selected mass. It can co-isolate more peptides and, since all peptides releases the same reporter ions, it could force an equal ratio between the reporter ions, once the majority of the proteins remains unaltered in the experiments. This leads to the compression of the reporter ion ratios, compromising quantification and, therefore, underestimating true variances in protein abundances. To avoid this issue, and applied whenever possible during this work experiments, samples were fractioned to many fractions to reduce peptide complexity, avoiding, thus, peptide co-isolation [155,156].

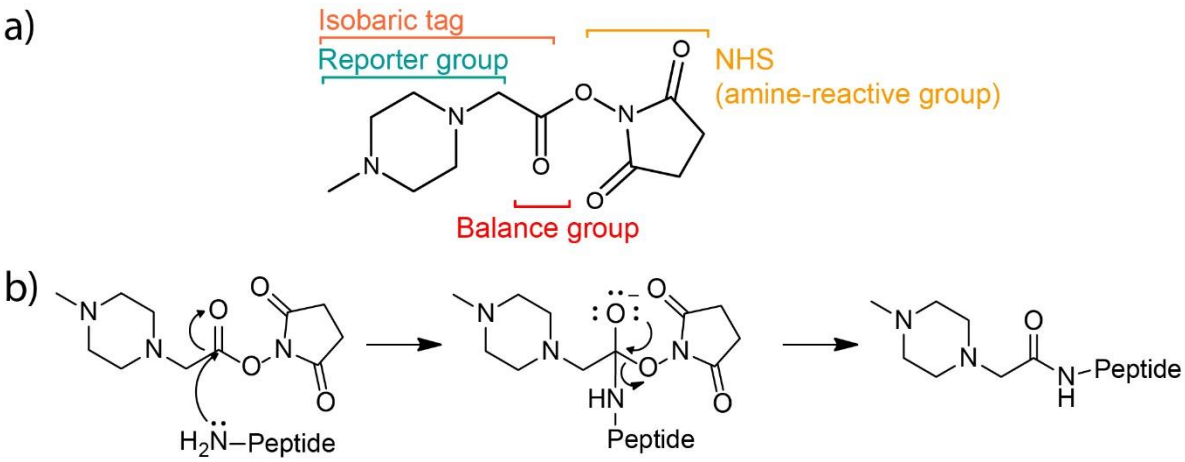

Figure 8. Isobaric tag chemical structure. (a) The NHS (N-hydroxysuccinimide ester) group undergo (b) a displacement reaction with unblocked primary amines to attach the tag to the molecule.

A standard protocol of relative quantification is as follows: up to 8 individual samples for iTRAQ or 10 for TMT are selected. The samples may vary between wild type, condition 1 and condition 2, all in triplicates or another setup depending on the experiment objective. The samples are individually prepared, proteins purified and digested. Later, samples are isobaric labeled, each with one single channel (tag) of the TMT (or iTRAQ) kit. After labeling, samples are pooled together in a ratio of 1:1. Phosphopeptide enrichment and other fractionation methods are usually compatible with the labeled peptides. Pooled samples are LC/MS measured. The same exact peptide from all conditions elute at the same time and are MS survey scan measured. Later, those peptides are isolated together, because they have the same mass, and MS^2 fragmented. The MS^2 spectrum will acquire the fragmented reporter ions. The signal intensity of the different reporter ions will allow the

relative quantification, in which higher the signal, higher is the presence of this peptide/protein in the sample (Figure 9). This might indicate how the presence or absence of the protein influence organism homeostasis.

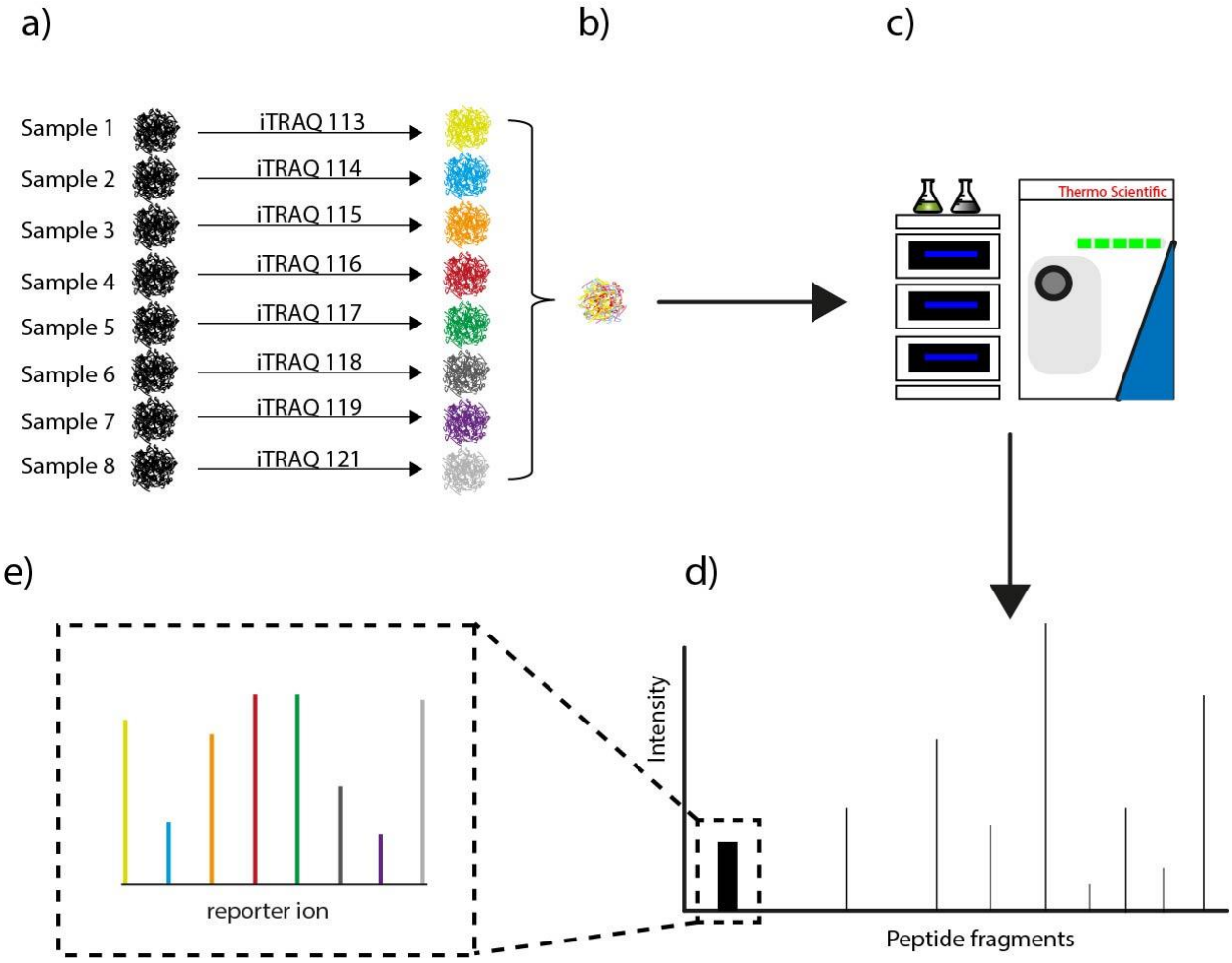

Figure 9. Isobaric label workflow. The same protocol is adopted for TMT. a) Digested peptides from 8 different samples are individually iTRAQ labeled and (b) pooled in a ratio of 1:1. c) The pooled sample is separated and measured by the LC/MS system. Since the peptides from the 8 different samples possess the same mass and physico-chemical properties, they elute together and are isolated together for MS^2 fragmentation. d) The spectrum of those peptides contain a region for peptide amino acid structure identification and a region containing the iTRAQ reporter ion (dashed line). e) Zoom in of the iTRAQ reporter ions. Signal intensity from the different reporter ions are used for peptide/protein relative quantification. Figure based on the workflow presented in the ThermoFisher website [157].

5.10 Label free quantification

A straightforward quantification method, the label free is the choice for studies that want to avoid extra steps of sample processing, costs of the isobaric labels or the possibility of inefficient labeling that might occur with iTRAQ or TMT. Taking into consideration the Figure 9, label free protocol consists in, after samples digestions, individual measurement of all samples. Instead of pooling eight samples and applying one single measurement, as with the isobaric labels, for label free would be necessary the measurement of each individual condition. In ideal conditions, the same peptide would elute at the same retention time in every MS measurement. The peak area from the peptide, which is directly proportional to the abundance of the analyte, would be compared between all runs, and the ion abundance of all peptides from a single protein would allow protein quantification between the samples [115].

Label free quantification takes longer MS measuring time when compared to chemical labeling. It is as well rely on highly reproducible liquid chromatography separation and mass spectrometry accuracy, once stable retention time is a vital factor for successful quantification. Measurement of the same sample amount between samples is as well highly important. In addition, off-line fractionation methods and enrichment of PTMs often have less reliable protein/PTM quantification than chemical labeling, since is harder to achieve reproducibility of samples manipulated in different times. However, computational software available, as Progenesis QI (Nonlinear Dynamics), automatically align retention times from the different runs and consider mass accuracy, performing peak abundance normalization, may reduce the problems state before.

6 Objective

The objective of this work was to characterize signaling networks in yeast mitochondria.

For this, the work was divided in two fronts:

1. The proteome of a yeast cell line with a mutation in the gene encoding MAS1 was quantitatively compared with a yeast wild type. Since around 99% of the mitochondrial proteins are imported from the cytosol, the MPP is responsible for a maturation process by enzymatic cleavage of proteins designated to the matrix and inner membrane. The impairment of the MAS1 could lead to a whole non-functional MPP and thus non-maturation of newly imported proteins. The comparison between the mutant yeast and wild type yeast in terms of protein quantification could elucidate by direct observation protein localization inside the mitochondrion. Also, alterations in the phosphoproteome could give hints about phosphorylation cascades related to the protein import.
2. Development of new techniques to increase (phospho)proteome coverage, giving a better overview of the sample. First, a broad-specificity enzyme was chosen due to lack of limitations for digestion sites. This enzyme was characterized and evaluated in terms of compatibility with bottom-up experiments and techniques. Second, a more mild mitochondrial purification technique was compared to the current purification protocol in terms of phosphorylation recovery.

After development and validation of the new techniques, they would be put to practice to boost mitochondrial signaling studies by increasing (phospho)proteome coverage.

7 Material and Methods

Chemicals and reagents

Chemical/Reagent	Purity	Abbreviation	Manufacturer
84 % Acetonitrile, 0.1 % FA	UPLC-grade	-	Biosolve BV, (Volkenwaard, The Netherlands - NL)
Acetonitrile	LC-grade	ACN	Biosolve BV, (Volkenwaard, NL)
Ammonium bicarbonate	≥ 99,5 %	ABC	Sigma Aldrich (Steinheim, Germany - G)
BCA assay	-	-	Pierce Thermo Scientific (Bremen, G)
Benzonase	> 90 %	-	Merck (Darmstadt, G)
Calcium Chloride	≥ 98 %	$CaCl_2$	Merck (Darmstadt, G)
complete Mini EDTA free	-	-	Roche Diagnostics (Mannheim, G)
Dithiothreitol	≥ 97 %	DTT	Roche Diagnostics (Mannheim, G)
Ethanol	≥ 99,9 %,	EtOH	Merck (Darmstadt, G)
Ethylene Diamine Triacetic Acid	pure	EDTA	Merck (Darmstadt, G)
Formic Acid	99% ULC/MS	FA	Biosolve BV, (Volkenwaard, NL)
Guanidine Hydrochloride	≥ 99 %	GuHCl	Sigma Aldrich (Steinheim, G)
Iodoacetamide	≥ 99 %	IAA	Sigma Aldrich (Steinheim, G)
Magnesium Chloride	≥ 98 %	$MgCl_2$	Sigma Aldrich (Steinheim, G)
PhosSTOP	-	-	Roche Diagnostics (Mannheim, G)
Potassium Chloride	Suprapur	KCl	Merck (Darmstadt, G)
Sodium Chloride	Suprapur	NaCl	Merck (Darmstadt, G)
Sodium dodecyl sulfate	≥ 99 %	SDS	AppliChem (Darmstadt, G)
Sodium Hydrogen Phosphate	99,95%	Na_2HPO_4	Sigma Aldrich (Steinheim, G)
Subtilisin P5380	-	-	Sigma Aldrich (Steinheim, G)
Trifluoroacetic acid	ULC/MS	TFA	Biosolve BV, (Volkenwaard, NL)
Tris(hydroxymethyl)-aminomethane	≥ 99,9 %	Tris	Applichem (Darmstadt, G)
Trypsin T1426	> 90 %	-	Sigma Aldrich (Steinheim, G)
iTRAQ 8plex	-	iTRAQ	Sciex (Darmstadt, G)
TMT 10plex	-	TMT	Thermo Scientific (Bremen, G)
Triethylammonium bicarbonate	-	TEAB	Sigma Aldrich (Steinheim, G)
Methylphosphonic acid	98%	-	Sigma Aldrich (Steinheim, G)
Potassium phosphate monobasic	≥ 99 %	KH_2PO_4	Sigma Aldrich (Steinheim, G)
Ammoniun hydroxide	puriss. p.a., 25%	-	Sigma Aldrich (Steinheim, G)
Dulbecco's Modified Eagle's medium	-	DMEM	Sigma Aldrich (Steinheim, G)
Fetal Bovine Serum	-	FCS	Sigma Aldrich (Steinheim, G)

Instruments and components

Instrument/Components	Manufacturer
ZORBAX 300SB-C18 column , 1 mm × 150 mm, pore size 300 A, 5 µm particle size	Agilent Technologies (Böblingen, G)
PolyWAX column, 4.6 mm x 100 mm, 300 A pore size, 5 µm particles	PolyLC INC (Columbia, USA)
Hypersep POROS SCX 10-200 mL cartridges	Thermo Scientific (Bremen, G)
POLYSULFOETHYL A column, 1 mm x 150 mm, 5 µm particle size, 200 Å pore size)	PolyLC INC (Columbia, USA)
SPEC C18 AR Tips - 4 mg, 15 mg	Agilent Technologies (Böblingen, G)
Acclaim PepMap-HPLC trap column, 2 cm x 100 µm, 2 µm particle size, 100 Å pore size	Thermo Scientific (Bremen, G)
Acclaim PepMap-HPLC main column, 50 cm x 75 µm, 2 µm particle size, 100 Å pore size	Thermo Scientific (Bremen, G)
LTQ-Orbitrap Velos Pro	Thermo Scientific (Bremen, G)
Q-Exactive HF	Thermo Scientific (Bremen, G)
Orbitrap Fusion Lumos	Thermo Scientific (Bremen, G)
C18 3M Empore™ SPE Extraction Disks	3M Bioanalytical Tech. (St. Paul, USA)
Oligo R3 Bulk Media	Applied Biosystems (Darmstadt, G)
UltiMate 3000 RSLCnano HPLC System	Thermo Scientific (Bremen, G)
5417R Refrigerated Centrifuge	Eppendorf (Hamburg, G)
Thermomixer comfort (0.5 mL, 1.5 mL, 2.0 mL)	Eppendorf (Hamburg, G)
UltiMate 3000 HPLC System	Thermo Scientific (Bremen, G)
Titansphere™ TiO Bulk Material, 5 µm particle size	GL Sciences Inc (Tokyo, Japan)
TSKgel Amide-80 Bulk Material	Tosoh Bioscience (Tokyo, Japan)
Vortex-Genie 2	Scientific Industrie (NY, USA)
0.5/1.5/2.0/5.0 mL LoBind Eppendor tubes	Eppendorf (Hamburg, G)
0.5/1.5/2.0 mL Safelock Eppendorf tubes	Eppendorf (Hamburg, G)
0.1-2.5 µL, 0.5-10 µL, 1-20 µL, 10-100 µL, 20-200 µL, 100-1000 µL Pipettes	Eppendorf (Hamburg, G)

7.1 MAS1 experiments

7.1.1 MAS1 mutant cultivation

The working group of Prof. Dr. Chris Meisinger and Dr. Nora Voegtle, Faculty of Biochemistry, University of Freiburg, Germany, offered the MAS1 temperature sensitive yeast cells and yeast mitochondria.

Yeast mitochondria purification protocol is based on Meisinger et al[158]. The protocol described below was applied for 3 biological replicates sets of 6 samples (wild type 0 h, 2 h and 4 h; MAS1 mutant 0 h, 2 h and 4 h), in which 0 h samples were grown always at 22 °C (permissive conditions),

while 2 h and 4h were temperature shifted to 37 °C (non-permissive conditions). Permissive conditions allow the normal translation of the MAS1 gene, while, during non-permissive conditions, the translation of the MAS1 gene is impaired.

MAS1 mutant strain (Matα, ura3-52, trp1-1, leu2-3, leu2-112, his3-11, his3-15)[159] and wild type (strain YPH499) were cultivated overnight in respiratory (YPG) medium (1% w/v yeast extract, 2% w/v bacto peptone, and 3% w/v glycerol (pH 5.0)) at 22 °C (permissive condition) with gentle shaking (130 rpm). After reaching a cell density of 1-3 OD_{600nm}, the culture was divided in two aliquots, in which half of the cells were shifted to 37 °C (non-permissive condition) while the other half was kept at 22 °C. At the time points 0, 2 and 4 h after the temperature shift, aliquots from each condition (22 and 37 °C) were removed and cells were pelleted by centrifugation at 3,000 x *g* for 5 min. Pellet was resuspended in homogenization buffer (10 mM Tris-HCl, pH 7.4, 0.6 M sorbitol, 0.2% (w/v) bovine serum albumin, 1 mM phenylmethylsulfonyl fluoride and 1 mM ethylenediaminetetraacetic acid. Homogenization was performed at 4 °C, using 15 stokes of a glass teflon homogenizer to homogenize the sample. The homogenate was centrifuged for 5 min at 1,500 x *g* to pellet cell parts, as nuclei and cell debris. The supernatant was collected and isolated mitochondria was obtained by an extra centrifugation step at 12,000 x *g* for 15 min. The pellet containing mitochondria was resupended in SEM buffer (250 mM sucrose, 1 mM EDTA, 10 mM MOPS-KOH, pH 7.2).

A second purification to remove contaminants such as vacuoles or endoplasmic reticulum was performed using a four-step sucrose density gradient centrifugation. A centrifuge tube was mounted pipetting 1.5 mL of a 60% sucrose solution to the bottom. New layers of 4 mL 32% sucrose, 1.5 mL 23% sucrose and 1.5 mL 15% sucrose were added on top of the bottom layer. Pre purified mitochondria was centrifuged for 1.5 h at 134,000 x *g*, and a highly purity mitochondria fraction was obtained between 32% and 60% sucrose, which was carefully removed, diluted with SEM buffer and centrifuged for 30 min at 10,000 x *g*.

7.1.2 Sample preparation for ChaFRADIC

Protocol was based on the one published by Venne et al [151]and described here. For each batch from the yeast and yeast mitochondria, samples were resuspended in 150 mM sodium chloride (NaCl), 1% (w/v) sodium dodecyl sulfate (SDS), and 50 mM Tris-Cl (pH 7.8), plus Complete Mini and PhosSTOP (Roche, Switzerland) as a protease and phosphatase inhibitor cocktail, respectively. Only the yeast lysate was incubated with 5 µL benzonase nuclease (25 units/µL) (Merck, Germany), to

reduce sample viscosity, for 30 min at 37 °C, followed by centrifugation at 18,000 x *g* for 30 min at 4 °C. The pellet was discarded. Bicinchoninic acid assay (BCA) was performed for all samples to verify protein concentrations. Samples were carbamidomethylated with dithiothreitol (DTT) 10 mM to reduce cysteines bonds for 30 min at 56 °C and iodoacetamide (IAA) 30 mM for alkylation for 20 min at room temperature in the dark. Afterwards, 100 µg of each sample was protein precipitated with 10-fold diluted with -40 °C ethanol and incubated for 1 h at -40 °C. Samples were then centrifuged at 18,000 x *g* for 30 min at 4 °C and the supernatant discarded. Pellets were resuspended in 10 µL 10 % SDS, and diluted with 40 µL of 0.5 M triethylammonium bicarbonate (TEAB), 20% (v/v) isopropanol to a final 2% SDS concentration. Each one of the six samples from each batch were iTRAQ 8plex labeled (Sciex, Germany), adding 80 µL isopropanol to the each iTRAQ channel and transferring individually to each sample. One iTRAQ set was used per sample batch, i.e. from the 8 possible iTRAQ channels (113:114:115:116:117:118:119:121), only 6 were used per batch, using a new iTRAQ set for the next sample batch. iTRAQ incubation took 2 h at room temperature (RT). Labeling reaction was stopped with 60 mM glycine for 10 min (RT), followed by addition of 130 mM hydroxylamine for extra 10 min at RT. Labeled samples had N-termini and lysines blocked with the iTRAQ reagent. Samples from each batch were pooled together and protein precipitated as described above. Pooled samples were resuspended in 6 M guanidine hydrochloride (GuHCl), diluted 30 fold with 200 mM TEAB, pH 8.0. Samples were individually digested with trypsin (Sigma Aldrich, Germany), digestion ratio of 20:1 (sample:enzyme), addition of 2 mM calcium chloride ($CaCl_2$, final concentration), incubation at 37 °C overnight. Samples were desalted using SPEC Pt C18AR (Agilent, Germany). SPEC tips were activated with 100 µL ACN (high organic solvent), equilibrated twice with 100 µL 0.1% triflouracetic acid (TFA) to , samples was loaded twice into the tip, washed twice with 0.1% TFA and finally eluted twice with 50 µL 70% ACN, 0.1%.TFA. An aliquot of 1 µg of each eluate were separated for future LC/MS analysis to determine possible iTRAQ correction ratios and labeling efficiency. The eluates were then dried under vacuum.

7.1.3 ChaFRADIC

The steps described below were performed for each pooled sample individually. Dried samples were resolubilized in 150 µL 10 mM KH_2PO_4, 20% ACN, pH 2.7 (SCX A). One third (50 µL) were injected in an Ultimate 3000 HPLC system (Thermo Scientific, Germany), mounted with a 150 x 1 mm POLYSULFOETHYL A column (PolyLC, Columbia, US, 5 µm particle size, 200 Å pore size). Sample was fractionated using a 3 buffer system, SCX A (10 mM KH_2PO_4, 20% ACN, pH 2.7), SCX B (10 mM

KH_2PO_4, 250 mM KCl, 20% ACN, pH 2.7) and SCX C (10 mM KH_2PO_4, 600 mM NaCl, 20% ACN, pH 2.7) (pH adjusted with the addition of pure phosphoric acid), at a flow rate of 80 µL/min. Buffer composition during fractionation is summarized in Table 1 Buffer composition was optimal for separation peptide by charge state, and a total of 13 fractions were automatically collected using the fractionation option available for the HPLC. Fraction collection is summarized in Table 21 and time points were optimized previously[151].

Table 1 . Buffer composition during SCX fractionation from the ChaFRADIC samples.

	SCX buffer in %		
Min	A	B	C
0	100	0	0
10	100	0	0
19.7	85	15	0
25	85	15	0
33	70	30	0
44	70	30	0
49	0	100	0
53	0	100	0
54	0	0	100
59	0	0	100
60	100	0	0
80	100	0	0

Table 2 . Fractions collected during SCX fractionation of the ChaFRADIC samples

Fraction	Collection period (min)
1	1.0 - 1.8
2	1.8 - 2.8
3	2.8 - 9.0
4	9.0 - 11.0
5	11.0 - 14.5
6	14.5 - 16.0
7	16.0 - 32.0
8	32.0 - 34.0
9	34.0 - 36.0
10	36.0 - 49.0
11	49.0 - 51.0
12	51.0 - 53.0
13	53.0 - 65.5

From each fraction, 5 µL were measured by liquid chromatography coupled with mass spectrometry (LC/MS). Separation was perfomerd by liquid chromatography (LC) using a trap column (100 µm × 2 cm C18 Acclaim Pepmap, Thermo Fischer, Germany) and a main column (75 µm × 50 cm C18 Acclaim Pepmap, Thermo Fisher). Samples were pre-concentrated on the trap column in 0.1% TFA for 5 min at a flow rate of 20 µL/min followed by separation on the main column at a constant flow rate of 250 nL/min, starting with 97% buffer A, 0.1 % formic acid (FA), ranging from 3-45% buffer B, 0.1% FA and 84% acetonitrile (ACN), in 55 min. Mass spectrometer acquisition was performed in an Orbitrap Velos Pro (Thermo Fisher, Germany), with the following parameters: MS survey scans were acquired in the Orbitrap between 300-1500 m/z, resolution of 60,000, using a lock mass of 371.1012. MS/MS scans were acquired in the ion trap, using Top 10 mode, with an injection time of 150 ms,

collision energy set to 35, isolation window of 1 m/z, dynamic exclusion of 30 s and using CID activation.

Data analysis of the MS raw files was performed using Proteome Discoverer 1.4 (Thermo Scientific), samples searched against Saccharomyces Genome Database (SGD) downloaded in September 2011 using Mascot 2.4. Samples were filtered to 1 % FDR at the peptide level performed by the software percolator 3.048[160]. Search parameter were: enzyme "trypsin", 2 missed cleavages, MS and MS/MS scans were set with 10 ppm and 0.5 Da mass tolerance, respectively. Carbamidomethylation of Cys (+57.0215 Da) and oxidation of Met (+15.9949 Da) were set as fixed and variable modification, respectively.

Identified peptides were evaluated for net charge. Total net charge was the sum of all lysines, arginines and histidines contained in the peptide backbone. Fractions with similar amount of peptides with the same net charge were combined. For the yeast samples, fraction 1 was discarded and combined fractions were 2 and 3, 4 to 7, 8 to 10, 11 and 12, 13 alone. For the mitochondrial samples, fractions 1 and 2 were discarded and combined fractions were: 3 alone, 4 to 6, 7 alone, 8 and 9, 10 alone, 11 and 12, 13 alone.

Combined fractions were desalted as described in chapter 7.1.2, resuspended in 200 µL of 200 mM Na_2HPO_4, pH 8.0. Final sample pH was around pH 7. Samples were incubated with 20 mM d3-NHS (final concentration) for 1 h at 37 °C, follow by a second incubation with 10 mM NHS trideutero acetate (final concentration) for 1 h at 37 °C. This step was necessary to derivatize new N-termini generated after digestion with trypsin. Derivatization reaction was stopped with addition of 60 mM glycine for 10 min (RT), followed by heat incubation at 95 °C for 5 min. Samples were acidified adding triflouracetic acid to a final concentration of 10% and desalted as described in chapter 7.1.2. Combined fractions were resuspended in 50 µL SCX A and followed a 2^{nd} SCX dimension fractionation, following the same parameters for the 1^{st} fractionation. Derivatized N-terminal peptides loose at least 1 charge state of their net charge, shifting elution position during the SCX gradient, while non derivitazed peptides (original protein N-terminal) remain with the same charge state. In that sense, all fractions beside the ones of interest were discarded, i.e. yeast combined fractions 2 and 3, for instance, were re-injected for the 2^{nd} SCX dimension, and from the new 13 generated fractions, only fractions 2 and 3 were kept and again combined. All combined fractions were once again desalted, dried, resuspended in 22 µL 0.1% TFA and 2/3 measured by LC/MS.

LC was performed as described previously in this chapter, but with a longer gradient of 90 min per sample. MS was performed in data dependent acquisition (DDA) in an Orbitrap Fusion Lumos

(Thermo Scientific), positive mode, with specific parameters summarized in Table 3. For charge state reduction, a solution of 10% NH_4OH was placed near the ion source, as suggested by Thingholm et al[161].

Table 3.ChaFRADIC MS parameters.

	Full MS	MS/MS		
		iTRAQ quantification	Peptide measurement	
Charge	All charges	All charges	+1 to +3	+4 to +8
m/z scan range	300-1500	-	-	-
First mass (m/z)	-	90	120	120
Resolution	120000	15000	-	-
Injection time (ms)	50	100	300	100
AGC	$2x10^5$	$1x10^5$	$2x10^3$	$1x10^4$
Mode	-	TopS 3s	TopS 3s	TopS 3s
Activation	-	HCD	HCD	EThcD
Collision energy	-	60%	35%	30 % HCD
Isolation window (m/z)	-	1.0	1.0	1.0
Acquisition	Orbitrap	Orbitrap	ion trap	ion trap

Data analysis of the MS raw files was performed using Proteome Discoverer 1.4 (Thermo Scientific) (Table 4), samples searched against Saccharomyces Genome Database (SGD) downloaded in September 2011 using Mascot 2.4. Samples were filtered to 1% FDR using percolator 3.048. A two-search strategy was performed and results later combined.

Since there is the possibility of endogenous protein N-terminal acetylation, one single search was focused to identify acetylated peptides. Identical peptide spectral matches (PSMs) had their iTRAQ reporter ion areas averaged. The normalization factors descendant from the global analysis corrected all PSMs' iTRAQ reporter ion areas in order to compensate possible different sample amount pooling after iTRAQ labeling.

Table 4. Proteome Discoverer 1.4[1,2] search parameters.

	Tolerances		**Modifications**	
	MS1	**MS2**	**Fixed**	**Variable**
N-termini iTRAQ	10 ppm	0.5 Da	Carbamidomethyl (C), iTRAQ8plex (N-term, K)	Oxidation (M), iTRAQ8plex (Y)
N-termini acetylation	10 ppm	0.5 Da	Carbamidomethyl (C), iTRAQ8plex (K), Acetyl (N-term)	Oxidation (M), iTRAQ8plex (Y)

1 - Trypsin: maximum of 2 missed cleavages

2 - Carbamidomethyl (C) (+57.0215 Da), iTRAQ8plex (+304.2054 Da), Oxidation (M) (+15.9949 Da), Acetylation (acetyl, + 42.0105 Da)

ChaFRADIC workflow is summarized in Figure 10. ChaFRADIC of the mitochondrial samples only differ in combination of samples pooled together after first SCX fractionation.

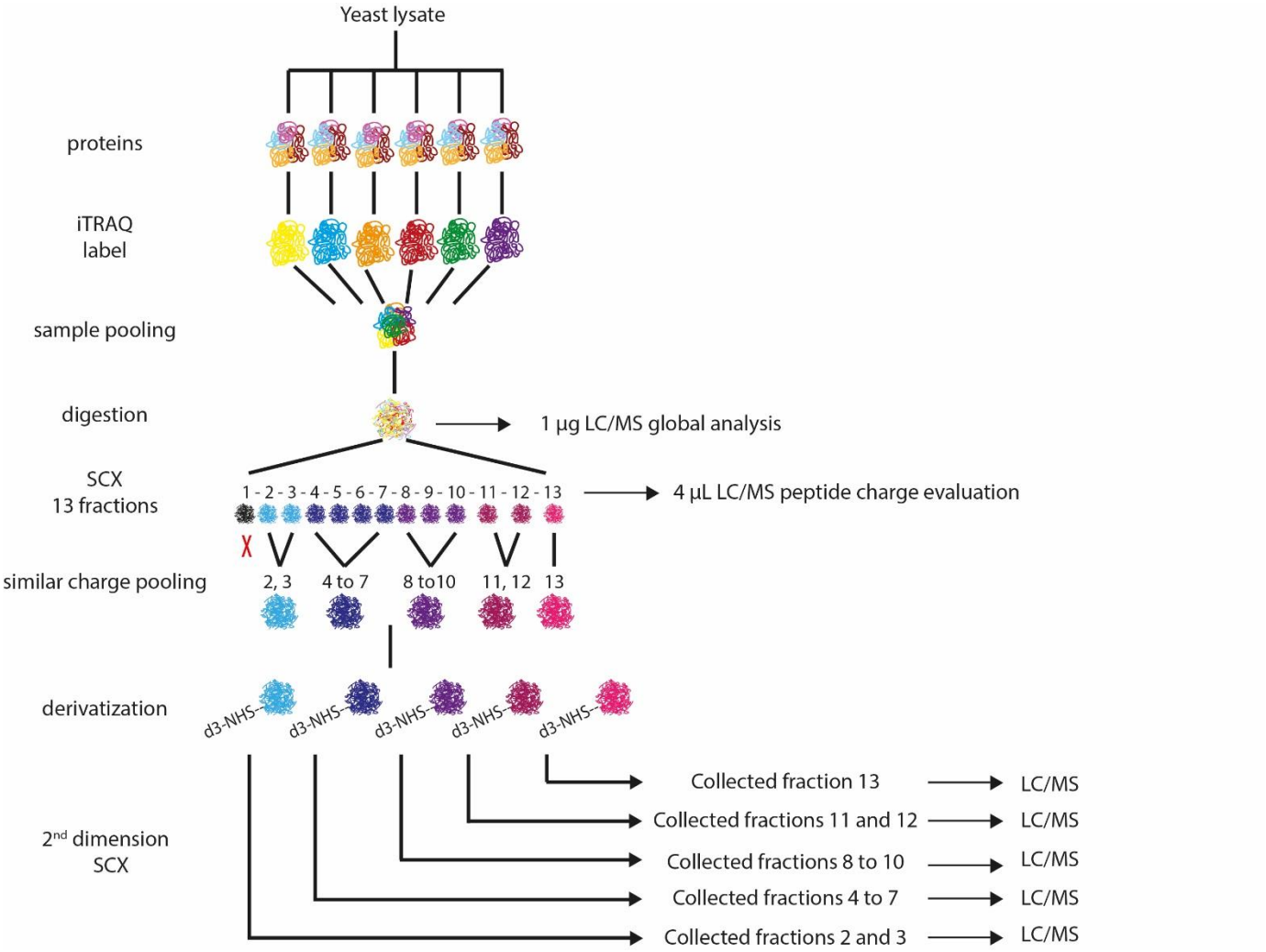

Figure 10. ChaFRADIC simplified workflow from yeast biological replicates. Proteins from the different conditions of the batch are iTRAQ labeled, pooled together in a ratio of 1:1, digested with trypsin, strong cationic exchange (SCX) fractionated in 13 fractions. A part of each fraction is measured by liquid chromatography coupled with mass spectrometry (LC/MS) to evaluate peptide charge state. Samples with the majority of the peptides with similar charge state were pooled together, derivatized with NHS trideutero acetate (d3-NHS), followed by a second SCX fractionation of each pooled sample. Same fractions per pooled samples were collected back together and measured by LC/MS.

7.1.4 ChaFRADIC sample normalization abundance and statistics

As indicated in Figure 10, 1 µg of sample was separated for global analysis. This step is important to correct iTRAQ ratio distortion inherent from wrong pipetting or due to imprecise protein

concentration done by BCA assay. Since it is expected that only a small group of proteins are significantly up or down regulated, the general trend of ratios between iTRAQ reporter ions should be 1:1 (the majority of proteins keep the same abundance in every sample).

Only peptides with values for all used iTRAQ channels were considerate. First, a sum of all intensities from each individual iTRAQ channel was performed. Secondly, a median of the sums (MD1) OF the iTRAQ channels was performed. Later, each iTRAQ channel sum was divided by the MD1, creating the normalization factors (NF) for each channel. This procedure was performed for each batch.

After creating the NF with the sample for global analysis, this was applied to normalize the values of the fractions of the 2nd SCX dimension. Only peptide spectral matches (PSMs) with all used iTRAQ channels were considerate. To generate normalized values, the corresponding NF from the global analysis divided the corresponding channel, e.g. NF 113 divided the intensity value of the iTRAQ channel 126 of each PSM. Individually for each PSM, a median (MS3) was taken across the 6 iTRAQ channels. The MS3 divided each normalized value per PSM (all 6 channels individually), creating normalized abundance values (NAVs) for the ChaFRADIC data.

This procedure was performed as well for each batch with the corresponding NF per batch. All 3 NAVs from each condition were averaged, e.g. the wild type 0 h NAV from batch 1, 2 and 3 were averaged. For each time point, average mutant values was divided by average wild type value, e.g. average mutant 0 h was divided by average wild type 0 h. A Student's T-test was performed for each time point comparison and the ratios between mutant and wild type for each time point were log2 transformed. Only phosphopeptides with a Student's T-test < 0.05 and -1 < log2 or log2 > 1 were considered as possibly regulated.

7.1.5 Sample preparation for phosphopeptide enrichment

Only the yeast mitochondria were selected for phosphospeptide enrichment. Samples were prepared as described in chapter 7.1.2 until carbamidomethylation. From each sample, 200 µg were diluted fold with -40 °C ethanol (previously incubated overnight at – 40 °C freezer) for 1 h, followed by centrifugation at 18,000 x *g* for 30 min at 4 °C. Supernatant was discarded and pellet was resuspended with 6 M GuHCl. Samples were diluted with 100 mM triethylammonium bicarbonate (TEAB), pH 8.0, until 0.2 M GuHCl, supplemented with 2 mM $CaCl_2$ (final concentration) and incubated overnight with trypsin in a ratio of 20:1 (sample:trypsin). Digestion reaction was quenched adding TFA to final concentration of 1% and dried under vacuum. Samples were resuspended in 100 µL 100 mM TEAB, pH 8.0, and incubated with 0.8 mg TMT 10plex (Thermo

Scientific) for 1 h at 25 °C. TMT aliquots were previously prepared by adding to each channel 41 µL acetonitrile (ACN) as described by the manufacture's protocol. Each mitochondrial batch used one single set of the TMT 10plex, i.e. from the 6 mitochondrial samples per batch, each used one of the 10 TMT channels available per set, and each batch used one TMT 10plex set. Reaction was quenched with 8 µL of 5% hydroxylamine and incubate for 15 minutes. For each batch, TMT labeled samples were pooled together in a ratio of 1:1 (sample concentration determined previously by BCA assay) and desalted as described in chapter 7.1.2. After desalting, 25 µg of each sample was separated for global analysis.

7.1.6 Global analysis of the mitochondrial proteome and statatistics

The 25 µg aliquots separated in chapter 7.1.5 were dried under vacuum. Samples were resuspended in 15 µL of 10 mM ammonium acetate, pH 8.0 (buffer A) and fractionated on an Ultimate 3000 LC (Thermo Scientific). Peptides were fractionated on a 1 mm × 150 mm C18 (ZORBAX 300SB-C18, pore size 300 A, 5 µm particle size, Agilent Technologies) column with a 45 min LC gradient ranging from 3 to 45% buffer B (84% ACN in 10 mM ammonium acetate, pH 8.0) at a flow rate of 12.5 µL/min. After fractionation, 16 fractions were collected in concatenated manner using 60 s intervals, starting again with the first fraction after 16 min. Fractions were dried under vacuum and resuspended in 15 µL of 0.1% TFA for LC/MS analysis.

LC was performed as described in chapter 7.1.3 for the second dimension ChaFRADIC. MS was performed in data dependent acquisition (DDA) in a QExactive HF (Thermo Scientific) with the parameters summarized in Table 5. Differences between resolution, automatic gain control (AGC) and collision energy are due to previous maximum peptide identification optimization performed in-house for different sample types. For instance, to identify as much as possible peptides with high confidence site location, it is necessary to use lower collision energy than for not phosphopeptide enriched samples.

Data analysis of the MS raw files was performed using Proteome Discoverer 1.4 (Thermo Scientific), samples searched against Saccharomyces Genome Database (SGD) downloaded in September 2011 using Mascot 2.4. Samples were filtered to 1 % FDR using the percolator 3.048 software. Other parameters details are summarized in Table 6. After database search, Proteome Discoverer provides, at the protein level, 5 TMT channels divided by one single fixed channel. Based on Kollipara et al[162] for statistics applied to isobaric labels, the ratios were transformed into normalized

abundance values (NAVs). For that, first, a hypothetical ratio for channel 126/126 was created to generate 6 data points per protein (e.g. 126/126, 127N/126, 127C/126, 128N/126, 128C/126, 129N/126), followed by log2 transformation of each ratio comparison. A median of all values of each ratio was taken (e.g. a median was taken from all TMT values from all proteins of the ratio comparison 127N/126), generating an median value (MV1) per ratio comparison. Then a median of all MV1s from the ratio comparisons were taken, generating an overall median (MV2). Each AV1 was later subtracted with the AV2 to generate the normalization factors (NF) of each TMT channel. Later, NFs values subtracted the respective log 2 transformed ratio comparison of each protein to obtain the normalized ratios (e.g. NF 126/126 subtracted the log2 transformed value of the 126/126 ratio comparison for each protein). To finalize, individually for each protein, a third median (MV3) was taken across the 6 ratio comparisons. The MV3 subtracted each normalized ratio per protein (all 6 channels individually), log 2 transformed values were transformed again in decimal values, finally reaching the NAVs.

This procedure was performed for each batch. Then all 3 NAVs from each condition were averaged, e.g. the wild type 0 h NAV from batch 1, 2 and 3 were averaged. For each time point, average mutant values was divided by average wild type value, e.g. average mutant 0 h was divided by average wild type 0 h. A Student's T-test was performed for each time point comparison and the ratios between mutant and wild type for each time point were log2 transformed. Only proteins with a Student's T-test < 0.05 and -1 < log2 or log2 > 1 were considered as possibly regulated.

Table 5. Global analysis and MAS1 phosphoproteome mass spectrometer parameters.

Experiment	Full MS							MS/MS								
	Instrument	Mass analyzer	m/z	Resolution	AGC	Injection time (ms)	Lock mass	Mass analyzer	Mode	Resolution	AGC	Injection time (ms)	Collision energy	Isolation window (m/z)	Dynamic Exclusion (s)	Activation
High pH reversed phase fractionation	QExactiveHF	Orbitrap	300-1500	60000	$1x10^6$	120	371,1012	Orbitrap	DDA - Top15	60000	$5x10^4$	200	30	1	30	HCD
Mas1 phosphoproteome	QExactiveHF	Orbitrap	300-1500	60000	$1x10^6$	120	371,1012	Orbitrap	DDA - Top15	15000	$2x10^5$	200	27	1	30	HCD

Table 6.Proteome Discoverer 1.4[1,2] parameters.

Experiment	Tolerances		Modifications	
	MS1	MS2	Fixed	Variable
High pH reversed phase fractionation	10 ppm	0.02 Da	Carbamidomethyl (C), TMT 10plex (N-term, K)	Oxidation (M)
Mas1 phosphoproteome	10 ppm	0.02 Da	Carbamidomethyl (C), TMT 10plex (N-term, K)	Oxidation (M), Phosphorylation (Y,S,T)

1 - Trypsin: maximum of 2 missed cleavages

2 - Carbamidomethyl (C) (+57.0215 Da), TMT 10plex (+229.2634 Da), Oxidation (M) (+15.9949 Da), Phosphorylation (Y,S,T) (+79.9663 Da)

7.1.7 Phosphopeptide enrichment

The yeast mitochondrial samples were, after TMT labeling, dried under vacuum and then were resolubilized in 1 mL of 80% ACN, 5% TFA and 1 M glycolic acid (buffer 1) and individually subjected to phosphopeptide enrichment using titanium dioxide (TiO_2, Titansphere TiO, 5 µm particle size, GL Sciences Inc, Japan), according to Engholm-Keller et al [163] with slight modifications. First, (1) TiO_2 beads (6:1, TiO_2:peptide (w:w)) were added to the sample, incubated for 10 min on a shaker at room temperature. The sample was centrifuged for 30 s at 3,000 x *g*. (2) The supernatant was cautiously transferred to a 2nd eppendorf tube already containing TiO_2 beads (3:1), once more incubated and centrifuged as described in step 1. (3) The supernatant was then transferred to a 3rd tube already containing TiO_2 beads (1.5:1), incubated and centrifuged as shown in step 1. The supernatant was discarded, 100 µL buffer 1 was added to the 3rd tube and the TiO_2-slurry beads were transferred to the 2nd tube, mixed and transferred to the 1st tube, mixed and transferred to a fresh eppendorf tube. The sample with the TiO_2 slurry was centrifuged as in step 1 and the supernatant was discarded. Next, to the beads were added 100 µL buffer 2 (80% ACN, 1% TFA), sample was mixed for 15 s, centrifuged as in step 1 and the solution was discarded, followed by another wash step with buffer 3 (10% ACN, 0.1% TFA). The washing steps helps removing loosely bound peptides, which probably do not contain phosphorylation. The TiO_2 slurry beads were dried for 10 min under vacuum, followed by incubation with 100 µL of 1% (v/v) ammonium hydroxide (elution buffer), pH 11.3, for 10 min on a shaker at room temperature to dissociate phosphopeptides from the beads. Later, the TiO_2 beads were pelleted by centrifugation at 3,000 x *g* for 30 s, the eluate was carefully removed to avoid TiO_2 beads and acidified with 8 µL of 100% formic acid (FA) and 2 µL of 10% TFA to guarantee proper acidification and to avoid beta elimination. Another 30 µL of elution buffer were added to the beads, mixed for 15 s, centrifuged as before and the eluates were pooled. Samples were desalted with self-made stage tips, based on the protocol of Rappsilber et al [164] using C18 3M Empore™ SPE Extraction Disks (Sigma-Aldrich) and 30 µg OLIGO™ R3 Reversed-Phase resin (Applied Biosystems). Sample desalting was conducted as described in chapter 7.1.2, but elution was performed with 47 µL 98% ACN, 0.1% TFA (HILIC buffer A). HILIC fractionation was performed on an Ultimate 3000 RSLC (Thermo Scientific) using a 250 µm x 15 cm TSKgel Amide-80 (Tosoh Bioscience, Japan) column. After injection, the sample was loaded for 20 min at a constant flow of 3 µL/min with 1% buffer B (0.1% TFA). In 2.5 min, B was increased to 10%, followed by an increase to 35% B in 40 min while concurrently decreasing the flow rate from 3.0 to 2.5 µL/min to avoid column overpressure with higher concentrations of water. Next, HILIC

buffer B was increased to 80% in 5 min. A total of 12 fractions were collected per enzyme. Each fraction was dried under vacuum and re-suspended in 15 µL of 0.1% TFA for LC/MS analysis.

LC, MS and data analysis were performed as described in chapter 7.1.3. MS and Proteome Discoverer parameters are described in Table 5 and Table 6. For the data analysis, only peptide spectral matches (PSMs) containing phosphorylation site location > 99 % and all TMT channels present were considered. As considered in chapter 7.1.3, it was necessary to correct value distortions. Each PSM contained an intensity value for each of the 6 used TMT channels. To generate normalized values, the corresponding NF from the global analysis divided the corresponding channel, e.g. NF 126/126 (previously decimal transformed) divided the intensity value of the TMT channel 126 of each PSM. Individually for each PSM, a median (MS3) was taken across the 6 TMT channels. The MS3 divided each normalized value per PSM (all 6 channels individually), finally reaching the NAVs for the phosphopeptide data.

This procedure was performed for each batch. Then all 3 NAVs from each condition were averaged, e.g. the wild type 0 h NAV from batch 1, 2 and 3 were averaged. For each time point, average mutant values was divided by average wild type value, e.g. average mutant 0 h was divided by average wild type 0 h. A Student's T-test was performed for each time point comparison and the ratios between mutant and wild type for each time point were log2 transformed. Only phosphopeptides with a Student's T-test < 0.05 and -1 < log2 or log2 > 1 were considered as possibly regulated.

7.2 Subtilisin experiments

7.2.1 Cell culture

HeLa cells S2 (DSMZ, Germany) and A431 cells (DSMZ, Germany) were grown in 75 cm^2 cell culture flask in Dulbecco's Modified Eagle Medium (DMEM, PAN Biotech), containing 10% FCS (fetal calf serum), 1% (v/v) penicillin/streptomycin, at 37 °C in an atmosphere supplemented with 5% CO_2 to a final confluence of ~75%. The medium was removed and cells washed with 5 mL of phosphate saline buffer (PBS) with 137 mM NaCl, 2.7 mM KCl, 10 mM Na_2HPO_4, 2 mM KH_2PO_4. Cells were separated from the growing flask with 2 mL of 0.05% Trypsin, 0.02% ethylenediaminetetraacetic acid (EDTA) in PBS, incubated at 37 °C for 5 min. To inactivate trypsin, 8 mL of fresh medium were added, cells were as well resuspended and transferred to a falcon tube of 15 mL, spun down for 5 min at 300 x *g*. Later, cell pellet was again washed with the same PBS twice.

7.2.2 Subtilisin and trypsin efficiency under different digestion conditions

The HeLa S2 cell pellet was resuspended in 150 mM sodium chloride (NaCl), 1% (w/v) sodium dodecyl sulfate (SDS), and 50 mM Tris-Cl (pH 7.8), plus Complete Mini and PhosSTOP (Roche, Switzerland), a protease and phosphatase inhibitor cocktail, respectively. The lysate was then incubated with 5 µL benzonase nuclease (25 units/µL) (Merck, Germany), to reduce sample viscosity by degrading nucleic acid, for 30 min at 37 °C, followed by centrifugation at 18,000 x *g* for 30 min at 4 °C. The pellet was discarded. Bicinchoninic acid assay (BCA) (Thermo Scientific) was performed to verify protein concentrations. Dithiothreitol (DTT) 10 mM was used to reduce cysteines bonds for 30 min at 56 °C and iodoacetamide (IAA) 30 mM was used for alkylation for 20 min at room temperature in the dark. Sample was 10-fold diluted with -40 °C ethanol and incubated for 1 h at -40 °C for protein precipitation. Sample was then centrifuged at 18,000 x *g* for 30 min at 4 °C and the supernatant discarded. Sample was resuspended in 6 M guanidine hydrochloride (GuHCl), divided in aliquots containing each 10 µg of protein and diluted with 50 mM ammonium bicarbonate buffer (ABC), pH 7.8, to 0.2 M, 0.5 M, 1.0 M, 2.0 M and 4.0 M GuHCl in triplicates. All samples were equated with ABC buffer to keep constant volume. Samples were individually digested with trypsin (product number T1426, Sigma-Aldrich, Germany) or subtilisin (product number P5380, Sigma-Aldrich). Trypsin samples followed the protocol: digestion ratio 20:1 (sample:enzyme), addition of 2 mM calcium chloride ($CaCl_2$, final concentration) to improve enzyme stability[165], incubation at 37 °C overnight. Subtilisin samples followed the protocol: samples were pre-heated for 5 min at 56 °C, subtilisin was added in a ratio of 20:1 (sample:enzyme), incubated for 20 min at 56 °C. For both cases, digestion was stopped with 1% trifluoroacetic acid (TFA). Also, 0.2 M HeLa S2 aliquots were digested, in triplicate, using the subtilisin protocol, but with incubation times of 1, 5, 10 and 20 minutes (Figure 12).

All samples had 1 µg of the digest controlled in a monolithic column (chromatography parameters described below) for efficient digestion control, since this column may efficiently separate peptides and proteins, the firsts eluting earlier than the seconds. Also, 500 ng of the different subtilisin time points were measured by liquid chromatography coupled to the mass spectrometer (LC/MS) as described below. Extra 500 ng of the trypsin (0.2 M GuHCl) and subtilisin (0.2 M GuHCl, 20 min) samples were as well measured by LC/MS to evaluate enzyme reproducibility, as described below.

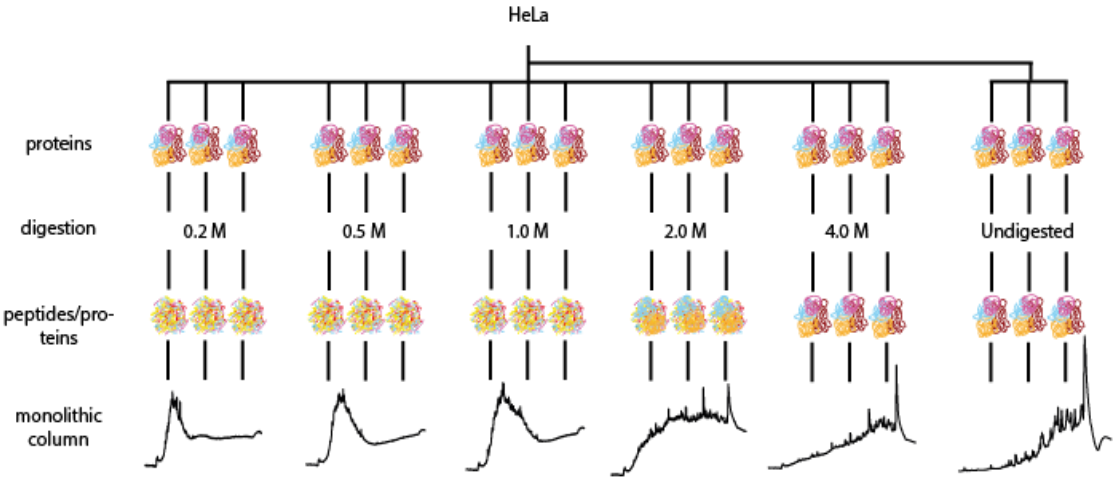

Figure 11. Evaluation of HeLa digested under different concentrations of guanidine hydrochloride (GuHCl). HeLa lysate was divided into different concentrations of GuHCl (0.2, 0.5, 1.0, 2.0 and 4.0 M GuHCl) and digested in triplicates by either trypsin or subtilisin. In addition, undigested HeLa was measured in a monolithic column as control. Depicted monolithic chromatograms represents HeLa

Digestion efficiency control was performed using a monolithic column (PepSwift monolithic PS-DVB PL-CAP200-PM, Dionex) coupled in a Ultimate 3000 HPLC (Dionex, Germany) by injecting 1 µg sample, using a binary gradient, starting with 95% buffer A (0.1% TFA), then increasing the gradient of buffer B (0.08% TFA, 84% acetonitrile) from 5% to 12% B in 5 min, follow by another increase from 12-50% B in 15 min. Flow rate was 2.2 µL/min and column oven set to 60 °C. UV traces were acquired at 214 nm.

Samples were separated and acquired in by LC/MS. Separation was done by liquid chromatography (LC) using a trap column (100 µm × 2 cm C18 Acclaim Pepmap, Thermo Fischer, Germany) and a main column (75 µm × 50 cm C18 Acclaim Pepmap, Thermo Fisher). Samples were pre-concentrated on the trap column in 0.1% TFA for 5 min at a flow rate of 20 µL/min followed by separation on the main column at a constant flow rate of 250 nL/min, starting with 3% buffer A, 0.1 % formic acid (FA), ranging from 3-45% buffer B, 0.1% FA and 84% acetonitrile (ACN), in 55 min. Mass spectrometer acquisition was done in an Orbitrap Velos Pro (Thermo Fisher), with the following parameters: MS survey scans were acquired in the Orbitrap between 300-1500 m/z, resolution of 60,000, using a lock mass of 371.1012. MS/MS scans were acquired in the ion trap, using Top 10 mode, with an injection time of 150 ms, collision energy set to 35, isolation window of 1 m/z, dynamic exclusion of 30 s and using CID activation.

Data analysis of the MS raw files was performed using Proteome Discoverer 2.2 (Thermo Scientific), samples searched against a human Uniprot database (20,194 target sequences, downloaded in September 2014,). Trypsin and subtilisin samples were searched using “trypsin” and “none” as enzyme, respectively. Trypsin samples allowed 2 missed cleavages and subtilisin

samples allowed zero miss cleavage. MS and MS/MS scans were set with 10 ppm and 0.5 Da mass tolerance, respectively. Carbamidomethylation of Cys (+57.0215 Da) and oxidation of Met (+15.9949 Da) were set as fixed and variable modifications, respectively.

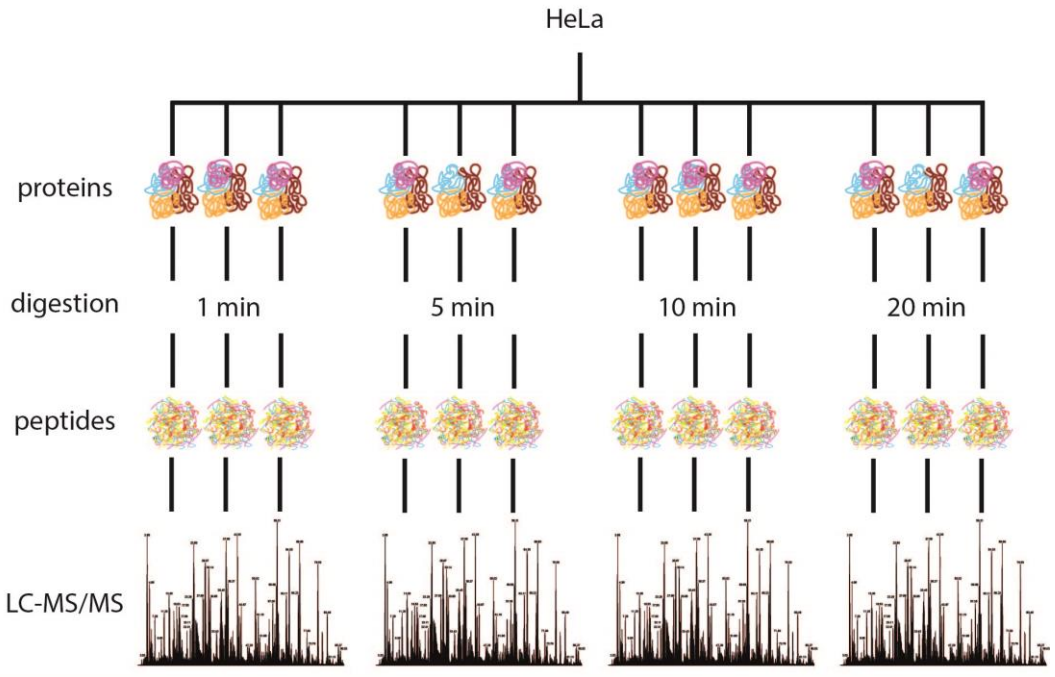

Figure 12. Evaluation of subtilisin digestion peptides over different time points. HeLa cell lysate was divided in 12 equal aliquots and digested with subtilisin, in triplicates, for 1, 5, 10 and 20 minutes. Digests were LC/MS measured for further peptide evaluation.

7.2.3 Systematic proteome comparison

A431 cell pellet was prepared as described in chapter 7.2.2. A431 cell line was this time selected to test subtilisin efficiency with different cell lines.

After resuspension in 6 M GuHCl, samples were diluted with 50 mM ABC buffer, pH 7.8, until a final concentration of 0.2 M GuHCl. Two aliquots of 25 µg each were digested either with trypsin or subtilisin following the protocol described in chapter 7.2.2. Incubation time for subtilisin for this experiments was of 20 min before enzymatic reaction stopped.

Samples were desalted using SPEC Pt C18AR (Agilent, Germany). SPEC tips were activated with 100 µL ACN, equilibrated twice with 100 µL 0.1% TFA, samples were loaded twice into the tip, washed twice with 0.1 % TFA and finally eluted twice with 50 µL 70% ACN. Eluate samples were dried under vacuum and resuspended in 15 µL of 10 mM ammonium acetate, pH 8.0 (buffer A). Samples were high pH reversed phase fractionated on a 1 mm × 150 mm C18 (ZORBAX 300SB-C18, pore size 300 A, 5 µm particle size, Agilent Technologies) column with a 45 min LC gradient ranging from 3-45% buffer B (84% ACN in 10 mM ammonium acetate, pH 8.0) at a flow rate of

12.5 µL/min. A total of 20 fractions were collected at intervals of 60 s in a concatenated manner, starting again sample collection from fraction tube number 1 after fraction 20 was over (Figure 13). Fractions were dried under vacuum and resuspended in 15 µL of 0.1% TFA for LC/MS analysis.

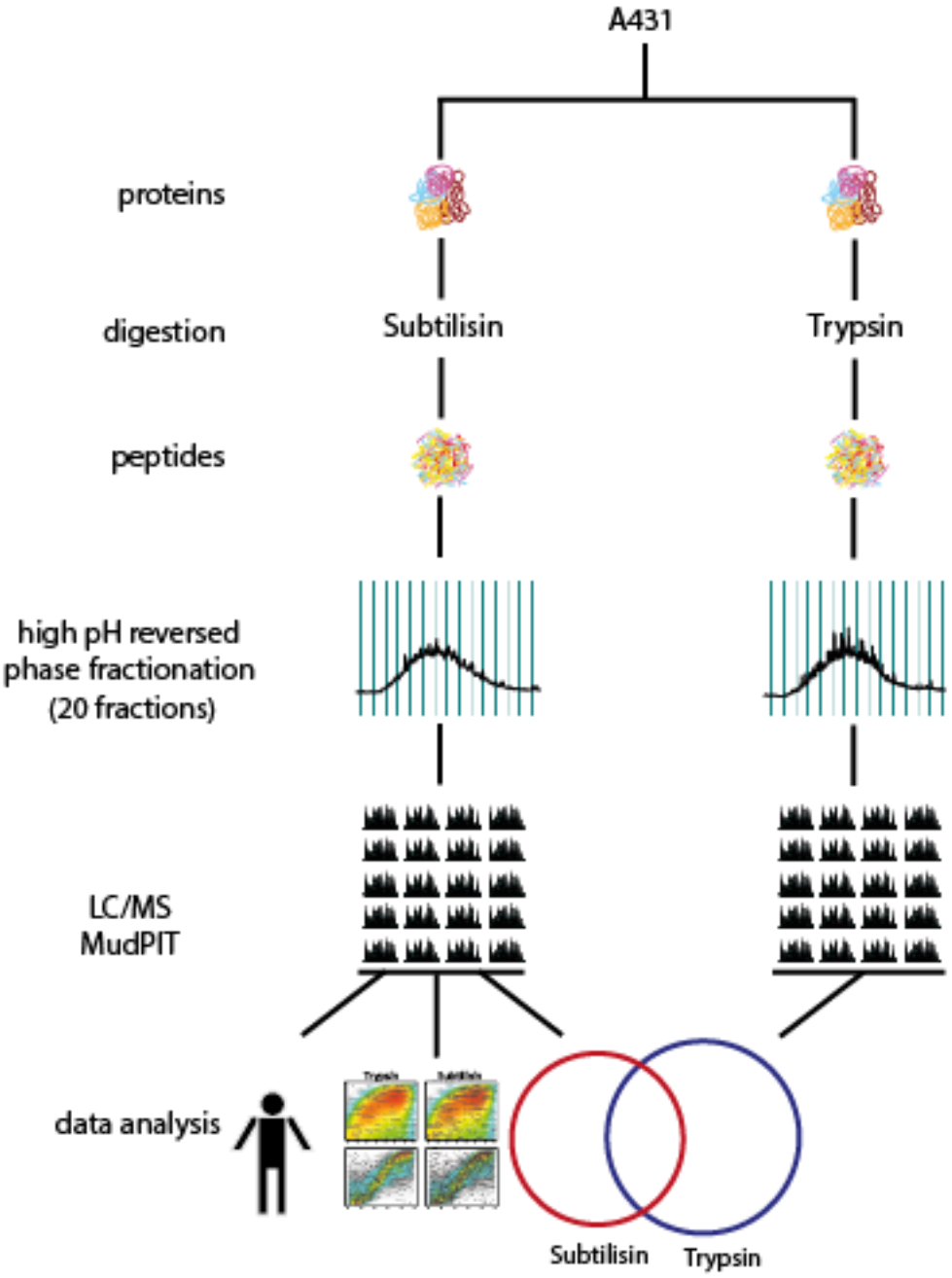

Figure 13 In-depth proteome coverage of A431 cell lysate subtilisin digested. A431 cell pellet was divided in 2 equal 25 µg aliquots and each individually digested either with subtilisin or trypsin. Digests were high pH reversed phase fractionated in 20 fractions for each aliquot digest. Fractions were LC/MS measured and searched against a human database in MudPIT mode (all measurements are combined and searched as one file in the Proteome Discoverer software). Subtilisin digest was evaluated for (1) contribution to proteome coverage, (2) enrichment of proline-rich regions and (3) additional proteins to trypsin digest.

7.2.4 Systematic phosphoproteome comparison

A HeLa S2 cell pellet was processed as described in chapter 7.2.2. After 30-fold dilution with 50 mM ABC (6 M to 0.2 M GuHCl), the sample was divided into 8 aliquots of 300 µg each. Four aliquots each were digested either with trypsin or subtilisin as in chapter 7.2.2, desalted as described in chapter 7.1.2 and dried under vacuum.

Two aliquots digested with trypsin and two aliquots digested with subtilisin were resolubilized in 1 mL of 80% ACN, 5% TFA and 1 M glycolic acid (buffer 1) and individually subjected to phosphopeptide enrichment using titanium dioxide (TiO_2, Titansphere TiO, 5 µm particle size, GL Sciences Inc, Japan), according to Engholm-Keller et al[163] with slight modifications. Enrichment steps were performed as described in chapter 7.1.7. For the other four digests, phosphopeptides were enriched by ERLIC-SCX/RP. Samples were separated using an Ultimate HPLC (LCPackings/ Thermo Scientific) equipped with a 4.6 x 100 mm PolyWAX column (300 A pore size, 5 µm particles, PolyLC) using buffer A (20 mM methylphosphonic acid, 70% ACN pH 2.0) and buffer B (200 mM triethylammonnium phosphate, 60% ACN, pH 2.0). Peptides were resuspended in 20 µL buffer A and separated using a 3-step gradient: 100% A for 10 min, a linear increase to 100% B in 10 min and 100% B for 10 min at a flow rate of 1 mL/min. 1 min-fractions were collected from retention time 2-6 min, 2 min fractions were collected from retention time 6-20 min and a 6 min-fraction was collected from retention time 20-26 min. All fractions were dried under vacuum. Fractions 1-6 were re-dissolved in 200 µL SCX A (20 mM KH_2PO_4, 20% ACN, pH 2.7), loaded onto an equilibrated Hypersep POROS SCX 10-200 mL cartridges (Thermo Scientific) and the flow throughs were collected. Fractions 7-12 were re-dissolved in 0.1% TFA and loaded onto equilibrated Hypersep C18-RP 10-200 µL cartridges. After washing with three column volumes of 0.1% TFA, peptides were eluted using three column volumes 60% ACN. All samples were dried under vacuum, reconstituted in 0.1% TFA and around 50% of each fraction was subjected to LC/MS (Figure 14).

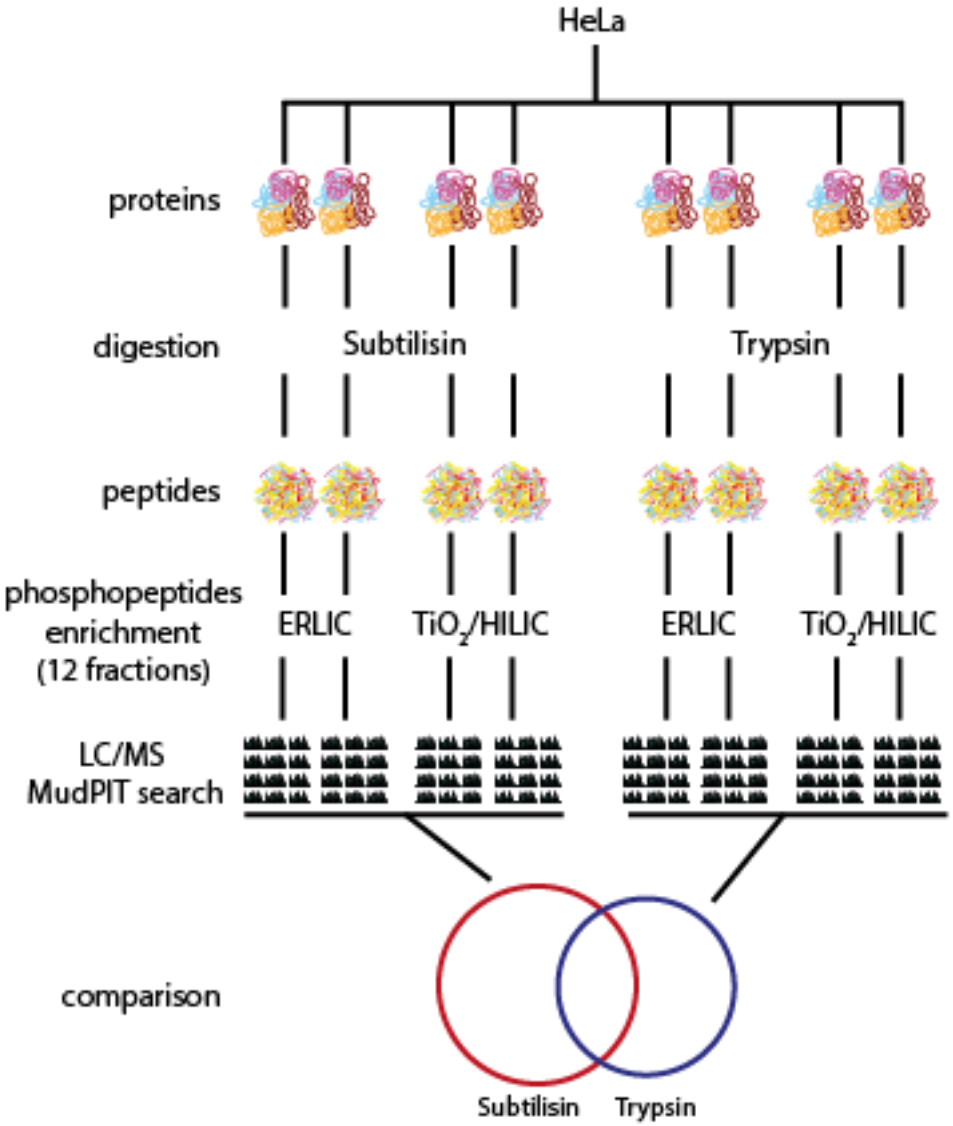

Figure 14. Phosphoproteome coverage comparison between subtilisin and trypsin. HeLa cell lysate was divided in 8 equal aliquots and half of the aliquots individually digested with subtilisin and the other half with trypsin. Two subtilisin aliquots were phosphopeptide enriched with TiO_2 and HILIC fractionated (12 fractions) and the other 2 aliquots phosphopeptide enriched by ERLIC fractionation (12 fractions). Same procedure was adopted for the trypsin aliquots. Fractions were LC-MS/MS measured and each fraction batch was individually searched in MudPIT mode. Subtilisin phosphorylation sites identifications (TiO_2/HILIC + ERLIC) were compared against trypsin phosphorylation sites identifications.

7.2.5 In-depth quantitative proteomics using chemical peptide labeling (iTRAQ)

Sixteen aliquots containing 150 µg of A431 cell pellet each were divided in 2 groups, in which the first group of 8 aliquots was digested with trypsin, as described in chapter 7.2.2 and the second group digested with subtilisin, incubation of 20 min with the enzyme, as described in chapter 7.2.2. All samples were desalted as described in chapter 7.1.2. Samples were reconstituted in 30 µL of 0.5 M triethylammonium bicarbonate buffer (TEAB), pH 8.0. Samples

were labeled with iTRAQ 8plex (Sciex, Germany). Each iTRAQ reagent was mixed with 80 µL isopropanol and transferred to one single sample, with 2 h incubation at 25 °C. Each group used one set of iTRAQ 8plex. Next, subtilisin samples were pooled in a ratio of 1:2:3:4:5:6:7:8 (113:114:115:116:117:118:119:121; sample named as SI), with the respective amounts of peptide for each label: 7.8 µg (113), 15.6 µg (114), 23.3 µg (115), 31.1 µg (116), 38.9 µg (117), 46. 7 µg (118), 54.4 µg (119) and 62.2 µg (121), to obtain a total of 280 µg. The trypsin samples were multiplexed using the same sample amounts, but in a reversed order of 8:7:6:5:4:3:2:1 (113:114:115:116:117:118:119: 121; sample named as TI). After pooling, samples were desalted as described in chapter 7.1.2. A total of 500 ng of each multiplexed sample (TI and SI) were measured by LC/MS. Later, 250 µg of the multiplexed subtilisin (SI) and trypsin (TI) samples, individually, were subjected to phosphopeptide enrichment based on TiO_2/HILIC protocol described in chapter 7.1.7. Each fractions was dried under vacuum and resuspended in 15 µL of 0.1% TFA for LC/MS analysis (Figure 15). To complete, a final STI sample composed by pooling 30 µg of the TI sample and 30 µg of the SI was prepared, in which 25 µg of the STI sample was subjected to high pH reversed phase fractionation (as described in chapter 7.1.6) and further measurement of the fractions by LC/MS. Data analysis is described in the next chapters.

The reason to use different ratio pooling allows the observation of subtle changes in the proteome and how precise the ratios can be determined. The mixed STI is useful to observe if the quantification is still possible for highly complex samples and to avoid false ratio observance due to co-isolation issues.

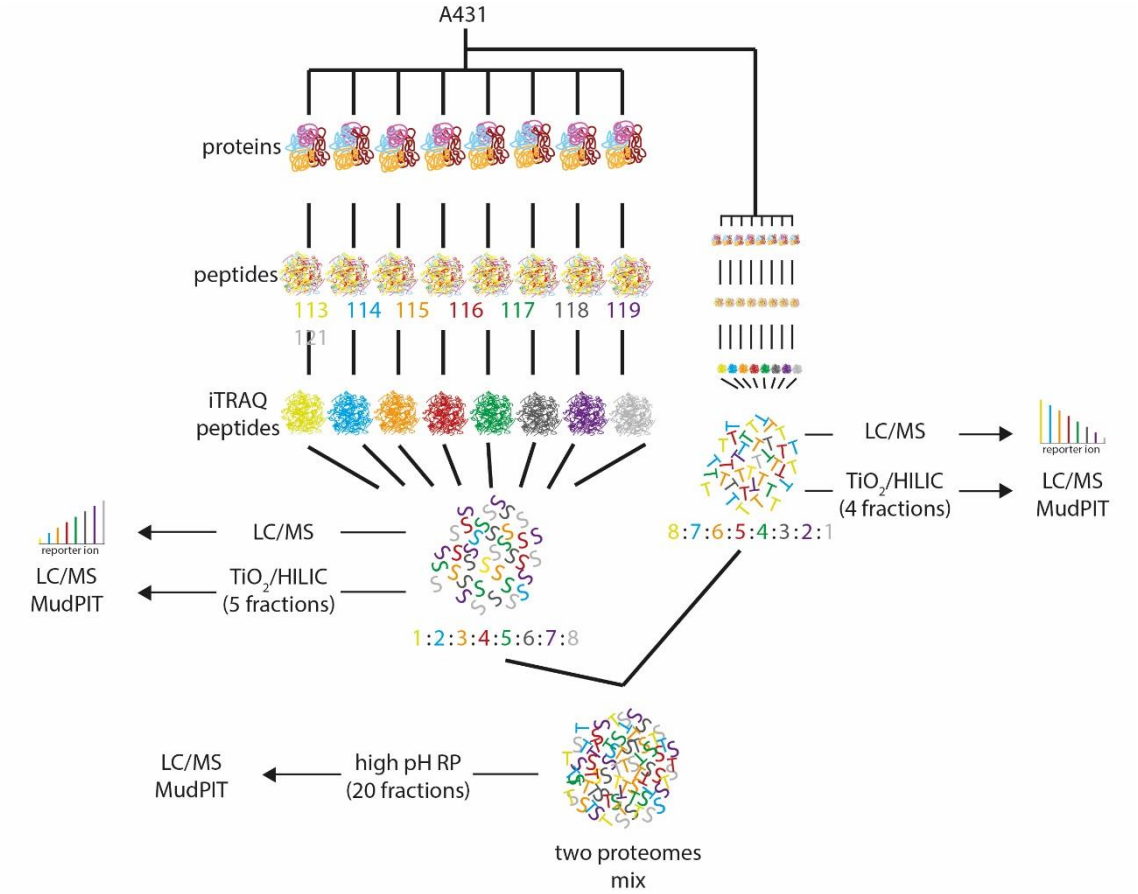

Figure 15. Compatibility between subtilisin digestion and quantification using chemical labeling. A431 cell lysate was divided in 16 equal aliquots prior digestion. Half of the aliquots were subtilisin digested and the other half trypsin digested. Each subtilisin aliquot was individually iTRAQ 8plex labeled and pooled together in a 1:2:3:4:5:6:7:8 proportion (113-121). Trypsin aliquots were also iTRAQ 8plex labeled and pooled together in a reversed proportion of 8:7:6:5:4:3:2:1 (113-121). Trypsin and subtilisin pooled samples were (1) measured by LC/MS, (2) TiO_2/HILIC phosphopeptide enriched and fractions measured by LC/MS and (3) mixed both in a ratio of 1:1 (subtilisin:trypsin) and high pH reversed-phase fractionated and fractions measured LC/MS.

7.2.6 LC/MS parameters

Offline LC was solely done for sample fractionation. Chromatography parameters are summarized in chapter 7.2.2.

On-line LC separations were performed in an Ultimate 3000 RSLCnano HPLC, coupled with trap columns (100 µm × 2 cm, C18 Acclaim Pepmap viper and main columns (75 µm × 50 cm, C18 Acclaim Pepmap viper; all Thermo Fisher Scientific). Samples were pre-concentrated in 0.1% TFA for 5 min at a flow rate of 20 µL/min followed by separation on the main column at 250 nL/min using binary buffer (A: 0.1% FA; B: 84% ACN, 0.1% FA) at 60 °C (column oven). Gradients are summarized in Table 8.

Mass spectrometer parameters for the different experiments are summarized in Table 9.

7.2.7 Database search

MS raw files were searched with Proteome Discoverer 2.2 (Thermo Scientific), using Mascot 2.4 against the human Uniprot database, with 20,194 target sequences (downloaded September 2014). Fractions were searched using the Multidimensional Protein Identification Technology (MudPIT) option (this option combines all fractions and search as if it was one single file). Proteome Discoverer 2.2 parameters are summarized in Table 10. Phosphorylation site probabilities were determined using the node ptmRS[39]. Only phosphorylation sites with site localization probabilities ≥ 99% were considered. For false discovery rate (FDR) estimation, percolator 3.048 was used. Data were filtered at <1% FDR on the peptide spectral match (PSM) and peptide level. For the global proteome, data was filtered at <1% FDR on the protein. For the iTRAQ data, only PSMs containing all used iTRAQ channels (113, 114, 115, 116, 117, 118, 119, 121) were considered for data analysis.

Table 7. Offline liquid chromatography parameters.

Experiment	HPLC	Column	Fractions	Buffer A	Buffer B	Gradient/duration 1	Gradient/duration 2	Gradient/duration 3	Flow rate
High pH reversed phase fractionation	Ultimate 3000 LC	1 mm × 150 mm C18 (ZORBAX 300SB)	20[1]	10 mM ammonium acetate, pH 8.0	84% ACN, 10 mM ammonium acetate, pH 8.0	3-45% B / 45 min	-	-	12.5 µL/min
HILIC, Phosphoproteome	Ultimate 3000 nanoRSLC	250 µm x 15 cm TSKgel Amide-80 (Tosoh, Japan)	12	98% ACN, 0.1% TFA	0.1% TFA	1-10% B / 2.5 min	10-35% B / 40 min	35-80% B / 5 min	3 - 2.5[4] µL/min
HILIC, iTRAQ phosphoproteome	Ultimate 3000 nanoRSLC	250 µm x 15 cm TSKgel Amide-80 (Tosoh, Japan)	4[2], 5[3]	98% ACN, 0.1% TFA	0.1% TFA	1-10% B / 2.5 min	10-35% B / 40 min	35-80% B / 5 min	3 - 2.5[4] µL/min
ERLIC, phosphoproteome	Ultimate 3000 LC	4.6 x 100 mm PolyWAX column (5 µm particles, 300 Å pore size, PolyLC)	12	20 mM methylphosphonic acid, 70% ACN	200 mM triethylammonnium phosphate, 60% ACN	100% A / 10 min	0-100% B / 10 min	100% B / 10 min	1 ml/min

1 - concatenated every 60 s intervals
2 - trypsin
3 - subtilisin
4 - gradient flow reduction between increase from 10 to 35% B

Table 8. “On-line” liquid chromatography parameters.

Experiment	Main column gradient (B)	Gradient duration (min)
High pH reversed phase fractions	3-35%	90
Phosphoproteome	3-42%	90
iTRAQ proteome (SI, TI)	3-42%	90
iTRAQ phosphoproteome (SI, TI)	3-42%	52
iTRAQ proteome Mix (STI)	3-35%	90

Table 9. Mass spectrometer parameters.

	MS1							MS2								
Experiment	**Instrument**	**Mass analyzer**	**m/z**	**Resolution**	**AGC**	**Injection time (ms)**	**Lock mass**	**Mass analyzer**	**Mode**	**Resolution**	**AGC**	**Injection time (ms)**	**Collision energy**	**Isolation window (m/z)**	**Dynamic Exclusion (s)**	**Activation**
High pH reversed phase fractionation	Fusion Lumos	Orbitrap	300-1500	60000	$4x10^5$	70	445,1200	Orbitrap	DDA - TopS 3s	30000	$3x10^4$	150	31	1	60	HCD
Phosphoproteome	QExactiveHF	Orbitrap	300-1500	60000	$1x10^6$	120	371,1012	Orbitrap	DDA - Top15	15000	$5x10^4$	120	27	2	30	HCD
iTRAQ proteome	QExactiveHF	Orbitrap	300-1500	60000	$1x10^6$	120	371,1012	Orbitrap	DDA - Top15	15000	$2x10^5$	200	30	1	30	HCD
iTRAQ phosphoproteome	QExactiveHF	Orbitrap	300-1750	60000	$1x10^6$	120	371,1012	Orbitrap	DDA - Top15	15000	$2x10^5$	200	32	1	30	HCD
iTRAQ proteome Mix	QExactiveHF	Orbitrap	300-1500	60000	$1x10^6$	120	371,1012	Orbitrap	DDA - Top15	15000	$2x10^5$	200	30	0,4	30	HCD

Table 10. Proteome Discoverer 2.2 parameters.

	Tolerances		Modifications	
Experiment	**MS1**	**MS2**	**Fixed**	**Variable**
High pH reversed phase fractionation	10 ppm	0.02 Da	Carbamidomethyl (C)	Oxidation (M)
Phosphoproteome	10 ppm	0.02 Da	Carbamidomethyl (C)	Oxidation (M), Phosphorylation (Y,S,T)
iTRAQ proteome	10 ppm	0.02 Da	Carbamidomethyl (C), iTRAQ8plex (N-term, K)	Oxidation (M), iTRAQ8plex (Y)
iTRAQ phosphoproteome	10 ppm	0.02 Da	Carbamidomethyl (C), iTRAQ8plex (N-term, K)	Oxidation (M), Phosphorylation (Y,S,T), iTRAQ8plex (Y)
iTRAQ proteome Mix	10 ppm	0.02 Da	Carbamidomethyl (C), iTRAQ8plex (N-term, K)	Oxidation (M), iTRAQ8plex (Y)

1 - Trypsin: maximum of 2 missed cleavages

2 - Carbamidomethyl (C) (+57.0215 Da), iTRAQ8plex (+304.2054 Da), Oxidation (M) (+15.9949 Da), Phosphorylation (Y,S,T) (+79.9663 Da)

7.2.8 Missing areas of the proteome

The proteome of the subtilisin fractions of the A431 systematic proteome comparison (chapter 7.2.3) was compared with the Peptide Atlas[86] (www.peptideatlas.org), in which peptide sequences from all world human proteome experiments are stored. A total of 1,222,862 peptide sequences were downloaded from Peptide Atlas website in October, 2017, and mapped to the employed Uniprot human database.

7.2.9 Mapping phosphopeptide sequences to proline-dense regions

Take into consideration the proteins of the downloaded Uniprot database, proline-rich regions were screened to determine the proline density at each region of the protein to evaluate proline recovery after digestion by each enzyme (trypsin and subtilisin). Using the position vector or all prolines from a protein, the kernel density function has been calculated and multiplied by the number or prolines in the protein, from which the absolute measure of proline density (bandwidth = 10, n= 16,384) can be determined. Regions with a density > 0.2 were considered proline-rich (approximately accounting for at minimum 25% of the proline residues inside a 25 amino acids regions). Proteins were plotted taking into consideration the relative position of the proline-rich regions and proline-rich regions can be observed by the color gradient. Identified peptides inside the proline-rich region were marked as black dots.

7.2.10 iTRAQ data analysis

To determine iTRAQ ratios, the reporter ion intensities from the PSM level were selected. For each PSM, the mean of the intensities of each iTRAQ channel (113, 114, 115, 116, 117, 118, 119 and 121) was performed. Later, each iTRAQ channel intensity was individually divided by the recently calculated mean and corrected by multiplying by 4.5 (the mean of the previous ratio 1:2:3:4:5:6:7:8 in which TI and SI samples were mixed). A boxplot was plotted to verify how accurate each iTRAQ channel was from the expected value. Closer the observed value to the expected ratio, better was the digestion reproducibility. Boxplot whiskers span all data points with the maximum being the most extreme data point and it is no more than 1.5 times the interquartile range.

7.2.11 Mitochondrial phosphoproteome

Highly purified mitochondria from yeast cell cultures were offered by the working group Prof. Dr. Chris Meisinger, Faculty of Biochemistry, University of Freiburg.

Yeast mitochondria purification protocol is based on Meisinger et al[158]. Yeast cells (strain YPH499) were cultivated overnight in respiratory (YPG) medium (1% w/v yeast extract, 2% w/v bacto peptone, and 3% w/v glycerol (pH 5.0)) at 30 °C with gentle shaking (130 rpm). After reaching a cell density of 1-3 OD_{600nm}, cells were pelleted by centrifugation at 3,000 x *g* for 5 min and resuspended in homogenization buffer (10 mM Tris-HCl, pH 7.4, 0.6 M sorbitol, 0.2% (w/v) bovine serum albumin, 1 mM phenylmethylsulfonyl fluoride and 1 mM ethylenediaminetetraacetic acid). Homogenization was performed at 4 °C, using 15 stokes of a glass teflon homogenizer to homogenize the sample. The homogenate was centrifuged for 5 min at 1,500 x *g* to pellet cell parts as nuclei and cell debris. The supernatant was collected and isolated mitochondria was obtained by an extra centrifugation step at 12,000 x *g* for 15 min. The pellet containing mitochondria was resupended in SEM buffer (250 mM sucrose, 1 mM EDTA, 10 mM MOPS-KOH, pH 7.2).

A second purification to remove contaminants such as vacuoles or endoplasmic reticulum was performed using a four-step sucrose density gradient centrifugation. A centrifuge tube was mounted pipetting 1.5 mL of a 60% sucrose solution to the bottom. New layers of 4 mL 32% sucrose, 1.5 mL 23% sucrose and 1.5 mL 15% sucrose were added on top of the bottom layer. Pre-purified mitochondria were centrifuged for 1.5 h at 134,000 x *g*, and a highly purity mitochondria fraction was obtained between 32% and 60% sucrose, which was carefully removed, diluted with SEM buffer and centrifuged for 30 min at 10,000 x *g*. The pellet containing the mitochondria was treated as show in chapter 7.2.2 to obtain the organelle lysate. After dilution from 6 M GuHCl to 0.2 M GuHCl with 50 mM ABC buffer, three equal aliquots of 500 µg each were digested with either trypsin, GluC (Promega, Germany) and subtilisin. Trypsin and GluC digestion followed the described protocol for trypsin, while the aliquot digested with subtilisin was incubated for 20 min. All digestions were stopped with 1% TFA and digestion efficiency controlled by the monolithic column.

Samples were desalted and phosphopeptide enriched by TiO_2/HILIC as described in chapter 7.1.7. Fractions were measured by LC/MS using the samples parameters for the "phosphoproteome" described in Table 8 and Table 9.

Data analysis of the MS raw files was performed using Proteome Discoverer 1.4 (Thermo Scientific), samples searched against Saccharomyces Genome Database (SGD) downloaded in September 2011 using Mascot 2.4. Samples were filtered to 1 % FDR. Trypsin and GluC samples

allowed 2 miss cleavages and enzymes were selected as “trypsin” and “GluC”, respectively. Subtilisin samples allowed zero miss cleavage and enzyme was selected as “none”. Full MS and MS/MS allowed, respectively, 10 ppm and 0.02 Da mass tolerance. Carbamidomethylation of the cysteine and oxidation of the methionine were selected as “fixed” and “variable”, respectively.

7.2.12 Super-fast sample preparation using subtilisin

HeLa S2 cells and mitochondrial used for this experiment were grown and purified as described in chapters 7.2.1 and 7.2.11, respectively.

Heart tissue: left ventricles of 8-week old male C57BL/6J mice were used for the experiments. They were obtained from mice after cervical dislocation. Hearts were quickly excised, washed in ice-cold PBS and right ventricles and atria were removed. Care of the animals was performed in accordance with the Committee on Animal Research of the regional government (LANUV, Germany).

All buffers were freshly prepared before conducting the experiments. Liquid nitrogen frozen mouse heart was grinded to powder with a pestle for approximately 5 min. Powdered mouse heart, HeLa cells and crude yeast mitochondria were lysed in 6 M GuHCl, 50 mM ABC, pH 7.8, followed by sonication with an ultrasonic probe (20% duty cycle, 1 × 20 s, 2 s pulse). Cysteines were reduced with 10 mM DTT for 20 min at 56 °C and alkylated with 30 mM IAA for 20 min in the dark, at room temperature. Meanwhile, a BCA (Thermo Scientific) was used to determine protein concentrations. Samples were diluted with 50 mM ABC, pH 7.8, to a final concentration of 0.5 M GuHCl. Next, samples were pre-heated for 5 min at 56 °C, followed by digestion with subtilisin in a ratio of 20:1 (sample:enzyme) for 2 min at 56 °C. Digestion was quenched by acidification with TFA to a final concentration of 1%. Before LC-MS measurement, samples were spun down for 1 min at 18,000 x g and an aliquot corresponding to 1 µg of peptide from each sample was diluted to 15 µL with 0.1 % TFA and immediately analyzed by LC/MS on an Orbitrap Fusion Lumos.

LC buffers were the same as described in chapter 7.2.6, with a gradient of 5-32 % B in 52 min. MS parameters are summarized in Table 11.

MS raw files were searched with the help of Proteome Discoverer v1.4 (Thermo Scientific), using Mascot v2.4 against either (i) a human Uniprot database (downloaded September 2014, 20,194 target sequences), (ii) a mouse Uniprot database (downloaded July 2015, 16,749 target sequences) or the *Saccharomyces* Genome Database (SGD) (downloaded September 2011, 6,717 target sequences). Other Proteome Discoverer parameters are summarized in Table 12.

Table 11. Mass spectrometer parameters of the super-fast digestion protocol. Mitochondria had special measurement parameter due to specificities of the sample.

	MS1							MS2								
Experiment	**Instrument**	**Mass analyzer**	**m/z**	**Resolution**	**AGC**	**Injection time (ms)**	**Lock mass**	**Mass analyzer**	**Mode**	**Resolution**	**AGC**	**Injection time (ms)**	**Collision energy**	**Isolation window (m/z)**	**Dynamic Exclusion (s)**	**Activation**
Super-fast	Fusion Lumos	Orbitrap	300-1500	$12x10^4$	$2x10^5$	50	445.120002	Orbitrap	DDA - Top15	15000	$5x10^4$	150	34	0.8	30	HCD
Super-fast mitochondria	Fusion Lumos	Orbitrap	300-1500	$12x10^4$	$2x10^5$	50	445.120002	Orbitrap	DDA - Top15	15000	$5x10^4$	150	34	1.2	30	HCD

Table 12. Proteome Discoverer 1.4 parameters of the super-fast digestion protocol.

	Tolerances		Modifications	
Experiment	**MS1**	**MS2**	**Fixed**	**Variable**
Super-fast	10 ppm	0.02 Da	Carbamidomethyl (C)	Oxidation (M)
Super-fast mitochondria	10 ppm	0.02 Da	Carbamidomethyl (C)	Oxidation (M), Phosphorylation (Y,S,T), Acetyl (Protein N-term)

1 Samples digested with trypsin allowed a maximum of 2 missed cleavages

2 Samples digested with subtilisin allowed a maximum of 0 missed cleavages

3 Carbamidomethyl (C) (+58.005 Da), Oxidation (M) (+15.995 Da), Phosphorylation (Y,S,T) (+79.966 Da), Acetyl (+42.011 Da)

7.2.13 Label free quantification of super-fast prepared samples

Human fibroblasts were cultured in DMEM containing 10% FCS (both Sigma Aldrich). At a confluency of 70%, cells were collected (scraped down of the culture dish) and washed thrice with ice-cold PBS via centrifugation at 2,000 rpm and 4°C. Afterwards, purified cell pellets were immediately snap-frozen in liquid nitrogen and stored at -80°C until further sample preparation.

Human fibroblasts cell pellets of three biological replicates from healthy (control) and three biological replicates with a mutation in VCP on chromosome 9p13 were treated as described in chapter 7.2.2. Prior to digestion, all samples were divided in two aliquots: one aliquot of each sample was digested with subtilisin as described in chapter 7.1.12 and the other aliquot digested with trypsin in a ratio of 20:1 (sample:enzyme) overnight at 37 °C in the presence of 2 mM $CaCl_2$. Digestion was stopped with 1% TFA (final concentration). After digestion, all samples were processed as above and measured in triplicates by LC/MS on an Orbitrap Fusion Lumos.

Data analysis for label free quantification was performed with the Progenesis QI for proteomics software version 3.0 from Nonlinear Dynamics (Newcastle upon Tyne, UK). MS raw files were automatically aligned, followed by peak picking. Only peptides with charge states +2, +3 and +4 were considered for peptide statistics, analysis of variance (one-factor ANOVA) and principal component analysis (PCA). Only MS/MS spectra with ranks 1-10 were exported as peak lists with a limited fragment ion count of 100 and using de-isotoping and charge deconvolution. Using the software searchGUI version 3.5[166], spectra were searched against a target/decoy version of the human Uniprot database (downloaded September 2014, containing 20,194 target sequences) using X!Tandem Vengeance (2015.12.15.2). Additionally, spectra were searched using Mascot 2.4. Search parameters were: “none” as enzyme with a maximum of zero miss cleavage, carbamidomethylation of Cys set as fixed modification, oxidation of Met set as variable modification, MS and MS/MS tolerances of 10 ppm and 0.02 Da, respectively. PeptideShaker 1.4.0[167] was used to combine all search result files and filter data at an FDR of 1 % on the protein and peptide level. Obtained identifications were exported using the advanced PeptideShaker features that allow direct re-import of the quality-controlled data into Progenesis.

Only proteins quantified with at least one unique peptide were exported from Progenesis. Then, for each protein, the average of the normalized abundances (obtained from Progenesis) from the biological replicate analyses was calculated to determine the ratios between the patients and controls. Later, each patient/control ratio was log2 transformed. Up and down regulation cut-offs

were calculated by the median of all patient/control ratios, plus (up-regulation) or minus (down-regulation) two times the standard deviation of the all patient/control ratios. . Proteins showing at least 2.31- (trypsin) and 2.03-fold (subtilisin) change and additionally having t-test p-values <0.05 were considered as regulated.

7.3 Subtilisin, PKA, antibody experiments

Prof. Dr. Tim Hucho, University Hospital of Cologne, Cologne, Germany, supplied PKA-Cα and anti-Cα, in order to evaluate, by mass spectrometry, the PKA epitope. The blockage of this epitope with the antibody could avoid a phosphorylation and PKA-Cα activity could be evaluated.

Murine PKA catalytic subunit isoform α1 (PKA-Cα, ~40 kDa) were expressed in E. coli BL21 DE3 and purified using an IP20-resin. Anti-Cα antibody was obtained from mouse monoclonal anti-Cα (1:500, clone 5B, BD Transduction Laboratories, #610980).

Approximately 15 µg of PKA-Cα were resuspended in 50 mM ammonium bicarbonate (ABC, Sigma-Aldrich, Germany), pH 7.8 and carbamidomethylated as described in chapter 7.1.2. Possible PKA degradations products were removed by ultrafiltration at 10,000 x g for 10 min at 4 °C in an Amicon MWCO 30 kDa Ultra-0.5 mL centrifugal filter (Merck Millipore, Darmstadt, Germany).

PKA incubation with the antibody followed two distinct processes.

First, PKA-Cα was incubated with anti-Cα at 37 °C, 1h, in 50mM ABC, pH 7.8. After, PKA and antibody (PKA/AB) were incubated with subtilisin (protease:protein ratio of 1:20) for 5 min at 56 °C. After digestion, PKA/AB was ultra-filtrated as described above and washed 5 times with 100 µL 50 mM ABC/per wash at 4 °C. The ultra-filtrate or flow through (what could pass through the filter) was dried under vacuum. To elute the peptides bound to the antibody, the concentrate (what could not pass through the filter) was incubated 5 min with 50 µL 0.1 % TFA, pH 2.1, at 4 °C. To separate the formerly bound peptides from intact PKA protein, subtilisin and antibody, the solution passed through another ultrafiltration step, followed by one washing step with 100 µL 0.1 % TFA and another ultrafiltration step. The 150 µL of the new ultra-filtrate (or eluate) were dried under vacuum. The PKA epitope should be highly abundant in the eluate. First flow through and eluate were reconstituted in 20 µL 0.1 % TFA and measured in a monolithic column and by LC/MS (Figure 16a). Also, PKA-Cα, anti-Cα, PKA/AB, pre and post digestion, were measured in a monolithic column.

Second, PKA was first digested with subtilisin (protease:protein ratio of 1:20) at 56 °C in 50 mM ABC, pH 7.8, for 5 min. PKA digest solution was ultrafiltrated in a 30 kDa filter at 4 °C, as described above, in order to remove the enzyme. The ultra-filtrate or the PKA peptides were then incubated with the antibody at 37 °C, 1h, in 50mM ABC, pH 7.8. The PKA peptides/antibody solution was ultra-filtrated and washed 5 times with 100 µl 50 mM ABC/per wash at 4 °C. The ultra-filtrate or flow through was dried under vacuum. The concentrate was incubated 5 min with 50 µL 0.1 % TFA, pH 2.2, at 4 °C, followed by ultrafiltration, and one more washing step with 100 µL 0.1 % TFA. The 150 µL of the new flow through or eluate were dried under vacuum. The PKA epitope should be highly abundant in the eluate. Sample was resuspended in 20 µL 0.1 % TFA and measure by LC/MS (Figure 16b).

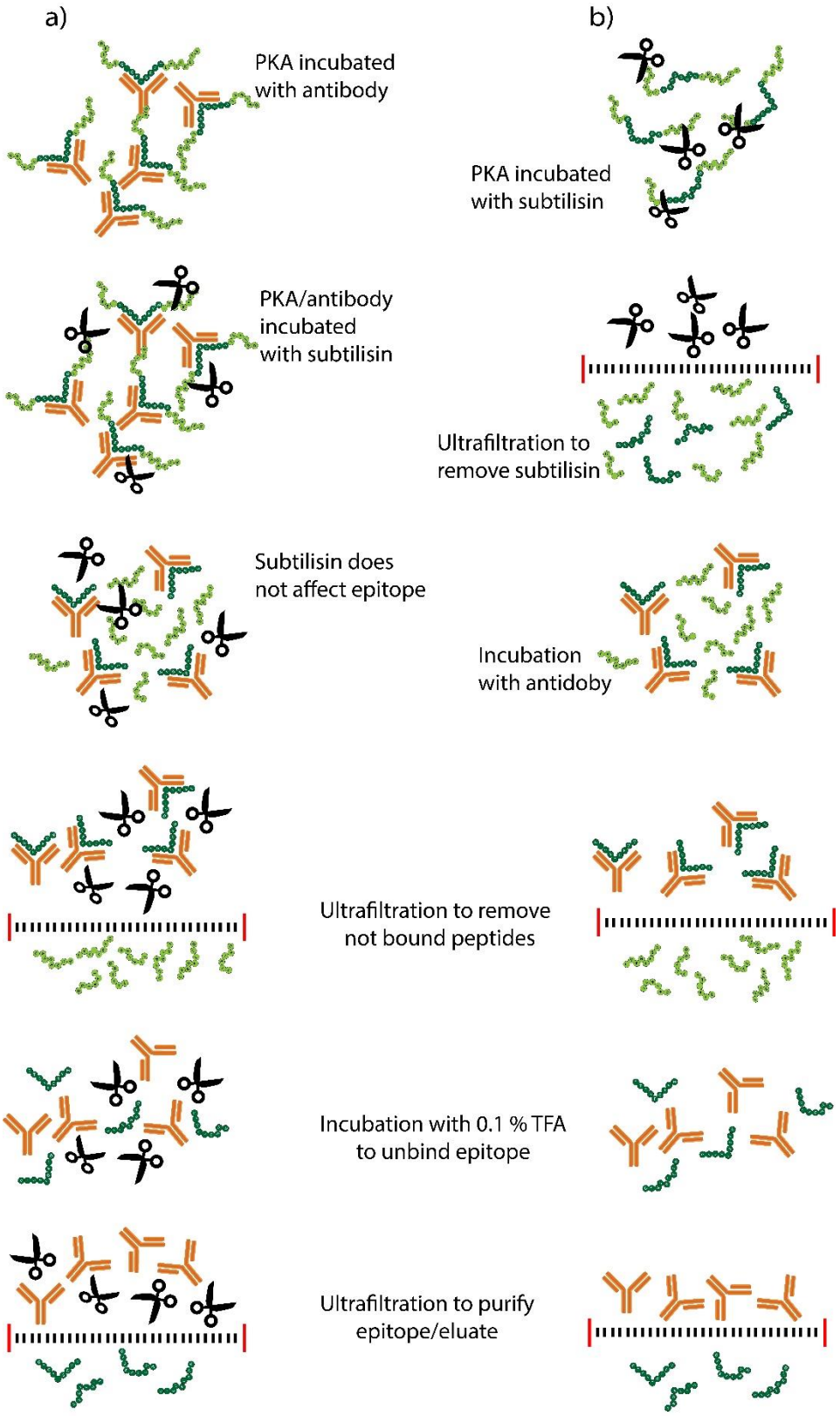

Figure 16.Epitope identification workflow. Two procedures were adopted to identify PKA-Cα, a) with intact protein/antibody incubation and b) PKA-Cα peptides incubated with antibody.

LC was performed as described in chapter 7.2.6 with a gradient ranging from 3-35% B in 55 min. MS measurements were acquired in an Orbitrap Fusion Lumos, with the following parameters: MS survey scan was acquired in the orbitrap from 300 to 1500 m/z, AGC of 2 x 10^5, maximum injection time of 50 ms; MS/MS was acquired in the orbitrap using TopS mode 3 s, HCD activation at 32 eV collision energy, AGC of 5 x 10^3 ions, maximum injection time of 150 ms, resolution of 30,000 and no dynamic exclusion.

MS raw files were searched using Proteome Discoverer 1.4, using Mascot 2.4 against a Mus musculus Uniprot database (downloaded July 2015, 16684 target sequences), with the following paramenters: enzyme selected as "none", carbamidomethylation of the cysteine and oxidation of the methionine as fixed and variable modification, respectively, MS survey and MS^2 mass tolerances was set to 10 ppm and 0.02 Da , respectively. Percolator 3.048[160] was used for false discovery rate (FDR) estimation at 1 % FDR on the PSM level.

7.4 New yeast mitochondria purification protocol

A more simplified and efficient mitochondrial purification protocol was developed in order to increase yeast mitochondria phosphoproteome coverage. The protocol was based on the method described in chapter 7.2.11 with a few modifications.

Mitochondria from yeast cell cultures were provided by the working group Prof. Dr. Chris Meisinger, Faculty of Biochemistry, University of Freiburg.

Yeast mitochondria purification protocol is based on Meisinger et al[158]. Yeast cells (strain YPH499) were cultivated overnight in respiratory (YPG) medium (1% w/v yeast extract, 2% w/v bacto peptone, and 3% w/v glycerol (pH 5.0)) at 30 °C with gentle shaking (130 rpm). After reaching a cell density of 1-3 OD_{600nm}, cells were divided in two aliquots, one followed the purification protocol described in chapter 7.2.11 and the other aliquot was pelleted by centrifugation at 5,850 x *g* for 10 min and resuspended in homogenization buffer (10 mM Tris-HCl, pH 7.4, 0.6 M sorbitol, 0.2% (w/v) bovine serum albumin, 1 mM phenylmethylsulfonyl fluoride and 1 mM ethylenediaminetetraacetic acid) complemented with PhosStop (Roche) and cOmplete EDTA-free (Roche). Homogenization was performed on ice, using 30 stokes of a glass teflon homogenizer to homogenize the sample. The homogenate was centrifuged for 5 min at 2,000 x *g* and 4 °C to pellet cell parts as nuclei and cell debris. The supernatant was collected and isolated mitochondria were obtained by an extra centrifugation step at 16,800 x *g* for 15 min, 4 °C. The pellet containing mitochondria was

resupended in SEM buffer (250 mM sucrose, 1 mM EDTA, 10 mM MOPS-KOH, pH 7.2) and snap frozen in liquid nitrogen.

Both aliquots were further processed with trypsin only and measured by LC/MS as described in chapter 7.2.11.

8 Results and discussion

8.1 MAS1 mutant experiments

The MAS1 temperature sensitive mutant experiment focused in achieving new information on how the mitochondrial processing peptidase (MPP) influences on the overall (phospho)proteome of the organelle. As well, it was analyzed possible new imported proteins that could pass through the MPP for maturation.

The temperature sensitive mutant is an excellent technique to evaluate function of genes and proteins that are essential for cell viability, in which critical functions cannot be replaced by other pathways or redundant genes/proteins with similar functions[168-170]. Alternative techniques, as gene deletion or interference RNA (iRNA), totally impair gene translation, causing cell death for lack of essential proteins. The temperature sensitive technique shows great use once 20% of the genome of the yeast are essential for cell viability[171]. Temperature sensitive mutants possesses gene sequences added in into the DNA, more specifically in the vicinity of the gene of interest, that causes instability of the gene of interest after a temperature shift, i.e. the gene is functional in permissive temperatures and not functional in non-permissive temperature. In the case of the studied MAS1 mutants, the gene was stable at the temperature of 22 °C, in which translation of the gene was theoretically occurring with no impairment. After temperature shift to 37 °C, the gene is no longer functional and translation of the gene is highly impaired, and the lack of the MAS1 protein would cause a functional impairment of the MPP, and further newly imported proteins would suffer no maturation, affecting mitochondrial homeostasis and possibly mitochondrial (phospho)proteome composition. In addition, whole yeast cell proteome composition could be altered, since possibly the proteome would be altered to compensate the impaired mitochondrial, especially what concerns cell energy production, since the yeast can alternate energy production in aerobic (by the mitochondrion) or anaerobic (by fermentation) depending on the current need.

8.1.1 Mitochondrial MAS1 ChaFRADIC experiments

As discussed, the MAS1 protein is an essential subunit of the MPP that acts cleaving the signaling sequence of imported proteins. The comparison between the wild type and MAS1 mutant using the ChaFRADIC workflow enables to observe differences between protein N-termini that pathway is

intricate with the MPP. Possible proteome change might occur as well, as a matter of an attempt to keep cell homeostasis.

To make this analysis, three biological replicates of wild type and temperature sensitive MAS1, each collected in permissive (0 h) and non-permissive (2 h and 4 h) time points (6 samples per biological replicate) were prepared as defined in the ChaFRADIC protocol. After iTRAQ labeling, sample pooling and digestion, each set of biological replicate was fractionated in a SCX system. All biological replicates showed a similar chromatogram during the fractionation, attesting a similar and reproducible procedure so far (Supplemental Figure 1a). In total, 13 fractions for each biological replicate was collected. Each fraction was analyzed by LC/MS to evaluate peptide charge state (Supplemental Table 1). Fractions with similar charge state were polled together, derivatized and passed through a new phase of SCX fractionation using exactly the same gradient as before. For each fraction, only the exact corresponding fractions were collected (Supplemental Figure 1b) and further LC/MS measured. This derivatization step combined with a second SCX fractionation works to enrich original protein N-termini and exclude the N-termini generated after digestion, since the derivatization step reduces one charge of the peptide generated after digestion while does not affect the original protein N-termini. During the SCX chromatography, original protein N-termini maintain elution gradient (i.e. elute at the same time as before), while non-original N-termini peptides shift elution to lower charges areas (i.e. those peptides elute before than original protein N-termini, since they have now at least one charge less).

Finally, each fraction from each biological replicate was measured by LC/MS, and database searches were performed as described in material and methods. Three biological replicates generated 3 different search results. The identified peptides of each search are iTRAQ labelled, generating a reporter ion intensity for each channel. To obtain one single table to be able to compare results, identical peptides in terms of amino acid sequence and modifications from the different biological replicates were combined, and iTRAQ reporter ion intensities averaged, e.g. the peptide “MLAAKNILNR”, from the protein YJR045C with an endogenous acetylation, had reporter ion normalized abundance for the wild type sample 0 h of 1.01 (biological replicate 1), 1.03 (biological replicate 2) and 0.92 (biological replicate 3), with a final value of 0,99 after combining all biological replicates.

To assess the peptides that significantly vary between the wild type and temperature sensitive MAS1 samples, volcano plots between the respective time points samples (MAS1 0 h x wt 0 h, MAS1

2 h x wt 2 h, MAS1 4 h x wt 4 h) were created. Since a functional MPP removes signaling peptide sequences, the focus was to identify up-regulated N-termini peptides, once these peptides would accumulate in an impaired MPP complex. Since some disadvantages of temperature sensitive mutants involve possible side effects and induced heat shocks after temperature shift [168], proteins up-regulated in the MAS1 0 h x wt 0 h comparison were disregarded if present in the other time point comparison.

Considering a 2-fold difference as regulation (p-value $\leq$ 0.05), a volcano plot was performed for all time points (0 h, 2 h and 4 h). The 0 h comparison only presented 15 up-regulated peptides from 9 different proteins (ALD4, LEU4, ICL2, HEH2, PDH1, FPR2, RIP1, CAT2, CYB2) (Supplemental Figure 2a and Supplemental Table 2). Even though a few proteins have been assigned as matrix proteins, they were discarded if present as regulated in the other time points. The comparison 2 h showed only 7 up-regulated peptides (not considering the ones found in 0 h) from 6 different proteins (YFH1, GRX5, ACN9, ALT1, YMR31 and STF1) (Supplemental Figure 2b and Supplemental Table 3). The comparison 4 h showed 33 regulated peptides from 29 proteins (YFH1, TUF1, SSC1, SOD2, SEC4, SDH1, RPL22A, QCR2, PRX1, MSS51, MRPL4, MRPL10, MIC17, MDJ1, ILV1, HSP60, GRX5, GLR1, ENB1, CRP1, CIT1, CIR2, ATP3, ATP16, APE2, ALT1, AIM45, ACP1 and ACN9) (Supplemental Figure 2c and Supplemental Table 4). It is promptly observed that at least 4 h of temperature shift is necessary to observe major changes in the peptidome composition. The peptides of the STF1 and YRM31 from the 2 h were not regulated as well in the 4 h dataset. Even though present in slightly higher amounts in the 4 h dataset compared to time point 0 h, those proteins could be a false positive or regulation level decreased due to a lower protein biosynthesis. Since signaling sequences varies between 20 to 60 amino acids[172], it was evaluated the peptides that were a substrate of the MPP for maturation. Also, proteins that are a substrate of the MPP are expected to be localized or in the matrix of the inner membrane. A recent paper by Voegtle et al[173] summarized over 800 mitochondrial proteins to different subcompartments of the organelle. The mitochondrial protein subcompartment of identified proteins in this study were based in the protein subcompartment localization described in the paper previously cited. The up-regulated peptides are shown in Table 13 and present some interesting information. First, there are strong evidences that the proteins SSC1, SOD2, GRX2, AIM45, SDH1, CIR2, CIT1, ILV1, MDJ1, MSS51, MRPL4, SSC1, ATP3, YFH1, ACP1, TUF1, PRX1 and ALT1 are processed by the MPP. There are 3 main reasons: (1) the net charge of the peptide in question, considering that signal peptides have a positive net charge, (2) the starting position of the peptide N-terminal, considering that the signal peptides are usually 20 to 60 amino acids, (3) presence of

the protein in the matrix or loosely associated to the inner part of the inner membrane, considering that proteins that follow the MPP pathway are destined to one of those 2 compartments.

Table 13.Up-regulated peptides from the temperature MAS1 x wild type. Protein presence in the subcompartment is indicate with an "X", as described in Ref [173].

Sequence	Net charge	Protein	Fold change (log2)	Position N-terminal	Matrix	Inter membrane	Outer membrane	Inter-membrane space
MLAAKNILNR	+2	SSC1	3,06	1	X	-	-	-
MFAKTAAANLTKKGGLSLLSTTAR	+4	SOD2	2,80	1	X	-	-	-
MFLPKFNPIR	+2	GRX5	2,47	1	X	-	-	-
MLSATKQTFR	+2	GLR1	1,77	1	X	-	-	-
MFKSLAAVLPR	+2	AIM45	1,16	1	X	-	-	-
MLSLKKSALSKLTLLR	+4	SDH1	3,34	1	-	X	-	-
MIKFTNENLIR	+1	CIR2	2,12	1	-	X	-	-
MNNKLIYR	+2	ACN9	2,23	1	-	-	-	-
MLETDHSR	+3	ENB1	1,29	1	-	-	-	-
SAILSTTSKSFLSR	+3	CIT1	3,73	2	X	-	-	-
SATLLKQPLCTVVR	+3	ILV1	2,62	2	-	X	-	-
AFQQGVLSR	+2	MDJ1	2,36	2	-	X	-	-
TVLYAPSGATQLYFHLLR	+3	MSS51	1,20	2	-	X	-	-
SFHSQGGPLR	+3	MRPL4	2,73	5	-	X	-	-
SSLSSSFR	+2	SSC1	2,50	11	X	-	-	-
SVMCHQAQVGILYKTNPVR	+4	ATP3	2,74	13	-	X	-	-
SLNFVAKR	+2	ATP16	2,59	13	-	-	-	-
IAAAGGER	+1	YFH1	2,86	22	X	-	-	-
ASTMAAPVHPQQQQQPNAYSHPPAAGAQTR	+4	MIC17	1,31	22	-	-	-	-
SVMSNTILAQR	+2	ACP1	1,81	24	X	-	-	-
SIAAHPR	+3	APE2	1,58	28	-	-	-	-
MLTSVAGNDIFFR	+2	MRPL10	1,70	30	-	-	-	-
SQTTTSYAAAFDR	+2	TUF1	1,70	32	X	-	-	-
ATAPILCKQFKQSDQPR	+4	PRX1	1,51	32	X	-	-	-
QQQQPNAYSHPPAAGAQTR	+3	MIC17	2,81	33	-	-	-	-
SLSGQSSLNDLR	+2	ALT1	2,15	77	X	-	-	-
VYDVTDER	+2	SEC4	1,08	99	-	-	X	-
TNEAAGDGTTSATVLGR	+2	HSP60	1,29	102	X	-	-	-
YQVTPEEDEEEDEE	+1	RPL22A	1,75	108	-	-	-	-
AAGLNGLAGPLHGR	+3	CIT1	1,16	301	X	-	-	-
NYVAVGDVSNLPYLDEL	+1	QCR2	1,14	352	-	X	-	-
YVAVGDVSNLPYLDEL	+1	QCR2	1,02	353	-	X	-	-
APKLPLTDEQTAEGR	+3	CRP1	1,15	374	-	-	-	-

The protein ATP16 is part of the ATP synthase complex. Albeit not present in any of the subcompartments presented in the table, this complex has already been described to be located in the inner membrane[68]. This result suggest that ATP16 follows the MPP pathway and is attached in the inner membrane by the matrix side.

MRPL10 is part of the mitochondrial ribosome dedicated to protein biosynthesis encoded from the mitochondrial DNA, including essential components of the respiratory chain[174]. Beside the observed use of the MPP pathway, the MRPL10 has been described as matrix protein[24] and loosely attached to the inner membrane [174]. Still, a defective MPP could impair proper function of the respiratory chain by lack of mature ribosomal units to synthetize essential proteins.

ACN9, known as well as SDH7, has been reported as a chaperone fundamental for the assembly of succinate dehydrogenase complex [175], a complex involved in both mitochondrial electron transport chain and the citric acid cycle. This protein has been reported in both intermembrane space [176] and matrix [175]. As showed here, the ACN9 is maturated by the MPP complex, indicating the protein as part of the matrix or inner membrane. Again becomes evident the importance of the MPP for the indirect assembly of vital components of the mitochondrion.

MIC17 (or MIX17) is a protein described to be located in the intermembrane space due a protein motif that indicates another import pathway [177]. Still, the evidence of a positively charged sequence raging the first protein amino acids and the up-regulation in MAS1 mutants indicate to be a matrix or inner membrane protein.

ENB1 had been described in yeast as part of de endosome by similarity and APE2 have been described as part of the mitochondrion, but none has proved evidence of location in the yeast. HSP60, CIT1, QCR2 are matrix or inner membrane protein, but up-regulated peptide does not coincide with the 20 to 60 amino acid expectation for signaling peptides. SEC4 is an outer membrane protein, CRP1 was described to be part of the nucleus and RPL22A was described as cytoplasmic. Those proteins should be further investigated to understand their appearance in the table. Coincidently, they present lower fold regulation than the majority of the peptides described above, increasing the chance of a false positive. In that sense, no conclusion can be made so far for those proteins.

To give an overview of the analyzed up-regulated proteins, a protein correlation using the software STRING was performed (Figure 17). Only up-regulated proteins were selected, once the objective

was to characterize proteins that accumulate with an impaired MPP. STRING [178] gives the possibility to view protein-protein interaction that might be physical and/or functional. The STRING uses published material, computational prediction, organism gene orthology and information described in other databases to perform the connection database. The protein correlation using STRING from the proteins clearly show a high level of communication between the proteins. With the present study, the protein network connections between MAS1 and MAS2 proteins (inserted in STRING just for visualization purposes) and the regulated proteins may be better understood. APE2, SEC4 and CRP1 are proteins with no sort of interaction with other proteins, increasing chance of a false-positive identification of those proteins.

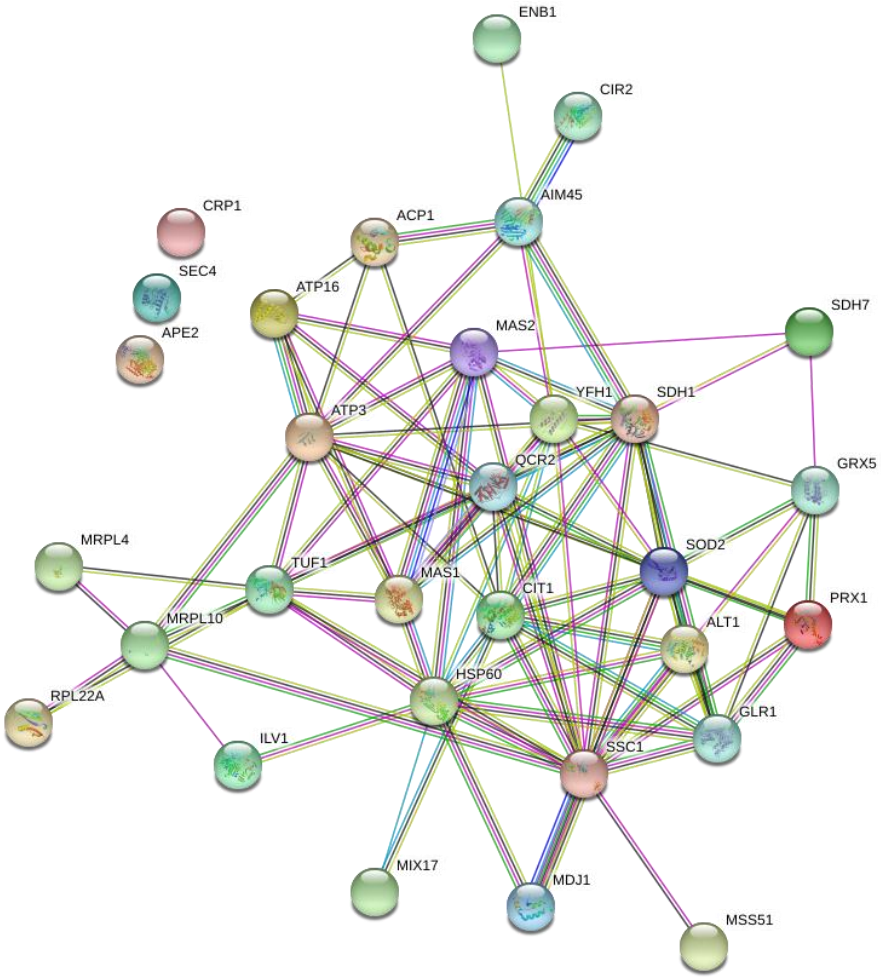

Figure 17. Using the software STRING, it is possible to observe the correlation of the up-regulated proteins from the MAS1 temperature sensitive study. It is evident the high amount of interactions between the up-regulated proteins. MAS1 and MAS2 (proteins of the MPP) were inserted to have a better overview of protein interaction.

8.1.2 Yeast MAS1 ChaFRADIC experiments

Albeit was not observed a vast proteome change in the MAS1 mitochondrial ChaFRADIC, a whole yeast ChaFRADIC experiment was performed with the intention to observe possible side effects of caused by a defective MPP. The steps performed for the data analysis were the same performed for mitochondrial MAS1 data analysis.

For each biological replicate, there were 6 samples, wild type grown in permissive conditions (0 h) and non-permissive conditions (2 h and 4 h), MAS1 mutant grown in permissive conditions (0 h) and non-permissive conditions (2 h and 4 h), generating 6 samples per replicate. For each replicate, samples from were iTRAQ labelled, pooled, digested, SCX fractionated in 13 fractions, each fraction measured by LC/MS to determine peptide charge state, fractions with similar charge state were pooled together, samples were derivatized with d3-NHS to reduce charge state of non-original protein N-termini, and each fraction was SCX fractionated as before to enrich original protein N-termini. In the second SCX fractionation, only the correspondent injected fraction(s) were again collected and measured by LC/MS, e.g. the pooled fractions 2 and 3 were reinjected in the SCX, and from all 13 new existent fractions, only fractions 2 and 3 were collected, pooled again and LC/MS measured.

First, the 3 SCX chromatograms of the biological replicates were visually compared to observe sample reproducibility (Supplemental Figure 3a). After confirming that chromatograms had comparable elution peaks in all samples, confirming a reproducible sample preparation until this point, fractions were measured by LC/MS to evaluate the overall charge state of present peptides. Fractions with similar overall charge state were pooled together, as summarized in Supplemental Table 5. From 13 initial fractions, after pooling, only 5 fractions were present (2 and 3, 4-7, 8-10, 11 and 12, 13), while original fraction 1 was discarded.

Later, the pooled or not fractions were again, individually, fractionated in the SCX system and recollected to enrich original protein N-termini (Supplemental Figure 3b). Samples were then LC/MS measured for further peptide identification. Only peptides present in all 3 biological replicates were considered. During the data analysis, each peptide had individually abundances normalized, wherein a median of the intensities of the iTRAQ reporter ions from every channel was calculated,

and posteriorly each individual reporter ion intensity was divided by the median, creating normalized abundances for each channel.

To combine the data from all biological replicates, each condition had normalized abundance values averaged, e.g. the peptide VNYTDDIkQSASATR from the protein PFK1 had abundance values of 0.99, 0.72 and 0.81 in biological replicates 1, 2 and 3 respectively, and a final value of 0.81 (average of the 3 values) after combining the 3 datasets. Three comparisons were performed, always between the MAS1 x wild type for all time points (0 h, 2 h and 4 h). For each comparison, a volcano plot was performed to evaluate protein regulation, considering a 2-fold difference as regulation (p value $\leq$ 0.05). As discussed previously, proteins regulated in the 0 h comparison were discarded if present in the other comparisons, once these proteins could be false positives induced by the gene modification to create the MAS1 mutant.

Since the objective is to observe possible changes in the yeast proteome, it was analyzed both up and down-regulated proteins. The volcano plot of the time point zero indicated a total of 52 down-regulated proteins (AAT2, GRS1, TPI1, YIM1, TVP15, OYE3 ,RPS9B ,YER159C-A ,SNA2, SBA1, ATP2, RPN10, GCD11, AMS1, SNF7, JEN1, OM45, GCV2, IDI1, LAP3, RTN2, PDR5, TOM20, NEW1, RPS20, YOS1, RPT4, VAS1, SAC6, CPA2, RPN2, RPL33A, COB, GUP1, ERG9, YCL057C-A, ATO3, HSC82, RPL33B, AYR1, CTT1, GLC3, SOD1, PRB1, EFT2, PFK1, PIL1, HSP12, RPP0, FMP45, IRA2, MIA40) and 14 up-regulated proteins (ILV5, CDC19, , HXK2, SSE1, ACS2, , RPL3, NDE1, TEF2, PCK1, SAH1, SSB2, RPL7A, MET6, RPS24A) (Supplemental Figure 4a and Supplemental Table 6). Those proteins were unconsidered if present as regulated in the other two comparisons. Still, the amount of regulated proteins was higher than expected. Possibly is due to a dynamic variation between samples during non-harsh conditions. The volcano plot of the 2 h comparison resulted in 44 down-regulated proteins, in which only 17 pass the criteria discussed above (HSP60, HSP104, PUP2, YPR160W-A, PRO2, GSY2, PRE9, CYC8, SEC27, HSP82, HSP30, TCB1, RPL32, YSC84, PYC1, HSP26, GRE1) and 4 up-regulated protein, in which only one pass the criteria (RPL16A) (Supplemental Figure 4b and Supplemental Table 7). The volcano plot of the 4 h comparison resulted in no down-regulations and 15 up-regulations, in which 13 pass the criteria (SSC1, RRP7, RPS3, SSZ1, SSA1, SSA2, PUB1, PMA1, RLI1, PFK2, RVB2, CMD1, KEL1) (Supplemental Figure 4c and Supplemental Table 8).

At first, it was expected to see differentially regulated proteins from the fermentation energy production pathway, once mitochondrial energy production would be impaired by lack of essential components of the respiratory chain, since the MPP would fail to mature proteins directly or

indirectly involved in mitochondrial energy production. A failed energy production into the mitochondrion could have forced a change in the energy production pathway, pushing energy production to a level in which there is no necessity of the discussed organelle.

What is actually observed and controversial is the down-regulation of heat shock proteins in 2 h MAS1 mutant samples and, at 4 h, an up-regulation of another set of heat shock proteins. Also, none of the proteins up or down-regulated at 2 h appear regulated at 4 h and vice-versa, lacking of continuity (upscaling or downscaling) the protein amount through time. The protein HSP60, for instance, had 28 peptides identified, in which only 1 peptide presented a regulation. The similar phenomenon happens with the protein HSP82, in which 11 peptides were identified and only one was regulated. In both cases, the regulated peptides are far away from the position that could suggest them as a signaling sequence. This incongruence is observed to other proteins as well, not mattering if up or down-regulated at any time point. Since only one peptide could be observed as regulated, could be due to a false-positive identification or co-isolation with other peptide ions during fragmentation, generating biased reporter ion intensities. Due to the impossibility to obtain any reliable data from this experiment, it is only possible to conclude that for large-scale proteome analysis, the ChaFRADIC method is ineffective, serving so far to identify protease subtracts as presented here and before [149]. Another specific experiment could have been performed instead of the ChaFRADIC to analyze the proteome data. For the purified mitochondria, a global analysis was performed, in which more confidently the proteomic data was analyzed.

8.1.3 Mitochondrial MAS1 global proteome

As explained in chapter 8.1.2, a change of the yeast proteome could happen due to a non-functional MPP at the mitochondrion, taking into consideration that the peptidase is essential for cell viability. To evaluate the mitochondrial proteome, a similar approach of the ChaFRADIC was adopted. For each condition of each biological replicate, samples were digested, TMT labelled and pooled. An aliquot of the pool of each biological replicate was fractionated using a high pH reversed phase setup, and fractions were LC/MS measured for protein identification and quantification.

Similar as performed for the ChaFRADIC samples, but now for proteins, only proteins identified in all biological replicates were considered. The data was combined doing the average of the normalized abundance ratios for each protein. The protein reporter ion intensity is just the sum of all reporter ions of all identified unique peptides correspondent to that protein. Later, normalized abundances values were calculated using the same steps as performed for the ChaFRADIC experiments.

The proteome was evaluated for possible regulations. Again, volcano plots of the mutant against the wild type were created for all time points. A 2-fold regulation determined up or down-regulations ($p \leq 0.05$). Any protein regulated in the time point 0 h were not considered if present as regulated in time points 2 h and 4 h. The volcano plot of 0 h presented 2 down-regulated proteins (YJL045W and FMP16) and 3 up-regulated proteins (TOP2, HTZ1 and RVB1) (Supplemental Figure 5a and Supplemental Table 9). Not considering the regulated proteins in 0 h, the 2 h volcano plot presented 3 down-regulated proteins (PMA2, RTN2 and HSP12) and 2 up-regulated proteins (YLR307C-A and HTB1) (Supplemental Figure 5b and Supplemental Table 10). Not considering proteins regulated at 0 h, the 4 h volcano plot presented 4 down-regulated proteins (PMA2, TAT1, RTN2 and HSP12) and 3 up-regulated proteins (YLR307C-A, SPG5 and ADK2) (Supplemental Figure 5c and Supplemental Table 11).

It is possible to observe that both 2 h and 4 h have a good agreement between down-regulated proteins, while matching only one up-regulated protein. In the universe of over 1100 identified proteins, including non-mitochondrial proteins, it was expected to have higher regulation in other proteins involved in the MPP pathway or proteins that could indirectly be regulated to compensate the unbalance caused by the impaired MAS1 mutant. The protein PMA2 has been reported already as a contaminant often found in mitochondria [24,64], and regulation could be just a matter of different amounts of the protein co-purified with the mitochondrion. RTN2, HSP12, HTB1, SPG5 and TAT1 are also proteins not described as mitochondrial or with low confidence, suggesting a possible contamination during purification of the

mitochondria. Since YLR307C-A was not yet described, only ADK2, a GTP:AMP phosphotransferase, could have been a protein affected by an impaired MPP. Still, this protein was not identified in highly purified mitochondria of the largest study of mitochondrial proteome distribution in the subcompartments [173]. It seems that the proteome is stable even after the 4 h mitochondria with an impaired MPP complex. A better evaluation could occur after a long exposure to non-permissive conditions, in which more changes might happen in the proteome. A protein correlation of the regulated proteins with the proteins MAS1 and MAS2 performed by the STRING software was analyzed with the intention to observe if the considered false-positives could have any kind of relation with the MPP, but still no relation was present (Figure 18).

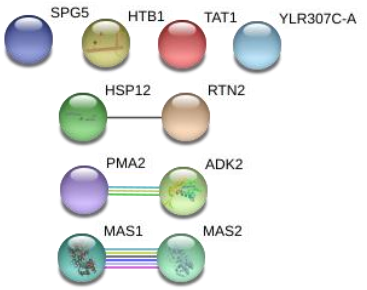

Figure 18.Correlation of the proteins founded as regulated in the mitochondrial global proteome analysis. Proteins found as regulated on the time point 0 h were not considered when found as regulated in the 2 h and 4 h comparison. MAS1 and MAS2 were not found as regulated, but added just to evaluate possible relationships with the proteins found as regulated. If any relationship between the MPP and the other regulated proteins was present, a line would connect the "found as regulated" proteins with MAS1 or MAS2. Still, no observable relation between the proteins and MAS1 or MAS2 is present, what could indicate false positive regulation of the proteins.

Those results could have raised questions about the real efficiency of the MAS1 mutant as functional. Interestingly, MAS1 was down-regulated in both 2 h and 4 h time points of the mitochondrial ChaFRADIC experiments (Supplemental Figure 2b, c) and appear to be down-regulated in the proteome analysis in both time points as well, with a ratio between the abundances of MAS1 mutant against the wild type of 0.63 and 0.64 (respectively 2 h and 4 h) and a stable ratio of 1.07 in the time point 0 h. In that sense, it possible to observe a down-regulation of MAS1 in the mutant, confirming an impaired MAS1 protein after the temperature shift. The MAS1 abundance reduction after 2 h appears to be stable until 4 h, what could indicate a lower MAS1 protein turnover once there is no import of new functional MAS1 protein to replace old but active MAS1 proteins. Other protein component of the MPP, MAS2, had ratios between the mutant and wild type of 0.95, 1.03 and 0.97 (time points 0 h, 2 h and 4 h respectively). A lower appearance of the MAS1 in the mutants did not affected the presence of the MAS2. Together with the high stability of the proteome, MAS2 could be performing protein maturation alone and only specific proteins might require

the full MPP for maturation. In that line of thinking, two extra experiments would be necessary, longer non-permissive time point incubation to evaluate further/different regulations and a full knockout of the MAS1 gene to observe the changes in the mitochondrial, and possibly the whole yeast, proteome.

8.1.4 Mitochondrial MAS1 mutant phosphoproteome experiment

Little is known about protein import regulation by means of phosphorylation, limiting the knowledge only to outer membrane import proteins. For instance, during fermentative energy production, the protein kinase A (PKA) is active and phosphorylates TOM70 (at serine 174), TOM22 (at threonine 76) and TOM40 (at serine 54), impairing protein import into the mitochondria by inhibiting receptor activity and decreasing precursor protein binding to the TOMM complex or by impeding biogenesis of the TOMM complex into the outer membrane. This occurs probably due to a lesser necessity of the organelle for energy production [179-183]. On the other hand, casein kinase 1 (CK1) phosphorylates TOM22 at position threonine 57 promoting biogenesis of the TOMM complex into the outer membrane [179]. This dual signaling events might occur because even in cases of fermentation energy production, the mitochondria still exert vital functions for the yeast, such as iron-sulfur cluster biogenesis, independently on the energy production metabolic pathway [184]. This demonstrates the complex signaling events happening concomitantly in order to maintain cell homeostasis during different conditions [183].

Due to this knowledge, before analyzing the mitochondrial phosphoproteome of an impaired MAS1 mutant, it was expected different levels of phosphorylation on TOMM components, in special the ones cited above[185]. Besides that, it was taken into consideration possible other phosphorylations that could be differentially regulated an impaired MPP.

Following the data analysis steps procedures performed for both ChaFRADIC and global proteome experiments, the same was applied for the phosphoproteome. In that sense, for each biological replicate, after each condition digestion, samples were TMT labeled, pooled in a ratio of 1:1 and phosphopeptide enriched and fractionated prior LC/MS with TiO_2/HILIC. After phosphorylated peptide identification with a phosphorylation site localization of at least 99% confidence, data from all biological replicates were combined, in which exact equal peptides in amino acids sequence, phosphorylation site and possible other modifications had normalized abundance values averaged. A volcano plot with a 2-fold regulation as threshold was performed for all time points, and phosphopeptides regulated in time point 0 h were unconsidered if regulated in time points 2 h and 4 h.

The time point zero (0 h) volcano plot presented 18 and 99 down and up-regulated phosphorylation sites respectively (Supplemental Figure 6a and Supplemental Table 12). The 2 h volcano plot presented 17 and 3 down and up-regulated sites respectively (Supplemental Figure 6b and Supplemental Table 13). The 4 h volcano plot presented 27 and 22 down and up-regulated site respectively (Supplemental Figure 6c and Supplemental Table 14). It is remarkable the amount of regulations present in the 0 h comparison. This is due to the high sensitivity of the mass spectrometer that is able to acquire even low abundant peptides. For instance, from the 99 up-regulated sites in the time point 0 h, they belong to 77 proteins, in which only 10 are mitochondrial, meaning that the other 67 are probably contaminants that were still identified. In the best-case scenario where no other than mitochondrial proteins should be present, the contaminants might have been co-purified with the organelle in different amounts between the mutant and wild type, causing the notable effect of many non-mitochondrial proteins with regulations.

It was previously expected to see phosphorylation changes in TOM70, TOM40, TOM22, but Table 14 and Table 15 that present all identified regulated phosphorylation sites in time points 2 h and 4 h do not show any of those proteins present. Only TOM71 appears to be regulated at time point 2 h, but same effect is not observable at time point 4 h, in which regulation must be further confirmed with further experiments targeting this specific site. The relevant phosphorylation sites of the three proteins cited first were further investigated if they appeared in any of the biological replicates, since it could not be present in time point 0 h, but present in time points 2 h and 4 h demonstrating a possible regulation. Still, no evidence of this sites was identified, suggesting either no regulation or no mass spectrometer identification.

Table 14. Down-regulated phosphorylation sites observed in the MAS1 mutant when compared to the wild type at time points 2 h and 4 h. Values presented are shown in log2. Standard deviations (SD) where calculated on the log2 values of the protein ratios. In addition, it is identified if the protein is known as mitochondrial or not.

Protein	Phosphorylation site	2 h	SD	4 h	SD	Mitochondrial
ALR1	S176	-1,85	0,08	-1,46	0,01	no
BUD4	S149	-1,00	0,10	-	-	no
ECM21	S33	-1,32	0,07	-1,41	0,07	no
EFR3	S570	-1,01	0,09	-1,26	0,04	yes
EFR3	S564, S570	-	-	-1,02	0,13	yes
FLC1	S713	-	-	-1,06	0,12	no
FRE7	T517, S519, S522	-	-	-1,08	0,12	no
HBT1	S218	-1,83	0,10	-2,05	0,07	no
HBT1	T731	-1,54	0,14	-1,51	0,07	no
JIP4	S726	-1,07	0,08	-	-	no
JIP4	S86	-1,22	0,07	-1,01	0,06	no
LSP1	T233	-	-	-1,09	0,04	yes
MRH1	S299	-	-	-1,03	0,10	yes
NTE1	S634	-1,39	0,10	-1,14	0,07	no
PDR5	S70	-	-	-1,05	0,18	yes
PIL1	S163	-	-	-1,03	0,08	yes
PRM5	S268	-1,18	0,12	-1,04	0,08	no
RGD1	S336	-	-	-1,04	0,08	no
RTN2	S278	-1,37	0,09	-1,44	0,10	no
SBH1	S35	-	-	-1,16	0,12	no
SLM1	S533	-1,03	0,08	-1,15	0,10	yes
SLM1	S536	-1,48	0,03	-1,66	0,11	yes
TAT1	S13, S20	-1,32	0,07	-1,55	0,07	no
TAT1	S84	-1,32	0,14	-1,19	0,07	no
TCB3	S128	-	-	-1,05	0,07	yes
TCB3	S88	-	-	-1,11	0,10	yes
YDR348C	S439	-1,26	0,06	-1,07	0,07	no
YFL042C	S149	-	-	-1,19	0,11	no
YOP1	S20	-	-	-1,05	0,13	no
YPL150W	S620	-1,07	0,11	-	-	no

Table 15. Up-regulated phosphorylation sites observed in the MAS1 mutant when compared to the wild type at time points 2 h and 4 h. Values presented are shown in log2. Standard deviations (SD) where calculated on the log2 values of the protein ratios In addition, it is identified if the protein is known as mitochondrial or not.

Protein	Phosphorylation site	2 h	SD	4 h	SD	Mitochondrial
MRH1	T295	1,38	0,08	-	-	yes
NUP53	S372	1,15	0,12	-	-	no
TOM71	S55	1,02	0,03	-	-	yes
ALD4	S56	-	-	1,54	0,07	yes
CIT1	S462	-	-	1,86	0,11	yes
COX6	S41	-	-	1,14	0,05	yes
FBP1	S12	-	-	1,08	0,13	no
FRT1	S34	-	-	1,02	0,08	no
GAT1	S288	-	-	1,59	0,14	no
HRK1	S661	-	-	1,02	0,04	no
HSP60	S141	-	-	1,01	0,05	yes
IES4	S28	-	-	1,15	0,09	no
ISW2	T774	-	-	1,54	0,15	no
MRH1	S289, T295	-	-	1,46	0,14	yes
NUP53	S369	-	-	1,10	0,10	no
RCO1	S683	-	-	1,06	0,12	no
RPH1	S689	-	-	2,14	0,19	no
RTG3	S246	-	-	1,79	0,09	no
STF2	S69	-	-	1,24	0,12	no
TAF4	S80	-	-	1,25	0,12	no
VHS2	S84	-	-	1,89	0,06	no
WHI2	S131	-	-	1,10	0,09	no
YAT2	S786	-	-	1,05	0,11	no
YDR186C	S692	-	-	1,06	0,05	no
YDR348C	T436	-	-	1,31	0,16	no

Some proteins presented in the table above are listed as mitochondrial [173] with reservations, once data was not entirely conclusive. Since it was not possible to find further support whether proteins are mitochondrial or not in this study, they were not considered for the next evaluation step. Protein correlation was created using STRING for the mitochondrial down and up-regulated proteins from Table 14 and Table 15, in order to evaluate possible connections between the phosphoproteome and the MPP (Figure 19).

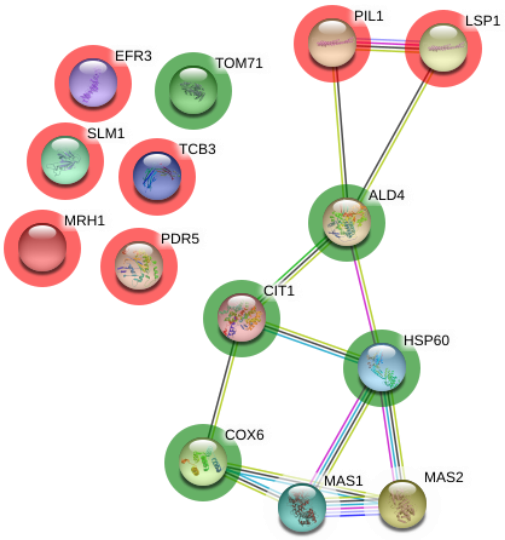

Figure 19. Using the STRING software, correlation from the proteins with up (green) and down (red) regulated phosphorylation sites from the MAS1 mutant phosphoproteome experiment. Interestingly is possible to observe a network concerning most of the proteins with up-regulated phosphorylation sites, in which the MPP could influence signaling events by phosphorylation. MAS1 and MAS2 proteins were included just to observe possible interaction with the proteins.

It is immediately possible to observe a connection between most of the up-regulated proteins phosphorylation sites to the MPP. The biological reason of the phosphorylation sites is yet unknown, once phosphorylations can both increase of decrease protein activity. Active PIL1 and LSP1 have been shown to down-regulate the PKC1-MAP kinase pathway and protein kinase YPK1 pathway, both important for cell growth and proliferation [186]. The down-regulation of both phosphorylation sites might be a signaling event to control cell growth and proliferation in a not partially functional mitochondria due to an impaired MPP. Interestingly, SLM1 protein is phosphorylated and active by the TORC2 complex under favorable growth conditions. TORC2 complex is part of the downstream signaling pathway of the YPK1 kinase [187,188]. This finding suggests that, since SLM1 phosphorylation sites are down-regulated, the cell has no favorable growth conditions, in which PIL1 and LSP1 are active and not phosphorylated, down-regulating the PKC1-MAP and YPK1 pathways. In a certain way, this regulations might influence cell energy production by up-regulation of COX6 and CIT1, but still the biological reason is not yet understood and requires further specific studies. PDR5 has been associated to detoxification of the cell during exponential cellular growth[189]. This suggests that PDR5 is only active when phosphorylated, since the cell appears to not be currently under growth and PDR5 has a phosphorylation site that is down-regulated. Curiously, TCB3 and MRH1 have been previously reported as phosphorylated in regular mitochondria [68], but under the current situation appear to be less phosphorylated, in which cause might be related to the MPP.

Yet, this study was mainly to characterize possible protein and pathways candidates that are in any level related to the MPP pathway. With a list of possible candidates, supported by literature knowledge, further laboratorial experimental strategies must be applied to increase knowledge and confidence in the findings brought to light in this study. In that way, to overcome the limitations that exists in mass spectrometry, different strategies were developed to give a boost in such kind of studies. The strategies with method validations are further described in this thesis.

8.2 Subtilisin experiments

First, HeLa cells and A431 cells were selected due to high knowledge about the cell's characteristics obtained from various other studies using human cell lines, besides the easiness to work with those cell lines in matter of cellular growth, replication and material amount, turning them a hand-on for methodological studies. Both are cancerous cell, originally from cervix [190] and skin [191] cancers, respectively, and further information can be retrieved from the Humam Protein Atlas [192-194] and their website "www.proteinatlas.org".

The subtilisin protease has been used for a diverse amount of proteomic experiments, but so far, no one has characterize specificities of this broad specificity enzyme, as much has already been done for extensive used specific proteases, as trypsin, GluC, ArgC, LysC and others. Since it was observed the potential use of the subtilisin to increase knowledge of the proteome, due to its interesting observable characteristic of the lack of specific site for cleavage as observed for the enzymes cited above. In the sense, no matter how many times one digests a specific proteome with one of the specific enzymes, in theory, the obtained peptide proteome for further analysis by mass spectrometry remains the same. Only advances in instrument technology that may be a gain to increase knowledge of the proteome and, consequently the post-translational modifications (PTMs) associated with the proteome.

Since it was not observed for subtilisin the same characteristics as for trypsin, such as specific site cleavage and some digestion efficiency impairments, and since subtilisin has no amino acid site digestion specificity, proteomes digested with this broad specificity enzyme could generate peptides suitable for mass spectrometry that is not possible to obtain after tryptic digestion. Consequently, PTMs from those new available peptides would be newly identified, what could boost the knowledge in mitochondria signaling pathways mediated by PTMs.

In that sense, first was necessary to bring to light subtilisin characteristics to use it in an efficient and reproducible way, and, obviously, to verify to the real compatibility with mass spectrometry. The experiment using different quantities of guanidine hydrochloride (GuHCl) was performed to verify possible limits of the chaotropic agent to sample digestion. High concentrations of GuHCl is commonly used to resuspend cell pellets into the solution and to preserve an unfolded protein shape, in order to facilitate enzymatic attack of the proteins. High concentrations indeed help resuspending cell pellet, but as well inactive the enzyme for the digestion, and reducing GuHCl concentration allow proper enzyme efficacy.

Always comparing subtilisin with the already well studied trypsin, triplicates of HeLa cell lysate in solution with the presence of 0.2, 0.5, 1.0, 2.0 and 4.0 M GuHCl were incubated with trypsin or subtilisin, always individually (Figure 20).

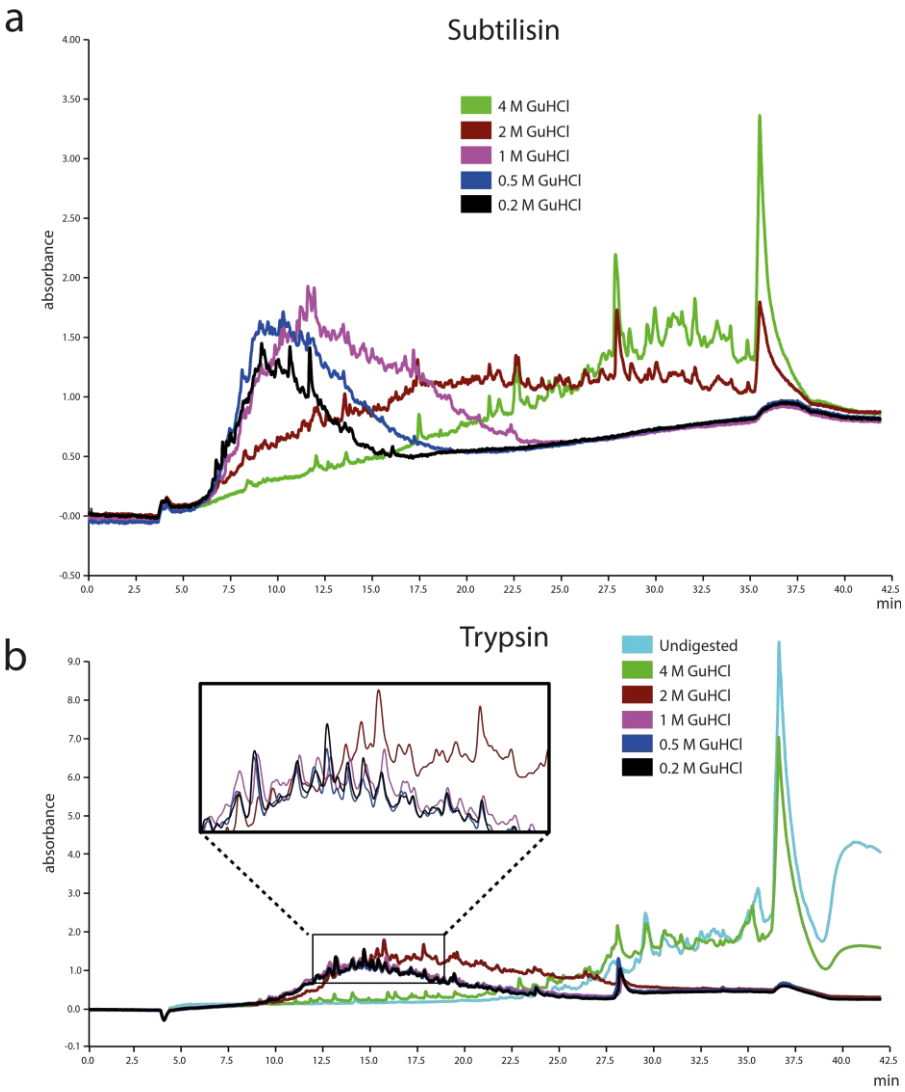

Figure 20. Monolithic HPLC chromatogram of HeLa cell lysate digested with (a) subtilisin and (b) trypsin, respectively, in the presence of 0.2 M, 0.5 M, 1 M, 2 M and 4 M guanidine hydrochloride (GuHCl) in digestion buffer. Trypsin chromatogram contain undigested HeLa.

The monolithic chromatograms indicate, in general, the degree of peptide/protein length. Normally, longer the amino acid chain, higher is the chance to be present hydrophobic amino acids, increasing the interaction between hydrophobic column and molecule. In that sense, usually smaller peptides elute earlier than longer peptides, and proteins elute at the end of the gradient. Until the minute 25th from the monolithic chromatogram, the UV signals can be considered as peptides, and after the minute 25th, mainly longer peptides or proteins, not suitable for MS analysis.

In Figure 20, it is possible to observe that subtilisin efficiently digests until 0.5 M GuHCl concentration and efficiency decreases up to 1 M GuHCl. Meanwhile, trypsin is functional up to 1 M GuHCl. For both proteases, 4 M GuHCl almost totally impair digestion activity. Since the optimized lab protocol for in-solution digestion with trypsin is set to a concentration of 0.2 M GuHCl, and subtilisin as well obtained an efficient digestion with that GuHCl concentration, 0.2 M was chosen for the further experiments involving subtilisin.

With the idea that subtilisin has no amino acid cleavage specificity [115], digestion could occur faster than the specific cleavage site proteases, due to the lack of necessity of finding specific amino acids in the protein composition. For that reason, HeLa cells were digested for 1, 5, 10 and 20 min (Figure 21).

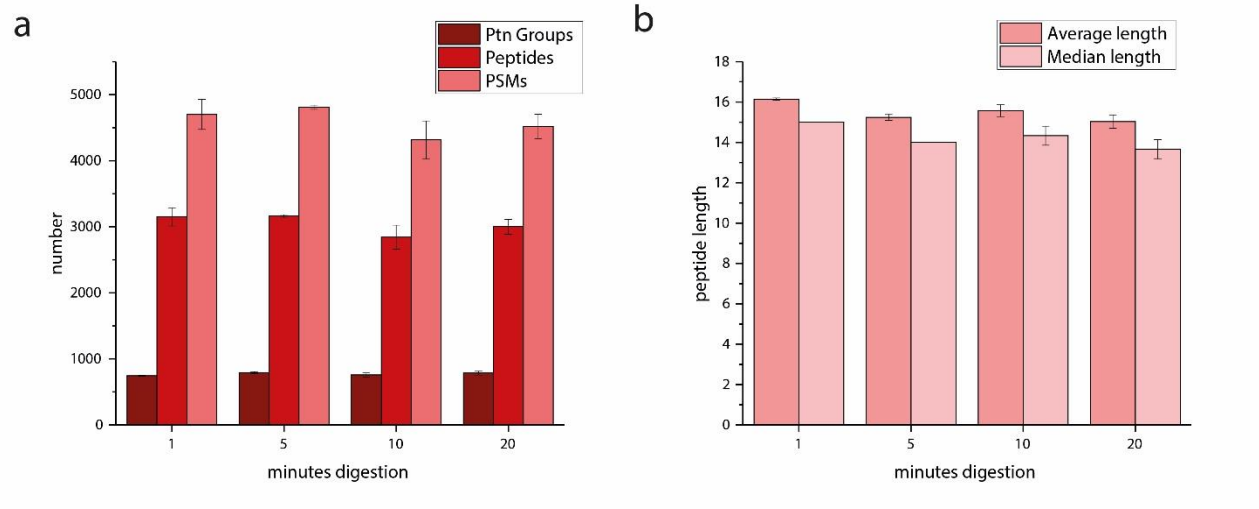

Figure 21. HeLa incubated with subtilisin with different time points. a) HeLa cell lysate digested with subtilisin for 1, 5, 10 and 20 minutes in triplicates. Protein groups, peptide and peptide spectral matches (PSMs) after Proteome Discoverer 2.2 search are displayed. b) Average and median peptide length of each time point.

Incredibly, efficient digestion of HeLa cell lysate was possible down to 1 min incubation with subtilisin (Figure 21a). Usually, digestions using the common proteases for bottom-up mass spectrometry take a period between 9 to 24 h until reaction is finally stopped and sample is digested. Subtilisin is possibly the fastest enzyme for efficient sample digestion ever reported in the literature [195], taking into consideration the ratio of 20:1 between sample and enzyme.

Burkhart et al [196] observed that trypsin generated optimal average peptide length for bottom-up mass spectrometry, of approximately 14 amino acids long. In good agreement with trypsin, the average subtilisin peptide is ~15 amino acids after incubation times of 5, 10 and 20 minutes (Figure 21b), while only 1 min incubation time generates longer peptides, much likely due to the short digestion time. It is also possible to observe one amino acid difference between the median and average peptide length. This occurs because the average takes into account all peptides lengths, meaning that if there is too short or too long peptides, it will influence the result. Meanwhile, the median takes only the middle value from all values, avoiding interferences from outlier values. If the median and average are close, it means that the dataset is evenly distributed.

Albeit being a broad specificity enzyme, subtilisin digestion reproducibility was evaluated. For large scale proteomics works, it is necessary to have reproducible system in order to be possible to replicate experiments. To evaluate the reproducibility, subtilisin reproducibility rates were compared to trypsin, in which the peptides of 3 individually digests of HeLa lysate from subtilisin (0.2 M GuHCl) and 3 digests of trypsin were plotted, per enzyme, in a Venn diagram (Figure 22).

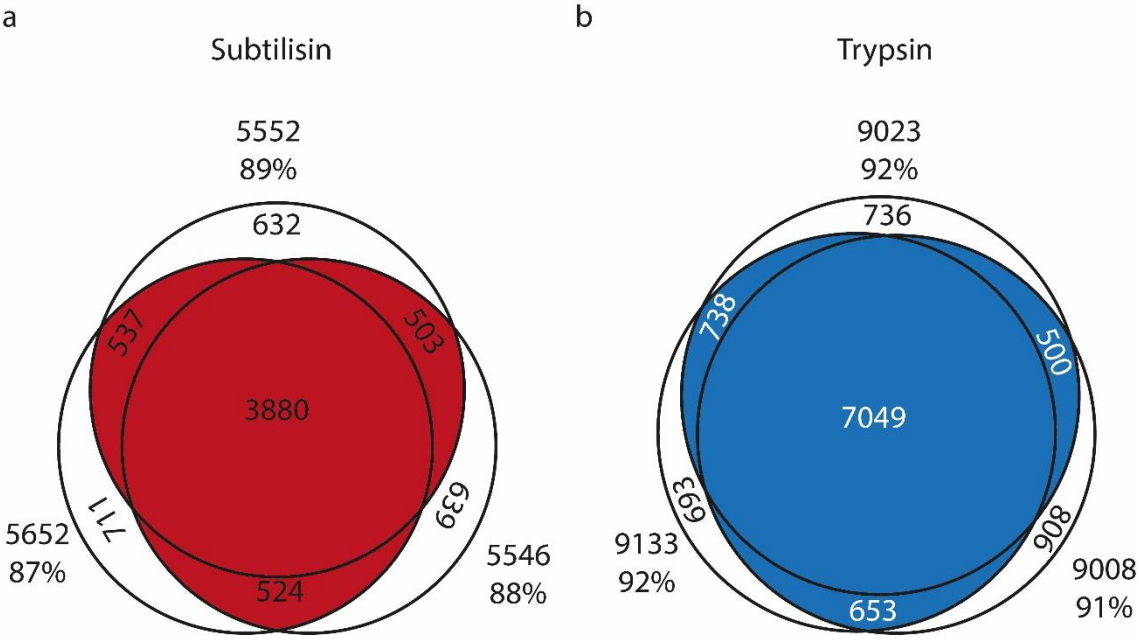

Figure 22. Enzyme reproducibility. HeLa cell lysate aliquots individually digested with subtilisin or trypsin in triplicates for each enzyme, in the presence of 0.2 M GuHCl. Aliquots were LC/MS measured and generated peptides (protein accession plus amino acid sequence, e.g. Q8TDD5; SCSSHEEENRCNFN) from each individual digestion of (a) subtilisin and (b) trypsin were compared by Venn diagram. Peptides present in at least 2 out of 3 replicates (red and blue area) were considered for the reproducibility rate.

Always taking into consideration the peptides present in at least 2 out of the 3 replicates, subtilisin presents a comparable reproducibility rate to trypsin. The reproducibility of a replicate is calculated by the number of peptides present in at least 2 out of 3 replicates, divided by the total identified peptides from this replicate. Subtilisin presents an average of 88% reproducibility (Figure 22a) between the 3 replicates, while trypsin has an average of 92% (Figure 22b). It was already expected a better performance of trypsin, due to specificity on digestion, but subtilisin surprised with high rates. By those results, it has been later investigated if subtilisin had some amino acid cleavage preference during digestion.

In Figure 22 it is still perceptible that trypsin yields a higher identification of peptides than subtilisin. This probably derives from single shot MS analysis, in which there is an undersampling of peptides due to high amount of similar peptides generated by subtilisin. Another explanation might be general Mascot ion score given by the search algorithm, wherein higher is the score, more trustable is the identification. Generally, subtilisin identifications presents lower ion scores than trypsin, probably due the beneficial presence of positive charges present in both C- and N-terminal of the tryptic peptide and also optimized search algorithms for trypsin (Figure 23).

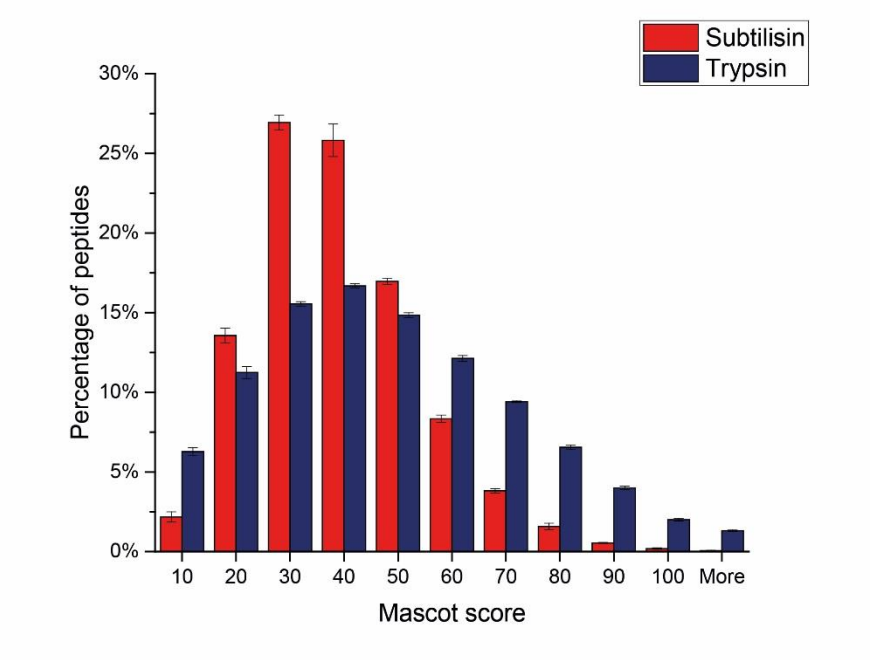

Figure 23. Histogram of peptide score distibution of subtilisin (red) and trypsin (blue) from reproducibility dataset. Tryptic peptides tend to receive better scores from Mascot.

Observed in chromatograms, e.g. the monolithic chromatograms in Figure 20, subtilisin peptides tend to have a lower hydrophobicity than tryptic peptides, what makes a big amount of peptides elute together at the beginning of the gradient, meanwhile tryptic peptides are more evenly distributed by the

throughout the gradient, allowing a lower sample complexity for MS analysis. In that sense, gradient for subtilisin samples were further adapted to improve peptide identification.

Beside the aforementioned issues, single shot LC/MS measurements proved to be too complex for optimal subtilisin peptide identification, due to complex digests including the presence of overlapping peptides (peptides that differ by only one, two or more amino acids) decreasing sensitivity and increasing undersampling[195]. For that reason, the next step was to evaluate subtilisin for in depth (phospho)proteome by lowering sample complexity with high pH reversed phase fractionation.

For this, two aliquots of 25 µg of A431 cell lysate were digested one with subtilisin and the other with trypsin. After digestion, samples were fractionated by high pH reversed phase fractionation, resulting in a total of 20 fractions per enzyme. Fractions were measured by LC/MS and proteins identified with a FDR $\leq$ 1% on the protein level.

Not surprisingly, trypsin yielded a higher identification of proteins (8,363 vs 6,807), peptides (99,127 vs 77,194) and PSMs (164,827 vs 103,837) than subtilisin due to probably undersampling, as explained earlier in this chapter (Figure 24a). Still, it is immediately possible to observe that subtilisin yields already an increase of 283 unique proteins not found in the trypsin dataset.

Checking the proteome more intrinsically, it was possible to observe an interesting “enrichment” of proline amino acids (Pro) in the subtilisin dataset (Figure 24b). The human Uniprot proteome was screened to determine the position of a proline within the protein. Since the distribution of the proline is not contiguous in the protein and varies from protein to protein, the kernel density estimation appears as a tool to estimate the unknown probability distribution of proline. The kernel density function was calculated using the position vector of all prolines from the protein. The calculated kernel density function was multiplied by absolute number of Pro within the protein, resulting in the measure of the density of prolines (bandwidth = 10, n= 16,384). Regions in which the density was higher than 0.2 were considered proline rich regions, accounting approximately for at least 25% of the Pro within 25 amino acids. The proline prot was created concentrating in the same area the Pro dense regions, as indicated by the color gradient scale. Since trypsin is impaired when the proline residue is in the vicinity of the cleavage site [197], it might reduce the amount of this peptide residue in the identified proteome composition. In the other hand, by the amount of Pro found in the subtilisin dataset, it does not cause any ineffectiveness of the enzyme or the different amount cleavage sites persecuted may overcome the limitation caused by the proline residue.

The Global Proteome Machine [198] proposed in their website (www.thegpm.org, 12th January 2017) a set of proteins that can be an indicative of how well the preparation protocol was performed to achieve peptides from integral membrane proteins. Those proteins are 13 mitochondrially expressed proteins, i.e. proteins encoded by the mitochondrial DNA and translated in the matrix by mitochondrial ribosomes. The proteins belong to the respiratory electron transport chain and are necessary for the oxidative phosphorylation, and some parts of the proteins domains are considered one of the most hydrophobic of the human proteome. Nine out of the 13 described proteins were better recovered after subtilisin digestion, indicating subtilisin as a possible powerful tool to achieve a higher proteome coverage of hydrophobic proteins by LC/MS (Figure 24c).

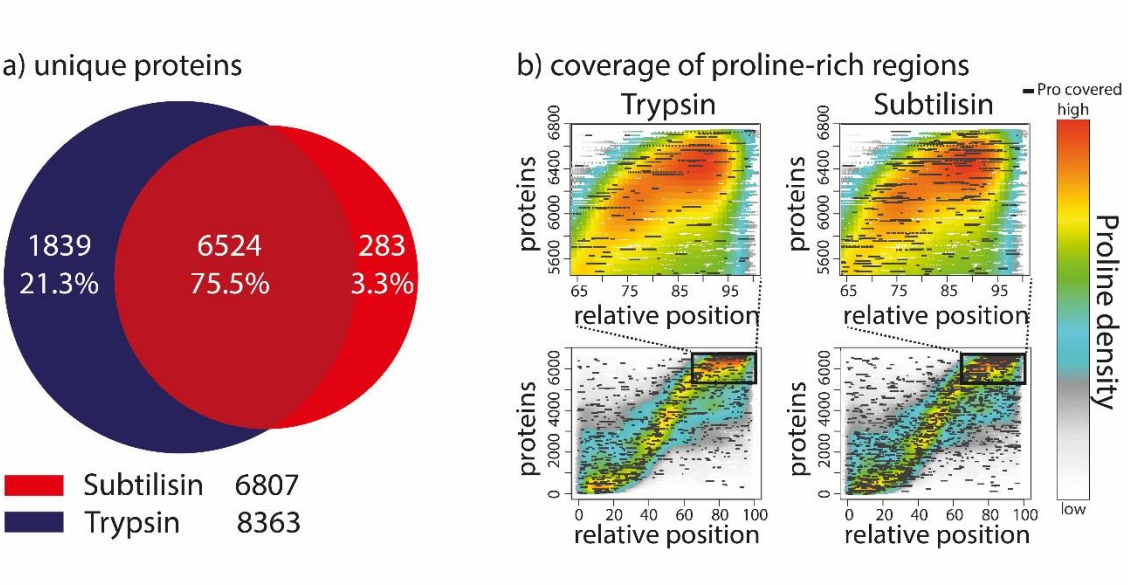

Figure 24. Proteome of the A431 cell line evaluated after subtilisin digestion. (a) Comparison between proteins with at least 1 unique peptide identified by trypsin and subtilisin. (b) Proline-rich regions are more frequently identified after subtilisin digestion, with the proline amino acid being identified twice more with subtilisin than trypsin (36,857 x 20,484). (c) Improved identification with subtilisin of mitochondrial integral membrane proteins from the reference set of proteins proposed by the Global Proteome Machine (GPM) to evaluate digestion efficiency.

The subtilisin peptide dataset was evaluated by iceLogo[199] to identify possible cleavage consensus amino acids. The software iceLogo[199] uses probability theory to identify conserved patterns in a protein or peptide

sequence. From the high confidence identified peptides, the five last amino acids of the sequence, including the C-terminal amino acid, was compared to the last 5 amino acid of all other identified peptides to possibly identify a pattern in the cleavage are. As well, the same procedure was performed for the 5 first amino acids after the cleavage site of the identified peptide (Figure 25). Indeed, differently from trypsin that lysine and arginine predominate in the position 4, subtilisin present a diverse set of amino acids at the cleavage site, presenting amino acids with different chemical properties. Nevertheless, after the cleavage site, subtilisin present a preference for acidic amino acid residues, the aspartic (D) and glutamic acid (E) and the nonpolar proline amino acid (Figure 25). This indicate that subtilisin might has a bigger affinity for acidic regions to perform the cleavage. In addition, the high presence of proline might be the reason for the higher amount of peptides containing proline residues than trypsin (Figure 24b).

Subtilisin yielded the identification of a protein classified as “missing protein”, in the sense of proteins not yet highly confident identified by mass spectrometry as demanded by the guidelines of the Human Proteome Organization [200-202]. To achieve the status of “evidence at the protein level”, a protein should be identified by mass spectrometry with FDR 1% at the protein level, at least 2 unique peptides with no less than 9 amino acids long and make the spectra of the identified peptides available. The peptides should not overlap each other as well. Meeting all this criteria, a proteoform of Mucolipin-3, a nonselective ligand-gated cation channel, has been detected with 3 unique peptides (^{185}CFFVEPDEPFHIG^{197}, ^{539}LEDDPPVSLF^{548} and ^{10}SCSSHEEENRCNFN^{23}) (Figure 26).

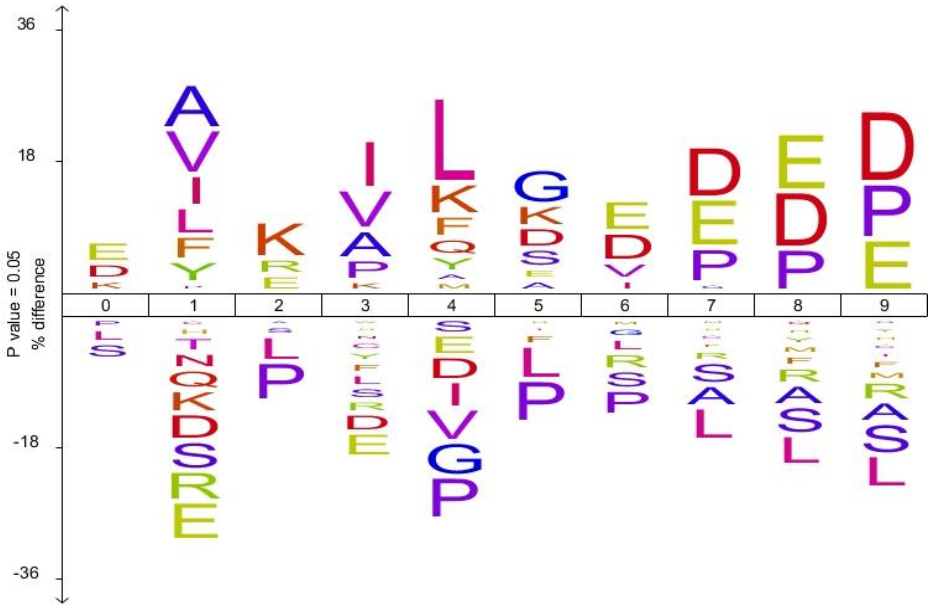

Figure 25. IceLogo of the peptides from the in-depth subtilisin proteome dataset. It is possible to observe the trend of amino acids around the cleavage site. Amino acids from the position 0 to 4 indicate the most frequent (above) and less frequent (under) amino acids in the relative position of the cleavage site, C-terminal position indicated by position 4. Amino acids from 5 to 9 are the most or less frequent amino acids after the cleavage site, being the position 5 the new N-terminal after the cleavage site. In that way, IceLogo indicates a preference of subtilisin for cleavage after a few specific amino acids (indicated in position 4) and a bigger affinity for acidic amino acids after the cleavage site.

The subtilisin and trypsin peptides were searched against the whole Peptide Atlas [86] repository of human proteins, accounting for 1,222,862 peptide sequences (October 2017). Subtilisin increased the sequence coverage of 3,636 proteins, corresponding to an increase of 0.40% of human proteome coverage yet identified by mass spectrometry experiments. In the other hand, trypsin could increase the sequence coverage of 1,652 proteins, corresponding to an increase of 0.15 % of the human proteome coverage. Since subtilisin is so far a proper tool for MS, the results were expected, once there is already a saturation of new sequences generated after trypsin digestion.

Next, subtilisin was evaluated for its compatibility for large scale phosphoproteomics. Aliquots of 300 µg HeLa cell lysate were digested either with trypsin or subtilisin. For both enzymes, 2 aliquots were phosphopeptide enriched with TiO_2 and further fractionated with HILIC (TiO_2/HILIC) and 2 other aliquots were enriched with ERLIC, in a total of 4 aliquots (2 TiO_2/HILIC and 2 ERLIC) per enzyme.

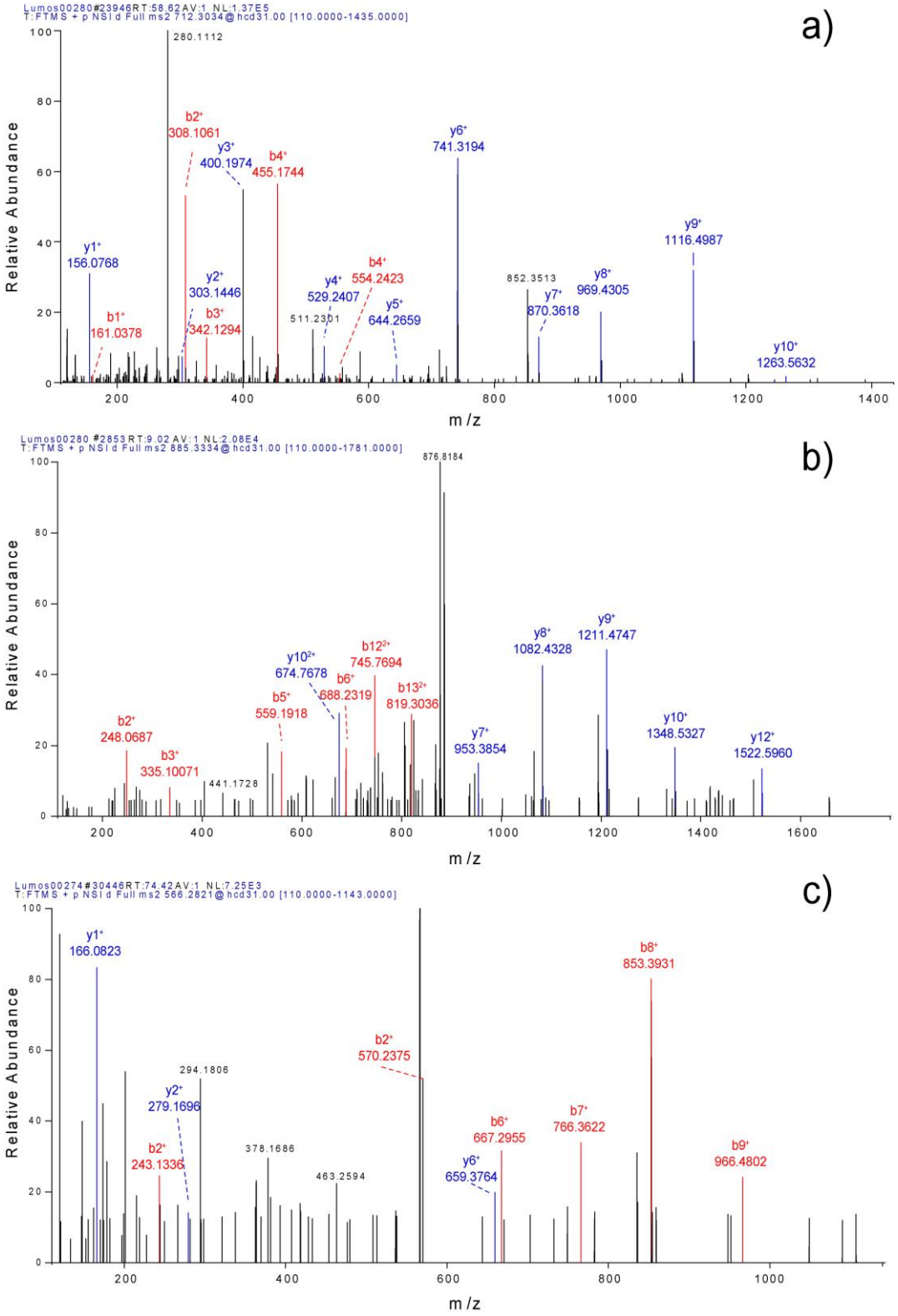

Figure 26.Spectra of the identified peptides of the protein Mucolipin-3. a) ^{185}CFFVEPDEPFHIG^{197}, b) ^{10}SCSSHEEENRCNFN^{23} and c) ^{539}LEDDPPVSLF^{548}.

Phosphorylation sites were filtered to site probability of at least 99 % [203], i.e. the algorithm gives a confidence probability in which higher the confidence percentage, higher is the chance of the correct phosphorylation assignment to the amino acid. Surprisingly, subtilisin could increase phosphoproteome coverage of over 1/3 of the sites found (Figure 27a).

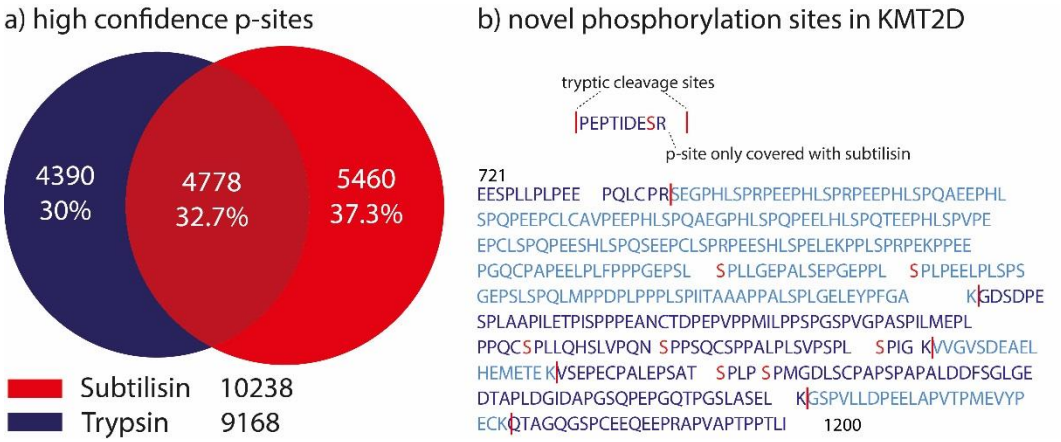

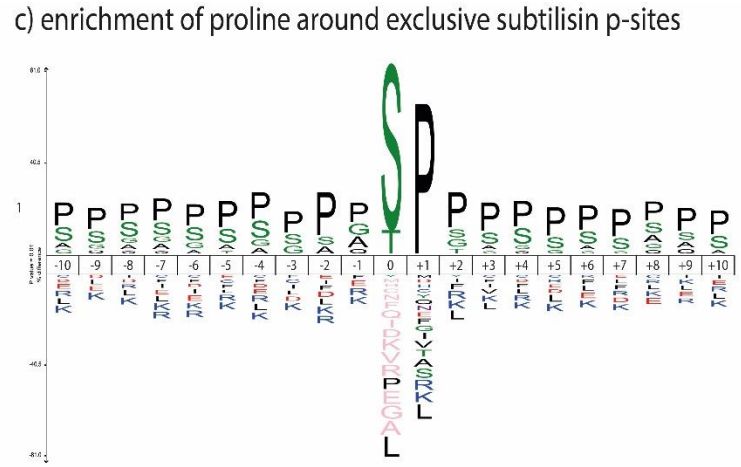

Figure 27. Phosphoproteome coverage of subtilisin. a) Subtilisin increases over 1/3 of the phosphoproteome coverage when used along with trypsin. b) Excerpt of a considered proline rich region of the protein KMT2D, in which tryptic peptides (limited by the red bars) would generate non suitable MS peptides, while it was possible to identify the phosphorylated amino acids (red letters) after subtilisin digestion. c) IceLogo of the 925 phosphorylation sites exclusively found in the subtilisin dataset showing a significant enrichment of prolines around the phosphorylated amino acid.

In total, it was possible to identify 10,238 high confident phosphorylation sites for subtilisin and 9,168 phosphorylation sites for trypsin. Further, an *in silico* digestion of the human proteome was performed with the enzymes ArgC, ArgN, LysC, LysN and GluC, and it was verified if the position within the protein of the phosphorylated amino acid found only in the subtilisin dataset could be covered by one of the peptides generated after the *in silico* digestion. As an example, from the exclusively subtilisin phosphoproteome dataset, if the phosphorylated serine at the position 31st of the amino acid sequence of protein "X" is not covered by any peptide *in silico* generated, that means this phospho-serine, in theory, cannot be covered by any other of the cited enzymes. It was possible to observe that 9.2 % (925) of the subtilisin

phosphorylation sites could not be covered by either trypsin or one of the *in silico* peptides, meanwhile only 1 % (92) of the trypsin phosphorylation sites could not be covered by subtilisin or one of the *in silico* peptides.

The protein Histone-lysine meethyltransferase (KMT2D), for instance, had 41 phosphorylation sites exclusively identified with subtilisin, in which 25 of those sites were not included in the PhosphoSitePlus[204] database, a repository for identified phosphorylation sites, accounting circa of 300,000 reported phosphorylations in different tissues under a varied amount of conditions [145,205] (Figure 27b). Interestingly, an iceLogo of the 925 exclusively subtilisin phosphorylation sites reveals another proline enrichment near the phosphorylated amino acid (Figure 27c).

Trypsin and subtilisin peptides of the global proteome and phosphoproteome studies went through further evaluation, focusing now on physicochemical characteristics that may increase knowledge about general peptide aspects after digestion. First, the pI and Gravy index [206] were evaluated. The Gravy index is a hydropathy scale that, taking into consideration the characteristics of all amino acids present in the peptide sequence, indicates its inclination to more hydrophobic (0>) or more hydrophilic (<0). It is possible to observe that subtilisin tends to have a lower pI and a higher hydrophilicity than trypsin for the peptides, while the values for phosphopeptides do not change much (Figure 28).

Second, the peptide sequence of peptides and phosphopeptides from the global (phospho)proteome were evaluated, assessing the median peptide length (Figure 29a, b) and relative contribution of each of the 20 amino acids (Figure 29c). Also, medians do not verify much for both enzymes, but it is observable the majority of peptides of subtilisin concentrate around the median, while for trypsin the peptides are more spread over through the graph (Figure 29a, b). This range around the median concentrate the best peptide length for mass spectrometry identification[196]. Compared to Figure 21b, the peptide median is lower. This is due the reason that experiments from the first and second reported median were performed with CID and HCD acquisitions in the mass spectrometer. The HCD method generate higher confidence peptides due the peptide measurement in the orbitrap, once peptides fragments from CID methods were acquired in the ion trap, which has lower resolution. Since smaller peptides are usually harder to confidently identify, the HCD method contributes to an improved identification of those peptides. It is as well possible to observe that subtilisin peptides have a higher share of aspartic acid (D) and glutamic acid (E), while the have a similar share of those amino acids for the phosphopeptides (Figure 29c). This remark explains the lower Gravy index for subtilisin peptides (Figure 28b), due to the higher concentration of acidic amino acids, and the similar index for the phosphopeptides, due an almost equal share of those amino acids.

Subtilisin as well possesses a higher amount of prolines in the amino acids composition, corroborating with the observations done in Figure 24b.

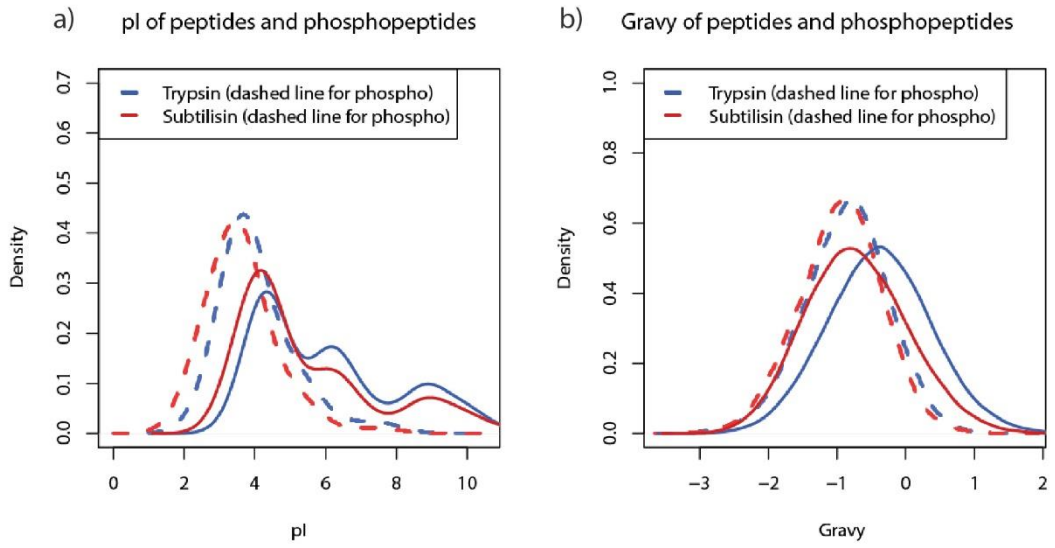

Figure 28. pI and Grave index for peptides and phosphopeptides. Subtilisin peptides tend to have a lower (a) pI and a higher (b) Grave index, while these characteristics are mild for the phosphopeptides. Chromatography separation might be optimized in selection of the gradient and pH.

To finalize the systematic peptide analysis of the peptides from global proteome (Figure 30) and the global phosphoproteome (Figure 31), for each amino acid, their occurrence per peptide was evaluated. It was already expected that subtilisin peptides would have acidic peptides (aspartic and glutamic acid) and proline appearing more times in a subtilisin peptide than in a tryptic peptide. The acidic amino acids influence the pI and Gravy index to have lower values. In that sense, since subtilisin present lower pI and Gravy index than tryptic peptides, it is expected to see a higher participation of the acidic amino acids in the subtilisin peptides, with a higher probability to have a two or more from the same amino acid. Due to the results presented in Figure 24b, it was, as well, expected that subtilisin would have a higher share of proline amino acids in the peptide sequence.

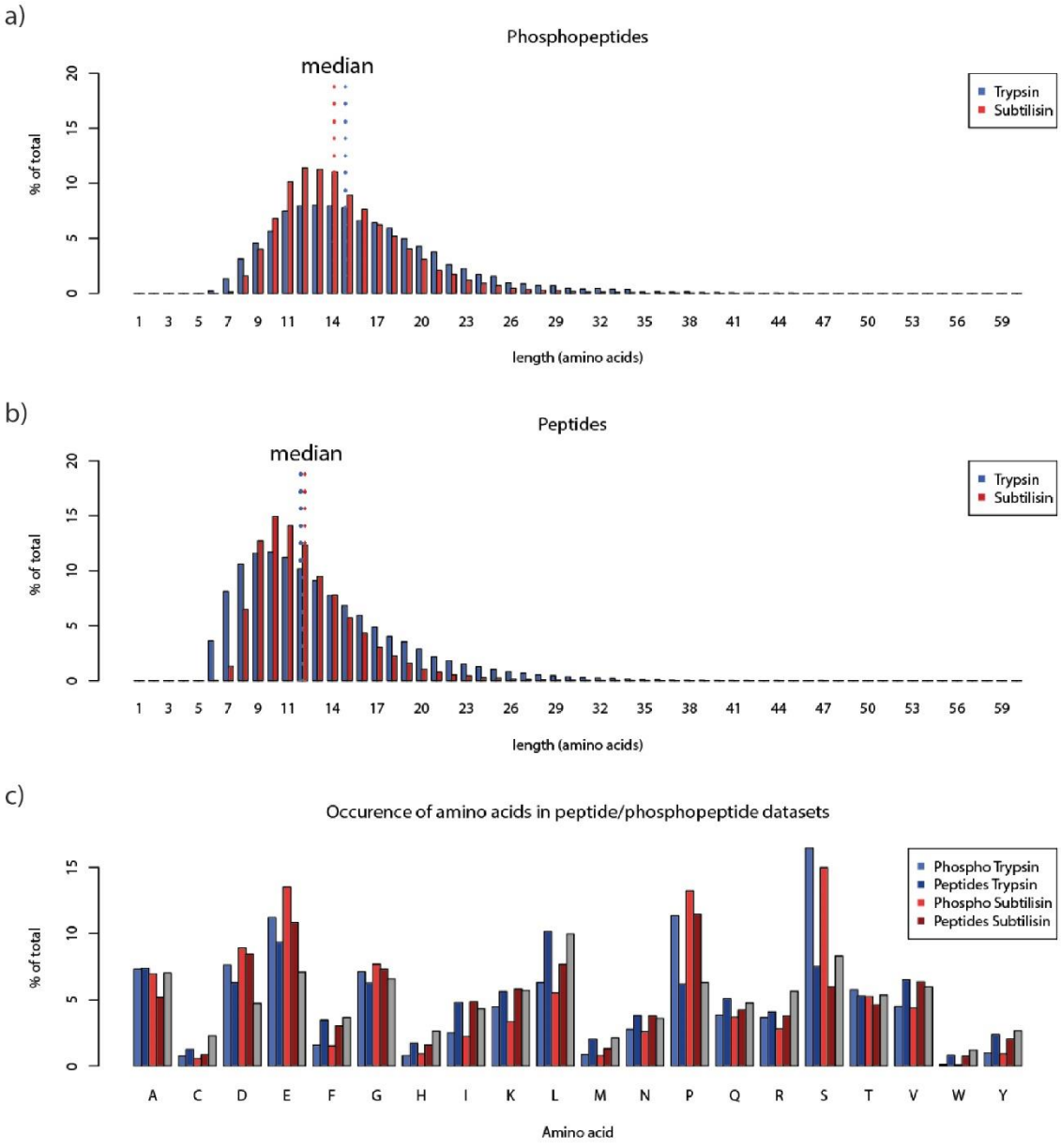

Figure 29.Peptide analysis of the subtilisin and trypsin (phospho)peptides. Subtilisin and trypsin have a similar peptide length for both cases (a, b), but the first possesses a distribution near to the median. The ideal peptide length for mass spectrometry identification is around 14 amino acids[196], showing that subtilisin also generate (phospho)peptides suitable for LC/MS.(c) Share of different amino acids of the (phospho)peptide composition from both enzymes.

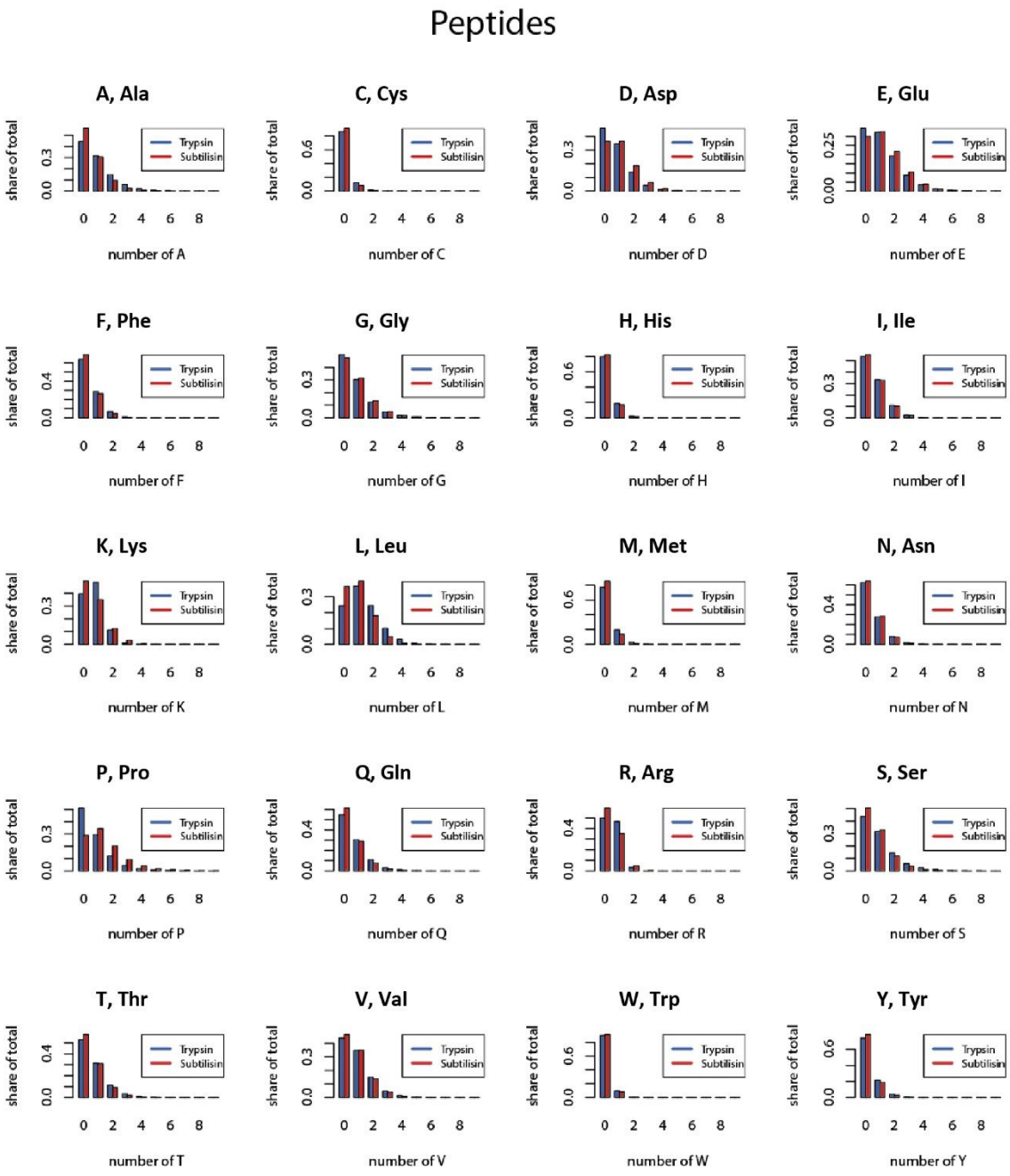

Figure 30. Occurrence of each amino acid per peptide from the global proteome dataset. Subtilisin tends to have more acidic amino acids (Asp, Glu) then trypsin, what could explain lower pI and higher Grave index for subtilisin peptides (Figure 28).

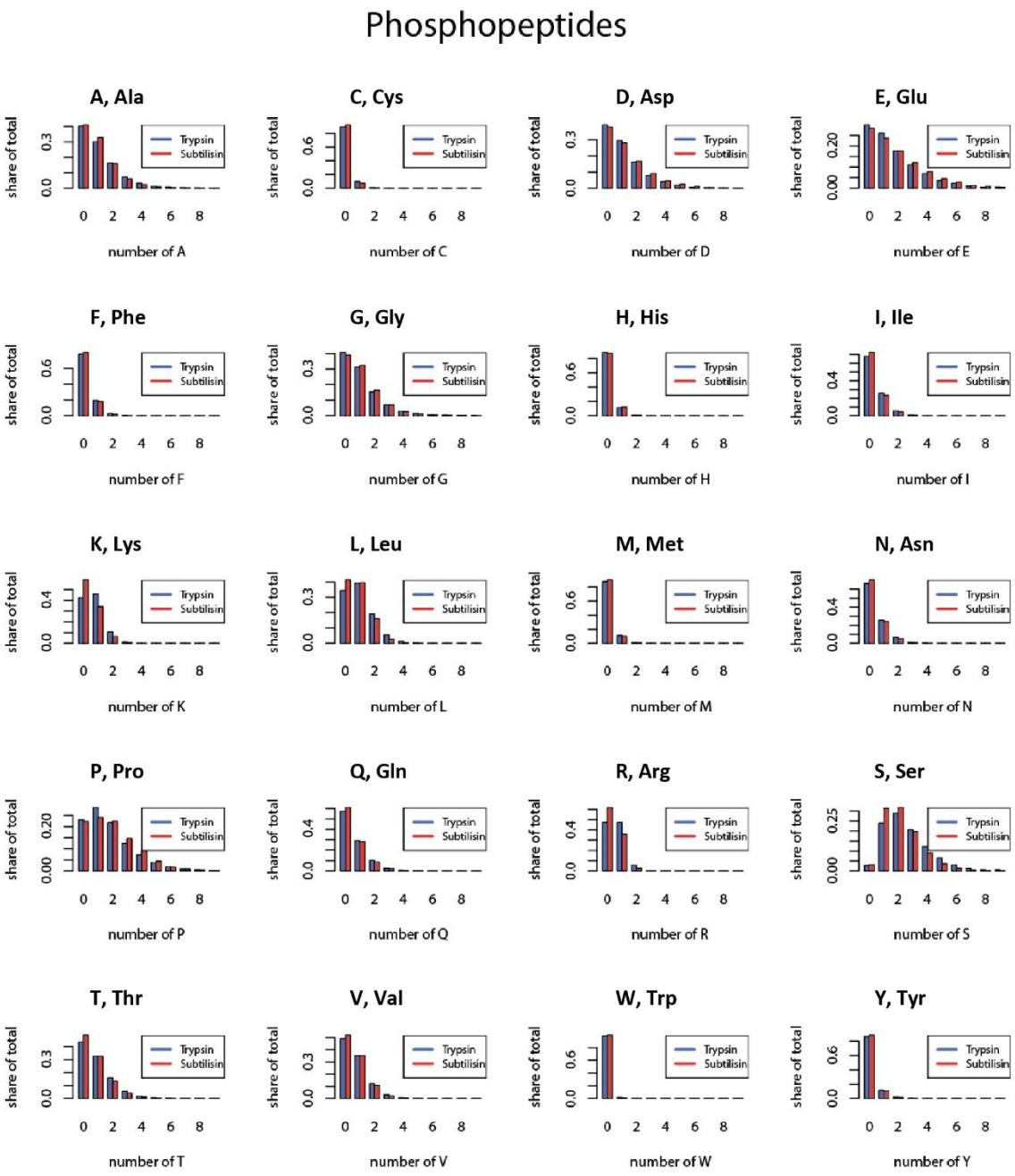

Figure 31. Occurrence of each amino acid per peptide from the global phosphoproteome dataset. Acidic amino acids (Glu, Asp) shows almost the same share for subtilisin phosphopeptide as for trypsin phosphopeptides. This might explain a similar pI and Grave index for both trypsin and subtilisin phosphopeptides (Figure 28).

Next, it was evaluated if subtilisin digestion could be explored for quantitative proteomics based on chemical labeling using iTRAQ 8plex. This labeling technology is based in peptide derivatization using chemical labels with different reporter ions, wherein the labeled peptides have the same nominal mass, appearing as a single peak in full MS scans (the sum intensity of all different labeled version of the same peptide backbone). The peptide are then co-isolated and MS/MS fragmented to analysis, in which

quantification is based on the relative intensities of the reporter ions [207,208]. That means iTRAQ 8plex quantification can only be performed between identical peptides coming from the different labeled samples. In order to obtain similar protein digestion from two or more samples with the same proteome, it is mandatory the occurrence of a reproducible digestion.

To perform this assessment, aliquots of 150 µg of A431 cell lysate were individually digested either with subtilisin or trypsin. After digestion, 8 aliquots of the subtilisin were labeled with one set of iTRAQ 8plex and other 8 aliquots of trypsin were labeled as the previous. For subtilisin, the 8 aliquots were pooled in a ratio of 1:2:3:4:5:6:7:8 (iTRAQ channels 113:114:115:116:117:118:119:121 respectively). For trypsin, the aliquots were pooled in a reversed ratio of 8_{113}:7_{114}:6_{115}:5_{116}:4_{117}:3_{118}:2_{119}:1_{121}. Most method development studies use a 1:1:1:1:1:1:1:1 ratio, but using different ratio pooling allows to observe subtle changes in the proteome and how precise the ratios can be determined. The different ratio model also allowed observing how precise the quantification for extremely complex proteomes is.

First, a 500 ng aliquot of subtilisin and trypsin iTRAQ samples were individually measured by LC/MS and 250 µg of each sample were TiO_2/HILIC phosphopetide enriched and fractions also measured by LC/MS. The iTRAQ ratios were treated as explained in chapter 7.2.10 and boxplot were plotted. Subtilisin observed ratios of the proteome were close to the expected ratios, having a result comparable as trypsin, guarantying the compatibility of subtilisin with chemical labeling methods (Figure 32a). For the phosphoproteome, even with a slight distortion caused by the low abundance of phosphospeptides, the same occurrences observed in the proteome could be observed for the phosphoproteome, confirming the possibility of using subtilisin for low stoichiometric events as phosphorylations and possibly other PTMs (Figure 32b). In general, two affirmations can be done: subtilisin is compatible with iTRAQ labeling methods and digestion is reproducible, otherwise ratios would be totally distorted from what was expected.

To exclude chances of co-isolation (when two or more different peptides are isolated together for further MS/MS fragmentation) [156,209,210], a new experiment was designed and performed (Figure 32c). The biggest problem of co-isolation is that it could mild wrong ratios, leveling every iTRAQ channel to an average ratio. The boxplot themselves should have been enough to demonstrate that the majority of the peptides are close to their theoretical ratio. Still, iTRAQ subtilisin (1_{113}:2_{114}:3_{115}:4_{116}:5_{117}:6_{118}:7_{119}:8_{121}) and trypsin (8_{113}:7_{114}:6_{115}:5_{116}:4_{117}:3_{118}:2_{119}:1_{121}) were mix together in a ratio of 1:1, creating a super complex proteomic sample with antagonistic ratio and, due to different digestion types, different background. This mixed sample was high pH reversed phase fractionated and fractions measured by LC/MS (Figure 32d).

Indeed, it was already predictable the ratios not nicely distributed as before, due to sample complexity, but the trend of the expected ratios for both enzymes was clearly present. In that sense, co-isolation problems can be definitely excluded for obtaining the correct quantitative ratios observed for the proteome and phosphoproteme.

During data analysis of the super complex sample, all identified peptides with a typical trypsin cleavage were considered part of the trypsin proteome, meanwhile the subtilisin proteome was composed by peptides not tryptic or semitryptic (the new peptide N-terminal coming after a lysine or arginine or the C-terminal being a lysine or arginine). That means all the rest of peptides were part of the subtilisin dataset, including peptides from wrongly trypsin miss cleavages and/or in-source fragmentation, contributing to a higher distortion in the subtilisin ratio variation. Still, as showed before, even with the apparent iTRAQ compression, subtle ratio changes (e.g. 1:2, or 7:8) to higher variances (e.g. 1:8) are visible in the super complex sample, excluding possibilities that would impair the use of subtilisin as for quantification proteomics.

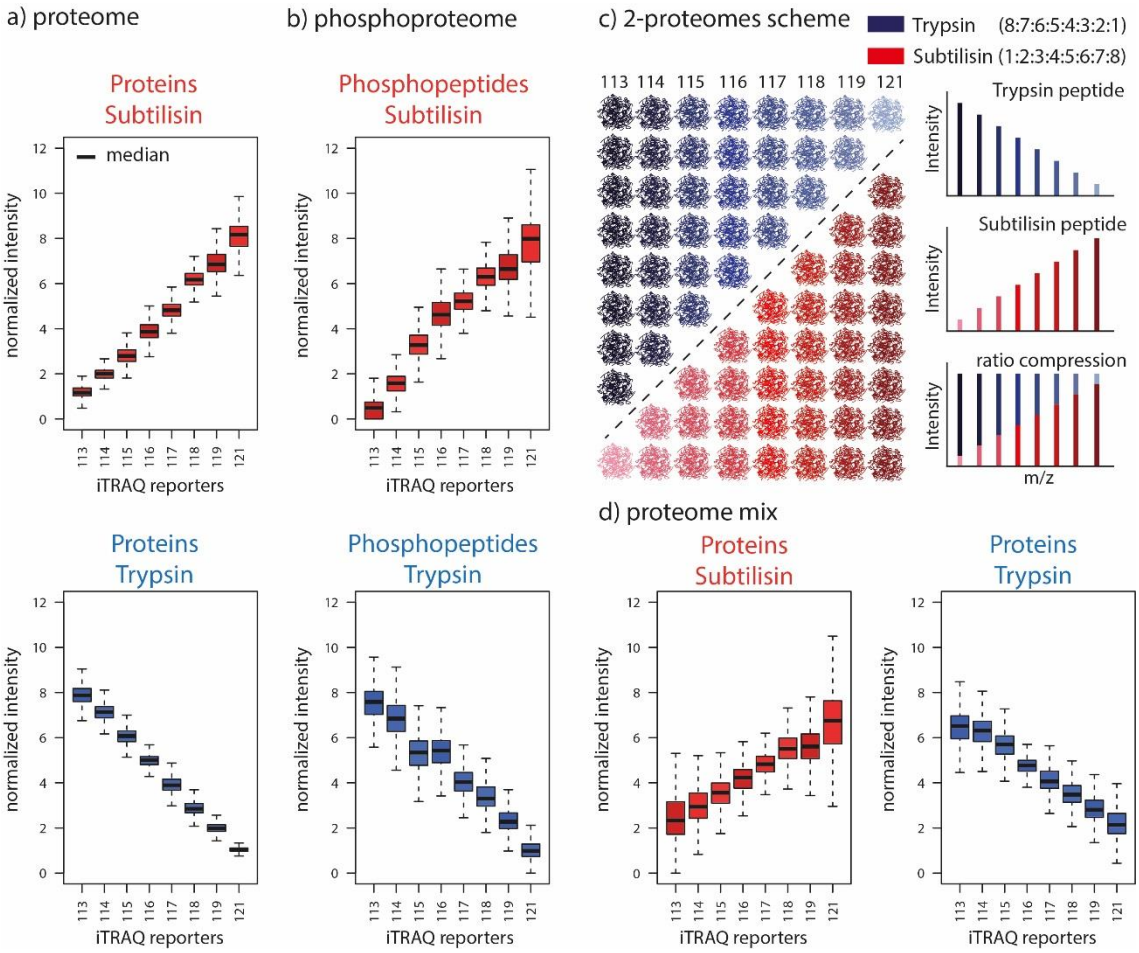

Figure 32. Subtilisin iTRAQ compatibility evaluation.a) The iTRAQ labelled subtilisin peptides of the A431 cell proteome presents the expected ratio of $1_{113}:2_{114}:3_{115}:4_{116}:5_{117}:6_{118}:7_{119}:8_{121}$, in which precision is comparable to tryptic peptides pooled in a reversed ratio order ($8_{113}:7_{114}:6_{115}:5_{116}:4_{117}:3_{118}:2_{119}:1_{121}$. The iTRAQ ratios intensities were normalized to the expected ratios as described in chapter 7.2.10. For each iTRAQ channel, closer the observed ratios are to the expected ratios, more reproducible and confident that digestion is. b) The same observation is done for the phosphopeptides, but will a lower precision due to low peptide abundance. c) Overview of the subtilisin and trypsin multiplexing scheme, generating d) a super complex proteome, but still present the expected ratios for both enzymes.

Interestingly, it was observed that subtilisin iTRAQ data had more PSMs or peptides quantified per protein than trypsin. If the same is PSM is measured a couple of time, more accurate will be the peptide reporter ion intensities. Higher the amount of identified peptides from the same protein, higher is the confidence of the protein quantification. In that sense, the data is more reliable, because the peptide and protein intensities are determined by the average intensity of the PSM and peptides, respectively. This event happens not only for the peptides, but for phosphopeptides as well (Figure 33).

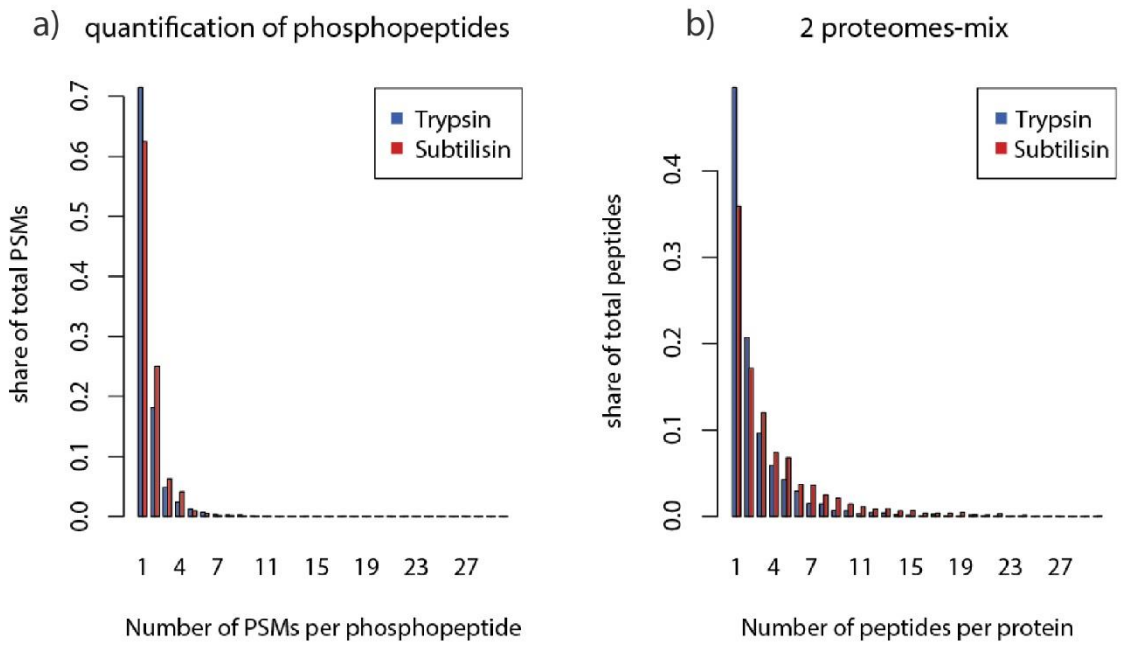

Figure 33. Amount of PSMs identified per phosphopeptide and peptides identified per protein. a) Each phosphopeptide identified might have one or more PSM. It is possible that higher the number of PSMs, higher is also the chance of a clear spectrum to assign confidently a phosphorylation site. b) Higher the number of peptides identified for a protein in an iTRAQ experiment, higher the chance of a better protein quantification. a, b) Subtilisin had a total more quantified PSMs and peptides per protein, giving more reliable data for the performed iTRAQ experiment.

After an extensive characterization of subtilisin, subtilisin was put to test with a different organism than human cells, and the target for the development of the presented study for this enzyme. Yeast mitochondria aliquots were individually digested with either subtilisin, trypsin or GluC. After digestion, samples were TiO_2/HILIC phosphopeptide enriched and fractions were measured by LC/MS. Total amount of phosphopeptides with a site probability $\geq$ 99 % identified by each of the enzymes were compared by Venn diagrams (Figure 34).Trypsin, subtilisin and GluC identify exclusively 656, 506 and 126 mitochondrial phosphorylation sites, respectively. In theory, the use of subtilisin together with trypsin could increase in almost 50 % the phosphoproteome coverage from mitochondrial studies due to unrevealing sites not covered only with tryptic digestion, increasing knowledge about the studied sample.

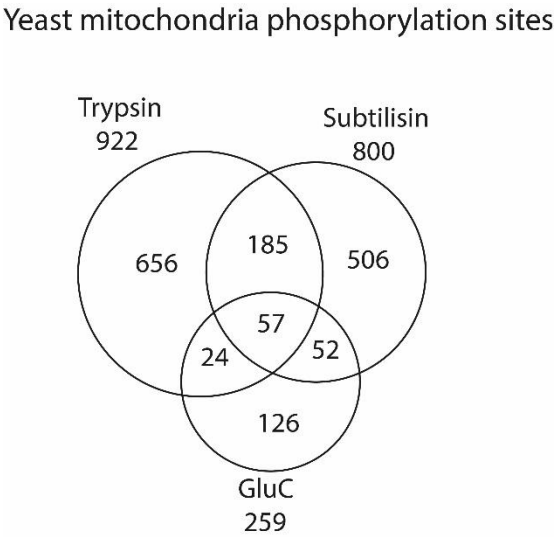

Figure 34. Amount of yeast mitochondria phosphorylation sites found after trypsin, subtilisin and GluC digestion.

To finalize, taking into consideration results observed in Figure 21a, a super-fast protocol was planned to reduced sample preparation time. Since subtilisin could fully digest samples down to 1 min, a few protocol modifications during sample preparation were performed in order to adapt the super-fast sample preparation. In that sense, a sample preparation protocol could be reduced to one hour (Table 16).

Table 16. Time demanded for sample preparation until digestion. Subtilisin super-fast sample preparation (depicted as fast-subtilisin) may take 5 min in case of tissue sample preparation.

	Time (min)		
Procedure	Trypsin	Subtilisin	Fast-subtilisin
Cell lysis	40	40	2-5
CMC + BCA	60	60	40
EtOH	90	90	-
Resuspension	10	10	-
Final sample preparation and digestion	840	25	7
Total time	1040	225	52

The fast protocol spanned a total of two hours from lysis to database search, including carbamidomethylation, BCA assay, digestion and a 52 min LC/MS analysis. It was possible to identify 863 proteins from yeast mitochondria, 2179 from HeLa and 1011 from mouse heart with at least 1 unique peptide at 1 % FDR. Indeed identifications were lower for samples prepared with the usual protocol and longer LC gradient times. Still, the protocol is valid for fast sample analysis, in which results can be achieve in 2 h, making a mark for bottom-up proteomics. Depending on the different projects and needs, adaptations can be made in order to increase protein identification.

Moreover, the super-fast protocol was tested for rapid label free quantitative profiling. Thus, human healthy fibroblasts and mutant fibroblasts with a mutation in VCP on chromosome 9p13 were analyzed, each, in biological triplicates. VCP encodes for the transitional endoplasmic reticulum ATPase and is required for the fragmentation of Golgi stacks and the formation of the transitional endoplasmic reticulum. The mutation causes an inclusion body myopathy, characterized by disabling muscle weakness, osteolytic bone lesions consistent with Paget disease, and premature frontotemporal dementia (disease reference code: IBMPFD1; OMIM: # 167320) [211]. Using PeptideShaker [167] and Progenesis (Nonlinear Dynamics), 1423 proteins were quantified, 1140 of which with at least 2 unique peptides, demonstrating a high reproducibility across replicates (Figure 35a). The reproducible workflow enabled the robust quantification of IBMPFD1 and control samples indicating significant proteomic changes in line with the neuropathological phenotype of the patients (Figure 35b) and showing a good correlation to trypsin-based quantitative data (Figure 35c). Thus, a network of secreted proteins of the extracellular matrix showed significantly reduced expression, including alpha-Collagens, Thrombospondin-1 and 2, Tenascin-X (TNXB), Gremlin-1, the serine protease HTRA1 and the procollagen C-endopeptidase enhancer 1. This is in agreement with the demonstrated role of VCP in secretion via modulation of ER-Golgi trafficking. Moreover, proper secretion of proteins and composition of the extracellular matrix is crucial for neuronal communication and muscle function. Neuronal vulnerability is indicated by reduced levels of LSAMP which is involved in neuronal growth and axon targeting, whereas proteins involved in neuronal/axonal regeneration such as Tenascin-X, Adducins and DCLK1 might be of potential relevance.

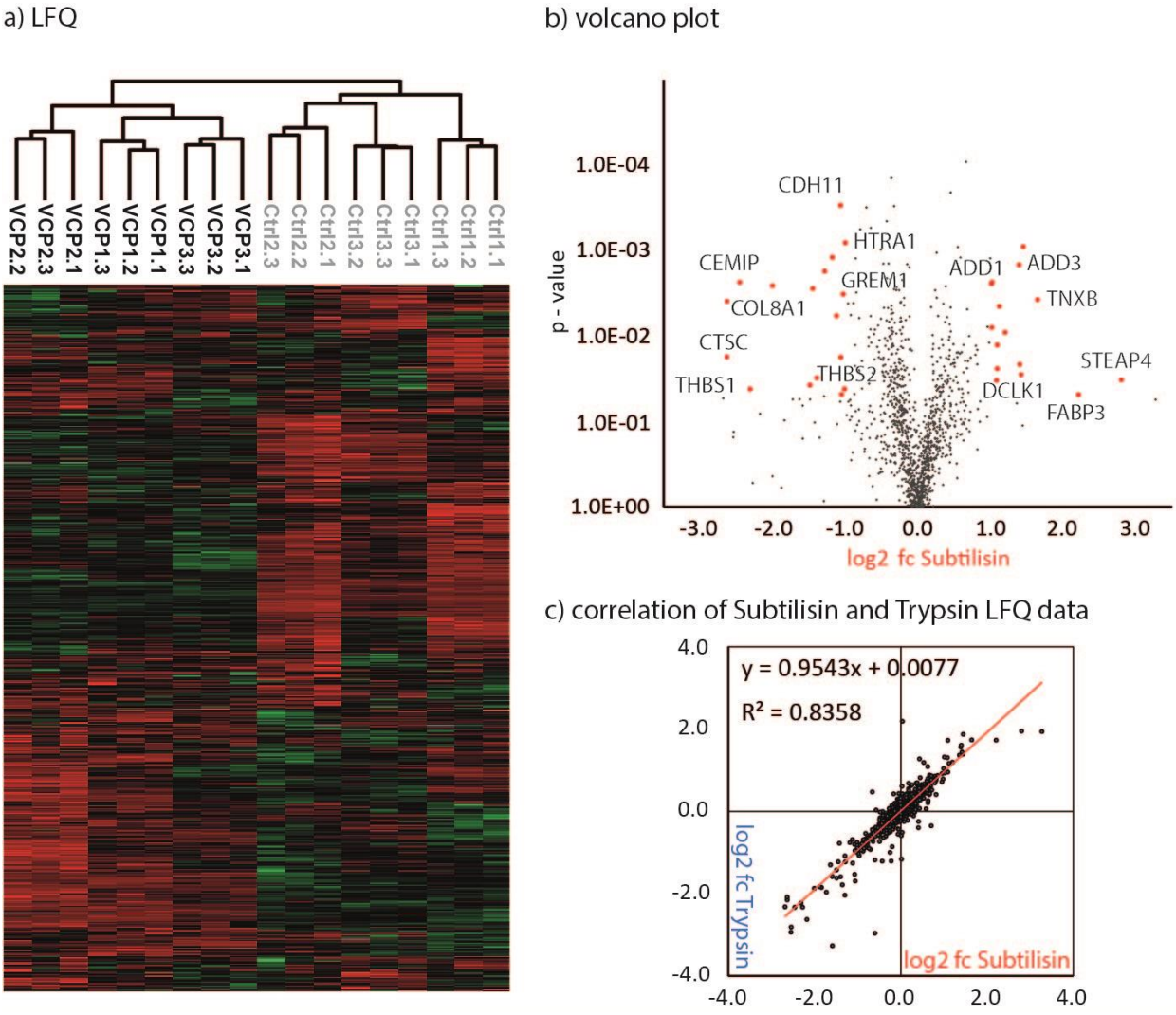

Figure 35. Label free quantification (LFQ) of sample treated with the super-fast protocol. a) Label free quantification of fibroblasts from healthy controls and IBMPFD1 patient. b) Significantly differential protein hits are labeled in red ($p<0.05$, >2-fold change). c) Log2 fold-changes (fc) from LFQ data show a good correlation for subtilisin and trypsin samples.

8.3 Subtilisin, PKA and antibody experiments

PKA protein isoforms have been reported to regulate biological functions, such as cellular differentiation and cell survival, besides been involved in processes such as memory formation and pain sensitization. PKA phosphorylates several proteins, both in the nucleus and in the cytoplasm of the cell [212-216]. The catalytic subunit α (Cα) possesses a phosphorylatable epitope that is necessary to regulate the kinase activity by conformational changes and protein association, which allowed to analyze and model its activation cycle in primary sensory neurons [217].

8| Results and Discussion

The use of monoclonal antibodies to enrich low abundant or interesting proteins of the proteome is a common technique described as immunoaffinity. If subtilisin demonstrates a potential for epitope mapping, it could also be used, together with a monoclonal antibody for a specific phosphorylated peptide, to enrich relevant phosphorylation sites not visible by common bottom-up approaches associated with phosphopeptide enrichment.

To identify the mentioned epitope, an approach joint of mass spectrometry and subtilisin was performed. The antibody (anti-Cα), PKA-Cα protein and both combined were analyzed by separation in the monolithic column pre and post subtilisin digestion, in order to verify the molecules stability when incubated with the enzyme. While the antibody shows an expected degradation stability [218] (Figure 36a,b), as well when incubated with PKA (Figure 36e, f), the kinase was enzymatically digested into peptides when incubated with subtilisin(Figure 36c, d). Due the antibody resistance against digestion, the identification of the epitope strategy was set, in which was based in the protein epitope-antibody activity. As showed previously, first the intact protein was incubated with the antibody. In theory, the epitope of interest is not susceptible to enzymatic digestion, once it is protected by the epitope/antibody binding, but the rest of the kinase is unguarded for proteolysis. After the ultrafiltration using the 30 kDa MWCO membrane, the peptides pass through the membrane, while the epitope/antibody stay over the membrane, as the concentrate, since the antibody has a volume bigger than the membrane cut-off porous. Incubation of the concentrate with an acidic pH induces elution of the epitope/antibody conjugate. Finally, a final ultrafiltration step was performed to purify the epitope (eluate) from the antibody, and, by MS, it was possible to measure the eluate and identify the epitope´s amino acid composition.

For the second applied strategy, the PKA peptides, generated after subtilisin digestion, were incubated with the antibody. After an ultrafiltration step, only the epitope conjugated with the antibody remained as the concentrate, while the not bound peptides passed as the flow through. Later, the same procedures explained above were adopted to unbind epitope/antibody and posterior epitope identification by mass spectrometry.

The LC/MS measurement showed that, of the total peptide identification, 44% (479 PSMs) and 80% (161 PSMs) belonged to the ^{50}GRGSFGRVM^{58} peptide identified in the first and second strategy, respectively (Figure 37a, b). Since the second strategy had an extra ultrafiltration step, the recovery of peptides was smaller, reducing the amount of identified PSMs. These results support each other and strongly suggest the mentioned peptide as the antibody epitope. It was further investigated the composition of peptides identified after PKA digestion by subtilisin without any kind of antibody enrichment, in which the peptide

^{50}GRGSFGRVM^{58} counted as much as 4% from the total, confirming the epitope enrichment by the antibody. Moreover, this amino acid sequence revealed to be within the N-lobe of the catalytic core, in which this is part of the glycine rich loop (GxGxxG) (Figure 38) (3D structure obtained from the Protein Data Bank[219] and modified with PyMol[220]). This loop is essential to bind the phosphoryl groups of ATP, being greatly conserved between the eukaryotic protein kinases [221].

The current results may bring other possibilities of the use of subtilisin, even though not addressed here, it will be suggested further use of the enzyme for related proteomics studies. The mild subtilisin attack to superficial substrates indicate a possibility to use the enzyme in studies of protein import, protein subcellular localization and protein function in yeast mitochondria. Some studies, for instance, have used proteinase K to cleave the external domains of protein/receptors from the outer mitochondrial membrane. In its turn, the cleaved proteins/receptors lose their function, leading to proteomics changes to keep mitochondrial organelle homeostasis. Other studies [173,222-225] have used the enzyme proteinase K to cleave surface proteins from intact cells/organelles. Later, the newly generated peptides were separated from the still intact cell/organelle and measured by LC/MS, in which peptide identification led to protein subcellular localization, i.e. the external membrane. In mitochondrial studies, quite often the enzyme proteinase K for is used for those purposes, but use of subtilisin could facilitate the logistics of the work, since it has been characterized and could be used for more deeper approaches, as (phospho)proteome mapping and quantification strategies.

Moreover, it was presented the potential of the combination use of subtilisin and monoclonal antibody to enrich epitope. As previously commented in this chapter, this technique could have a high value in phosphopeptide enrichment of interest phosphorylation sites when associated with immunoaffinity. Since the protein import into the mitochondrion is mediated by transient phosphorylations, this technique could be applied to increase chances of identification of specific sites in a complex mixture of (phospho)peptides. For instance, identification of phosphorylation sites from the TOM22, TOMM 40 or TOM70 from the MAS1 mutant experiments could be given a better overview of the protein import upon an impaired mitochondrial processing peptidase (MPP).

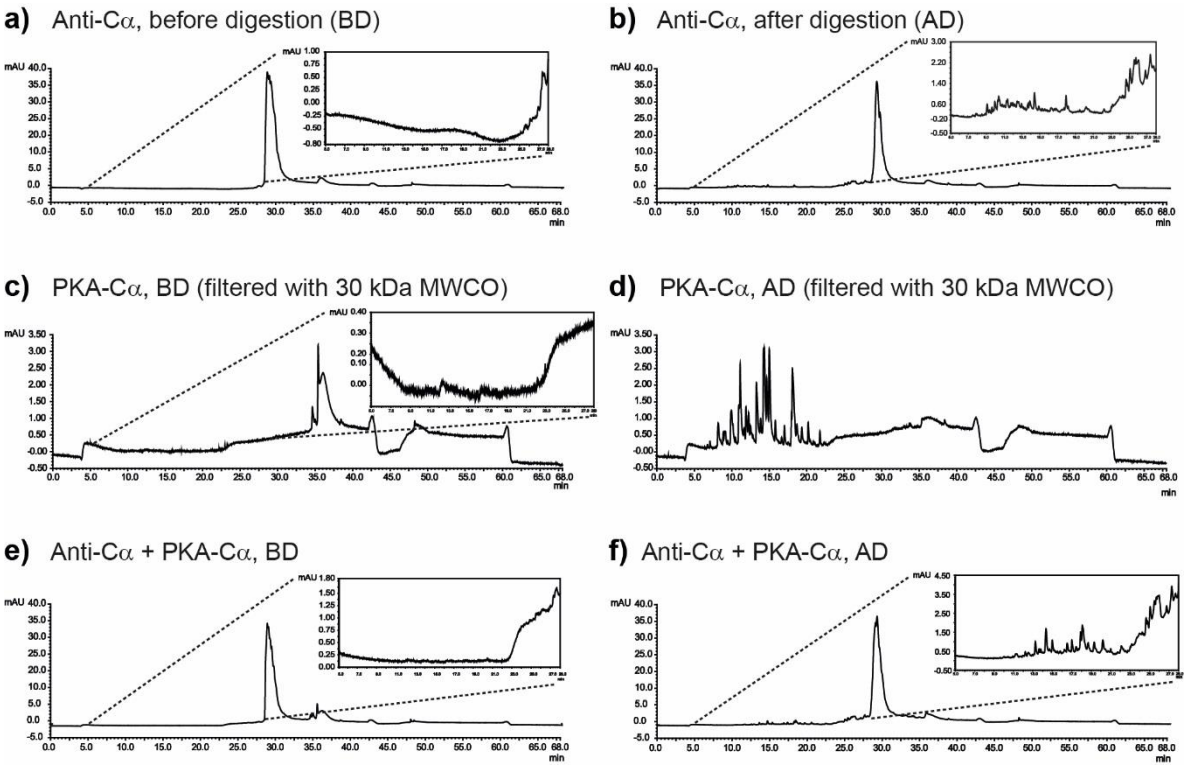

Figure 36.Monolithic chromatograms of anti-Cα antibody and PKA-Cα. To evaluate protein stability on the presence of active subtilisin, the antibody and protein where incubated with the enzyme and degradation profile checked on a monolithic column after digestion/incubation (AD). A control of the protein and antibody before digestions (BD) was also checked on the monolithic. a, b) Anti-Cα before and after digestion shows stability of the antibody against digestion. c, d) PKA-Cα is intact before digestion, but can be cleaved by subtilisin. e, f) incubation antibody and PKA shows anti-Cα stability. Zoomed UV traces are mainly peptide area elution. MWCO is molecular weight cut-off. BD = before digestion, AD = after digestion with subtilisin.

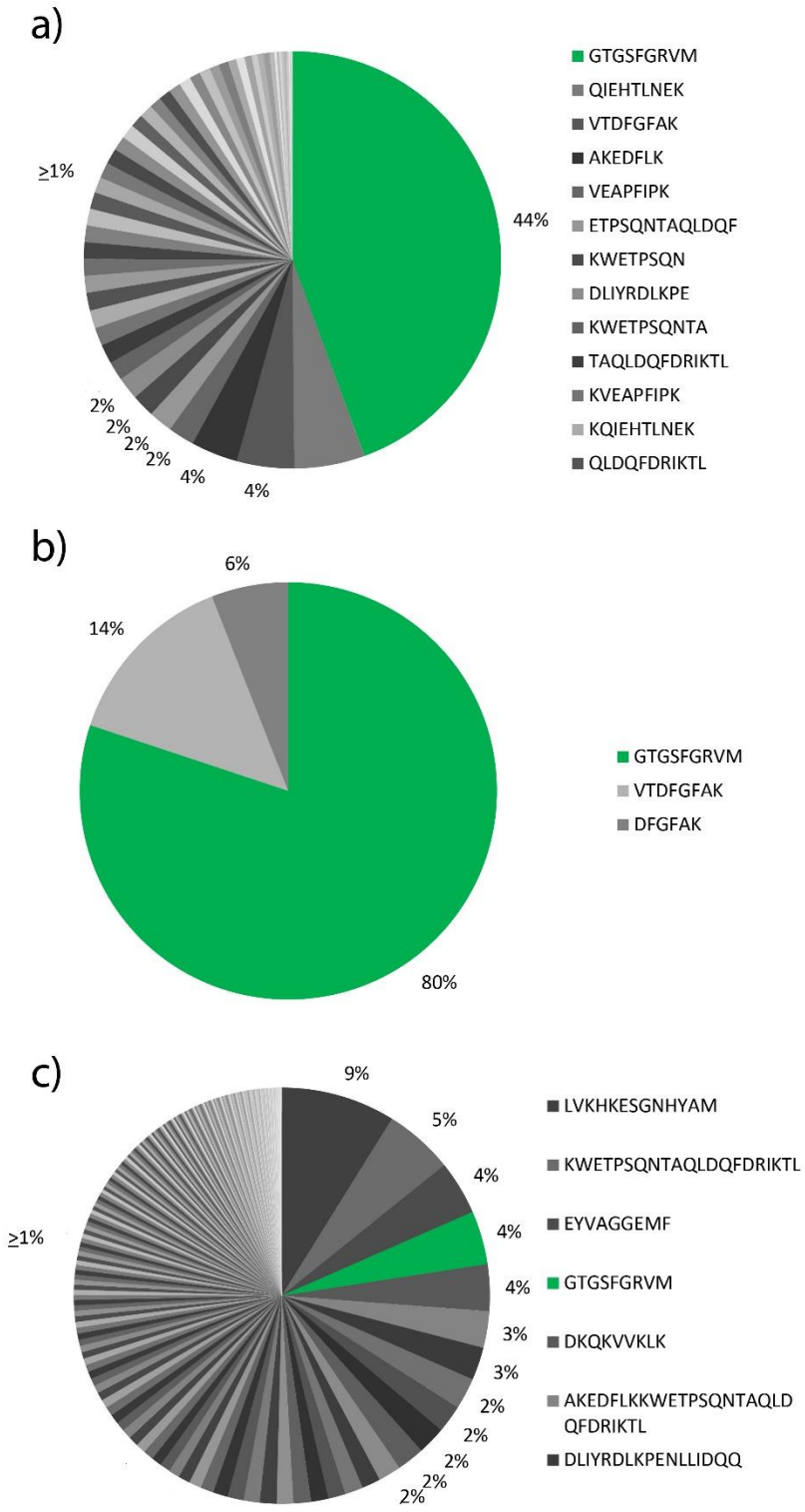

Figure 37. Identification of PKA-Cα epitope. a) Epitope identification through the intact protein and antibody incubation, in which 44 % of the identified peptides was the ^{50}GRGSFGRVM^{58} peptide.b) Epitope identification through digested PKA-Cα with the antibody, in which 80 % of the identified peptides was the ^{50}GRGSFGRVM^{58}. c) PKA-Cα digested with subtilisin indicates that the peptide ^{50}GRGSFGRVM^{58} does not naturally stand as the major peptide.

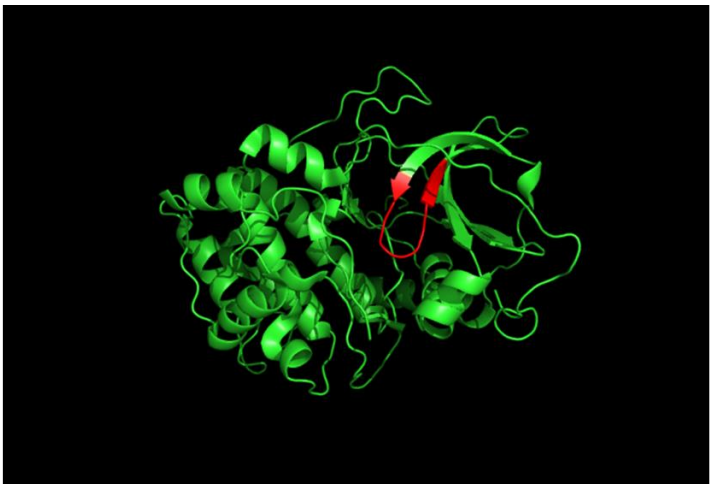

Figure 38. Glycine rich loop containing the ^{50}GRGSFGRVM^{58} peptide from the protein PKA-Cα is essential for binding the phosphoryl group of ATP. Structure obtained from the Protein Data Bank (entry 2GFC) and modified with the PyMol software.

8.4 New yeast mitochondria purification protocol

It has been already observed that phosphorylation takes a deep role in mitochondrial regulatory systems, spanning from protein import and protein maturation to vital functions as regulations of the respiratory chain [68,185,226-230]. To be able to perform such kind of studies, scientists rely on the development of phosphorylation preparation/identification techniques, in which, for bottom-up mass spectrometry, e.g., varies with the type on proteolytic enzyme, as previously presented. Already established, but not deeply studied, the mitochondrial purification treatment demonstrate an important factor on viability of phosphorylation sites. The phosphorylation lost during this step cannot be retrieved by any means during samples preparation for mass spectrometry. In that sense, it was investigated how this stage of sample preparation could influence in the final amount of phosphorylations identified by LC/MS.

To evaluate the new protocol, the number of identified proteins and phosphorylation sites were compared between the standard protocol (SP) and the new and faster protocol (NFP). The total amount of identified high confidence yeast proteins was for SP and NFP, respectively, 654 and 772 (Figure 39a). Yet, since the NFP had a less stringent mitochondrial purification, it was expected a higher concentration of protein contaminants from other yeast organelles. Still, the total number of identified mitochondrial protein between both purification methods do not vary deeply, with a total identification for SP and NFP, respectively, of 495 and 519 protein (Figure 39b). At first sight, the NFP method seem to be a bit more advantageous, since the purification step is faster and the number of total identifications are higher. Further qualitative analyses, in which was considered protein score (Figure 39c), total protein coverage

(Figure 39d) and amount of unique peptides per protein (Figure 39e) from the mitochondrial proteins identified by both purification steps, did not show a striking difference between both methods. There is no visible difference between the parameters mentioned above, with slightly higher medians for the NFP for the protein score (414 x 454) and protein coverage (29 x 31), and equal median for unique peptides per protein (8 x 8).

Another objective was to compare identification of phosphorylation sites after TiO_2/HILIC phosphopeptide enrichment. The NFP uses less amount of centrifugation steps, an immediate step of sample freezing after mitochondria purification and a cocktail of protease and phosphatase inhibitors. This could reduce loss of liable phosphorylation sites during sample preparation and reduce/impair the activity of enzymes that could degraded the phosphoprotein.

After LC/MS measurement, the total phosphorylation sites identified for the SP and NFP was, respectively, 783 and 1179, in which NFP conserved 3.6 times more unique sites than SP (Figure 40). Taking into consideration that, after the mitochondrial purification, all sample preparation steps were performed equality for all samples, the NFP apparently better conserves phosphoproteins intact, being a more suitable protocol for mitochondrial phosphoproteome coverage studies. As well, there is an increased chance of identification of phosphorylation sites of interest.

As an outcome, both purification protocols have similar results regarding the proteome, but the NFP has two observed advantages: (1) it is a faster purification protocol and (2) better conserve phosphorylation during the application of the protocol. To reach a final conclusion about this subject, it is necessary to repeat this experiment with more replicates to be able to generate confident statistical data to verify the observed data. Still, results showed one of the best phosphopeptide recovery studies ever performed in house, indicating the potential of the NFP as the model protocol for enrichment of mitochondria.

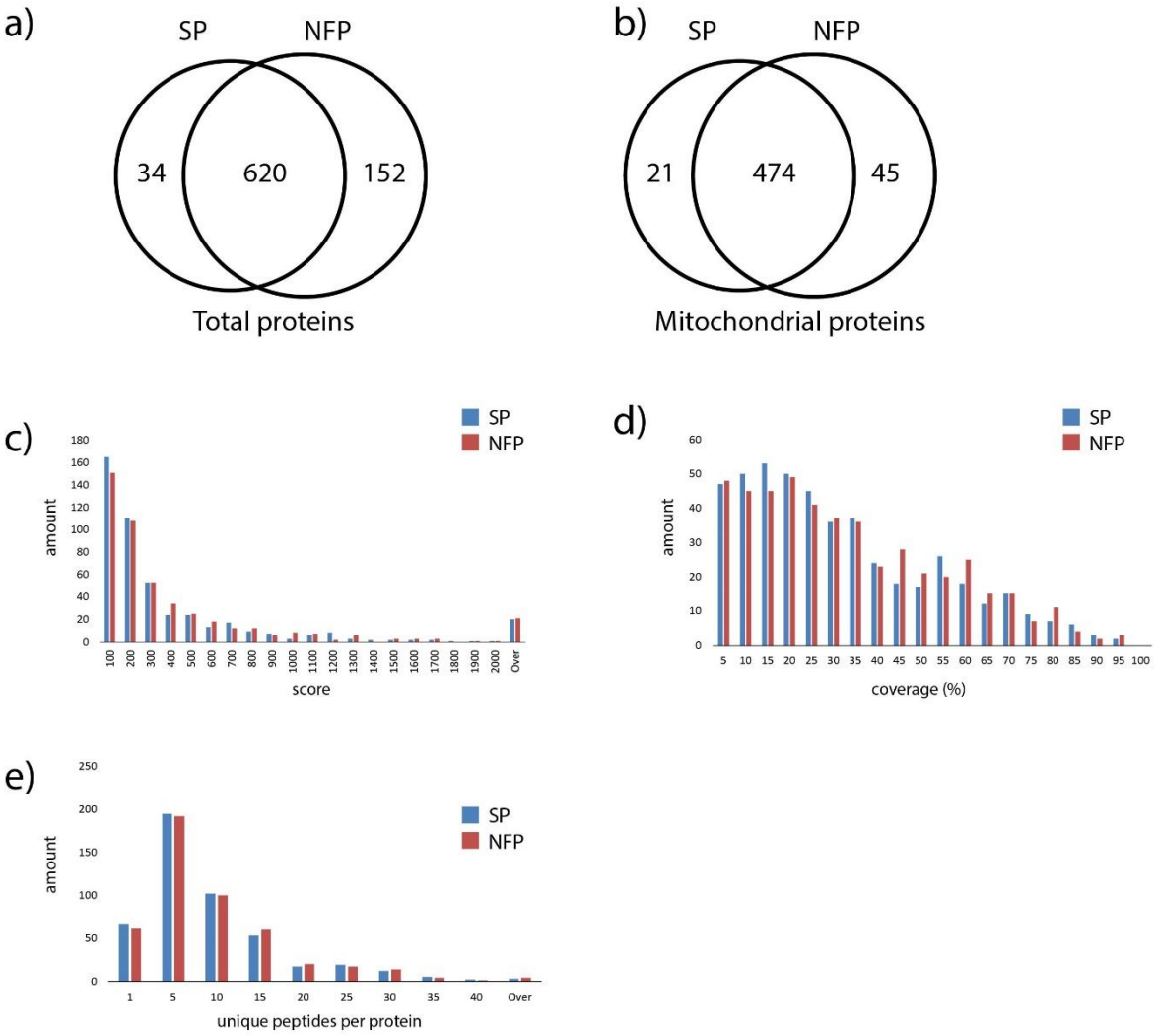

Figure 39. Comparison between two mitochondrial purification protocols, standard protocol (SP) and new and fast protocol (NFP). a) Total amount of identified proteins by LC/MS after application of both protocols, including contaminant proteins. b) Total amount of exclusively mitochondrial proteins identified. Taking into consideration exclusively mitochondrial proteins identified in both purification protocols, the protein score (c), the protein coverage (d) and unique peptides per protein (e) we compared, with no clear visible difference between both protocols. At (c), protein scores over 2000 were represented at the “over” bars.

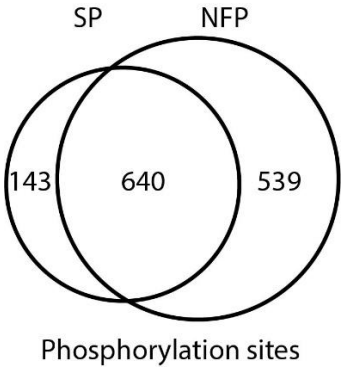

Figure 40. Venn diagram comparing the unique phosphorylation sites from mitochondria purified using the standard protocol (SP) and new and fast protocol (NFP). The phosphopeptides from both mitochondria purification protocol were enriched by TiO_2/HILIC and measured by LC/MS. The total amount of identified phosphorylation sites from both conditions were compared. NFP identify 3.6 times more unique phosphorylation sites than SP.

9 Conclusion

From all MAS1 mutant experiments, concerning the mitochondrial and whole yeast ChaFRADIC experiments, global proteome and phosphoprotome, only the mitochondrial ChaFRADIC presented conclusive results, consistently identifying 18 substrates that follows the mitochondrial processing peptidase (MPP) pathway for protein import into the organelles and increased the confidence about protein subcompartment location into the mitochondrion. Still, the number of substrates of the MPP appear to be low considering the suggested amount of matrix proteins and loosely associated proteins from the inner side of the inner membrane, considering the study of Voegtle et al [173]. One of the pointed reasons is possibly the low time for MAS1 protein turnover, which proteome variation between mutant and wild type was not visible under the current threshold applied for possible regulations. Lower thresholds could have been applied, but the overall confidence in the identifications would be impaired, in which the option lower identifications but higher confidence was chosen.

Besides the purified mitochondria, the whole yeast cell was also analyzed making use of ChaFRADIC technique, but with no conclusive results. First, there was no confident evidence in proteins enrolled with the MPP pathway. Second, there was no congruency between the identified regulated peptides in the different time points studied. In that case, ChaFRADIC was observed to be a technique not suitable to evaluate possible small proteins changes in a complex proteome. The ChaFRADIC technique is based in protein N-terminal enrichment, protein quantification could mainly be done by the comparison between the abundance of original protein N-terminal peptides. In a complex environment, in which all cell/organelle proteome is reduced to peptides, original N-terminal peptide from regulated proteins might be low abundant. If this peptide is not acquired in the mass spectrometer in data dependent acquisition, this regulation would not even be recorded and information would be lost. As well, a technique in which more peptides from a single protein could be measured, higher the chance to identify proteins and with more confidence.

A global proteome analysis of the mitochondrial MAS1 mutant demonstrated a very stable proteome, not affected by the impaired MPP, increasing the chance of a 4 h non-permissive time shift was not sufficient to observe meaningfulness changes in the proteome, and for a better conclusive work, higher times of non-permissive temperature shift should be applied. Still, this result make clear that observed regulations, such as phosphorylation patterns, were strictly related to different stoichiometry of modifications between the two conditions, and not related to an increase of the protein abundance. In other words, if

an observed phosphorylation site is up-regulated, it is not due to an up-regulation of the protein itself, but solely an increased amount of the phosphorylation.

In addition, the phosphoproteome investigation of the mitochondrial MAS1 mutant revealed a net of proteins possibly regulated by kinases that responded to an impaired MPP, with impact to the whole yeast. This initial study of the phosphoproteome was mainly to identify possible signaling pathways related to a deficient protein import machinery, and phosphorylation site specificity should be further studied to confirm the observations showed in this study. Important sites involved in the protein import into the mitochondria were not identified in this study, in which sites could give a clear overview of organelle behavior when an essential component of the system is miss functioning.

In that sense, the strategy became to develop techniques that could overcome issues presented above, as low identification of proteins related to the MPP pathway using ChaFRADIC and, consequently, loss of information, as PTM, due to impossibility of peptide/protein identification. For this, the new developed techniques were focused in reaching hard parts for identification of the (phospho)proteome by LC/MS, targeting specific regions of the proteome that have a real relevance and conserving unaltered the phosphoproteome using more gently sample handling techniques that would allow a higher stability of phosphorylation sites.

The proteolytic enzyme subtilisin was chosen to boost (phospho)proteome identification for samples compatible with bottom-up proteomics. With subtilisin, it was possible to increase sample coverage and almost double phosphopeptide identification compared to the enzyme-of-choice, trypsin. Besides other remarkable achievements, it was verified that subtilisin is compatible with labeling techniques such as iTRAQ and TMT, since subtilisin showed reproducibility between individual digestions. The reproducibility rate was not as high as observed for trypsin, but unexpectedly high for a broad specificity enzyme.

The combination of trypsin and subtilisin to evaluate the MAS1 experiments probably would increase information about the proteome and consequently the phosphoproteome as well. With adaptation to the experiment plan, as increasing the non-permissive incubation time, probably the proteome could have larger alterations that could be confidently detected, revealing some yet unknown protein functions.

Further, a technique combining subtilisin and antibody affinity showed the possibility of enrichment of specific targets. Subtilisin, aligned with ultrafiltration techniques, showed a great capability to reveal protein epitope. In the case of enrichment of specific phosphorylations, for instance, the monoclonal antibody would specifically selected the target, while the subtilisin would reduce sample complexity allowing identification of the phosphorylation site. This could be an advantage to enrich several targets in one single shot LC/MS analysis.

9| Conclusion

The high digestion reproducibility rates between replicates led to test efficiency of subtilisin when facing biological replicates on a label free quantification (LFQ) experiment. For comparison, the same samples were digested with trypsin. The LFQ data showed a good correlation for the subtilisin and trypsin samples, confirming the possibility to use the broad specificity enzyme for other quantification methods than only labeled based.

The LFQ was designed using a protocol that could encompass sample preparation and peptide identification in as little as 2 h. The enzyme:sample ratio of 1:20 was sufficient to digest the proteome of a complex sample in only 2 minutes using subtilisin, generating reproducible peptides for the LFQ experiment. Optimized liquid chromatography gradient allowed a better peptide distribution throughout an almost 50 min gradient and about 10 min peptide search. Since it takes about 1 h for cell lysis, protein concentration measurement and proteome digestion, the sample preparation time length summed with the LC/MS/database search time length is equal to approximately one 2 h.

The last experiment focused on more gently mitochondrial purification techniques to avoid loss of fragile phosphorylations sites. The combination of reduced centrifugation steps, the addition of phosphatases inhibitors and sample snap freeze allowed the identification of almost the double of phosphorylation sites in comparison with the current protocol described by Meisinger et al [158].

Indeed, the importance to confirm the data is strikingly necessary for two main reasons: (1) even being already published such protocol, it is mandatory to adequate the experiments to the well established scientific method, using at least replicates, to strength confidence of the data and (2) since such new mitochondria purification protocol has a promising outcome for phosphoproteomics and possibly other PTMs, more effort should be spend to validate it.

Combining the new mitochondrial protocol with the newly developed subtilisin protocol is a “worth trying” experiment to increase phosphoproteome coverage in mitochondria. A higher coverage in a single experiment may increase the knowledge about cascade of events driven by phosphorylation, elucidating signaling events in yeast mitochondrial, which pathways could be applied as basis for diseases in human mitochondria.

To conclude, MAS1 mutant experiments allowed the identification of specific proteins that follows the import pathway to the inner membrane and matrix. Further bottom-up techniques with a new proteolytic enzyme were developed to boost the experiment identifications and other related experiments.

10 References

1 Goffeau, A. *et al.* Life with 6000 Genes. *Science* **274**, 546-567, doi:10.1126/science.274.5287.546 (1996).
2 Karathia, H., Vilaprinyo, E., Sorribas, A. & Alves, R. Saccharomyces cerevisiae as a Model Organism: A Comparative Study. *PLoS ONE* **6**, e16015, doi:10.1371/journal.pone.0016015 (2011).
3 Lasserre, J. P. *et al.* Yeast as a system for modeling mitochondrial disease mechanisms and discovering therapies. *Disease models & mechanisms* **8**, 509-526, doi:10.1242/dmm.020438 (2015).
4 Lasserre, J.-P. *et al.* Yeast as a system for modeling mitochondrial disease mechanisms and discovering therapies. *Disease Models & Mechanisms* **8**, 509-526, doi:10.1242/dmm.020438 (2015).
5 Foury, F., Roganti, T., Lecrenier, N. & Purnelle, B. The complete sequence of the mitochondrial genome of Saccharomyces cerevisiae. *FEBS letters* **440**, 325-331 (1998).
6 de Zamaroczy, M. & Bernardi, G. The primary structure of the mitochondrial genome of Saccharomyces cerevisiae — a review. *Gene* **47**, 155-177, doi:http://dx.doi.org/10.1016/0378-1119(86)90060-0 (1986).
7 Otterstedt, K. *et al.* Switching the mode of metabolism in the yeast Saccharomyces cerevisiae. *EMBO Reports* **5**, 532-537, doi:10.1038/sj.embor.7400132 (2004).
8 Horvath, S. E. & Daum, G. Lipids of mitochondria. *Progress in lipid research* **52**, 590-614, doi:10.1016/j.plipres.2013.07.002 (2013).
9 Lill, R. & Mühlenhoff, U. Iron–sulfur-protein biogenesis in eukaryotes. *Trends in Biochemical Sciences* **30**, 133-141, doi:http://dx.doi.org/10.1016/j.tibs.2005.01.006 (2005).
10 Stehling, O. & Lill, R. The Role of Mitochondria in Cellular Iron–Sulfur Protein Biogenesis: Mechanisms, Connected Processes, and Diseases. *Cold Spring Harbor Perspectives in Biology* **5**, a011312, doi:10.1101/cshperspect.a011312 (2013).
11 Ferreira, G. C., Andrew, T. L., Karr, S. W. & Dailey, H. A. Organization of the terminal two enzymes of the heme biosynthetic pathway. Orientation of protoporphyrinogen oxidase and evidence for a membrane complex. *Journal of Biological Chemistry* **263**, 3835-3839 (1988).
12 Ohara, K., Kokado, Y., Yamamoto, H., Sato, F. & Yazaki, K. Engineering of ubiquinone biosynthesis using the yeast coq2 gene confers oxidative stress tolerance in transgenic tobacco. *The Plant Journal* **40**, 734-743, doi:10.1111/j.1365-313X.2004.02246.x (2004).
13 Wang, S. S. & Brandriss, M. C. Proline utilization in Saccharomyces cerevisiae: sequence, regulation, and mitochondrial localization of the PUT1 gene product. *Molecular and Cellular Biology* **7**, 4431-4440 (1987).
14 Butow, R. A. & Avadhani, N. G. Mitochondrial Signaling: The Retrograde Response. *Molecular Cell* **14**, 1-15, doi:https://doi.org/10.1016/S1097-2765(04)00179-0 (2004).
15 Pereira, C. *et al.* Mitochondria-dependent apoptosis in yeast. *Biochimica et Biophysica Acta (BBA) - Molecular Cell Research* **1783**, 1286-1302, doi:https://doi.org/10.1016/j.bbamcr.2008.03.010 (2008).
16 DiMauro, S. & Schon, E. A. Mitochondrial respiratory-chain diseases. *The New England journal of medicine* **348**, 2656-2668, doi:10.1056/NEJMra022567 (2003).
17 Vafai, S. B. & Mootha, V. K. Mitochondrial disorders as windows into an ancient organelle. *Nature* **491**, 374-383, doi:10.1038/nature11707 (2012).
18 Schapira, A. H. V. Mitochondrial disease. *The Lancet* **368**, 70-82, doi:https://doi.org/10.1016/S0140-6736(06)68970-8.

10| References

19 Skladal, D., Halliday, J. & Thorburn, D. R. Minimum birth prevalence of mitochondrial respiratory chain disorders in children. *Brain : a journal of neurology* **126**, 1905-1912, doi:10.1093/brain/awg170 (2003).

20 Pfeffer, G., Majamaa, K., Turnbull, D. M., Thorburn, D. & Chinnery, P. F. Treatment for mitochondrial disorders. *The Cochrane database of systematic reviews*, CD004426, doi:10.1002/14651858.CD004426.pub3 (2012).

21 Bolender, N., Sickmann, A., Wagner, R., Meisinger, C. & Pfanner, N. Multiple pathways for sorting mitochondrial precursor proteins. *EMBO Reports* **9**, 42-49, doi:10.1038/sj.embor.7401126 (2008).

22 Meisinger, C., Sickmann, A. & Pfanner, N. The Mitochondrial Proteome: From Inventory to Function. *Cell* **134**, 22-24, doi:https://doi.org/10.1016/j.cell.2008.06.043 (2008).

23 Cherry, J. M. *et al.* Saccharomyces Genome Database: the genomics resource of budding yeast. *Nucleic acids research* **40**, D700-705, doi:10.1093/nar/gkr1029 (2012).

24 Sickmann, A. *et al.* The proteome of Saccharomyces cerevisiae mitochondria. *Proceedings of the National Academy of Sciences of the United States of America* **100**, 13207-13212, doi:10.1073/pnas.2135385100 (2003).

25 Harbauer, A. B., Zahedi, R. P., Sickmann, A., Pfanner, N. & Meisinger, C. The protein import machinery of mitochondria-a regulatory hub in metabolism, stress, and disease. *Cell metabolism* **19**, 357-372, doi:10.1016/j.cmet.2014.01.010 (2014).

26 Truscott, K. N. *et al.* A presequence- and voltage-sensitive channel of the mitochondrial preprotein translocase formed by Tim23. *Nat Struct Mol Biol* **8**, 1074-1082 (2001).

27 Chacinska, A., Koehler, C. M., Milenkovic, D., Lithgow, T. & Pfanner, N. Importing mitochondrial proteins: machineries and mechanisms. *Cell* **138**, 628-644, doi:10.1016/j.cell.2009.08.005 (2009).

28 Schmidt, O., Pfanner, N. & Meisinger, C. Mitochondrial protein import: from proteomics to functional mechanisms. *Nature reviews. Molecular cell biology* **11**, 655-667, doi:10.1038/nrm2959 (2010).

29 Neupert, W. A perspective on transport of proteins into mitochondria: a myriad of open questions. *Journal of molecular biology* **427**, 1135-1158, doi:10.1016/j.jmb.2015.02.001 (2015).

30 Koehler, C. M. Protein translocation pathways of the mitochondrion. *FEBS letters* **476**, 27-31 (2000).

31 Roesch, K., Curran, S. P., Tranebjaerg, L. & Koehler, C. M. Human deafness dystonia syndrome is caused by a defect in assembly of the DDP1/TIMM8a–TIMM13 complex. *Human Molecular Genetics* **11**, 477-486, doi:10.1093/hmg/11.5.477 (2002).

32 Davey, K. M. *et al.* Mutation of DNAJC19, a human homologue of yeast inner mitochondrial membrane co-chaperones, causes DCMA syndrome, a novel autosomal recessive Barth syndrome-like condition. *Journal of Medical Genetics* **43**, 385-393, doi:10.1136/jmg.2005.036657 (2006).

33 Agsteribbe, E. *et al.* A Fatal, Systemic Mitochondrial Disease with Decreased Mitochondrial Enzyme Activities, Abnormal Ultrastructure of the Mitochondria and Deficiency of Heat Shock Protein 60. *Biochemical and Biophysical Research Communications* **193**, 146-154, doi:http://dx.doi.org/10.1006/bbrc.1993.1602 (1993).

34 Briones, P. *et al.* A new case of multiple mitochondrial enzyme deficiencies with decreased amount of heat shock protein 60. *Journal of Inherited Metabolic Disease* **20**, 569-577, doi:10.1023/a:1005303008439.

35 Fontaine, B. *et al.* A New Locus for Autosomal Dominant Pure Spastic Paraplegia, on Chromosome 2q24-q34. *American Journal of Human Genetics* **66**, 702-707 (2000).

36 Hansen, J. J. *et al.* Hereditary Spastic Paraplegia SPG13 Is Associated with a Mutation in the Gene Encoding the Mitochondrial Chaperonin Hsp60. *American Journal of Human Genetics* **70**, 1328-1332 (2002).

37 Takakubo, F. *et al.* An amino acid substitution in the pyruvate dehydrogenase E1 alpha gene, affecting mitochondrial import of the precursor protein. *American Journal of Human Genetics* **57**, 772-780 (1995).

38 Purdue, P. E., Takada, Y. & Danpure, C. J. Identification of mutations associated with peroxisome-to-mitochondrion mistargeting of alanine/glyoxylate aminotransferase in primary hyperoxaluria type 1. *J Cell Biol* **111**, 2341-2351 (1990).

39 Purdue, P. E., Allsop, J., Isaya, G., Rosenberg, L. E. & Danpure, C. J. Mistargeting of peroxisomal L-alanine:glyoxylate aminotransferase to mitochondria in primary hyperoxaluria patients depends upon activation of a cryptic mitochondrial targeting sequence by a point mutation. *Proceedings of the National Academy of Sciences of the United States of America* **88**, 10900-10904 (1991).

40 Danpure, C. J. & Jennings, P. R. Peroxisomal alanine:glyoxylate aminotransferase deficiency in primary hyperoxaluria type I. *FEBS Letters* **201**, 20-34, doi:10.1016/0014-5793(86)80563-4 (1986).

41 MacKenzie, J. A. & Mark Payne, R. Mitochondrial Protein Import and Human Health and Disease. *Biochimica et biophysica acta* **1772**, 509-523, doi:10.1016/j.bbadis.2006.12.002 (2007).

42 Vögtle, F.-N. *et al.* Intermembrane Space Proteome of Yeast Mitochondria. *Molecular & Cellular Proteomics* **11**, 1840-1852, doi:10.1074/mcp.M112.021105 (2012).

43 Herrmann, J. M. & Riemer, J. The Intermembrane Space of Mitochondria. *Antioxidants & Redox Signaling* **13**, 1341-1358, doi:10.1089/ars.2009.3063 (2010).

44 Koehler, C. M. & Tienson, H. L. Redox regulation of protein folding in the mitochondrial intermembrane space. *Biochimica et biophysica acta* **1793**, 139-145, doi:10.1016/j.bbamcr.2008.08.002 (2009).

45 Geissler, A. *et al.* The mitochondrial presequence translocase: an essential role of Tim50 in directing preproteins to the import channel. *Cell* **111**, 507-518 (2002).

46 Wiedemann, N. *et al.* Machinery for protein sorting and assembly in the mitochondrial outer membrane. *Nature* **424**, 565-571 (2003).

47 Schägger, H. in *Methods in Cell Biology* Vol. Volume 65 231-244 (Academic Press, 2001).

48 Chacinska, A. *et al.* Essential role of Mia40 in import and assembly of mitochondrial intermembrane space proteins. *The EMBO Journal* **23**, 3735-3746, doi:10.1038/sj.emboj.7600389 (2004).

49 Rehling, P. *et al.* Protein insertion into the mitochondrial inner membrane by a twin-pore translocase. *Science* **299**, 1747-1751, doi:10.1126/science.1080945 (2003).

50 Frazier, A. E. *et al.* Pam16 has an essential role in the mitochondrial protein import motor. *Nature structural & molecular biology* **11**, 226-233, doi:10.1038/nsmb735 (2004).

51 Meisinger, C., Sommer, T. & Pfanner, N. Purification of Saccharomcyes cerevisiae mitochondria devoid of microsomal and cytosolic contaminations. *Analytical biochemistry* **287**, 339-342, doi:10.1006/abio.2000.4868 (2000).

52 Meisinger, C. *et al.* Protein import channel of the outer mitochondrial membrane: a highly stable Tom40-Tom22 core structure differentially interacts with preproteins, small tom proteins, and import receptors. *Molecular and cellular biology* **21**, 2337-2348, doi:10.1128/mcb.21.7.2337-2348.2001 (2001).

53 Kumar, A. *et al.* Subcellular localization of the yeast proteome. *Genes & Development* **16**, 707-719, doi:10.1101/gad.970902 (2002).

54 Sickmann, A. *et al.* The proteome of Saccharomyces cerevisiae mitochondria. *Proceedings of the National Academy of Sciences* **100**, 13207-13212, doi:10.1073/pnas.2135385100 (2003).

55 Reinders, J., Zahedi, R. P., Pfanner, N., Meisinger, C. & Sickmann, A. Toward the Complete Yeast Mitochondrial Proteome: Multidimensional Separation Techniques for Mitochondrial Proteomics. *Journal of Proteome Research* **5**, 1543-1554, doi:10.1021/pr050477f (2006).

56 Scharfe, C. *et al.* MITOP: database for mitochondria-related proteins, genes and diseases. *Nucleic Acids Research* **27**, 153-155 (1999).
57 Ong, S.-E. *et al.* Stable Isotope Labeling by Amino Acids in Cell Culture, SILAC, as a Simple and Accurate Approach to Expression Proteomics. *Molecular & Cellular Proteomics* **1**, 376-386, doi:10.1074/mcp.M200025-MCP200 (2002).
58 Böttinger, L. *et al.* A complex of Cox4 and mitochondrial Hsp70 plays an important role in the assembly of the cytochrome c oxidase. *Molecular Biology of the Cell* **24**, 2609-2619, doi:10.1091/mbc.E13-02-0106 (2013).
59 Böttinger, L. *et al.* Mitochondrial Heat Shock Protein (Hsp) 70 and Hsp10 Cooperate in the Formation of Hsp60 Complexes. *The Journal of Biological Chemistry* **290**, 11611-11622, doi:10.1074/jbc.M115.642017 (2015).
60 Cheng, M. Y. *et al.* Mitochondrial heat-shock protein hsp60 is essential for assembly of proteins imported into yeast mitochondria. *Nature* **337**, 620-625 (1989).
61 Lytovchenko, O. *et al.* The INA complex facilitates assembly of the peripheral stalk of the mitochondrial F(1)F(o)-ATP synthase. *The EMBO Journal* **33**, 1624-1638, doi:10.15252/embj.201488076 (2014).
62 Barrientos, A. Yeast Models of Human Mitochondrial Diseases. *IUBMB Life* **55**, 83-95, doi:10.1002/tbmb.718540876 (2003).
63 Lasserre, J.-P. *et al.* Yeast as a system for modeling mitochondrial disease mechanisms and discovering therapies. *Disease Models and Mechanisms* **8**, 509-526, doi:10.1242/dmm.020438 (2015).
64 Zahedi, R. P. *et al.* Proteomic Analysis of the Yeast Mitochondrial Outer Membrane Reveals Accumulation of a Subclass of Preproteins. *Molecular Biology of the Cell* **17**, 1436-1450, doi:10.1091/mbc.E05-08-0740 (2006).
65 Ellenrieder, L., Mårtensson Christoph, U. & Becker, T. in *Biological Chemistry* Vol. 396 1199 (2015).
66 Distler, A. M., Kerner, J. & Hoppel, C. L. Proteomics of mitochondrial inner and outer membranes. *PROTEOMICS* **8**, 4066-4082, doi:10.1002/pmic.200800102 (2008).
67 Cherry, J. M. *et al.* Saccharomyces Genome Database: the genomics resource of budding yeast. *Nucleic Acids Research* **40**, D700-D705, doi:10.1093/nar/gkr1029 (2012).
68 Reinders, J. *et al.* Profiling Phosphoproteins of Yeast Mitochondria Reveals a Role of Phosphorylation in Assembly of the ATP Synthase. *Molecular & Cellular Proteomics* **6**, 1896-1906, doi:10.1074/mcp.M700098-MCP200 (2007).
69 Dudkina, N. V., Kouřil, R., Peters, K., Braun, H.-P. & Boekema, E. J. Structure and function of mitochondrial supercomplexes. *Biochimica et Biophysica Acta (BBA) - Bioenergetics* **1797**, 664-670, doi:http://dx.doi.org/10.1016/j.bbabio.2009.12.013 (2010).
70 Vonck, J. & Schäfer, E. Supramolecular organization of protein complexes in the mitochondrial inner membrane. *Biochimica et Biophysica Acta (BBA) - Molecular Cell Research* **1793**, 117-124, doi:http://dx.doi.org/10.1016/j.bbamcr.2008.05.019 (2009).
71 Smith, P. M., Fox, J. L. & Winge, D. R. Biogenesis of the cytochrome bc(1) complex and role of assembly factors. *Biochimica et Biophysica Acta* **1817**, 276-286, doi:10.1016/j.bbabio.2011.11.009 (2012).
72 Cruciat, C.-M., Brunner, S., Baumann, F., Neupert, W. & Stuart, R. A. The Cytochrome bc 1 and Cytochromec Oxidase Complexes Associate to Form a Single Supracomplex in Yeast Mitochondria. *Journal of Biological Chemistry* **275**, 18093-18098, doi:10.1074/jbc.M001901200 (2000).
73 Schägger, H. Respiratory Chain Supercomplexes. *IUBMB Life* **52**, 119-128, doi:10.1080/15216540152845911 (2001).

74 de Vries, S. & Marres, C. A. M. The mitochondrial respiratory chain of yeast. Structure and biosynthesis and the role in cellular metabolism. *Biochimica et Biophysica Acta (BBA) - Reviews on Bioenergetics* **895**, 205-239, doi:http://dx.doi.org/10.1016/S0304-4173(87)80003-4 (1987).

75 de Vries, S. & Grivell, L. A. Purification and characterization of a rotenone-insensitive NADH: Q6 oxidoreductase from mitochondria of Saccharomyces cerevisiae. *European Journal of Biochemistry* **176**, 377-384, doi:10.1111/j.1432-1033.1988.tb14292.x (1988).

76 Baker, M. J., Tatsuta, T. & Langer, T. Quality Control of Mitochondrial Proteostasis. *Cold Spring Harbor Perspectives in Biology* **3**, a007559, doi:10.1101/cshperspect.a007559 (2011).

77 Bohnert, M. *et al.* Role of mitochondrial inner membrane organizing system in protein biogenesis of the mitochondrial outer membrane. *Molecular Biology of the Cell* **23**, 3948-3956, doi:10.1091/mbc.E12-04-0295 (2012).

78 Höhr, A. I. C., Straub, S. P., Warscheid, B., Becker, T. & Wiedemann, N. Assembly of β-barrel proteins in the mitochondrial outer membrane. *Biochimica et Biophysica Acta (BBA) - Molecular Cell Research* **1853**, 74-88, doi:http://dx.doi.org/10.1016/j.bbamcr.2014.10.006 (2015).

79 Horvath, S. E. *et al.* Role of membrane contact sites in protein import into mitochondria. *Protein Science : A Publication of the Protein Society* **24**, 277-297, doi:10.1002/pro.2625 (2015).

80 Baker, E. S. *et al.* Mass spectrometry for translational proteomics: progress and clinical implications. *Genome medicine* **4**, 63, doi:10.1186/gm364 (2012).

81 Gillet, L. C., Leitner, A. & Aebersold, R. Mass Spectrometry Applied to Bottom-Up Proteomics: Entering the High-Throughput Era for Hypothesis Testing. *Annual review of analytical chemistry (Palo Alto, Calif.)* **9**, 449-472, doi:10.1146/annurev-anchem-071015-041535 (2016).

82 Wolters, D. A., Washburn, M. P. & Yates, J. R., 3rd. An automated multidimensional protein identification technology for shotgun proteomics. *Analytical chemistry* **73**, 5683-5690 (2001).

83 Tsiatsiani, L. & Heck, A. J. Proteomics beyond trypsin. *The FEBS journal* **282**, 2612-2626, doi:10.1111/febs.13287 (2015).

84 Brownridge, P. & Beynon, R. J. The importance of the digest: proteolysis and absolute quantification in proteomics. *Methods* **54**, 351-360, doi:10.1016/j.ymeth.2011.05.005 (2011).

85 Jones, P. *et al.* PRIDE: a public repository of protein and peptide identifications for the proteomics community. *Nucleic acids research* **34**, D659-663, doi:10.1093/nar/gkj138 (2006).

86 Desiere, F. *et al.* The PeptideAtlas project. *Nucleic acids research* **34**, D655-658, doi:10.1093/nar/gkj040 (2006).

87 Vizcaino, J. A. *et al.* ProteomeXchange provides globally coordinated proteomics data submission and dissemination. **32**, 223-226, doi:10.1038/nbt.2839 (2014).

88 Dickhut, C., Feldmann, I., Lambert, J. & Zahedi, R. P. Impact of digestion conditions on phosphoproteomics. *Journal of proteome research* **13**, 2761-2770, doi:10.1021/pr401181y (2014).

89 Benore-Parsons, M., Seidah, N. G. & Wennogle, L. P. Substrate phosphorylation can inhibit proteolysis by trypsin-like enzymes. *Arch Biochem Biophys* **272**, 274-280, doi:10.1016/0003-9861(89)90220-8 (1989).

90 Thiede, B. *et al.* Analysis of missed cleavage sites, tryptophan oxidation and N-terminal pyroglutamylation after in-gel tryptic digestion. *Rapid Commun Mass Spectrom* **14**, 496-502, doi:10.1002/(sici)1097-0231(20000331)14:6<496::aid-rcm899>3.0.co;2-1 (2000).

91 Hamady, M., Cheung, T. H. T., Tufo, H. & Knight, R. Does protein structure influence trypsin miscleavage? Using structural properties to predict the behavior of related proteins. *IEEE Eng Med Biol Mag* **24**, 58-66, doi:10.1109/memb.2005.1436461 (2005).

92 Vandermarliere, E., Mueller, M. & Martens, L. Getting intimate with trypsin, the leading protease in proteomics. *Mass spectrometry reviews* **32**, 453-465, doi:10.1002/mas.21376 (2013).

10| References

93 Giansanti, P., Tsiatsiani, L., Low, T. Y. & Heck, A. J. Six alternative proteases for mass spectrometry-based proteomics beyond trypsin. **11**, 993-1006, doi:10.1038/nprot.2016.057 (2016).

94 Giansanti, P. *et al.* An Augmented Multiple-Protease-Based Human Phosphopeptide Atlas. *Cell reports* **11**, 1834-1843, doi:10.1016/j.celrep.2015.05.029 (2015).

95 Gauci, S. *et al.* Lys-N and trypsin cover complementary parts of the phosphoproteome in a refined SCX-based approach. *Analytical chemistry* **81**, 4493-4501, doi:10.1021/ac9004309 (2009).

96 Guo, X., Trudgian, D. C., Lemoff, A., Yadavalli, S. & Mirzaei, H. Confetti: A Multiprotease Map of the HeLa Proteome for Comprehensive Proteomics. *Molecular & Cellular Proteomics : MCP* **13**, 1573-1584, doi:10.1074/mcp.M113.035170 (2014).

97 Huesgen, P. F. *et al.* LysargiNase mirrors trypsin for protein C-terminal and methylation-site identification. *Nature methods* **12**, 55-58, doi:10.1038/nmeth.3177 (2015).

98 The UniProt, C. The Universal Protein Resource (UniProt). *Nucleic Acids Research* **35**, D193-D197, doi:10.1093/nar/gkl929 (2007).

99 Lu, S. *et al.* Mapping native disulfide bonds at a proteome scale. *Nature methods* **12**, 329-331, doi:10.1038/nmeth.3283 (2015).

100 Polzien, L. *et al.* Identification of Novel in Vivo Phosphorylation Sites of the Human Proapoptotic Protein BAD: PORE-FORMING ACTIVITY OF BAD IS REGULATED BY PHOSPHORYLATION. *The Journal of Biological Chemistry* **284**, 28004-28020, doi:10.1074/jbc.M109.010702 (2009).

101 MacCoss, M. J. *et al.* Shotgun identification of protein modifications from protein complexes and lens tissue. *Proceedings of the National Academy of Sciences of the United States of America* **99**, 7900-7905, doi:10.1073/pnas.122231399 (2002).

102 Wu, C. C. & Yates, J. R., 3rd. The application of mass spectrometry to membrane proteomics. *Nature biotechnology* **21**, 262-267, doi:10.1038/nbt0303-262 (2003).

103 Zybailov, B. L., Florens, L. & Washburn, M. P. Quantitative shotgun proteomics using a protease with broad specificity and normalized spectral abundance factors. *Mol Biosyst* **3**, 354-360, doi:10.1039/b701483j (2007).

104 Schlosser, A., Vanselow, J. T. & Kramer, A. Mapping of phosphorylation sites by a multi-protease approach with specific phosphopeptide enrichment and NanoLC-MS/MS analysis. *Analytical chemistry* **77**, 5243-5250, doi:10.1021/ac050232m (2005).

105 Rietschel, B. *et al.* Elastase digests: new ammunition for shotgun membrane proteomics. *Mol Cell Proteomics* **8**, 1029-1043, doi:10.1074/mcp.M800223-MCP200 (2009).

106 Wang, B., Malik, R., Nigg, E. A. & Körner, R. Evaluation of the Low-Specificity Protease Elastase for Large-Scale Phosphoproteome Analysis. *Analytical chemistry* **80**, 9526-9533, doi:10.1021/ac801708p (2008).

107 Engel, J. *et al.* Targeting Drug Resistance in EGFR with Covalent Inhibitors: A Structure-Based Design Approach. *Journal of medicinal chemistry* **58**, 6844-6863, doi:10.1021/acs.jmedchem.5b01082 (2015).

108 Ottesen, M. The conversion of ovalbumin into plakalbumin, as followed in the pH-stat. *Archives of biochemistry and biophysics* **65**, 70-77, doi:http://dx.doi.org/10.1016/0003-9861(56)90177-1 (1956).

109 Linderstrom-Land, K. & Ottesen, M. A new protein from ovalbumin. *Nature* **159**, 807 (1947).

110 DeLange, R. J. & Smith, E. L. Subtilisin Carlsberg: I. AMINO ACID COMPOSITION; ISOLATION AND COMPOSITION OF PEPTIDES FROM THE TRYPTIC HYDROLYSATE. *Journal of Biological Chemistry* **243**, 2134-2142 (1968).

111 Jacobs, M., Eliasson, M., Uhlen, M. & Flock, J. I. Cloning, sequencing and expression of subtilisin Carlsberg from Bacillus licheniformis. *Nucleic acids research* **13**, 8913-8926 (1985).

112 Dodson, G. & Wlodawer, A. Catalytic triads and their relatives. *Trends in Biochemical Sciences* **23**, 347-352, doi:10.1016/S0968-0004(98)01254-7.

10| References

113 Hedstrom, L. Serine protease mechanism and specificity. *Chemical reviews* **102**, 4501-4524 (2002).

114 Reinders, J., Lewandrowski, U., Moebius, J., Wagner, Y. & Sickmann, A. Challenges in mass spectrometry-based proteomics. *Proteomics* **4**, 3686-3703, doi:10.1002/pmic.200400869 (2004).

115 Zhang, Y., Fonslow, B. R., Shan, B., Baek, M.-C. & Yates, J. R. Protein Analysis by Shotgun/Bottom-up Proteomics. *Chemical reviews* **113**, 2343-2394, doi:10.1021/cr3003533 (2013).

116 Wisniewski, J. R., Zougman, A., Nagaraj, N. & Mann, M. Universal sample preparation method for proteome analysis. *Nature methods* **6**, 359-362, doi:10.1038/nmeth.1322 (2009).

117 Shevchenko, A., Tomas, H., Havli, J., Olsen, J. V. & Mann, M. In-gel digestion for mass spectrometric characterization of proteins and proteomes. *Nature protocols* **1**, 2856, doi:10.1038/nprot.2006.468 (2007).

118 Medzihradszky, K. F. In-solution digestion of proteins for mass spectrometry. *Methods Enzymol* **405**, 50-65, doi:10.1016/s0076-6879(05)05003-2 (2005).

119 Steen, H. & Mann, M. The abc (and xyzs) of peptide sequencing. *Nature Reviews Molecular Cell Biology* **5**, 699, doi:10.1038/nrm1468

(2004).

120 Bélanger, J. M. R., Jocelyn Paré, J. R. & Sigouin, M. in *Techniques and Instrumentation in Analytical Chemistry* Vol. 18 (eds J. R. J. Paré & J. M. R. Bélanger) 37-59 (Elsevier, 1997).

121 Karpievitch, Y. V., Polpitiya, A. D., Anderson, G. A., Smith, R. D. & Dabney, A. R. Liquid Chromatography Mass Spectrometry-Based Proteomics: Biological and Technological Aspects. *The annals of applied statistics* **4**, 1797-1823, doi:10.1214/10-aoas341 (2010).

122 Wilm, M. & Mann, M. Analytical properties of the nanoelectrospray ion source. *Analytical chemistry* **68**, 1-8 (1996).

123 Scheltema, R. A. *et al.* The Q Exactive HF, a Benchtop Mass Spectrometer with a Pre-filter, High-performance Quadrupole and an Ultra-high-field Orbitrap Analyzer. *Molecular & Cellular Proteomics : MCP* **13**, 3698-3708, doi:10.1074/mcp.M114.043489 (2014).

124 N., P. D., C., P. D. J., M., C. D. & S., C. J. Probability-based protein identification by searching sequence databases using mass spectrometry data. *ELECTROPHORESIS* **20**, 3551-3567, doi:doi:10.1002/(SICI)1522-2683(19991201)20:18<3551::AID-ELPS3551>3.0.CO;2-2 (1999).

125 Dorfer, V. *et al.* MS Amanda, a Universal Identification Algorithm Optimized for High Accuracy Tandem Mass Spectra. *Journal of Proteome Research* **13**, 3679-3684, doi:10.1021/pr500202e (2014).

126 Yates, J. R. Pivotal role of computers and software in mass spectrometry - SEQUEST and 20 years of tandem MS database searching. *J Am Soc Mass Spectrom* **26**, 1804-1813, doi:10.1007/s13361-015-1220-0 (2015).

127 Gonczarowska-Jorge, H., Dell'Aica, M., Dickhut, C. & Zahedi, R. P. Variable Digestion Strategies for Phosphoproteomics Analysis. *Methods in molecular biology (Clifton, N.J.)* **1355**, 225-239, doi:10.1007/978-1-4939-3049-4_15 (2016).

128 Orbitrap, P. http://planetorbitrap.com/. (May, 2018 (date of access)).

129 Blume-Jensen, P. & Hunter, T. Oncogenic kinase signalling. *Nature* **411**, 355-365, doi:10.1038/35077225 (2001).

130 Hunter, T. Signaling--2000 and beyond. *Cell* **100**, 113-127 (2000).

131 Cohen, P. The origins of protein phosphorylation. *Nature Cell Biology* **4**, E127, doi:10.1038/ncb0502-e127 (2002).

132 Sefton, B. M. Overview of protein phosphorylation. *Current protocols in cell biology* **Chapter 14**, Unit 14.11, doi:10.1002/0471143030.cb1401s00 (2001).

133 Olsen, J. V. *et al.* Global, in vivo, and site-specific phosphorylation dynamics in signaling networks. *Cell* **127**, 635-648, doi:10.1016/j.cell.2006.09.026 (2006).

10| References

134 Dunn, J. D., Reid, G. E. & Bruening, M. L. Techniques for phosphopeptide enrichment prior to analysis by mass spectrometry. *Mass spectrometry reviews* **29**, 29-54, doi:10.1002/mas.20219 (2010).

135 Larsen, M. R., Thingholm, T. E., Jensen, O. N., Roepstorff, P. & Jorgensen, T. J. Highly selective enrichment of phosphorylated peptides from peptide mixtures using titanium dioxide microcolumns. *Mol Cell Proteomics* **4**, 873-886, doi:10.1074/mcp.T500007-MCP200 (2005).

136 Buszewski, B. & Noga, S. Hydrophilic interaction liquid chromatography (HILIC)—a powerful separation technique. *Analytical and Bioanalytical Chemistry* **402**, 231-247, doi:10.1007/s00216-011-5308-5 (2012).

137 Alpert, A. J. Hydrophilic-interaction chromatography for the separation of peptides, nucleic acids and other polar compounds. *Journal of chromatography* **499**, 177-196 (1990).

138 Yoshida, T. Peptide separation by Hydrophilic-Interaction Chromatography: a review. *Journal of biochemical and biophysical methods* **60**, 265-280, doi:10.1016/j.jbbm.2004.01.006 (2004).

139 Millipore, M. https://www.merckmillipore.com/BR/pt/analytics-and-sample-preparation/sequant/what-is-hilic/Ih2b.qB.xfgAAAFFw6IcWdZp,nav. (Accessed January, 2020).

140 Tosoh. https://www.separations.eu.tosohbioscience.com/OpenPDF.aspx?path=~/File%20Library/TBG/Products%20Download//Flyer/f15l13a.pdf. (Accessed January, 2020).

141 Larsen, M. R., Thingholm, T. E., Jensen, O. N., Roepstorff, P. & Jørgensen, T. J. D. Highly Selective Enrichment of Phosphorylated Peptides from Peptide Mixtures Using Titanium Dioxide Microcolumns. *Molecular & Cellular Proteomics* **4**, 873 (2005).

142 McNulty, D. E. & Annan, R. S. Hydrophilic interaction chromatography reduces the complexity of the phosphoproteome and improves global phosphopeptide isolation and detection. *Mol Cell Proteomics* **7**, 971-980, doi:10.1074/mcp.M700543-MCP200 (2008).

143 Otter, D. in *Encyclopedia of Food Sciences and Nutrition (Second Edition)* 4824-4830 (Academic Press, 2003).

144 Gilar, M., Olivova, P., Daly, A. E. & Gebler, J. C. Orthogonality of Separation in Two-Dimensional Liquid Chromatography. *Analytical chemistry* **77**, 6426-6434, doi:10.1021/ac050923i (2005).

145 Batth, T. S., Francavilla, C. & Olsen, J. V. Off-line high-pH reversed-phase fractionation for in-depth phosphoproteomics. *J Proteome Res* **13**, 6176-6186, doi:10.1021/pr500893m (2014).

146 Yang, F., Shen, Y., Camp, D. G. & Smith, R. D. High pH reversed-phase chromatography with fraction concatenation as an alternative to strong-cation exchange chromatography for two-dimensional proteomic analysis. *Expert Review of Proteomics* **9**, 129-134, doi:10.1586/epr.12.15 (2012).

147 Le Bihan, T., Duewel, H. S. & Figeys, D. On-line strong cation exchange µ-HPLC-ESI-MS/MS for protein identification and process optimization. *J Am Soc Mass Spectrom* **14**, 719-727, doi:https://doi.org/10.1016/S1044-0305(03)00208-3 (2003).

148 Alpert, A. J. & Andrews, P. C. Cation-exchange chromatography of peptides on poly(2-sulfoethyl aspartamide)-silica. *Journal of Chromatography A* **443**, 85-96, doi:https://doi.org/10.1016/S0021-9673(00)94785-X (1988).

149 Venne, A. S., Vogtle, F. N., Meisinger, C., Sickmann, A. & Zahedi, R. P. Novel highly sensitive, specific, and straightforward strategy for comprehensive N-terminal proteomics reveals unknown substrates of the mitochondrial peptidase Icp55. *J Proteome Res* **12**, 3823-3830, doi:10.1021/pr400435d (2013).

150 Van Damme, P. *et al.* A review of COFRADIC techniques targeting protein N-terminal acetylation. *BMC Proceedings* **3**, S6-S6, doi:10.1186/1753-6561-3-S6-S6 (2009).

151 Venne, A. S. *et al.* An improved workflow for quantitative N-terminal charge-based fractional diagonal chromatography (ChaFRADIC) to study proteolytic events in Arabidopsis thaliana. *Proteomics* **15**, 2458-2469, doi:10.1002/pmic.201500014 (2015).

10| References

152 Whitley, D., Goldberg, S. P. & Jordan, W. D. Heat shock proteins: A review of the molecular chaperones. *Journal of Vascular Surgery* **29**, 748-751, doi:https://doi.org/10.1016/S0741-5214(99)70329-0 (1999).

153 Ross, P. L. *et al.* Multiplexed protein quantitation in Saccharomyces cerevisiae using amine-reactive isobaric tagging reagents. *Mol Cell Proteomics* **3**, 1154-1169, doi:10.1074/mcp.M400129-MCP200 (2004).

154 Thompson, A. *et al.* Tandem mass tags: a novel quantification strategy for comparative analysis of complex protein mixtures by MS/MS. *Analytical chemistry* **75**, 1895-1904 (2003).

155 Ow, S. Y., Salim, M., Noirel, J., Evans, C. & Wright, P. C. Minimising iTRAQ ratio compression through understanding LC-MS elution dependence and high-resolution HILIC fractionation. *Proteomics* **11**, 2341-2346, doi:10.1002/pmic.201000752 (2011).

156 Savitski, M. M. *et al.* Measuring and managing ratio compression for accurate iTRAQ/TMT quantification. *J Proteome Res* **12**, 3586-3598, doi:10.1021/pr400098r (2013).

157 Scientific, T. https://www.thermofisher.com. (Accessed May, 2018.).

158 Meisinger, C., Pfanner, N. & Truscott, K. N. Isolation of yeast mitochondria. *Methods in molecular biology (Clifton, N.J.)* **313**, 33-39, doi:10.1385/1-59259-958-3:033 (2006).

159 Witte, C., Jensen, R. E., Yaffe, M. P. & Schatz, G. MAS1, a gene essential for yeast mitochondrial assembly, encodes a subunit of the mitochondrial processing protease. *Embo j* **7**, 1439-1447 (1988).

160 Kall, L., Canterbury, J. D., Weston, J., Noble, W. S. & MacCoss, M. J. Semi-supervised learning for peptide identification from shotgun proteomics datasets. *Nature methods* **4**, 923-925, doi:10.1038/nmeth1113 (2007).

161 Thingholm, T. E., Palmisano, G., Kjeldsen, F. & Larsen, M. R. Undesirable charge-enhancement of isobaric tagged phosphopeptides leads to reduced identification efficiency. *J Proteome Res* **9**, 4045-4052, doi:10.1021/pr100230q (2010).

162 Kollipara, L. *et al.* In-depth phenotyping of lymphoblastoid cells suggests selective cellular vulnerability in Marinesco-Sjögren syndrome. *Oncotarget* **8**, 68493-68516, doi:10.18632/oncotarget.19663 (2017).

163 Engholm-Keller, K. *et al.* TiSH--a robust and sensitive global phosphoproteomics strategy employing a combination of TiO2, SIMAC, and HILIC. *J Proteomics* **75**, 5749-5761, doi:10.1016/j.jprot.2012.08.007 (2012).

164 Rappsilber, J., Mann, M. & Ishihama, Y. Protocol for micro-purification, enrichment, pre-fractionation and storage of peptides for proteomics using StageTips. *Nature protocols* **2**, 1896-1906, doi:10.1038/nprot.2007.261 (2007).

165 in *Handbook of Metalloproteins*.

166 Vaudel, M., Barsnes, H., Berven, F. S., Sickmann, A. & Martens, L. SearchGUI: An open-source graphical user interface for simultaneous OMSSA and X!Tandem searches. *Proteomics* **11**, 996-999, doi:10.1002/pmic.201000595 (2011).

167 Vaudel, M. *et al.* PeptideShaker enables reanalysis of MS-derived proteomics data sets. *Nature biotechnology* **33**, 22-24, doi:10.1038/nbt.3109 (2015).

168 Ben-Aroya, S., Pan, X., Boeke, J. D. & Hieter, P. Making temperature-sensitive mutants. *Methods in enzymology* **470**, 181-204, doi:10.1016/S0076-6879(10)70008-2 (2010).

169 Tan, G., Chen, M., Foote, C. & Tan, C. Temperature-Sensitive Mutations Made Easy: Generating Conditional Mutations by Using Temperature-Sensitive Inteins That Function Within Different Temperature Ranges. *Genetics* **183**, 13-22, doi:10.1534/genetics.109.104794 (2009).

170 Varadarajan, R., Nagarajaram, H. A. & Ramakrishnan, C. A procedure for the prediction of temperature-sensitive mutants of a globular protein based solely on the amino acid sequence. *Proceedings of the National Academy of Sciences* **93**, 13908-13913, doi:10.1073/pnas.93.24.13908 (1996).

10| References

171 Ben-Aroya, S. *et al.* Toward a Comprehensive Temperature-Sensitive Mutant Repository of the Essential Genes of Saccharomyces cerevisiae. *Molecular cell* **30**, 248-258, doi:10.1016/j.molcel.2008.02.021 (2008).

172 Gakh, O., Cavadini, P. & Isaya, G. Mitochondrial processing peptidases. *Biochimica et Biophysica Acta (BBA) - Molecular Cell Research* **1592**, 63-77, doi:https://doi.org/10.1016/S0167-4889(02)00265-3 (2002).

173 Vögtle, F. N. *et al.* Landscape of submitochondrial protein distribution. *Nature communications* **8**, 290, doi:10.1038/s41467-017-00359-0 (2017).

174 Pfeffer, S., Woellhaf, M. W., Herrmann, J. M. & Forster, F. Organization of the mitochondrial translation machinery studied in situ by cryoelectron tomography. *Nature communications* **6**, 6019, doi:10.1038/ncomms7019 (2015).

175 Na, U. *et al.* The LYR factors SDHAF1 and SDHAF3 mediate maturation of the iron-sulfur subunit of succinate dehydrogenase. *Cell metabolism* **20**, 253-266, doi:10.1016/j.cmet.2014.05.014 (2014).

176 Dennis, R. A. & McCammon, M. T. Acn9 is a novel protein of gluconeogenesis that is located in the mitochondrial intermembrane space. *Eur J Biochem* **261**, 236-243, doi:10.1046/j.1432-1327.1999.00267.x (1999).

177 Pfanner, N. *et al.* Uniform nomenclature for the mitochondrial contact site and cristae organizing system. *The Journal of cell biology* **204**, 1083-1086, doi:10.1083/jcb.201401006 (2014).

178 Szklarczyk, D. *et al.* The STRING database in 2017: quality-controlled protein-protein association networks, made broadly accessible. **45**, D362-d368, doi:10.1093/nar/gkw937 (2017).

179 Gerbeth, C. *et al.* Glucose-induced regulation of protein import receptor Tom22 by cytosolic and mitochondria-bound kinases. *Cell metabolism* **18**, 578-587, doi:10.1016/j.cmet.2013.09.006 (2013).

180 Schmidt, O. *et al.* Regulation of mitochondrial protein import by cytosolic kinases. *Cell* **144**, 227-239, doi:10.1016/j.cell.2010.12.015 (2011).

181 Rao, S. *et al.* Biogenesis of the preprotein translocase of the outer mitochondrial membrane: protein kinase A phosphorylates the precursor of Tom40 and impairs its import. *Molecular Biology of the Cell* **23**, 1618-1627, doi:10.1091/mbc.E11-11-0933 (2012).

182 Dudek, J., Rehling, P. & van der Laan, M. Mitochondrial protein import: Common principles and physiological networks. *Biochimica et Biophysica Acta (BBA) - Molecular Cell Research* **1833**, 274-285, doi:https://doi.org/10.1016/j.bbamcr.2012.05.028 (2013).

183 Opalińska, M. & Meisinger, C. Mitochondrial protein import under kinase surveillance. *Microbial Cell* **1**, 51-57, doi:10.15698/mic2014.01.127 (2014).

184 Lill, R. & Muhlenhoff, U. Iron-sulfur-protein biogenesis in eukaryotes. *Trends Biochem Sci* **30**, 133-141, doi:10.1016/j.tibs.2005.01.006 (2005).

185 Schmidt, O. *et al.* Regulation of Mitochondrial Protein Import by Cytosolic Kinases. *Cell* **144**, 227-239, doi:http://dx.doi.org/10.1016/j.cell.2010.12.015 (2011).

186 Zhang, X., Lester, R. L. & Dickson, R. C. Pil1p and Lsp1p negatively regulate the 3-phosphoinositide-dependent protein kinase-like kinase Pkh1p and downstream signaling pathways Pkc1p and Ypk1p. *J Biol Chem* **279**, 22030-22038, doi:10.1074/jbc.M400299200 (2004).

187 Leskoske, K. L., Roelants, F. M., Marshall, M. N. M., Hill, J. M. & Thorner, J. The Stress-Sensing TORC2 Complex Activates Yeast AGC-Family Protein Kinase Ypk1 at Multiple Novel Sites. *Genetics* **207**, 179-195, doi:10.1534/genetics.117.1124 (2017).

188 Audhya, A. *et al.* Genome-wide lethality screen identifies new PI4,5P2 effectors that regulate the actin cytoskeleton. *Embo j* **23**, 3747-3757, doi:10.1038/sj.emboj.7600384 (2004).

189 Mamnun, Y. M., Schuller, C. & Kuchler, K. Expression regulation of the yeast PDR5 ATP-binding cassette (ABC) transporter suggests a role in cellular detoxification during the exponential growth phase. *FEBS letters* **559**, 111-117, doi:10.1016/s0014-5793(04)00046-8 (2004).

10| References

190 Scherer, W. F., Syverton, J. T. & Gey, G. O. Studies on the propagation in vitro of poliomyelitis viruses. IV. Viral multiplication in a stable strain of human malignant epithelial cells (strain HeLa) derived from an epidermoid carcinoma of the cervix. *The Journal of experimental medicine* **97**, 695-710 (1953).

191 Giard, D. J. *et al.* In vitro cultivation of human tumors: establishment of cell lines derived from a series of solid tumors. *Journal of the National Cancer Institute* **51**, 1417-1423 (1973).

192 Uhlen, M. *et al.* Proteomics. Tissue-based map of the human proteome. *Science* **347**, 1260419, doi:10.1126/science.1260419 (2015).

193 Uhlen, M. *et al.* Towards a knowledge-based Human Protein Atlas. *Nature biotechnology* **28**, 1248-1250, doi:10.1038/nbt1210-1248 (2010).

194 Thul, P. J. & Akesson, L. A subcellular map of the human proteome. **356**, doi:10.1126/science.aal3321 (2017).

195 Gonczarowska-Jorge, H. *et al.* Quantifying Missing (Phospho)Proteome Regions with the Broad-Specificity Protease Subtilisin. **89**, 13137-13145, doi:10.1021/acs.analchem.7b02395 (2017).

196 Burkhart, J. M., Schumbrutzki, C., Wortelkamp, S., Sickmann, A. & Zahedi, R. P. Systematic and quantitative comparison of digest efficiency and specificity reveals the impact of trypsin quality on MS-based proteomics. *J Proteomics* **75**, 1454-1462, doi:10.1016/j.jprot.2011.11.016 (2012).

197 Dickhut, C., Feldmann, I., Lambert, J. & Zahedi, R. P. Impact of digestion conditions on phosphoproteomics. *J Proteome Res* **13**, 2761-2770, doi:10.1021/pr401181y (2014).

198 Fenyö, D., Eriksson, J. & Beavis, R. Mass Spectrometric Protein Identification Using the Global Proteome Machine. *Methods in molecular biology (Clifton, N.J.)* **673**, 189-202, doi:10.1007/978-1-60761-842-3_11 (2010).

199 Colaert, N., Helsens, K., Martens, L., Vandekerckhove, J. & Gevaert, K. Improved visualization of protein consensus sequences by iceLogo. *Nature methods* **6**, 786-787, doi:10.1038/nmeth1109-786 (2009).

200 Baker, M. S., Ahn, S. B., Mohamedali, A. & Islam, M. T. Accelerating the search for the missing proteins in the human proteome. **8**, 14271, doi:10.1038/ncomms14271 (2017).

201 Omenn, G. S. *et al.* Metrics for the Human Proteome Project 2015: Progress on the Human Proteome and Guidelines for High-Confidence Protein Identification. *J Proteome Res* **14**, 3452-3460, doi:10.1021/acs.jproteome.5b00499 (2015).

202 Gaudet, P. *et al.* The neXtProt knowledgebase on human proteins: 2017 update. *Nucleic acids research* **45**, D177-d182, doi:10.1093/nar/gkw1062 (2017).

203 Taus, T. *et al.* Universal and confident phosphorylation site localization using phosphoRS. *J Proteome Res* **10**, 5354-5362, doi:10.1021/pr200611n (2011).

204 Hornbeck, P. V. *et al.* PhosphoSitePlus, 2014: mutations, PTMs and recalibrations. *Nucleic acids research* **43**, D512-520, doi:10.1093/nar/gku1267 (2015).

205 Sharma, K. *et al.* Ultradeep human phosphoproteome reveals a distinct regulatory nature of Tyr and Ser/Thr-based signaling. *Cell reports* **8**, 1583-1594, doi:10.1016/j.celrep.2014.07.036 (2014).

206 Kyte, J. & Doolittle, R. F. A simple method for displaying the hydropathic character of a protein. *Journal of molecular biology* **157**, 105-132 (1982).

207 Pichler, P. *et al.* Peptide Labeling with Isobaric Tags Yields Higher Identification Rates Using iTRAQ 4-Plex Compared to TMT 6-Plex and iTRAQ 8-Plex on LTQ Orbitrap. *Analytical chemistry* **82**, 6549-6558, doi:10.1021/ac100890k (2010).

208 Ross, P. L. *et al.* Multiplexed Protein Quantitation in Saccharomyces cerevisiae Using Amine-reactive Isobaric Tagging Reagents. *Molecular & Cellular Proteomics* **3**, 1154-1169, doi:10.1074/mcp.M400129-MCP200 (2004).

209 Ting, L., Rad, R., Gygi, S. P. & Haas, W. MS3 eliminates ratio distortion in isobaric multiplexed quantitative proteomics. *Nature methods* **8**, 937-940, doi:10.1038/nmeth.1714 (2011).

10| References

210 Erickson, B. K. *et al.* Evaluating multiplexed quantitative phosphopeptide analysis on a hybrid quadrupole mass filter/linear ion trap/orbitrap mass spectrometer. *Analytical chemistry* **87**, 1241-1249, doi:10.1021/ac503934f (2015).

211 Watts, G. D. J. *et al.* Inclusion body myopathy associated with Paget disease of bone and frontotemporal dementia is caused by mutant valosin-containing protein. *Nat Genet* **36**, 377-381, doi:10.1038/ng1332 (2004).

212 Pirino, G., Wescott, M. P. & Donovan, P. J. Protein kinase A regulates resumption of meiosis by phosphorylation of Cdc25B in mammalian oocytes. *Cell cycle (Georgetown, Tex.)* **8**, 665-670, doi:10.4161/cc.8.4.7846 (2009).

213 Baker, M. A., Hetherington, L., Curry, B. & Aitken, R. J. Phosphorylation and consequent stimulation of the tyrosine kinase c-Abl by PKA in mouse spermatozoa; its implications during capacitation. *Developmental biology* **333**, 57-66, doi:10.1016/j.ydbio.2009.06.022 (2009).

214 Taylor, S. S., Ilouz, R., Zhang, P. & Kornev, A. P. Assembly of allosteric macromolecular switches: lessons from PKA. *Nature reviews. Molecular cell biology* **13**, 646-658, doi:10.1038/nrm3432 (2012).

215 Taylor, S. S., Buechler, J. A. & Yonemoto, W. cAMP-dependent protein kinase: framework for a diverse family of regulatory enzymes. *Annual review of biochemistry* **59**, 971-1005, doi:10.1146/annurev.bi.59.070190.004543 (1990).

216 Herberg, F. W., Taylor, S. S. & Dostmann, W. R. Active site mutations define the pathway for the cooperative activation of cAMP-dependent protein kinase. *Biochemistry* **35**, 2934-2942, doi:10.1021/bi951647c (1996).

217 Isensee, J. *et al.* PKA-RII subunit phosphorylation precedes activation by cAMP and regulates activity termination. *The Journal of cell biology* (2018).

218 Jiskoot, W., Beuvery, E. C., de Koning, A. A., Herron, J. N. & Crommelin, D. J. Analytical approaches to the study of monoclonal antibody stability. *Pharmaceutical research* **7**, 1234-1241 (1990).

219 Berman, H., Henrick, K. & Nakamura, H. Announcing the worldwide Protein Data Bank. *Nature Structural Biology* **10**, 980, doi:10.1038/nsb1203-980 (2003).

220 Schrödinger, L., The PyMol Molecular Graphics System, 1.5.0.4; 2013.

221 Hemmer, W., McGlone, M., Tsigelny, I. & Taylor, S. S. Role of the glycine triad in the ATP-binding site of cAMP-dependent protein kinase. *J Biol Chem* **272**, 16946-16954 (1997).

222 Voegtle, F.-N. *et al.* Intermembrane space proteome of yeast mitochondria. *Molecular & Cellular Proteomics*, doi:10.1074/mcp.M112.021105 (2012).

223 Besingi, R. N. & Clark, P. L. Extracellular Protease Digestion to Evaluate Membrane Protein Cell Surface Localization. *Nature protocols* **10**, 2074-2080, doi:10.1038/nprot.2015.131 (2015).

224 Kang'ethe, W. & Bernstein, H. D. Stepwise Folding of an Autotransporter Passenger Domain Is Not Essential for Its Secretion. *The Journal of Biological Chemistry* **288**, 35028-35038, doi:10.1074/jbc.M113.515635 (2013).

225 Noinaj, N. *et al.* Structural insight into the biogenesis of β-barrel membrane proteins. *Nature* **501**, 385-390, doi:10.1038/nature12521 (2013).

226 Harbauer, Angelika B., Zahedi, René P., Sickmann, A., Pfanner, N. & Meisinger, C. The Protein Import Machinery of Mitochondria—A Regulatory Hub in Metabolism, Stress, and Disease. *Cell Metabolism* **19**, 357-372, doi:https://doi.org/10.1016/j.cmet.2014.01.010 (2014).

227 Kane, L. A., Youngman, M. J., Jensen, R. E. & Van Eyk, J. E. Phosphorylation of the F(1)F(o) ATP synthase β subunit: Functional and structural consequences assessed in a model system. *Circulation research* **106**, 504-513, doi:10.1161/CIRCRESAHA.109.214155 (2010).

228 Horbinski, C. & Chu, C. T. Kinase signaling cascades in the mitochondrion: a matter of life or death. *Free radical biology & medicine* **38**, 2-11, doi:10.1016/j.freeradbiomed.2004.09.030 (2005).

10| References

229 Gibson, B. W. The human mitochondrial proteome: oxidative stress, protein modifications and oxidative phosphorylation. *The international journal of biochemistry & cell biology* **37**, 927-934, doi:10.1016/j.biocel.2004.11.013 (2005).

230 Huttemann, M., Lee, I., Samavati, L., Yu, H. & Doan, J. W. Regulation of mitochondrial oxidative phosphorylation through cell signaling. *Biochimica et biophysica acta* **1773**, 1701-1720 (2007).

11 Supplemental Figures and Tables

11.1 Figures and Tables from 9.1.1 Mitochondrial MAS ChaFRADIC experiments

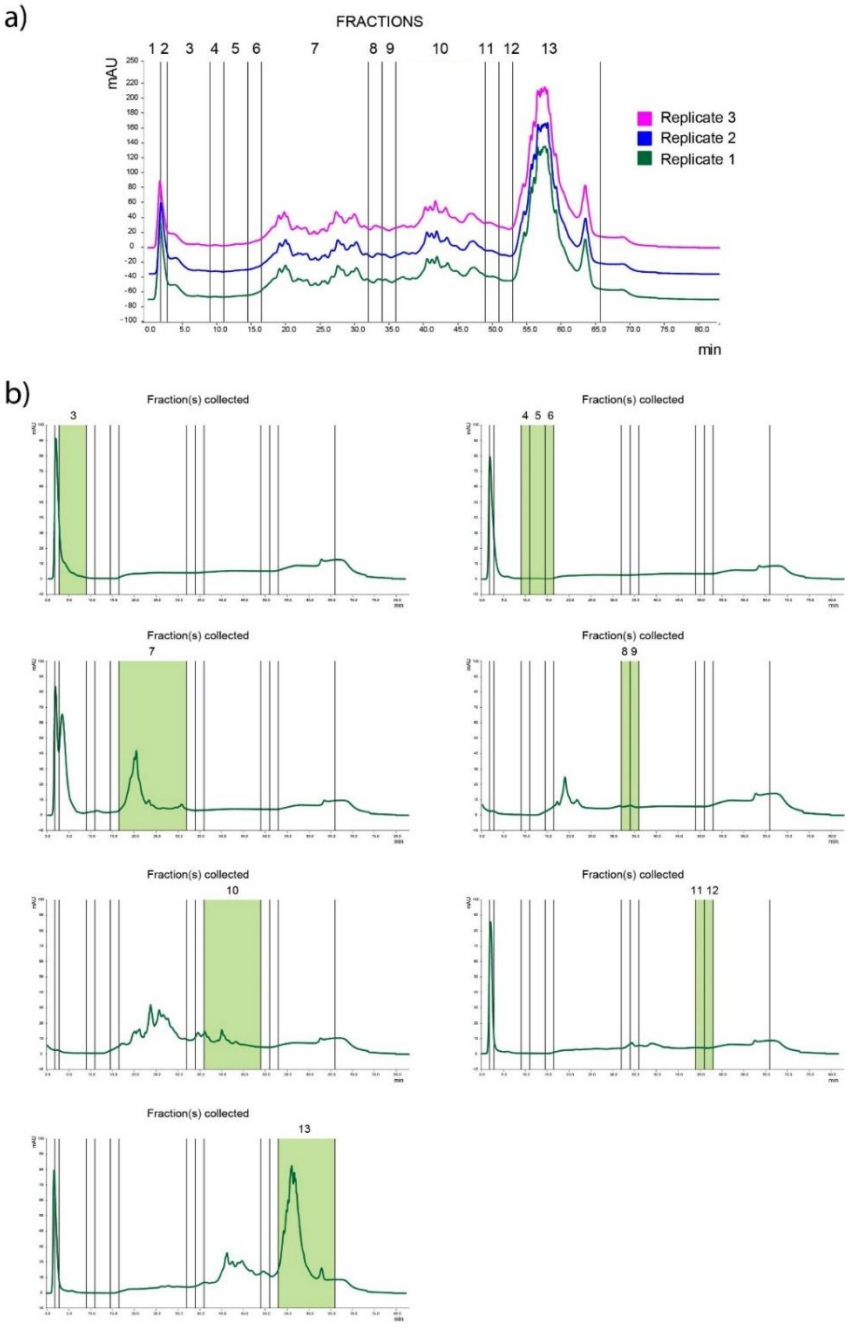

Supplemental Figure 1. Strong cationic exchange (SCX) fractionation of the mitochondrial biological replicates. a) Reproducibility from the 3 biological replicates can be seen by similar chromatograms. For each biological replicate SCX fractionation, 13 fractions were collected, measured by LC/MS and pooled together according to charge state. b) Second SCX fractionation of each fraction (individually or pooled). The injected fractions correspond to the collected fractions as well (green column), in which original protein N-termini remain in the same elution time point, while not original protein N-termini elute in earlier fractions, as described in the ChaFRADIC protocol. It is possible to observe peptides eluting in earlier fractions than injected due to derivatization.

11| Supplemental Figures and Tables

Supplemental Table 1. Peptide charge state composition of each fraction of the SCX chromatography ChaFRADIC MAS1 mitochondria experiment The 13 fractions collected after the first SCX dimension of the 3 yeast biological replicates. Each fraction was measured by LC/MS to determine overall peptide charge state. Fractions with similar charge state were pooled together (3, 4-6, 7, 8 and 9, 10, 11 and 12, 13). Total peptides identified for each fraction are determined below.

Replicate 1	Composition (in %)												
Fraction	1	2	3	4	5	6	7	8	9	10	11	12	13
no charge	0,0	0,0	0,0	0,0	0,0	0,0	0,0	0,0	0,0	0,0	0,0	0,0	0,0
charge +1	0,0	5,7	82,8	16,7	2,0	2,8	0,0	0,1	0,2	0,4	0,6	3,6	0,5
charge +2	0,0	85,7	17,2	83,3	98,0	97,9	86,2	6,7	6,8	4,6	3,6	5,8	6,0
charge +3	0,0	8,6	1,0	0,0	0,0	0,0	13,8	92,9	92,4	61,6	8,9	12,3	11,4
charge +4	0,0	0,0	0,0	0,0	0,0	0,0	0,0	0,3	0,8	32,9	85,7	76,8	50,2
charge +5	0,0	0,0	0,0	0,0	0,0	0,0	0,0	0,0	0,0	0,4	1,2	2,2	27,9
charge +6	0,0	0,0	0,0	0,0	0,0	0,0	0,0	0,0	0,0	0,0	0,0	0,0	4,5
total peptides	0	35	99	24	50	143	738	775	529	453	168	138	201
Replicate 2	Composition (in %)												
Fraction	1	2	3	4	5	6	7	8	9	10	11	12	13
no charge	0,0	0,0	0,0	0,0	0,0	0,0	0,0	0,0	0,0	0,0	0,0	0,0	0,0
charge +1	0,0	35,3	100,0	0,0	0,0	0,0	0,1	0,0	0,0	0,0	0,1	0,1	0,3
charge +2	0,0	34,1	0,0	100,0	99,6	100,0	66,6	2,1	2,2	0,5	2,1	2,2	0,6
charge +3	0,0	18,8	0,0	0,0	0,4	0,0	33,3	95,9	92,8	17,7	10,0	9,5	7,1
charge +4	0,0	11,8	0,0	0,0	0,0	0,0	0,0	2,1	5,1	79,8	67,5	64,2	29,7
charge +5	0,0	0,0	0,0	0,0	0,0	0,0	0,0	0,0	0,0	2,1	20,2	23,6	50,3
charge +6	0,0	0,0	0,0	0,0	0,0	0,0	0,0	0,0	0,0	0,0	0,0	0,4	11,9
total peptides	0	85	21	17	273	495	1857	582	277	435	989	692	310
Replicate 3	Composition (in %)												
Fraction	1	2	3	4	5	6	7	8	9	10	11	12	13
no charge	0,0	0,0	0,0	0,0	0,0	0,0	0,0	0,0	0,0	0,0	0,0	0,0	0,0
charge +1	0,0	10,1	100,0	12,7	5,4	1,7	0,1	0,0	0,0	0,0	0,3	0,5	0,2
charge +2	0,0	73,7	0,0	87,3	94,6	98,3	80,2	1,8	2,0	0,2	3,0	3,6	0,5
charge +3	0,0	9,2	0,0	0,0	0,0	0,0	19,7	94,3	92,1	34,6	9,2	8,1	6,0
charge +4	0,0	7,0	0,0	0,0	0,0	0,0	0,0	3,9	5,9	63,5	65,2	60,4	29,8
charge +5	0,0	0,0	0,0	0,0	0,0	0,0	0,0	0,0	0,0	1,7	22,3	26,7	56,3
charge +6	0,0	0,0	0,0	0,0	0,0	0,0	0,0	0,0	0,0	0,0	0,0	0,7	7,2
total peptides	0	42	17	23	125	221	1242	325	150	327	774	565	244

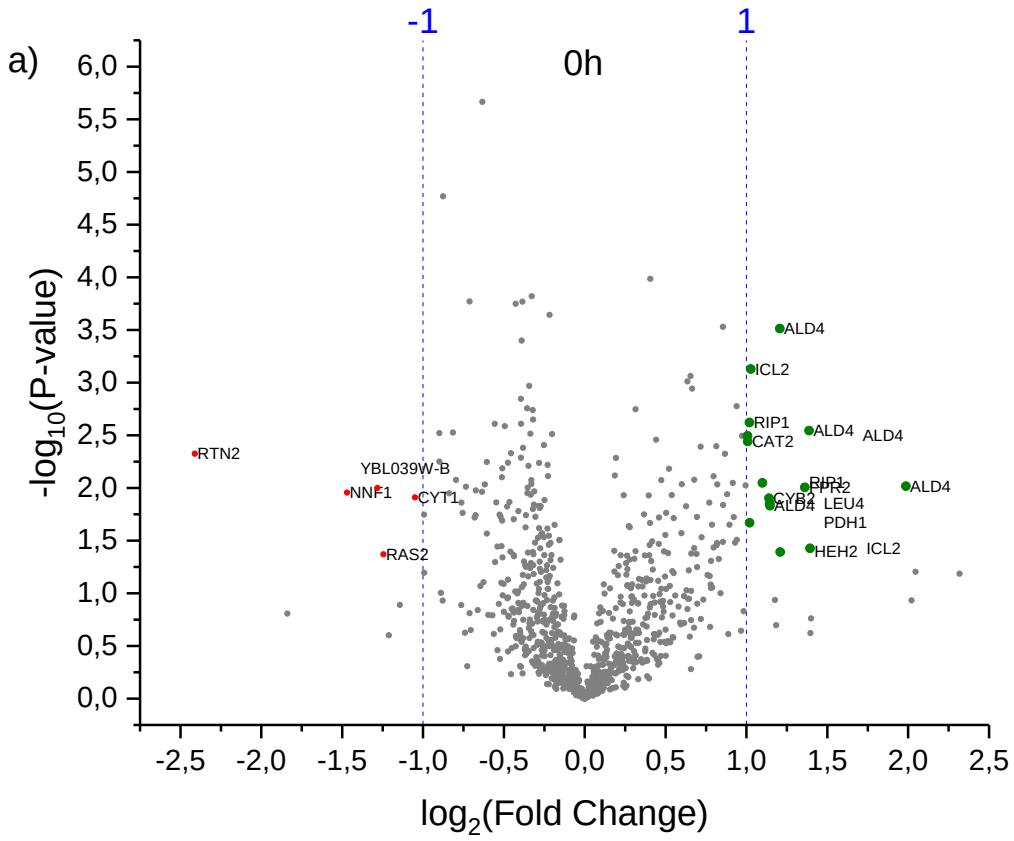

Supplemental Figure 2. Volcano plots of the mitochondrial temperature sensitive MAS1 mutant against the wild type. a), b) and c) present, respectively, the volcano plots of the 0 h, 2 h and 4 h time shift. Green dots indicate up-regulated proteins. A 2-fold sample difference was considered to evaluate regulation ($p \leq 0.05$). Up-regulated proteins in the 0 h were disregarded in the 2 h and 4 h analysis. Figure parts B and C are in the following pages due to size fitting.

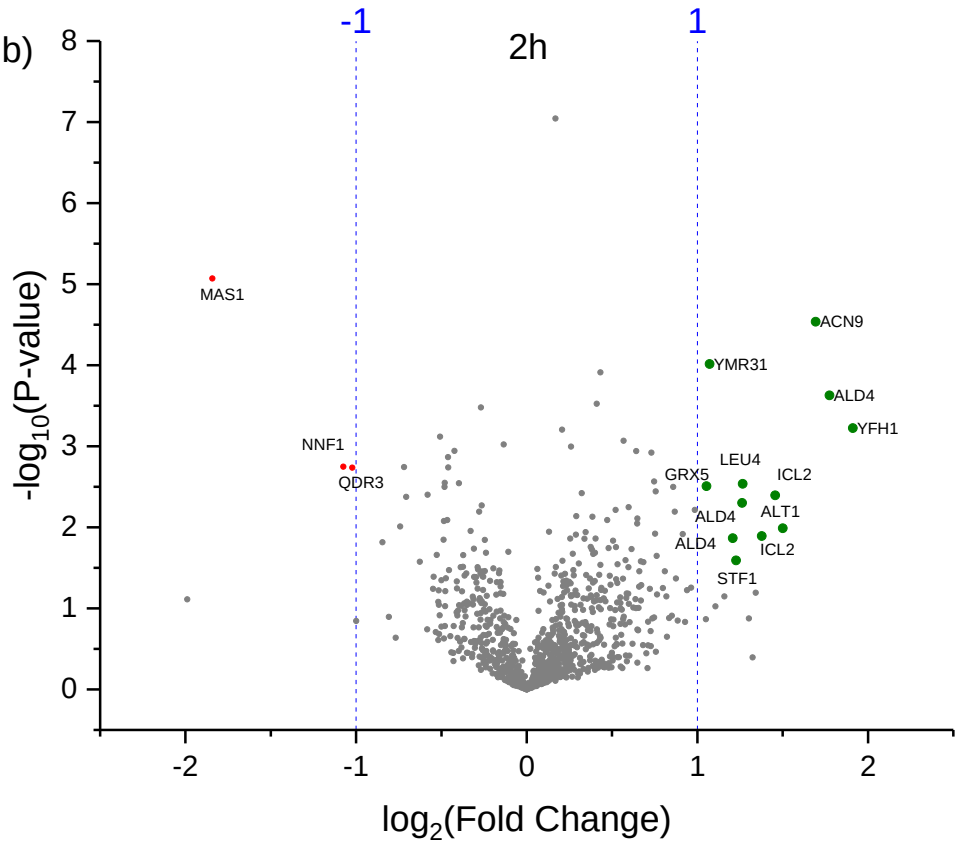

Supplemental Figure 2. Volcano plots of the mitochondrial temperature sensitive MAS1 mutant against the wild type. a), b) and c) present, respectively, the volcano plots of the 0 h, 2 h and 4 h time shift. Green dots indicate up-regulated proteins. A 2-fold sample difference was considered to evaluate regulation ($p \leq 0.05$). Up-regulated proteins in the 0 h were disregarded in the 2 h and 4 h analysis.

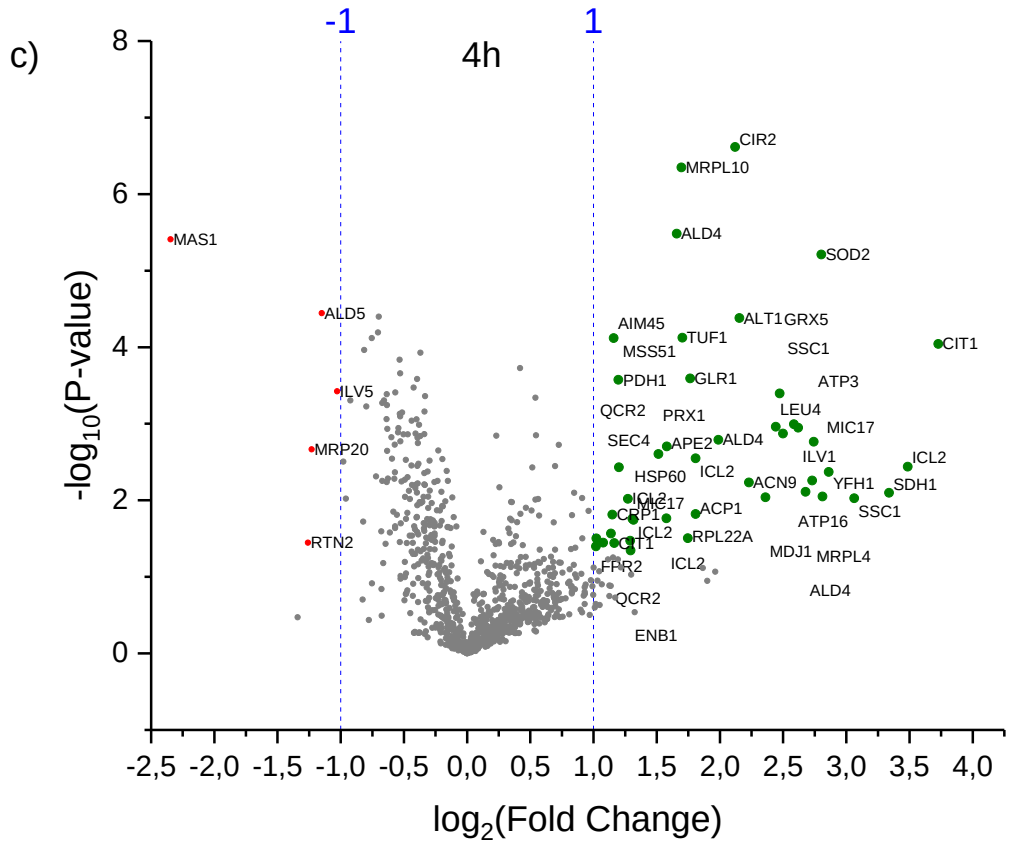

Supplemental Figure 2. Volcano plots of the mitochondrial temperature sensitive MAS1 mutant against the wild type. a), b) and c) present, respectively, the volcano plots of the 0 h, 2 h and 4 h time shift. Green dots indicate up-regulated proteins. A 2-fold sample difference was considered to evaluate regulation ($p \leq 0.05$). Up-regulated proteins in the 0 h were disregarded in the 2 h and 4 h analysis.

11| Supplemental Figures and Tables

Supplemental Table 2. Up- and down-regulated peptides from the 0 h time shift MAS1 mitochondrial ChaFRADIC experiment. At least a 2-fold regulation between the mutant and respective wild type was considered as regulation ($p \leq 0.05$). Wild type (WT) and mutant normalized abundance values are displayed.

Protein accession	gene	mito?	peptide	WT yeast batch1	WT yeast batch 2	WT yeast batch 3	Mas1 mutant batch1	Mas1 mutant batch 2	Mas1 mutant batch 3	T.TEST mutants against its respective wild types	Average WT	Average mutant	Mutant divided by its respective wild type	Log 2
YOR374W	ALD4	yes	sTLcLkTSASSIGR	0,45	0,61	0,70	1,78	1,36	1,47	0,00	0,59	1,54	2,62	1,39
YNL104C	LEU4	yes	vkESIIALAEHAASR	0,64	0,75	0,80	1,61	1,25	1,97	0,01	0,73	1,61	2,21	1,14
YDR519W	FPR2	no	gSLSDLEIGIIkR	0,26	0,53	0,35	1,15	0,80	0,99	0,01	0,38	0,98	2,57	1,36
YOR374W	ALD4	yes	lkTSASSIGR	0,37	0,56	0,37	1,55	1,36	2,24	0,01	0,43	1,72	3,96	1,99
YOR374W	ALD4	yes	kTSASSIGR	0,62	0,52	0,65	1,29	1,38	1,48	0,00	0,60	1,38	2,31	1,21
YPR002W	PDH1	yes	tATDYSDEVAR	0,66	0,95	0,95	1,49	2,17	1,53	0,02	0,85	1,73	2,03	1,02
YML054C	CYB2	yes	vTVDAPSLGQR	0,75	0,73	1,08	2,03	2,14	1,47	0,01	0,85	1,88	2,20	1,14
YPR006C	ICL2	yes	mINNkTFNR	0,66	0,65	0,82	1,55	1,35	1,46	0,00	0,71	1,45	2,04	1,03
YEL024W	RIP1	yes	iSQSLLASkSTYR	0,33	0,31	0,40	0,88	0,60	0,74	0,01	0,34	0,74	2,14	1,10
YEL024W	RIP1	yes	aLkDPQTDADR	0,47	0,29	0,37	0,74	0,73	0,81	0,00	0,38	0,76	2,03	1,02
YOR374W	ALD4	yes	eGREDDVEEAVQAADR	0,56	0,41	0,50	0,97	1,35	0,91	0,01	0,49	1,08	2,21	1,15
YDR458C	HEH2	no	kISETFDNQDEEDTSR	0,54	0,83	0,48	1,65	0,93	1,72	0,04	0,62	1,43	2,31	1,21
YPR006C	ICL2	yes	mINNkTFNR	0,69	0,73	1,15	2,02	3,08	1,64	0,04	0,86	2,25	2,63	1,39
YML042W	CAT2	yes	cLDLDQSPVTLEEkSR	0,92	1,06	0,87	2,20	1,75	1,77	0,00	0,95	1,91	2,01	1,01
YOR374W	ALD4	yes	dNGkAISSSR	0,40	0,36	0,37	0,73	0,68	0,87	0,00	0,38	0,76	2,01	1,01
YJR112W	NNF1	no	vNSHGIR	0,66	0,83	1,03	0,32	0,20	0,39	0,01	0,84	0,30	0,36	-1,47
YBL039W-B	YBL039W-B	no	gFFNNNPVIEFFHR	0,87	1,12	0,77	0,32	0,33	0,49	0,01	0,92	0,38	0,41	-1,28
YNL098C	RAS2	yes	sTTVVNAR	0,46	0,85	0,88	0,23	0,40	0,29	0,04	0,73	0,31	0,42	-1,24
YOR065W	CYT1	yes	vGVSHTNEEVR	1,13	1,42	1,71	0,71	0,69	0,66	0,01	1,42	0,69	0,48	-1,05
YDL204W	RTN2	no	dIEEELAAHQR	0,55	0,81	0,56	0,17	0,14	0,05	0,00	0,64	0,12	0,19	-2,41

Supplemental Table 3. Up- and down-regulated peptides from the 2 h time shift MAS1 mitochondrial ChaFRADIC experiment. At least a 2-fold regulation between the mutant and respective wild type was considered as regulation ($p \leq 0.05$). Wild type (WT) and mutant normalized abundance values are displayed.

Protein accession	gene	mito?	peptide	WT yeast batch1	WT yeast batch 2	WT yeast batch 3	Mas1 mutant batch1	Mas1 mutant batch 2	Mas1 mutant batch 3	T.TEST mutants against its respective wild types	Average WT	Average mutant	Mutant divided by its respective wild type	Log 2
YPR006C	ICL2	yes	mITmINNkTFNR	0,90	0,89	0,59	1,66	2,28	1,56	0,01	0,79	1,84	2,31	1,21
YDL120W	YFH1	yes	iAAAGGER	0,41	0,42	0,48	1,62	1,44	1,85	0,00	0,43	1,63	3,76	1,91
YOR374W	ALD4	yes	sTLcLkTSASSIGR	0,45	0,56	0,59	1,33	1,76	1,30	0,00	0,53	1,46	2,74	1,46
YNL104C	LEU4	yes	vkESIIALAEHAASR	0,60	0,59	0,58	1,36	1,70	1,20	0,01	0,59	1,42	2,40	1,26
YDR511W	ACN9	yes	mNNkLIYR	0,89	0,90	0,84	2,75	3,01	2,74	0,00	0,88	2,83	3,23	1,69
YPL059W	GRX5	yes	mFLPkFNPIR	0,84	0,95	0,79	1,61	1,69	2,06	0,00	0,86	1,79	2,08	1,05
YLR089C	ALT1	yes	sLSGQSSLNDLR	0,97	0,85	0,67	1,93	2,13	2,98	0,01	0,83	2,35	2,83	1,50
YOR374W	ALD4	yes	lkTSASSIGR	0,42	0,64	0,34	1,59	1,58	1,62	0,00	0,47	1,60	3,42	1,77
YPR006C	ICL2	yes	eVSPDFGDYPYDTVPNQVER	1,11	0,65	0,85	1,15	2,10	2,57	0,07	0,87	1,94	2,23	1,16
YOR374W	ALD4	yes	kTSASSIGR	0,71	0,62	0,66	1,66	1,82	1,34	0,00	0,67	1,60	2,41	1,27
YPR006C	ICL2	yes	mINNkTFNR	0,64	0,39	0,63	1,34	1,81	1,18	0,01	0,55	1,44	2,60	1,38
YPR006C	ICL2	yes	sGESFTETQF	1,10	0,65	0,71	0,90	2,45	1,74	0,14	0,82	1,70	2,07	1,05
YDR190C	RVB1	no	vAISEVkENPGVNSSNSGAVTR	0,70	1,11	0,91	2,68	2,10	1,09	0,09	0,91	1,96	2,15	1,11
YCR010C	ADY2	yes	tGGDNNEYIYIGR	1,36	0,97	0,88	0,95	6,11	0,98	0,40	1,07	2,68	2,50	1,32
YPR006C	ICL2	yes	mINNkTFNR	0,68	0,53	0,82	1,31	2,69	1,00	0,13	0,67	1,66	2,47	1,30
YDL130W-A	STF1	yes	dGPLGGAGPGNPQDIFIkR	0,85	1,00	0,96	2,74	1,52	2,32	0,03	0,94	2,19	2,34	1,23
YFR049W	YMR31	yes	mIATPIR	0,66	0,69	0,58	1,34	1,31	1,42	0,00	0,64	1,36	2,10	1,07
YJR112W	NNF1	no	vNSHGIR	1,34	1,65	1,36	0,66	0,69	0,72	0,00	1,45	0,69	0,47	-1,07
YBL039W-B	YBL039W-B	no	gFFNNNPVIEFFHR	1,20	1,15	2,34	0,84	0,44	1,07	0,14	1,57	0,78	0,50	-1,00
YLR340W	RPP0	no	sAASGDAAPAEEAAAEEEEESDDDmGFGLFD	0,49	0,79	0,54	1,08	2,23	1,29	0,06	0,61	1,53	2,54	1,34
YDL204W	RTN2	no	dIEEELAAHQR	5,02	3,54	1,42	0,68	1,12	0,71	0,08	3,33	0,84	0,25	-1,99
YBR043C	QDR3	no	nLESTASNSR	1,89	1,65	1,53	0,90	0,86	0,74	0,00	1,69	0,83	0,49	-1,02
YLR163C	MAS1	yes	sTISSQIPGTR	1,03	1,11	1,05	0,28	0,32	0,28	0,00	1,06	0,30	0,28	-1,84

11| Supplemental Figures and Tables

Supplemental Table 4. Up- and down-regulated peptides from the 4 h time shift MAS1 mitochondrial ChaFRADIC experiment. At least a 2-fold regulation between the mutant and respective wild type was considered as regulation ($p < 0.05$). Wild type (WT) and mutant normalized abundance values are displayed.

Protein accession	gene	mito?	peptide	WT yeast batch1	WT yeast batch 2	WT yeast batch 3	Mas1 mutant batch1	Mas1 mutant batch 2	Mas1 mutant batch 3	T.TEST mutants against its respective wild types	Average WT	Average mutant	Mutant divided by its respective wild type	Log 2
YNR001C	CIT1	yes	sAILSTTSkSFLSR	0,89	0,81	0,69	11,77	10,03	9,87	0,00	0,80	10,56	13,25	3,73
YPR006C	ICL2	yes	mITmINNkTFNR	0,67	0,78	0,53	8,97	7,92	5,27	0,00	0,66	7,39	11,21	3,49
YKL148C	SDH1	yes	mLSLkkSALSkLTLLR	1,02	1,19	0,98	7,32	10,74	14,14	0,01	1,06	10,74	10,11	3,34
YJR045C	SSC1	yes	mLAAkNILNR	0,92	0,84	0,87	6,75	5,27	9,93	0,01	0,88	7,32	8,36	3,06
YDL120W	YFH1	yes	iAAAGGER	0,41	0,34	0,37	3,45	2,60	2,08	0,00	0,37	2,71	7,27	2,86
YMR002W	MIC17	yes	qQQQPNAYSHPPAAGAQTR	0,69	1,05	0,50	4,26	4,37	7,12	0,01	0,75	5,25	7,02	2,81
YHR008C	SOD2	yes	mFAkTAAANLTkkGGLSLLSTTAR	0,87	0,90	0,71	5,96	5,83	5,47	0,00	0,83	5,75	6,97	2,80
YBR039W	ATP3	yes	sVmcHQAQVGILYkTNPVR	1,12	1,07	0,86	8,16	5,48	6,84	0,00	1,02	6,82	6,69	2,74
YLR439W	MRPL4	yes	sFHSQGGPLR	0,99	1,07	1,02	6,99	4,88	8,54	0,01	1,03	6,80	6,63	2,73
YOR374W	ALD4	yes	sTLcLkTSASSIGR	0,67	0,64	0,67	5,62	3,86	3,21	0,01	0,66	4,23	6,40	2,68
YER086W	ILV1	yes	sATLLkQPLcTVVR	0,75	0,95	0,68	4,09	4,77	5,75	0,00	0,79	4,87	6,15	2,62
YDL004W	ATP16	yes	sLNFVAkR	1,03	1,06	0,99	6,32	5,06	7,11	0,00	1,03	6,16	6,00	2,59
YJR045C	SSC1	yes	sSLSSSFR	0,97	0,92	0,99	5,12	4,67	6,53	0,00	0,96	5,44	5,66	2,50
YPL059W	GRX5	yes	mFLPkFNPIR	1,08	1,05	0,94	6,34	5,84	4,89	0,00	1,02	5,69	5,55	2,47
YNL104C	LEU4	yes	vkESIIALAEHAASR	0,34	0,31	0,34	2,10	1,50	1,78	0,00	0,33	1,79	5,43	2,44
YFL016C	MDJ1	yes	aFQQGVLSR	0,97	1,00	0,96	4,21	4,11	6,73	0,01	0,98	5,02	5,14	2,36
YDR511W	ACN9	yes	mNNkLIYR	1,11	1,10	1,16	6,59	5,33	3,91	0,01	1,12	5,28	4,69	2,23
YLR089C	ALT1	yes	sLSGQSSLNDLR	1,03	0,78	0,72	3,91	3,53	3,83	0,00	0,84	3,76	4,45	2,15
YOR356W	CIR2	yes	mIkFTNENLIR	0,88	1,02	0,99	4,22	4,21	4,16	0,00	0,96	4,20	4,35	2,12
YOR374W	ALD4	yes	lkTSASSIGR	0,45	0,55	0,38	1,69	1,62	2,17	0,00	0,46	1,83	3,97	1,99
YPR006C	ICL2	yes	mINNkTFNR	0,56	0,40	0,59	1,65	2,17	1,58	0,00	0,51	1,80	3,50	1,81
YKL192C	ACP1	yes	sVmSNTILAQR	1,01	1,04	0,95	3,23	2,60	4,67	0,02	1,00	3,50	3,50	1,81
YPL091W	GLR1	yes	mLSATkQTFR	0,92	1,28	0,95	3,82	3,24	3,63	0,00	1,05	3,57	3,40	1,77
YLR061W	RPL22A	no	yQVTPEEDEEEDEE	0,47	0,55	0,58	1,85	1,10	2,43	0,03	0,53	1,79	3,35	1,75
YOR187W	TUF1	yes	sQTTTSYAAAFDR	0,77	0,98	0,70	2,52	2,72	2,75	0,00	0,82	2,66	3,26	1,70
YNL284C	MRPL10	yes	mLTSVAGNDIFFR	0,85	0,85	0,93	2,81	2,88	2,84	0,00	0,88	2,84	3,24	1,70
YOR374W	ALD4	yes	kTSASSIGR	0,63	0,60	0,65	2,05	1,96	1,93	0,00	0,63	1,98	3,16	1,66
YKL157W	APE2	yes	sIAAHPR	0,92	1,07	0,82	3,26	2,42	2,72	0,00	0,94	2,80	2,99	1,58
YPR006C	ICL2	yes	eVSPDFGDYPYDTVPNQVER	0,57	0,72	0,57	1,91	1,28	2,35	0,02	0,62	1,85	2,98	1,58
YBL064C	PRX1	yes	aTAPILckQFkQSDQPR	1,00	1,10	0,85	3,32	2,50	2,60	0,00	0,98	2,81	2,86	1,51
YPR006C	ICL2	yes	nEVSPDFGDYPYDTVPNQVER	0,79	1,04	0,53	2,39	1,48	2,02	0,02	0,79	1,96	2,49	1,32
YMR002W	MIC17	yes	aSTMAAPVHPQQQQQPNAYSHPPAAGAQTR	0,72	0,85	0,70	2,19	1,31	2,11	0,02	0,75	1,87	2,48	1,31
YOL158C	ENB1	no	mLETDHSR	0,53	0,70	0,52	1,13	1,14	2,00	0,05	0,58	1,43	2,45	1,29
YLR259C	HSP60	yes	tNEAAGDGTTSATVLGR	0,85	1,12	0,76	1,67	2,02	3,01	0,03	0,91	2,23	2,45	1,29
YPR006C	ICL2	yes	tLVGSTNEVSPDFGDYPYDTVPNQVER	0,71	0,92	0,62	1,96	1,40	2,07	0,01	0,75	1,81	2,41	1,27
YPR002W	PDH1	yes	tATDYSDEVAR	0,40	0,59	0,48	1,31	1,03	1,05	0,00	0,49	1,13	2,30	1,20
YLR203C	MSS51	yes	tVLYAPSGATQLYFHLLR	0,73	0,88	0,67	1,77	1,64	1,82	0,00	0,76	1,74	2,29	1,20
YNR001C	CIT1	yes	aAGLNGLAGPLHGR	0,50	0,86	0,49	1,36	1,03	1,77	0,04	0,62	1,39	2,24	1,16
YPR004C	AIM45	yes	mFkSLAAVLPR	0,99	0,99	0,87	2,24	2,06	2,07	0,00	0,95	2,13	2,23	1,16
YHR146W	CRP1	no	aPkLPLTDEQTAEGR	1,08	1,02	0,47	1,91	1,61	2,19	0,02	0,86	1,90	2,22	1,15
YPR191W	QCR2	yes	nYVAVGDVSNLPYLDEL	0,55	0,72	0,51	1,61	0,93	1,36	0,03	0,59	1,30	2,20	1,14
YFL005W	SEC4	yes	vYDVTDER	0,39	0,52	0,84	1,48	0,93	1,28	0,04	0,59	1,23	2,11	1,08
YDR519W	FPR2	no	gSLSDLEIGIIkR	0,53	0,92	1,16	2,03	1,36	1,90	0,03	0,87	1,76	2,03	1,02
YPR191W	QCR2	yes	yVAVGDVSNLPYLDEL	0,48	0,55	0,72	1,51	0,86	1,17	0,04	0,58	1,18	2,03	1,02
YLR355C	ILV5	yes	sLFkEGR	1,44	1,44	1,27	0,71	0,71	0,61	0,00	1,38	0,68	0,49	-1,03
YER073W	ALD5	yes	ySQAPLR	1,14	1,10	1,18	0,55	0,51	0,48	0,00	1,14	0,51	0,45	-1,15
YDR405W	MRP20	yes	lASVVESSSkILDkSGSDR	1,21	1,08	0,94	0,52	0,46	0,39	0,00	1,08	0,46	0,43	-1,23
YDL204W	RTN2	no	dIEEELAAHQR	2,31	3,78	2,25	1,32	0,88	1,29	0,04	2,78	1,16	0,42	-1,26
YLR163C	MAS1	yes	sTISSQIPGTR	0,97	1,01	0,96	0,19	0,17	0,22	0,00	0,98	0,19	0,20	-2,35

11.2 Figures and Tables from 9.1.2 Yeast MAS1 ChaFRADIC experiments

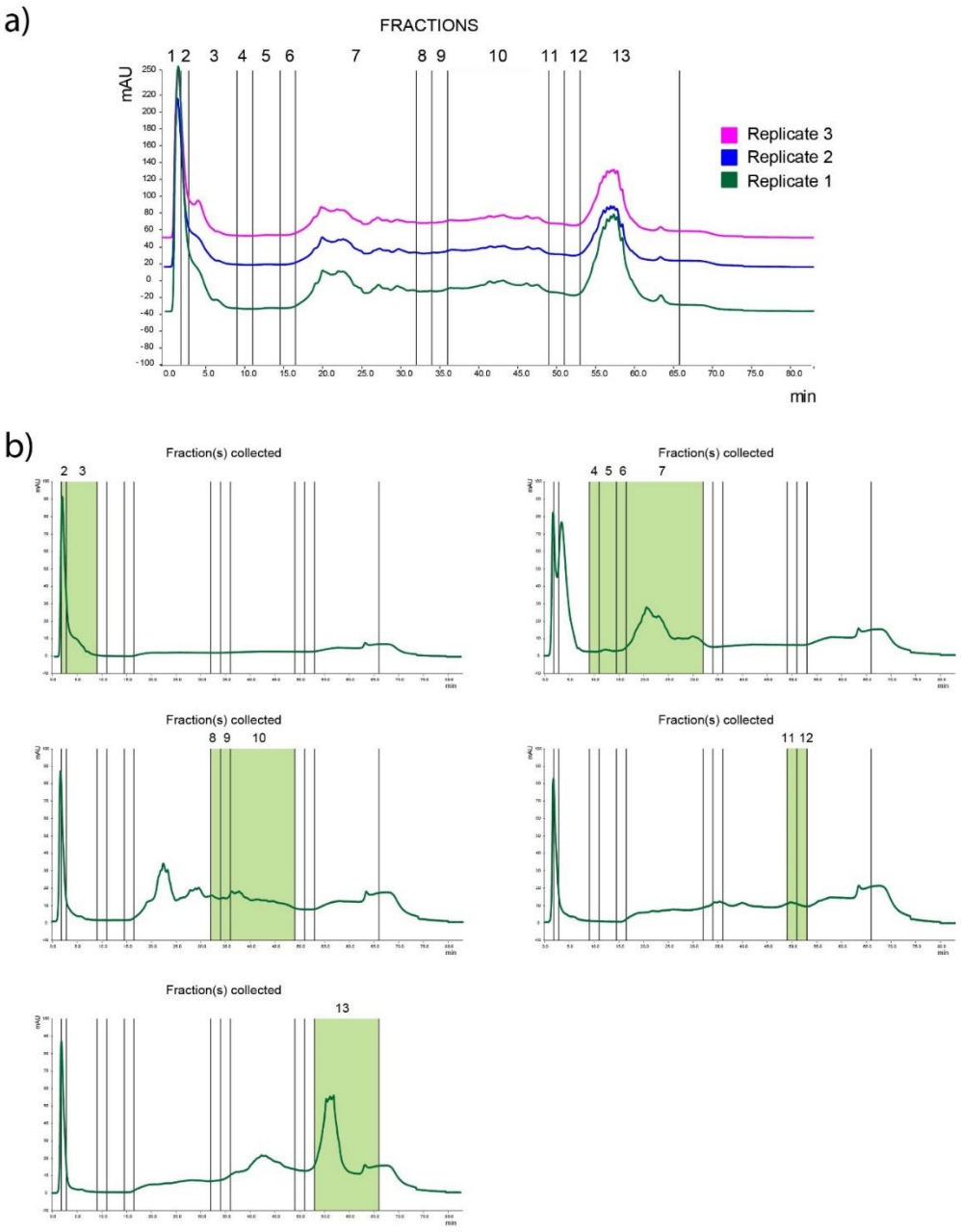

Supplemental Figure 3. Strong cationic exchange (SCX) fractionation of the yeast biological replicates. a) Reproducibility from the 3 biological replicates can be seen by similar chromatograms. For each biological replicate SCX fractionation, 13 fractions were collected, measured by LC/MS and pooled together according to charge state. b) Second SCX fractionation of each fraction (individually or pooled). The injected fractions correspond to the collected fractions as well (green column), in which original protein N-termini remain in the same elution time point, while not original protein N-termini elute in earlier fractions, as described in the ChaFRADIC protocol. It is possible to observe peptides eluting in earlier fractions than injected.

11| Supplemental Figures and Tables

Supplemental Table 5. Peptide charge state composition of each fraction of the SCX chromatography ChaFRADIC yeast mitochondria experiment The 13 fractions collected after the first SCX dimension of the 3 yeast biological replicates. Each fraction was measured by LC/MS to determine overall peptide charge state. Fractions with similar charge state were pooled together (2 and 3, 4-7, 8-10, 11 and 12, 13). Total peptides identified for each fraction are determined below.

Replicate 1	Composition (in %)												
Fraction	1	2	3	4	5	6	7	8	9	10	11	12	13
no charge	0,0	0,0	0,0	0,0	0,0	0,0	0,0	0,0	0,0	0,0	0,0	0,0	0,0
charge +1	4,2	75,0	100,0	0,0	0,0	0,0	0,0	0,1	0,1	0,5	0,0	0,0	0,0
charge +2	86,1	25,0	0,0	100,0	100,0	100,0	94,4	0,7	0,3	0,4	0,0	0,0	1,3
charge +3	9,7	0,0	0,0	0,0	0,0	0,0	5,6	99,2	99,5	87,7	4,3	0,0	5,1
charge +4	0,0	0,0	0,0	0,0	0,0	0,0	0,0	0,0	0,1	11,4	93,8	100,0	71,8
charge +5	0,0	0,0	0,0	0,0	0,0	0,0	0,0	0,0	0,0	0,0	1,9	0,0	21,8
charge +6	0,0	0,0	0,0	0,0	0,0	0,0	0,0	0,0	0,0	0,0	0,0	0,0	0,0
total peptides	72	4	68	13	107	235	713	1320	1051	569	162	35	78
Replicate 2	Composition (in %)												
Fraction	1	2	3	4	5	6	7	8	9	10	11	12	13
no charge	0,0	0,0	0,0	0,0	0,0	0,0	0,0	0,0	0,0	0,0	0,0	0,0	0,0
charge +1	18,8	88,9	100,0	8,3	1,0	0,0	0,0	0,2	0,1	0,0	0,3	0,9	1,5
charge +2	81,3	0,0	0,0	91,7	99,0	100,0	94,2	0,8	0,5	0,0	0,7	0,9	3,1
charge +3	0,0	0,0	0,0	0,0	0,0	0,0	5,8	98,9	99,3	90,5	7,3	11,1	6,9
charge +4	0,0	0,0	0,0	0,0	0,0	0,0	0,0	0,0	0,1	9,5	91,3	87,0	69,2
charge +5	0,0	0,0	0,0	0,0	0,0	0,0	0,0	0,0	0,0	0,0	0,3	0,0	18,5
charge +6	0,0	11,1	0,0	0,0	0,0	0,0	0,0	0,0	0,0	0,0	0,0	0,0	0,8
total peptides	16	9	39	12	105	163	740	1219	1220	485	289	108	130
Replicate 3	Composition (in %)												
Fraction	1	2	3	4	5	6	7	8	9	10	11	12	13
no charge	0,0	0,0	0,0	0,0	0,0	0,0	0,0	0,0	0,0	0,0	0,0	0,0	0,0
charge +1	0,0	50,0	100,0	9,1	2,0	0,0	0,0	0,1	0,1	0,3	0,3	0,0	1,1
charge +2	100,0	50,0	0,0	90,9	98,0	100,0	96,0	1,8	0,3	0,3	0,2	2,1	2,2
charge +3	0,0	0,0	0,0	0,0	0,0	0,0	4,0	98,1	99,4	89,5	5,0	10,7	4,4
charge +4	0,0	0,0	0,0	0,0	0,0	0,0	0,0	0,0	0,2	9,8	93,3	87,1	68,8
charge +5	0,0	0,0	0,0	0,0	0,0	0,0	0,0	0,0	0,0	0,1	1,2	0,1	21,3
charge +6	0,0	0,0	0,0	0,0	0,0	0,0	0,0	0,0	0,0	0,0	0,0	0,0	2,2
total peptides	2	6	31	11	103	172	699	1201	1087	457	221	103	87

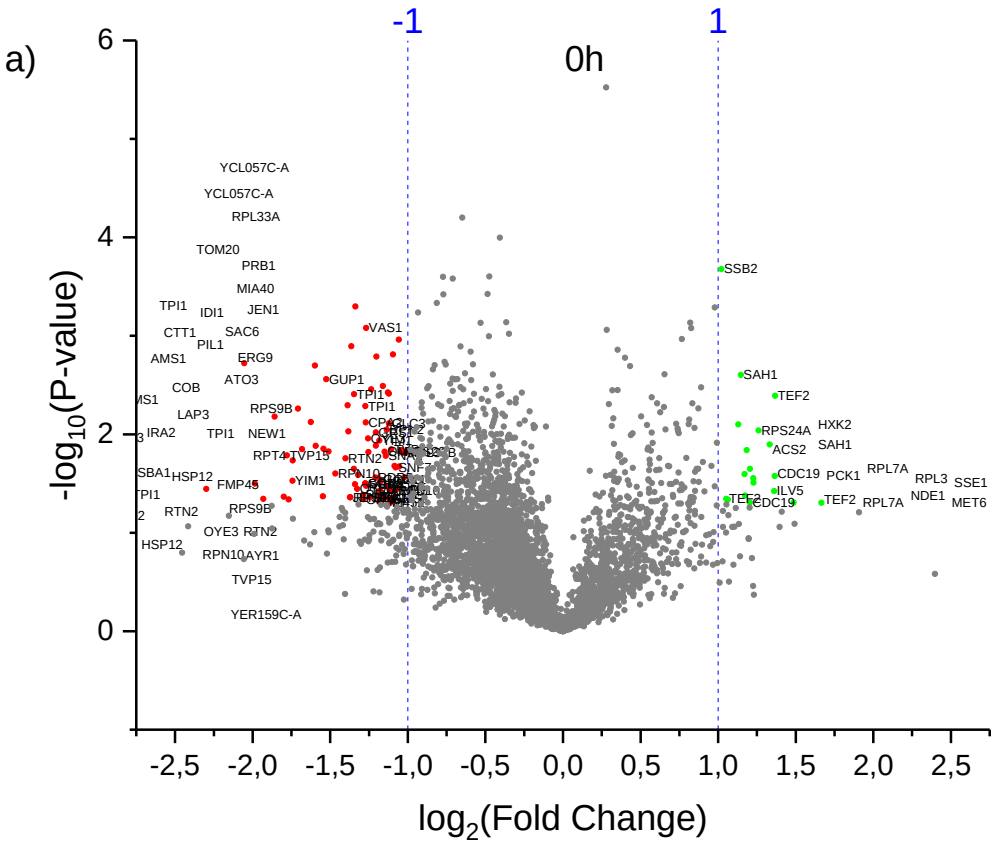

Supplemental Figure 4. Volcano plots of the yeast temperature sensitive MAS1 mutant against the wild type. a), b) and c) present, respectively, the volcano plots of the 0 h, 2 h and 4 h time shift. Green dots indicate up-regulated proteins and red dots indicate down regulated proteins. A 2-fold sample difference was considered to evaluate regulation ($p \leq 0.05$). Up or down-regulated proteins in the 0 h were disregarded in the 2 h and 4 h analysis. Figure parts B and C follows in the next pages due to size fitting.

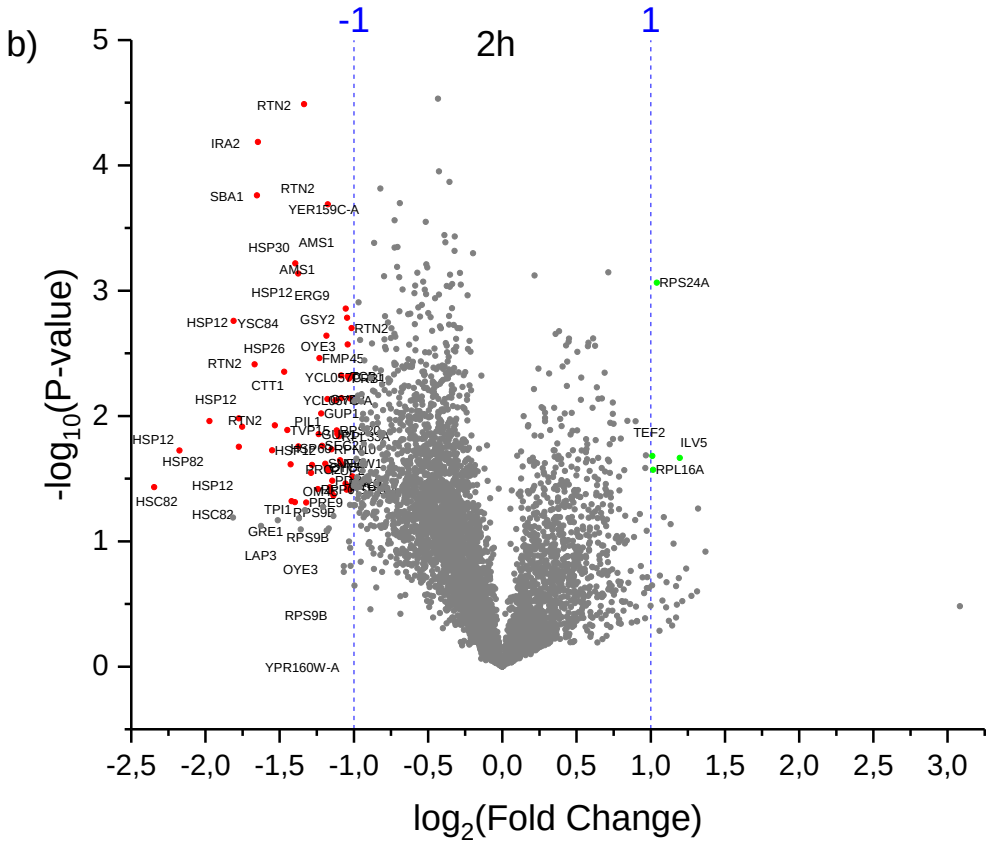

Supplemental Figure 4 Volcano plots of the yeast temperature sensitive MAS1 mutant against the wild type. a), b) and c) present, respectively, the volcano plots of the 0 h, 2 h and 4 h time shift. Green dots indicate up-regulated proteins and red dots indicate down regulated proteins. A 2-fold sample difference was considered to evaluate regulation ($p \leq 0.05$). Up or down-regulated proteins in the 0 h were disregarded in the 2 h and 4 h analysis.

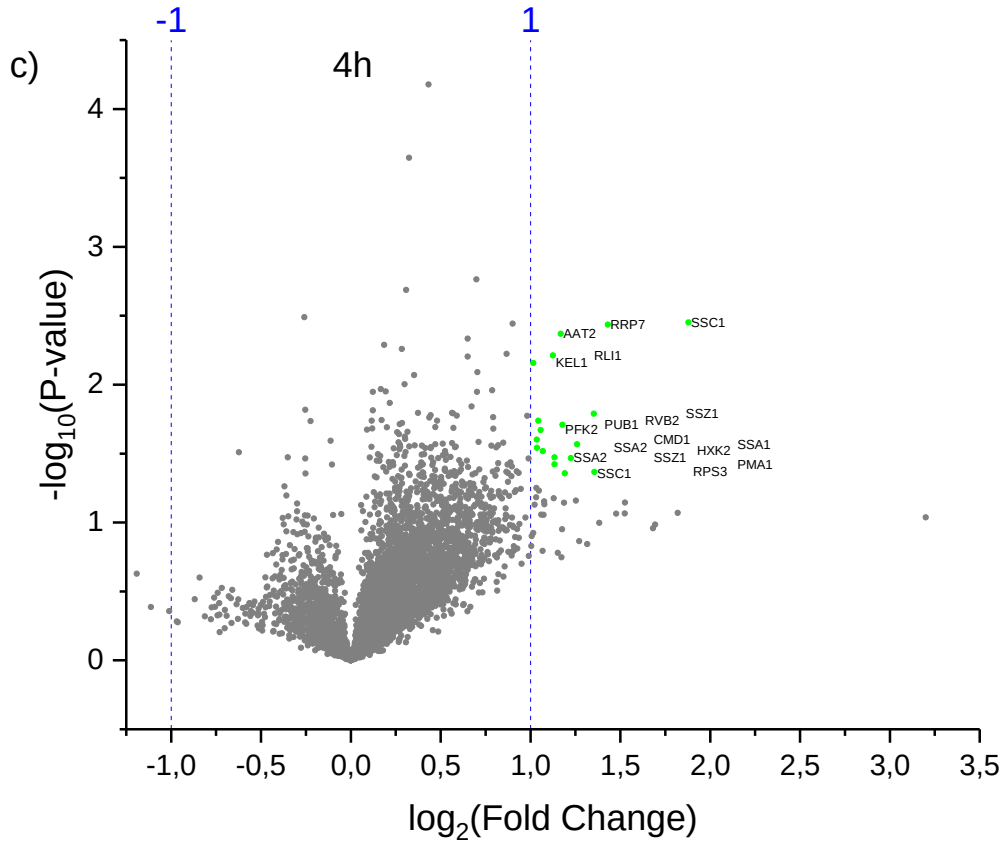

Supplemental Figure 4. Volcano plots of the yeast temperature sensitive MAS1 mutant against the wild type. a), b) and c) present, respectively, the volcano plots of the 0 h, 2 h and 4 h time shift. Green dots indicate up-regulated proteins and red dots indicate down regulated proteins. A 2-fold sample difference was considered to evaluate regulation ($p \leq 0.05$) Up or down-regulated proteins in the 0 h were disregarded in the 2 h and 4 h analysis.

12| Supplemental Information

Supplemental Table 6. Up- and down-regulated peptides from the 0 h time shift yeast MAS1 ChaFRADIC experiment. At least a 2-fold regulation between the mutant and respective wild type was considered as regulation ($p < 0.05$). Wild type (WT) and mutant normalized abundance values are displayed.

Protein accession	gene	peptide	WT yeast batch1	WT yeast batch 2	WT yeast batch 3	Mas1 mutant batch1	Mas1 mutant batch 2	Mas1 mutant batch 3	T.TEST mutants against its respective wild types	Average WT	Average mutant	Mutant divided by its respective wild type	Log 2
YGL076C	RPL7A	KSKAQQKTAEQVAAER	0,61	0,49	0,59	0,99	2,49	1,85	0,05	0,56	1,78	3,17	1,67
YER091C	MET6	DEVNDLEAA	1,07	0,20	0,95	1,29	2,44	2,48	0,05	0,74	2,07	2,80	1,49
YBR118W	TEF2	VIVLNHPGQISAGYSPVLDCHTAHIACR	0,73	0,41	0,64	1,64	1,65	1,27	0,00	0,59	1,52	2,58	1,37
YKR097W	PCK1	GALIAYSGVKTGR	0,62	0,69	0,88	1,23	2,17	2,25	0,03	0,73	1,88	2,57	1,36
YLR355C	ILV5	LAQYDVLR	0,45	0,75	0,73	1,40	2,27	1,27	0,04	0,64	1,65	2,57	1,36
YER043C	SAH1	DISLAAFGR	0,92	0,29	0,68	1,41	1,83	1,53	0,01	0,63	1,59	2,52	1,33
YER074W	RPS24A	KVISNPLLAR	0,51	0,67	0,60	1,09	1,65	1,52	0,01	0,59	1,42	2,40	1,26
YPL106C	SSE1	GVSYGIFKTDLPEGEEKPR	0,69	0,41	0,77	1,08	1,88	1,42	0,03	0,62	1,46	2,34	1,23
YOR063W	RPL3	TVVDTPPVVVVGVVGYVETPR	0,61	0,47	0,84	1,26	1,96	1,27	0,03	0,64	1,50	2,34	1,23
YGL076C	RPL7A	AQQKTAEQVAAER	0,64	0,62	0,73	1,13	1,95	1,50	0,02	0,66	1,53	2,31	1,21
YAL038W	CDC19	AASAVAAVFEQKAKAIIVLSTSGTTPR	0,63	0,36	0,59	0,79	1,24	1,59	0,05	0,52	1,21	2,30	1,20
YLR153C	ACS2	VSLKDGYLQNNATEGDAEHITPDNLRR	0,77	0,42	0,63	1,08	1,62	1,45	0,01	0,61	1,38	2,27	1,18
YMR145C	NDE1	VAPTTGVVAKQSFFKR	0,72	0,57	0,73	0,99	1,96	1,62	0,04	0,68	1,53	2,26	1,17
YAL038W	CDC19	AAVFEQKAKAIIVLSTSGTTPR	0,78	0,42	0,55	0,96	1,56	1,42	0,03	0,58	1,31	2,25	1,17
YGL253W	HXK2	DKPFVMDTSYPAR	0,50	0,98	0,76	1,41	1,79	1,72	0,01	0,75	1,64	2,19	1,13
YBR118W	TEF2	AFSEYPPLGR	0,81	0,64	0,41	1,30	1,65	0,94	0,05	0,62	1,30	2,09	1,06
YBR118W	TEF2	SEYPPLGR	0,81	0,67	0,38	1,31	1,61	0,94	0,05	0,62	1,29	2,07	1,05
YNL209W	SSB2	VAFTPQER	0,60	0,75	0,69	1,40	1,31	1,41	0,00	0,68	1,37	2,03	1,02
YOR259C	RPT4	QSHEQQPEQPQETEEHHEEEPSR	1,52	0,99	1,67	0,71	0,61	0,74	0,03	1,40	0,69	0,49	-1,02
YBR189W	RPS9B	EAAEEAEDEE	1,50	1,23	1,83	0,69	0,64	0,88	0,01	1,52	0,74	0,49	-1,04
YPL226W	NEW1	KEDDEADKENKFSGR	1,87	1,25	1,95	0,64	0,87	0,93	0,02	1,69	0,81	0,48	-1,05
YKL217W	JEN1	ASQDLLPTMLR	1,84	2,10	1,93	0,78	0,94	1,10	0,00	1,96	0,94	0,48	-1,06
YIL124W	AYR1	SDPVDVYR	1,91	1,11	1,86	0,84	0,89	0,59	0,04	1,63	0,77	0,48	-1,07
YHR200W	RPN10	DQPEQSEQPEQHQDK	1,54	1,04	1,85	0,71	0,54	0,85	0,04	1,48	0,70	0,47	-1,08
YEL060C	PRB1	NSAPWGLAR	1,57	1,52	1,39	0,85	0,71	0,54	0,00	1,50	0,70	0,47	-1,09
YDR100W	TVP15	IGDDDIDDDDDMI	1,55	1,09	1,58	0,78	0,50	0,68	0,01	1,41	0,65	0,46	-1,11
YDR385W	EFT2	DTDAEGKPLER	1,85	1,17	2,37	0,84	0,83	0,81	0,05	1,79	0,83	0,46	-1,11
YIL136W	OM45	LSKDEMDDLR	1,71	1,13	2,13	0,70	0,76	0,83	0,04	1,66	0,76	0,46	-1,12
YJR121W	ATP2	QHLGENTVR	1,52	1,15	2,17	0,65	0,81	0,76	0,04	1,61	0,74	0,46	-1,12
YER074W-A	YOS1	VAVLSEER	1,23	2,04	1,35	0,87	0,62	0,64	0,03	1,54	0,71	0,46	-1,12
YDR525W-A	SNA2	CHPYEENEAR	1,35	1,23	1,88	0,59	0,67	0,76	0,02	1,49	0,67	0,45	-1,14
YBR189W	RPS9B	AEASGEAAEEAEDEE	1,75	1,49	2,66	0,82	0,82	0,97	0,04	1,96	0,87	0,44	-1,18
YLR027C	AAT2	QSDAFQEDR	0,97	1,37	1,73	0,63	0,37	0,78	0,04	1,36	0,60	0,44	-1,19
YDR129C	SAC6	THTINEEERR	1,60	1,51	1,58	0,84	0,46	0,74	0,00	1,56	0,68	0,43	-1,20
YPL171C	OYE3	QFLDPHSNKR	1,87	1,21	1,74	0,66	0,59	0,77	0,01	1,61	0,67	0,42	-1,26
YGR094W	VAS1	HDQNDYNTGKR	1,68	1,48	1,70	0,54	0,66	0,81	0,00	1,62	0,67	0,42	-1,27
YJR109C	CPA2	STDFDEVDR	1,18	1,66	1,54	0,66	0,42	0,73	0,01	1,46	0,61	0,41	-1,27
YJR104C	SOD1	EIAGNSPNAER	1,33	2,14	1,30	0,82	0,58	0,57	0,03	1,59	0,66	0,41	-1,27
YMR189W	GCV2	SGAQGEYTGLR	1,98	1,08	1,97	0,79	0,63	0,65	0,03	1,67	0,69	0,41	-1,28
YPL171C	OYE3	FLDPHSNKR	1,97	1,06	1,98	0,56	0,56	0,88	0,04	1,67	0,67	0,40	-1,33
YPL117C	IDI1	DHELGIPEDETKTR	1,56	1,80	1,98	0,65	0,62	0,80	0,00	1,78	0,69	0,39	-1,36
YGR082W	TOM20	AIYFDYQR	1,70	1,70	2,33	0,78	0,69	0,73	0,01	1,91	0,73	0,38	-1,39
YHR200W	RPN10	QQQQDQPEQSEQPEQHQDK	1,68	1,22	2,22	0,48	0,51	0,86	0,03	1,71	0,62	0,36	-1,47
YNL239W	LAP3	NLPQQKASR	2,35	1,49	2,60	0,83	0,78	0,65	0,01	2,15	0,75	0,35	-1,51
YDR050C	TPI1	WVILGHSER	1,69	1,70	2,39	0,86	0,49	0,53	0,01	1,93	0,62	0,32	-1,62
YMR152W	YIM1	SCYQDDEVVIE	1,07	1,80	2,33	0,49	0,47	0,59	0,03	1,73	0,52	0,30	-1,74
YDR050C	TPI1	SLKPEFVDIINSR	1,52	1,28	2,72	0,49	0,54	0,56	0,04	1,84	0,53	0,29	-1,80
YNL239W	LAP3	HVDETSKLPLR	1,59	3,83	2,41	0,90	0,76	0,39	0,05	2,61	0,68	0,26	-1,93

12| Supplemental Information

Protein accession	gene	peptide	WT yeast batch1	WT yeast batch 2	WT yeast batch 3	Mas1 mutant batch1	Mas1 mutant batch 2	Mas1 mutant batch 3	T.TEST mutants against its respective wild types	Average WT	Average mutant	Mutant divided by its respective wild type	Log 2
YDR100W	TVP15	SIGDDDIDDDDDMI	1,55	1,16	2,19	0,85	0,55	0,79	0,05	1,64	0,73	0,45	-1,16
YGR088W	CTT1	TVGGESGTPDTAR	1,57	2,00	2,02	0,77	0,62	0,45	0,00	1,86	0,61	0,33	-1,60
YIL136W	OM45	SKDEMDDLR	1,73	1,08	2,28	0,62	0,69	0,78	0,05	1,70	0,70	0,41	-1,29
YBR121C	GRS1	AQAEAEAETD	1,15	1,22	1,65	0,53	0,55	0,66	0,01	1,34	0,58	0,43	-1,21
YKL217W	JEN1	SQDLLPTMLR	1,81	1,91	3,30	0,74	0,86	1,12	0,04	2,34	0,90	0,39	-1,37
YIL136W	OM45	GEQSEQQIAER	1,76	1,03	2,16	0,76	0,67	0,75	0,05	1,65	0,73	0,44	-1,18
YBR189W	RPS9B	EASGEAAEEAEDEE	1,84	1,59	3,04	0,72	0,78	1,00	0,04	2,16	0,83	0,39	-1,37
YDR050C	TPI1	DVGAKWVILGHSER	1,43	1,38	1,45	0,51	0,34	0,83	0,00	1,42	0,56	0,39	-1,35
YDR050C	TPI1	ADVDGFLVGGASLKPEFVDIINSR	1,17	1,51	1,13	0,65	0,44	0,49	0,01	1,27	0,53	0,41	-1,27
YGL156W	AMS1	GAGSTINPPDDNR	1,71	1,09	0,98	0,62	0,48	0,66	0,04	1,26	0,59	0,46	-1,10
YDR384C	ATO3	SLINANVR	1,61	1,93	2,36	0,62	0,82	1,12	0,01	1,97	0,85	0,43	-1,21
YIL075C	RPN2	LAYAGTGNNSAVKR	1,53	1,51	1,10	0,70	0,47	0,71	0,01	1,38	0,63	0,46	-1,14
YDR050C	TPI1	DKADVDGFLVGGASLKPEFVDIINSR	1,11	1,71	1,05	0,59	0,38	0,58	0,03	1,29	0,52	0,40	-1,32
YIL136W	OM45	SEPSEAQKR	1,78	1,16	1,32	0,65	0,72	0,55	0,02	1,42	0,64	0,45	-1,15
YKL117W	SBA1	ENDEEDEEEEIEPEVKA	1,79	0,97	1,89	0,83	0,48	0,65	0,04	1,55	0,66	0,42	-1,24
YDL204W	RTN2	TVDIEEELAAHQR	1,88	1,16	1,49	0,83	0,64	0,67	0,02	1,51	0,71	0,47	-1,09
YGL156W	AMS1	FKPVQGIYENR	2,02	1,38	1,53	0,39	0,27	0,69	0,01	1,64	0,45	0,28	-1,86
YER159C	YER159C-A	CVEEGQTQPEEESA	1,69	1,01	2,03	0,68	0,73	0,69	0,04	1,58	0,70	0,45	-1,17
YPL143W	RPL33A	DAQFYLGKR	1,52	1,70	1,78	0,54	0,72	0,97	0,00	1,67	0,75	0,45	-1,16
YOR234C	RPL33B	EAQFYLGKR	1,63	1,42	1,17	0,56	0,60	0,92	0,02	1,41	0,70	0,49	-1,02
YEL011W	GLC3	NFFAASSR	1,35	1,48	1,83	0,86	0,55	0,72	0,01	1,55	0,71	0,46	-1,12
YCL057C-A	YCL057C-A	GVGVFTSVLFFKR	1,55	1,76	1,58	0,58	0,57	0,78	0,00	1,63	0,64	0,40	-1,34
Q0105	COB	LVLPFTDR	1,54	1,95	1,20	0,76	0,38	0,47	0,01	1,56	0,54	0,34	-1,54
YGL156W	AMS1	GDGGGGPTEEMLQKMR	1,96	1,17	1,58	0,42	0,31	0,74	0,01	1,57	0,49	0,31	-1,68
YGL084C	GUP1	SPENPNYAR	1,63	1,58	2,08	0,63	0,48	0,73	0,00	1,76	0,61	0,35	-1,53
YHR200W	RPN10	QQQDQPEQSEQPEQHQDK	1,92	1,18	2,08	0,64	0,56	0,83	0,02	1,73	0,68	0,39	-1,35
YPL171C	OYE3	VTDPSLVEGEGEYSEGTNDF	1,91	1,05	1,86	0,72	0,40	0,79	0,03	1,61	0,63	0,39	-1,34
YOR153W	PDR5	NANDPENVGER	1,95	1,37	2,46	0,79	0,74	0,97	0,03	1,93	0,83	0,43	-1,21
YCL057C-A	YCL057C-A	TSVLFFKR	1,71	1,72	1,29	0,69	0,71	0,60	0,00	1,57	0,67	0,42	-1,24
YLR025W	SNF7	ENSVKDGEEEEDEEDEDEKALR	1,59	1,18	1,84	0,72	0,54	0,92	0,02	1,54	0,73	0,47	-1,08
YMR152W	YIM1	SKNSIER	1,76	1,23	1,32	0,71	0,48	0,71	0,01	1,44	0,63	0,44	-1,18
YHL015W	RPS20	EAPVQIVKR	1,73	1,48	2,12	0,70	0,80	1,11	0,02	1,78	0,87	0,49	-1,04
YFL014W	HSP12	AEKGKDNAEGQGESLADQAR	2,01	1,17	1,24	0,49	0,40	0,44	0,02	1,48	0,44	0,30	-1,74
YKL195W	MIA40	MASSPQFGR	1,26	1,62	1,28	0,72	0,60	0,58	0,00	1,39	0,63	0,46	-1,13
YHR190W	ERG9	EVLHGNVKIR	1,68	1,32	1,56	0,63	0,60	0,87	0,00	1,52	0,70	0,46	-1,12
YGL084C	GUP1	QASSPENPNYAR	1,82	2,54	2,02	0,60	0,42	0,52	0,00	2,12	0,51	0,24	-2,05
YER025W	GCD11	QEPTCPEPDCYR	1,42	1,27	2,09	0,68	0,57	0,87	0,03	1,59	0,71	0,44	-1,18
YFL014W	HSP12	GKDNAEGQGESLADQAR	1,97	1,13	1,40	0,72	0,73	0,54	0,03	1,50	0,66	0,44	-1,18
YGR086C	PIL1	QNPPPPPSTTKGR	1,71	1,85	1,19	0,59	0,53	0,70	0,01	1,58	0,61	0,38	-1,38
YDL204W	RTN2	TVPLIYDR	2,07	1,34	1,39	0,76	0,62	0,43	0,02	1,60	0,61	0,38	-1,40
YDR100W	TVP15	QFVEEPANFR	1,69	1,73	2,79	0,66	0,44	0,71	0,02	2,07	0,60	0,29	-1,78
YDL222C	FMP45	GFNSAPSTTR	1,84	1,23	1,27	0,72	0,56	0,53	0,02	1,45	0,61	0,42	-1,25
YGR240C	PFK1	GALLKIR	1,41	2,01	1,11	0,50	0,46	0,89	0,04	1,51	0,62	0,41	-1,29
YFL014W	HSP12	DNAEGQGESLADQAR	2,30	1,05	1,74	0,79	0,55	0,40	0,04	1,69	0,58	0,34	-1,55
YLR340W	RPP0	AAAEEEEESDDDMGFGLFD	1,86	1,33	2,50	0,73	0,67	0,96	0,03	1,89	0,79	0,42	-1,27
YFL014W	HSP12	EKGKDNAEGQGESLADQAR	2,41	1,30	1,24	0,41	0,41	0,44	0,03	1,65	0,42	0,25	-1,98
YOL081W	IRA2	GSIAFQR	2,18	1,45	1,67	0,64	0,51	0,47	0,01	1,77	0,54	0,31	-1,71
YDL204W	RTN2	VLFDKGVVSR	2,06	1,45	1,25	0,63	0,43	0,52	0,01	1,59	0,53	0,33	-1,59
YMR186W	HSC82	ASTEAPVEEVPADTEMEEVD	2,67	1,10	2,78	0,67	0,21	0,45	0,04	2,18	0,44	0,20	-2,30
YKL117W	SBA1	KENDEEDEEEEIEPEVKA	2,67	1,05	2,01	0,59	0,49	0,60	0,05	1,91	0,56	0,29	-1,77
YER043C	SAH1	SAPAQNYKIADISLAAFGR	0,79	0,47	0,73	1,35	1,56	1,50	0,00	0,66	1,47	2,21	1,15

Supplemental Table 7. Up- and down-regulated peptides from the 2 h time shift yeast MAS1 ChaFRADIC experiment. At least a 2-fold regulation between the mutant and respective wild type was considered as regulation ($p < 0.05$). Wild type (WT) and mutant normalized abundance values are displayed.

Protein accession	gene	peptide	WT yeast batch1	WT yeast batch 2	WT yeast batch 3	Mas1 mutant batch1	Mas1 mutant batch 2	Mas1 mutant batch 3	T.TEST mutants against its respective wild types	Average WT	Average mutant	Mutant divided by its respective wild type	Log 2
YLR355C	ILV5	LAQYDVLR	0,64	0,71	0,67	1,39	1,23	2,00	0,02	0,67	1,54	2,29	1,20
YIL133C	RPL16A	SVEPVVVIDGKGHLVGR	0,63	0,48	0,60	1,38	1,25	0,83	0,03	0,57	1,15	2,02	1,02
YER074W	RPS24A	KVISNPLLAR	0,63	0,53	0,60	1,14	1,32	1,13	0,00	0,58	1,20	2,06	1,04
YBR118W	TEF2	AFSEYPPLGR	0,70	0,84	0,38	1,27	1,11	1,50	0,02	0,64	1,29	2,01	1,01
YNL239W	LAP3	NLPQQKASR	1,12	2,12	2,34	0,88	0,35	0,85	0,05	1,86	0,69	0,37	-1,42
YDR050C	TPI1	WVILGHSER	1,14	1,81	2,08	0,82	0,74	0,50	0,03	1,68	0,69	0,41	-1,29
YLR259C	HSP60	VGGASEVEVGEKKDRYDDAL	1,48	2,23	2,17	1,02	0,75	0,95	0,01	1,96	0,91	0,46	-1,11
YPL226W	NEW1	KEDDEADKENKFSGR	1,26	1,69	2,13	0,86	0,80	0,73	0,02	1,69	0,80	0,47	-1,08
YGL062W	PYC1	NKLTSDDVR	1,31	1,81	2,00	0,88	0,46	1,14	0,04	1,71	0,83	0,49	-1,04
YGR135W	PRE9	DEDEEADEDMK	1,32	2,20	2,88	0,86	0,71	1,00	0,05	2,13	0,85	0,40	-1,32
YOR323C	PRO2	QDVSDLLDQDEYID	1,40	1,80	2,38	0,90	0,89	0,99	0,03	1,86	0,93	0,50	-1,01
YHR200W	RPN10	QQQQDQPEQSEQPEQHQDK	1,41	1,78	2,31	0,90	0,80	0,78	0,02	1,83	0,83	0,45	-1,15
YGR088W	CTT1	TVGGESGTPDTAR	1,23	2,08	1,72	0,77	0,71	0,46	0,02	1,68	0,65	0,39	-1,37
YBL092W	RPL32	IAHNISAKNR	1,22	1,70	2,15	0,76	0,72	0,96	0,03	1,69	0,81	0,48	-1,06
YGR253C	PUP2	EAAESPEEADVEMS	1,38	2,16	2,48	0,86	0,85	0,96	0,03	2,01	0,89	0,44	-1,17
YIL136W	OM45	SKDEMDDLR	1,43	1,43	2,29	0,90	0,75	0,88	0,04	1,72	0,84	0,49	-1,03
YBR189W	RPS9B	ASGEAAEEAEDEE	1,29	1,94	2,50	0,80	0,82	0,95	0,04	1,91	0,86	0,45	-1,15
YLL026W	HSP104	TLGDDDNEDSMEIDDDLD	1,53	2,24	2,73	0,91	0,94	1,28	0,04	2,16	1,05	0,48	-1,05
YBR189W	RPS9B	EASGEAAEEAEDEE	1,23	1,93	2,39	0,74	0,79	1,00	0,04	1,85	0,84	0,45	-1,14
YPL223C	GRE1	GSKADPYGEENQGNFPQR	1,50	3,33	2,35	0,87	0,97	0,88	0,05	2,39	0,91	0,38	-1,40
YBR112C	CYC8	QVEEDENYDD	1,43	1,91	2,49	0,81	0,77	1,00	0,03	1,94	0,86	0,44	-1,18
YLR258W	GSY2	GVNPAADDDDDGPYADDS	1,60	1,94	2,00	0,90	0,90	0,88	0,00	1,85	0,89	0,48	-1,05
YPL171C	OYE3	VTDPSLVEGEGEYSEGTNDFAYS	1,40	1,68	2,49	0,78	0,74	0,97	0,04	1,86	0,83	0,45	-1,16
YPR160W	YPR160W-A	NKAEDFQDR	1,53	2,32	2,71	0,85	0,73	1,12	0,02	2,18	0,90	0,41	-1,28
YDL204W	RTN2	TVDIEEELAAHQR	1,51	1,75	1,93	0,84	0,84	0,89	0,00	1,73	0,85	0,49	-1,02
YGL156W	AMS1	FKPVQGIYENR	1,48	1,46	1,69	0,82	0,73	0,49	0,00	1,54	0,68	0,44	-1,19
YGL137W	SEC27	QSEQQPEQGEAVPEPVEEES	1,34	1,81	2,24	0,74	0,72	0,86	0,02	1,80	0,77	0,43	-1,21
YER159C	YER159C-A	CVEEGQTQPEEESA	1,54	1,84	2,24	0,83	0,88	0,88	0,01	1,88	0,86	0,46	-1,12
YPL143W	RPL33A	DAQFYLGKR	1,29	1,48	1,89	0,69	0,90	0,58	0,01	1,55	0,72	0,47	-1,10
YOR086C	TCB1	DIAFKAHAR	1,55	1,68	2,02	0,82	0,74	0,99	0,00	1,75	0,85	0,49	-1,04
YCL057C-A	YCL057C-A	GVGVFTSVLFFKR	1,40	1,34	1,74	0,73	0,88	0,59	0,01	1,49	0,73	0,49	-1,03
YLR340W	RPP0	AEEEEESDDDMGFGLFD	1,50	1,53	2,52	0,78	0,60	0,97	0,04	1,85	0,78	0,42	-1,24
YGL156W	AMS1	GDGGGGPTEEMLQKMR	1,64	1,50	1,73	0,84	0,89	0,61	0,00	1,62	0,78	0,48	-1,05
YGL084C	GUP1	SPENPNYAR	1,46	1,59	2,13	0,75	0,82	0,65	0,01	1,72	0,74	0,43	-1,22
YBR189W	RPS9B	GEAAEEAEDEE	1,24	1,75	2,03	0,63	0,80	0,93	0,02	1,68	0,79	0,47	-1,09
YPL171C	OYE3	VTDPSLVEGEGEYSEGTNDF	1,60	1,77	1,78	0,80	0,64	1,05	0,00	1,71	0,83	0,49	-1,04
YOR153W	PDR5	NANDPENVGER	1,27	1,82	2,25	0,63	0,76	1,03	0,03	1,78	0,80	0,45	-1,14
YCL057C-A	YCL057C-A	TSVLFFKR	1,45	1,29	1,37	0,72	0,86	0,47	0,00	1,37	0,68	0,50	-1,01
YLR025W	SNF7	ENSVKDGEEEEDEEDEDEKALR	1,72	1,40	2,37	0,84	0,85	0,70	0,02	1,83	0,80	0,44	-1,19
YHL015W	RPS20	EAPVQIVKR	1,30	1,60	1,93	0,63	0,92	0,68	0,01	1,61	0,74	0,46	-1,12
YFL014W	HSP12	AEKGKDNAEGQGESLADQAR	1,88	2,96	1,96	0,91	0,60	0,51	0,01	2,27	0,67	0,30	-1,75
YDL204W	RTN2	ISNENKSSTSQR	1,79	1,82	2,05	0,85	0,84	0,81	0,00	1,89	0,84	0,44	-1,18
YPL171C	OYE3	VTDPSLVEGEGEYSEGTN	1,62	1,79	2,30	0,76	0,82	0,94	0,01	1,90	0,84	0,44	-1,18
YHR190W	ERG9	EVLHGNVKIR	1,53	1,31	1,77	0,71	0,83	0,63	0,00	1,54	0,72	0,47	-1,09
YFL014W	HSP12	GESLADQAR	1,78	3,09	2,07	0,82	0,78	0,77	0,02	2,31	0,79	0,34	-1,55
YGL084C	GUP1	QASSPENPNYAR	1,33	1,37	1,81	0,61	0,89	0,41	0,01	1,51	0,64	0,42	-1,24
YFL014W	HSP12	GKDNAEGQGESLADQAR	1,78	2,15	1,96	0,80	0,86	0,61	0,00	1,97	0,76	0,39	-1,37
YGR086C	PIL1	QNPPPPPSTTKGR	1,69	1,22	1,46	0,74	0,78	0,55	0,01	1,46	0,69	0,47	-1,08
YEL060C	PRB1	VIDTGVNINHKDFEKR	1,50	1,32	1,55	0,65	0,93	0,55	0,01	1,45	0,71	0,49	-1,03
YDL204W	RTN2	TVPLIYDR	1,55	1,70	1,65	0,67	0,66	0,61	0,00	1,64	0,65	0,40	-1,34
YDR100W	TVP15	QFVEEPANFR	1,44	1,75	2,33	0,61	0,82	0,59	0,01	1,84	0,67	0,37	-1,45
YCR021C	HSP30	GETAIHEPEPEAEQAVEDTA	2,32	2,73	2,65	0,96	0,81	1,16	0,00	2,57	0,98	0,38	-1,39
YBR072W	HSP26	VITLPDYPGVDAD	2,26	3,45	2,12	0,92	0,67	1,32	0,02	2,61	0,97	0,37	-1,43
YDL222C	FMP45	GFNSAPSTTR	1,83	1,64	1,38	0,74	0,77	0,55	0,00	1,62	0,69	0,43	-1,23
YDL204W	RTN2	ESPDLVGVLKPHIDR	1,97	2,53	2,94	0,73	0,81	0,80	0,00	2,48	0,78	0,31	-1,67
YFL014W	HSP12	DNAEGQGESLADQAR	1,97	3,42	2,72	0,72	0,88	0,77	0,01	2,71	0,79	0,29	-1,77
YFL014W	HSP12	EKGKDNAEGQGESLADQAR	2,20	2,41	1,78	0,77	0,57	0,48	0,00	2,13	0,61	0,29	-1,81
YMR186W	HSC82	STEAPVEEVPADTEMEEVD	2,09	3,11	3,98	0,69	0,90	1,09	0,02	3,06	0,89	0,29	-1,77
YOL081W	IRA2	GSIAFQR	1,99	1,80	1,78	0,66	0,55	0,57	0,00	1,86	0,59	0,32	-1,65
YDL204W	RTN2	VLFDKGVVSR	2,26	1,33	1,84	0,67	0,67	0,54	0,01	1,81	0,63	0,35	-1,53
YPL240C	HSP82	ASTAAPVEEVPADTEMEEVD	2,72	3,31	4,68	0,79	0,80	1,15	0,01	3,57	0,91	0,25	-1,97
YMR186W	HSC82	ASTEAPVEEVPADTEMEEVD	2,38	4,66	6,39	0,67	0,85	1,11	0,04	4,47	0,88	0,20	-2,34
YHR016C	YSC84	DTEYSRPNHSGR	2,05	2,08	2,71	0,56	0,93	0,98	0,00	2,28	0,82	0,36	-1,47
YKL117W	SBA1	KENDEEDEEEEIEPEVKA	2,43	2,30	2,60	0,65	0,74	0,95	0,00	2,45	0,78	0,32	-1,65
YFL014W	HSP12	GQGESLADQAR	2,48	4,93	3,28	0,64	0,96	0,77	0,02	3,56	0,79	0,22	-2,17

Supplemental Table 8. Up- and down-regulated peptides from the 4 h time shift yeast MAS1 ChaFRADIC experiment. At least a 2-fold regulation between the mutant and respective wild type was considered as regulation ($p < 0.05$). Wild type (WT) and mutant normalized abundance values are displayed.

Protein accession	gene	peptide	WT yeast batch1	WT yeast batch 2	WT yeast batch 3	Mas1 mutant batch1	Mas1 mutant batch 2	Mas1 mutant batch 3	T.TEST mutants against its respective wild types	Average WT	Average mutant	Mutant divided by its respective wild type	Log 2
YJR045C	SSC1	VQGGEEVNAE	0,17	0,53	0,39	1,51	1,11	1,38	0,00	0,36	1,33	3,68	1,88
YCL031C	RRP7	EAQAQEDVQSS	0,47	0,54	0,34	1,33	0,99	1,33	0,00	0,45	1,22	2,69	1,43
YNL178W	RPS3	RPAEETEAQAEPVEA	0,51	0,73	0,26	1,01	1,09	1,74	0,04	0,50	1,28	2,56	1,36
YHR064C	SSZ1	LISDYDADELAEA	0,39	0,77	0,20	1,08	1,27	1,14	0,02	0,46	1,16	2,55	1,35
YAL005C	SSA1	NFNDPEVQAD	0,33	0,84	0,33	0,99	1,38	1,23	0,03	0,50	1,20	2,39	1,26
YLL024C	SSA2	QAGGAPEGAAPGGFPGGAPPAPEAEG PTVEEVD	0,70	0,68	0,15	1,00	1,16	1,41	0,03	0,51	1,19	2,34	1,23
YJR045C	SSC1	GSSGLSENEIEQMVNDAEKFKSQDEAR	0,75	0,93	0,46	1,06	1,90	1,94	0,04	0,72	1,63	2,28	1,19
YNL016W	PUB1	NDQQQPVMSEQQQQQQQQQQQQ	0,46	0,68	0,26	0,89	1,04	1,23	0,02	0,47	1,06	2,26	1,18
YLR027C	AAT2	QSDAFQEDR	0,48	0,56	0,51	1,30	0,95	1,22	0,00	0,51	1,15	2,25	1,17
YHR064C	SSZ1	LISDYDADELAE	0,37	0,86	0,26	1,01	1,12	1,15	0,03	0,50	1,10	2,19	1,13
YGL008C	PMA1	DGQLVEIPANEVVPGDILQLEDGTVIPT DGR	0,45	0,78	0,17	0,95	1,11	1,02	0,04	0,47	1,02	2,19	1,13
YDR091C	RLI1	ATEDLQNDSASR	0,41	0,67	0,43	1,02	1,02	1,24	0,01	0,50	1,09	2,18	1,12
YGL253W	HXK2	VMDTSYPAR	0,59	0,80	0,27	0,98	1,19	1,33	0,03	0,55	1,16	2,10	1,07
YMR205C	PFK2	AAEENFNAD	0,45	0,82	0,35	1,00	1,24	1,14	0,02	0,54	1,13	2,08	1,06
YPL235W	RVB2	AQEEEVELS	0,44	0,79	0,35	1,07	0,99	1,20	0,02	0,53	1,09	2,06	1,04
YLL024C	SSA2	YQAGGAPEGAAPGGFPGGAPPAPEAE GPTVEEVD	0,60	0,71	0,21	0,95	1,10	1,08	0,03	0,51	1,04	2,05	1,04
YBR109C	CMD1	EVSDGSGEINIQ	0,38	0,81	0,38	0,99	1,01	1,21	0,03	0,52	1,07	2,05	1,03
YHR158C	KEL1	QVNEDADSDLL	0,52	0,72	0,42	1,19	0,99	1,18	0,01	0,55	1,12	2,02	1,02

11.3 Figures and Tables from 9.1.3 Mitochondrial MAS1 global proteome

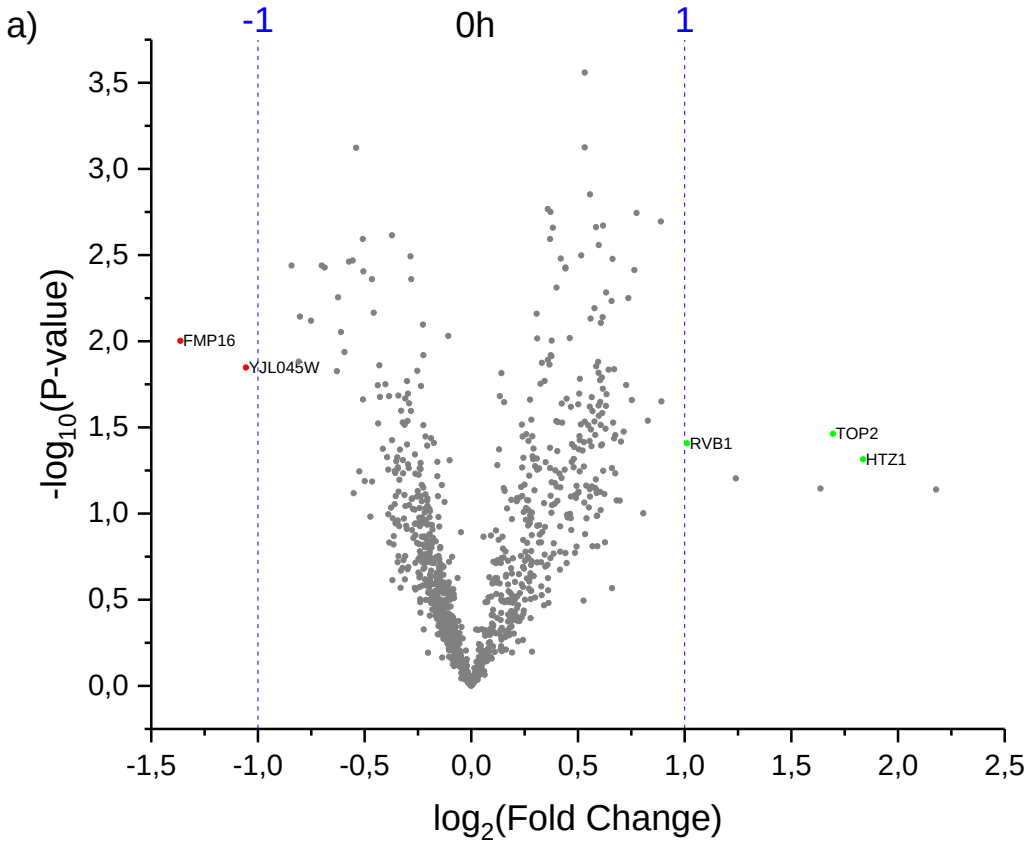

Supplemental Figure 5. Volcano plots of the global proteome of the mitochondrial temperature sensitive MAS1 mutant against the wild type. a), b) and c) present, respectively, the volcano plots of the 0 h, 2 h and 4 h time shift. Green dots indicate up-regulated proteins and red dots indicate down regulated proteins. A 2-fold sample difference was considered to evaluate regulation ($p \leq 0.05$). Up or down-regulated proteins in the 0 h were disregarded in the 2 h and 4 h analysis. Figure parts B and C are in the following pages due to size fitting.

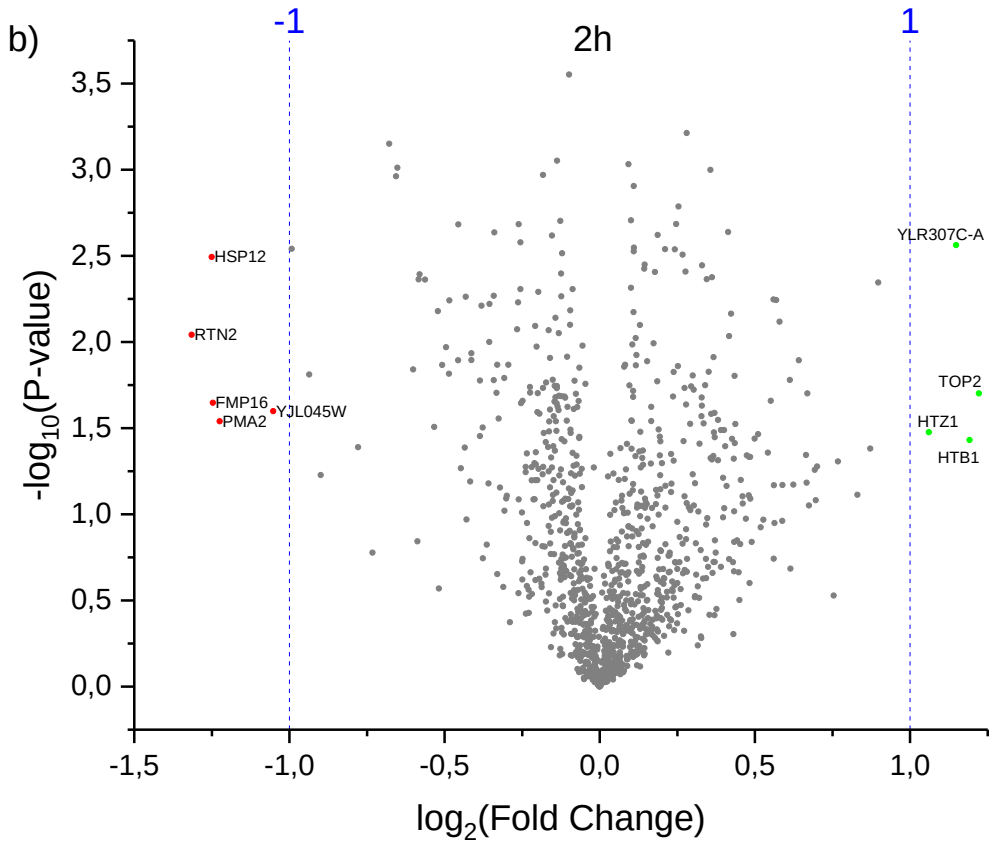

Supplemental Figure 5. Volcano plots of the global proteome of the mitochondrial temperature sensitive MAS1 mutant against the wild type. a), b) and c) present, respectively, the volcano plots of the 0 h, 2 h and 4 h time shift. Green dots indicate up-regulated proteins and red dots indicate down regulated proteins. A 2-fold sample difference was considered to evaluate regulation ($p \leq 0.05$). Up or down-regulated proteins in the 0 h were disregarded in the 2 h and 4 h analysis.

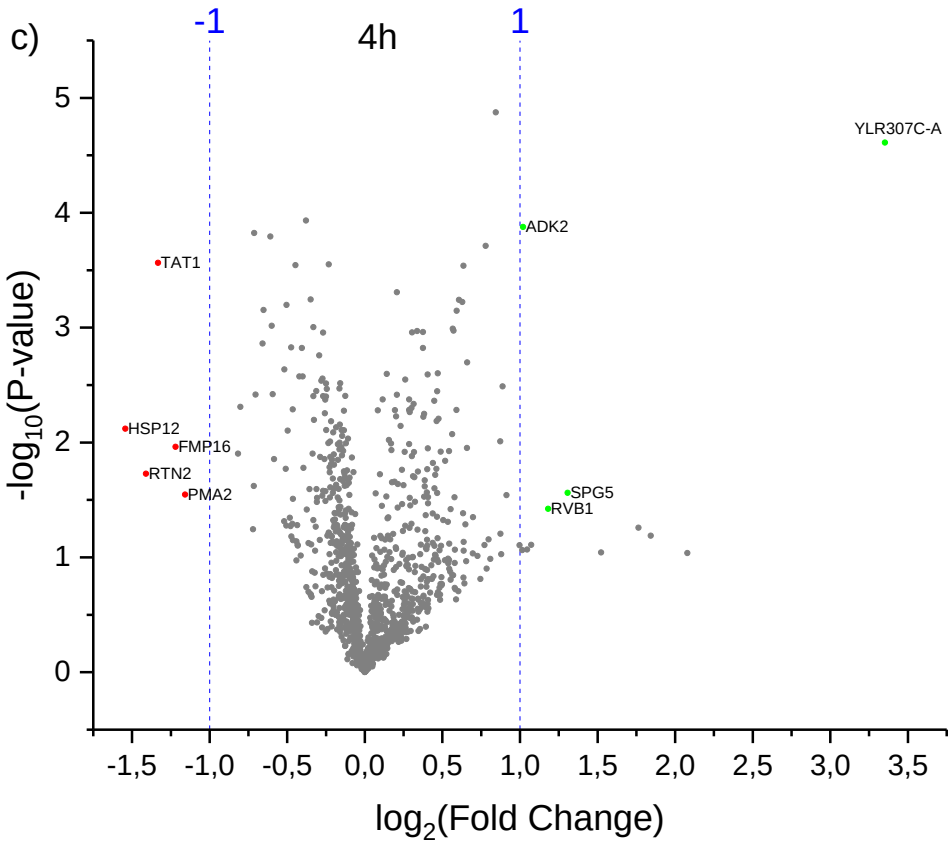

Supplemental Figure 5. Volcano plots of the global proteome of the mitochondrial temperature sensitive MAS1 mutant against the wild type. a), b) and c) present, respectively, the volcano plots of the 0 h, 2 h and 4 h time shift. Green dots indicate up-regulated proteins and red dots indicate down regulated proteins. A 2-fold sample difference was considered to evaluate regulation ($p \leq 0.05$). Up or down-regulated proteins in the 0 h were disregarded in the 2 h and 4 h analysis.

12| Supplemental Information

Supplemental Table 9. Up- and down-regulated proteins from the 0 h time shift MAS1 mitochondrial global proteome experiment. At least a 2-fold regulation between the mutant and respective wild type was considered as regulation ($p < 0.05$). Wild type (WT) and mutant normalized abundance values are displayed.

Protein accession	gene	WT yeast batch1	WT yeast batch 2	WT yeast batch 3	Mas1 mutant batch1	Mas1 mutant batch 2	Mas1 mutant batch 3	T.TEST mutants against its respective wild types	Average WT	Average mutant	Mutant divided by its respective wild type	Log 2
YOL012C	HTZ1	0,39	0,75	0,43	2,20	0,95	2,47	0,05	0,52	1,87	3,57	1,84
YNL088W	TOP2	0,50	0,73	0,45	2,05	1,06	2,35	0,03	0,56	1,82	3,24	1,70
YDR190C	RVB1	0,64	0,77	0,66	1,70	0,94	1,52	0,04	0,69	1,39	2,02	1,01
YJL045W	YJL045W	1,20	1,16	1,58	0,51	0,82	0,57	0,01	1,31	0,63	0,48	-1,06
YDR070C	FMP16	1,49	1,84	1,22	0,55	0,76	0,45	0,01	1,51	0,59	0,39	-1,36

Supplemental Table 10. Up- and down-regulated proteins from the 2 h time shift MAS1 mitochondrial global proteome experiment. At least a 2-fold regulation between the mutant and respective wild type was considered as regulation ($p < 0.05$). Wild type (WT) and mutant normalized abundance values are displayed.

Protein accession	gene	WT yeast batch1	WT yeast batch 2	WT yeast batch 3	Mas1 mutant batch1	Mas1 mutant batch 2	Mas1 mutant batch 3	T.TEST mutants against its respective wild types	Average WT	Average mutant	Mutant divided by its respective wild type	Log 2
YNL088W	TOP2	0,90	0,94	0,71	2,18	2,37	1,41	0,02	0,85	1,99	2,33	1,22
YDR224C	HTB1	0,98	1,02	0,72	2,21	2,64	1,38	0,04	0,91	2,08	2,28	1,19
YLR307C-A	YLR307C-A	0,55	0,79	0,72	1,58	1,32	1,67	0,00	0,69	1,52	2,22	1,15
YOL012C	HTZ1	0,88	1,05	0,78	2,22	2,13	1,29	0,03	0,90	1,88	2,09	1,06
YJL045W	YJL045W	1,05	1,38	1,74	0,70	0,76	0,55	0,03	1,39	0,67	0,48	-1,05
YPL036W	PMA2	1,81	2,47	1,37	0,75	0,79	0,88	0,03	1,88	0,81	0,43	-1,22
YDR070C	FMP16	1,19	2,08	1,74	0,58	0,71	0,82	0,02	1,67	0,70	0,42	-1,25
YFL014W	HSP12	2,13	2,20	1,76	0,60	0,95	1,00	0,00	2,03	0,85	0,42	-1,25
YDL204W	RTN2	2,85	2,06	2,05	0,99	1,12	0,69	0,01	2,32	0,93	0,40	-1,31

Supplemental Table 11. Up- and down-regulated proteins from the 4 h time shift MAS1 mitochondrial global proteome experiment. At least a 2-fold regulation between the mutant and respective wild type was considered as regulation ($p < 0.05$). Wild type (WT) and mutant normalized abundance values are displayed.

Protein accession	gene	WT yeast batch1	WT yeast batch 2	WT yeast batch 3	Mas1 mutant batch1	Mas1 mutant batch 2	Mas1 mutant batch 3	T.TEST mutants against its respective wild types	Average WT	Average mutant	Mutant divided by its respective wild type	Log 2
YLR307C-A	YLR307C-A	0,67	0,81	0,79	7,53	7,34	8,35	0,00	0,76	7,74	10,21	3,35
YMR191W	SPG5	0,89	0,98	0,87	3,02	1,70	2,05	0,03	0,91	2,26	2,47	1,31
YDR190C	RVB1	0,78	0,81	0,75	1,19	1,81	2,31	0,04	0,78	1,77	2,27	1,18
YER170W	ADK2	0,69	0,83	0,79	1,49	1,62	1,56	0,00	0,77	1,56	2,03	1,02
YPL036W	PMA2	2,04	1,81	1,14	0,73	0,70	0,80	0,03	1,66	0,75	0,45	-1,16
YDR070C	FMP16	1,86	1,30	1,65	0,84	0,77	0,45	0,01	1,60	0,69	0,43	-1,22
YBR069C	TAT1	0,90	1,01	0,90	0,40	0,31	0,41	0,00	0,94	0,37	0,40	-1,33
YDL204W	RTN2	2,27	2,28	3,58	1,01	0,90	1,15	0,02	2,71	1,02	0,38	-1,41
YFL014W	HSP12	3,24	2,66	4,12	1,39	1,05	1,00	0,01	3,34	1,15	0,34	-1,54

11.4 Figures and Tables from 9.1.4 Mitochondrial MAS1 mutant phosphoproteome experiment

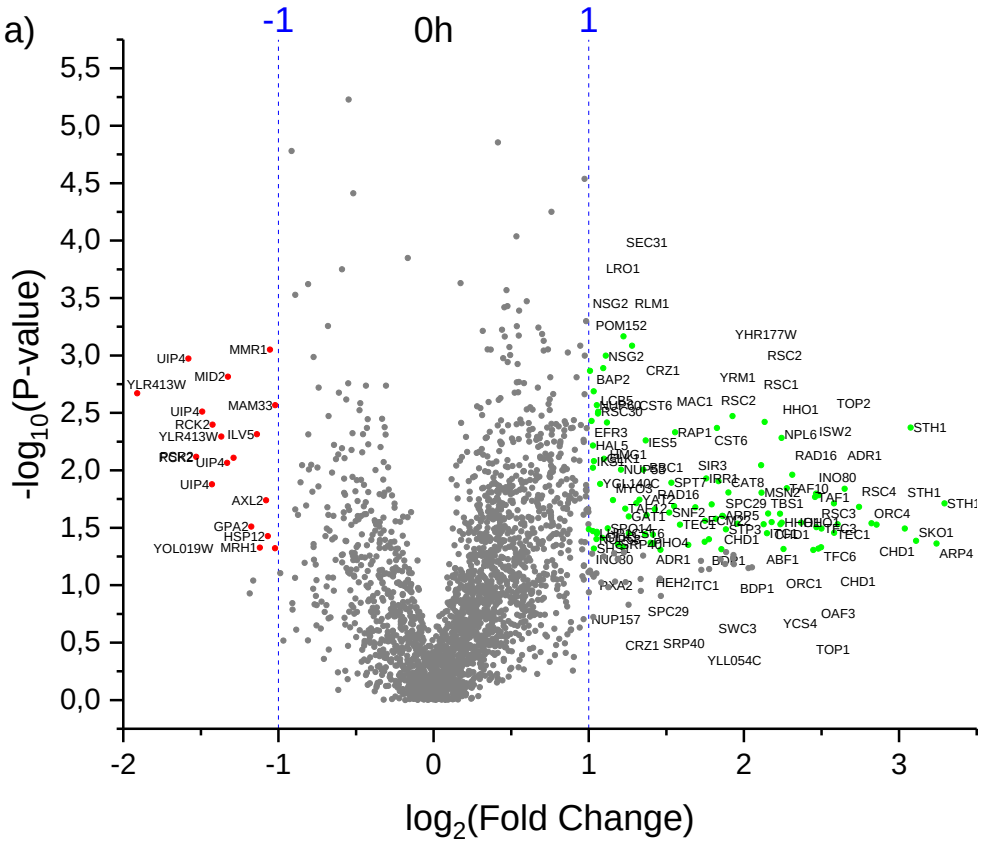

Supplemental Figure 6. Volcano plots of the phosphoproteome of the mitochondrial temperature sensitive MAS1 mutant against the wild type. a), b) and c) present, respectively, the volcano plots of the 0 h, 2 h and 4 h time shift. Green dots indicate up-regulated proteins and red dots indicate down regulated proteins. A 2-fold sample difference was considered to evaluate regulation ($p \leq 0.05$). Up or down-regulated proteins in the 0 h were disregarded in the 2 h and 4 h analysis. Figure parts B and C are in the following pages due to size fitting.

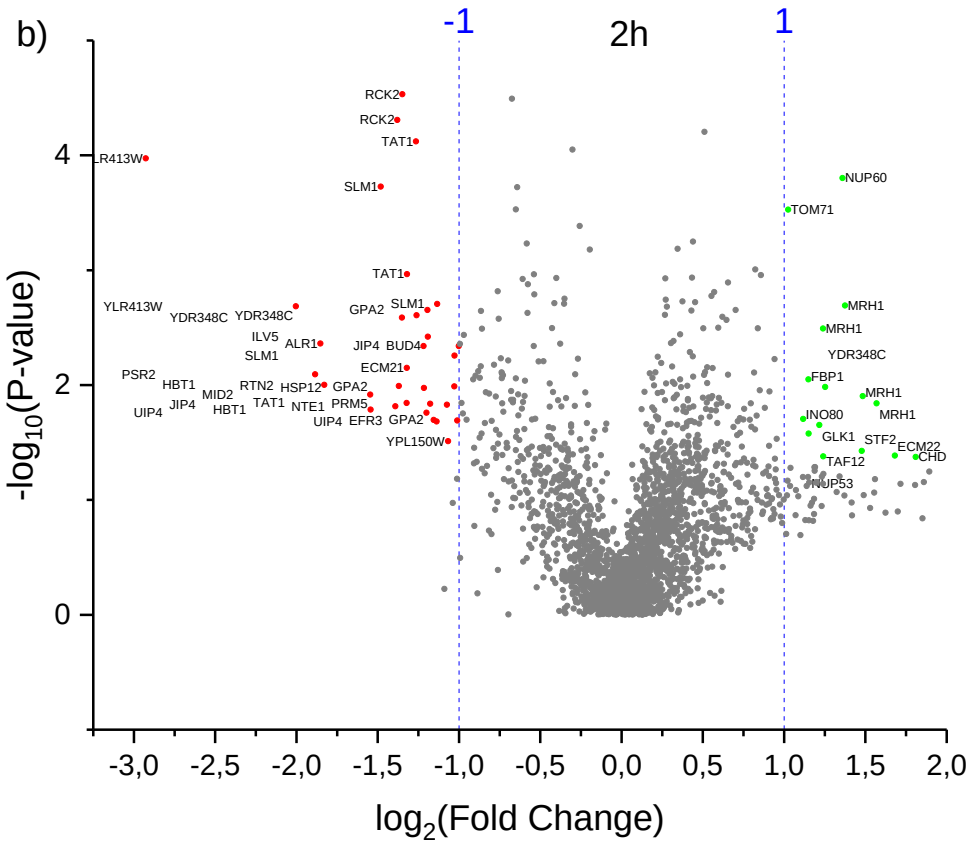

Supplemental Figure 6. Volcano plots of the phosphoproteome of the mitochondrial temperature sensitive MAS1 mutant against the wild type. a), b) and c) present, respectively, the volcano plots of the 0 h, 2 h and 4 h time shift. Green dots indicate up-regulated proteins and red dots indicate down regulated proteins. A 2-fold sample difference was considered to evaluate regulation ($p \leq 0.05$). Up or down-regulated proteins in the 0 h were disregarded in the 2 h and 4 h analysis.

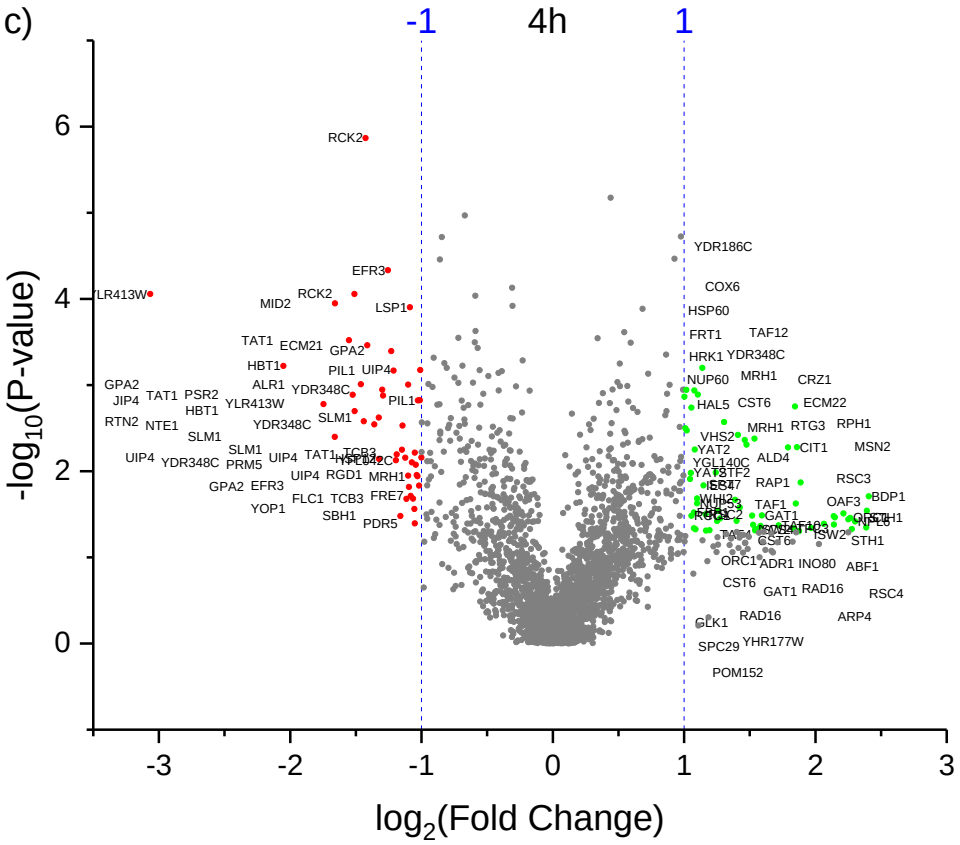

Supplemental Figure 6. Volcano plots of the phosphoproteome of the mitochondrial temperature sensitive MAS1 mutant against the wild type. a), b) and c) present, respectively, the volcano plots of the 0 h, 2 h and 4 h time shift. Green dots indicate up-regulated proteins and red dots indicate down regulated proteins. A 2-fold sample difference was considered to evaluate regulation ($p \leq 0.05$). Up or down-regulated proteins in the 0 h were disregarded in the 2 h and 4 h analysis.

12| Supplemental Information

Supplemental Table 12. Up- and down-regulated phosphopeptides from the 0 h time shift yeast MAS1 ChaFRADIC experiment. At least a 2-fold regulation between the mutant and respective wild type was considered as regulation ($p \leq 0.05$). Wild type (WT) and mutant normalized abundance values are displayed. “Phosphosite confidence” indicates percentage of binding confidence of the phosphorylation on the S, T or/and Y amino acid present in the peptide sequence. ”P-site” indicates amino acid and position within the protein.

Protein accession	Gene	Phosphosite confidence (%)	Peptide, protein, p-site	WT batch 1	WT batch 2	WT batch 3	Mas1 mutant batch1	Mas1 mutant batch 2	Mas1 mutant batch 3	T.TEST mutants against its respective wild types	WT average	Mutant average	Mutant divided by its respective wild type	Ratios log2
YIL126W	STH1	S(3): 100.0	INSIIDFIK;YIL126W;S329	0,20	0,49	0,16	1,94	1,05	2,33	0,019	0,20	1,94	9,80	3,29
YJL081C	ARP4	T(2): 0.0; T(4): 0.0; S(13): 100.0	VTPTEEKEQEAVSK;YJL081C;S349	0,14	0,53	0,20	2,03	0,72	1,93	0,043	0,20	1,93	9,45	3,24
YNL167C	SKO1	S(3): 100.0; T(6): 0.0; T(7): 0.0	KNSAVTTAPAQKDDVENNK;YNL167C;S399	0,12	0,38	0,15	1,42	0,53	1,32	0,041	0,15	1,32	8,63	3,11
YIL126W	STH1	S(1): 100.0; S(2): 0.0; Y(10): 0.0	SSAQLEQLLYR;YIL126W;S51	0,23	0,42	0,18	1,91	1,30	2,13	0,004	0,23	1,91	8,43	3,08
YIL126W	STH1	S(4): 100.0	KEDSEPLGR;YIL126W;S1045	0,19	0,47	0,13	1,60	0,88	2,23	0,032	0,19	1,60	8,21	3,04
YER164W	CHD1	Y(8): 0.0; S(12): 100.0	AAAHQQNYFNDSDDEDDEDNIK;YER164W;S36	0,19	0,45	0,21	1,62	0,71	1,52	0,030	0,21	1,52	7,24	2,86
YPR162C	ORC4	T(1): 0.0; S(3): 0.0; S(8): 100.0	TISEARLSPQVNLLPIKR;YPR162C;S9	0,20	0,50	0,20	1,84	0,80	1,45	0,029	0,20	1,45	7,08	2,82
YKR008W	RSC4	S(1): 0.0; T(2): 0.0; T(3): 0.0; S(4): 100.0	STTSDIEK;YKR008W;S406	0,24	0,46	0,20	1,62	0,86	1,84	0,021	0,24	1,62	6,69	2,74
YDR216W	ADR1	S(3): 100.0; S(5): 50.0; S(6): 50.0	KNSASSVK;YDR216W;S180	0,12	0,24	0,09	0,75	0,43	0,80	0,015	0,12	0,75	6,28	2,65
YER164W	CHD1	T(9): 0.0; S(12): 100.0; S(15): 0.0; T(17): 0.0	GPAALINNTRLSPNSPTPPLK;YER164W;S1336	0,18	0,49	0,26	1,90	0,81	1,57	0,029	0,26	1,57	6,08	2,60
YBR083W	TEC1	S(1): 0.0; S(6): 100.0; S(8): 0.0	SDDLKSPSAK;YBR083W;S86	0,18	0,41	0,21	1,26	0,56	1,24	0,035	0,21	1,24	5,98	2,58
YNL088W	TOP2	T(3): 100.0; S(5): 0.0; S(7): 0.0; T(9): 0.0	EKTPSVSETK;YNL088W;T1250	0,13	0,47	0,25	1,49	0,78	1,51	0,019	0,25	1,49	5,98	2,58
YAL001C	TFC3	S(8): 100.0	GFDELGKSR;YAL001C;S434	0,22	0,58	0,33	1,98	0,86	1,87	0,032	0,33	1,87	5,66	2,50
YDR362C	TFC6	S(1): 0.0; S(2): 0.5; S(3): 99.5; S(6): 0.0; S(7): 0.0	SSSPGSSLGQK;YDR362C;S145	0,26	0,54	0,29	1,72	0,68	1,65	0,047	0,29	1,65	5,65	2,50
YDR303C	RSC3	S(3): 100.0; T(8): 0.0; S(18): 0.0	KLSEDGVTDGDGKPIPESER;YDR303C;S236	0,16	0,38	0,27	1,49	0,83	1,69	0,016	0,27	1,49	5,59	2,48
YKR064W	OAF3	S(3): 99.6; T(4): 0.4	KQSTPAER;YKR064W;S73	0,17	0,49	0,29	1,85	0,66	1,59	0,048	0,29	1,59	5,58	2,48
YOR304W	ISW2	T(1): 0.0; S(2): 0.0; T(4): 0.0; T(8): 100.0; S(11): 0.0; S(15): 0.0; T(16): 0.0	TSATREDTPLSQNESTR;YOR304W;T1079	0,25	0,33	0,16	1,45	0,60	1,39	0,031	0,25	1,39	5,53	2,47
YGL150C	INO80	S(5): 100.0	NANLSDIINEK;YGL150C;S133	0,24	0,41	0,22	1,34	0,73	1,34	0,016	0,24	1,34	5,52	2,46
YGR274C	TAF1	S(5): 100.0	DNPASPK;YGR274C;S1064	0,24	0,36	0,25	1,37	0,74	1,46	0,017	0,25	1,37	5,50	2,46
YOL006C	TOP1	S(4): 0.0; S(7): 0.0; S(9): 0.0; Y(17): 0.0; S(19): 100.0; S(24): 0.0	KVASMNSASLQDEAEPYDSDEAISK;YOL006C;S49	0,13	0,82	0,23	1,43	0,83	1,27	0,049	0,23	1,27	5,46	2,45
YPL127C	HHO1	S(3): 100.0	EVSPKPK;YPL127C;S130	0,20	0,63	0,39	2,03	0,95	1,99	0,029	0,39	1,99	5,16	2,37
YBR114W	RAD16	S(3): 100.0; T(10): 0.0	DVSDDDEPLTK;YBR114W;S109	0,21	0,43	0,20	1,03	0,70	1,13	0,011	0,21	1,03	4,97	2,31
YDR167W	TAF10	S(8): 100.0; T(18): 0.0	EAVVDDGSENAFGIPEFTRK;YDR167W;S58	0,15	0,32	0,24	1,20	0,65	1,19	0,014	0,24	1,19	4,85	2,28
YML065W	ORC1	T(4): 0.0; T(6): 0.0; S(10): 100.0; T(14): 0.0	DKATQTAQISDAETR;YML065W;S237	0,25	0,37	0,27	1,49	0,55	1,31	0,049	0,27	1,31	4,77	2,25
YPL127C	HHO1	S(2): 0.0; S(3): 100.0; S(5): 0.0; S(6): 0.0; T(8): 0.0; Y(9): 0.0	ASSPSSLTYK;YPL127C;S174	0,26	0,53	0,33	1,58	0,78	1,61	0,029	0,33	1,58	4,74	2,24
YMR091C	NPL6	S(9): 100.0; T(15): 0.0	HVDEEEDLSEDKGVTR;YMR091C;S86	0,21	0,40	0,29	1,36	1,02	1,65	0,005	0,29	1,36	4,73	2,24
YLR272C	YCS4	S(4): 100.0; T(7): 0.0; T(11): 0.0	KVESQETLNDTIER;YLR272C;S464	0,26	0,43	0,30	1,40	0,73	1,65	0,030	0,30	1,40	4,71	2,24
YPL127C	HHO1	S(3): 0.0; S(4): 100.0; S(6): 0.0; S(7): 0.0; T(9): 0.0; Y(10): 0.0	KASSPSSLTYK;YPL127C;S174	0,27	0,65	0,35	1,63	0,90	1,64	0,024	0,35	1,63	4,70	2,23
YER164W	CHD1	S(2): 0.0; S(5): 100.0; T(7): 0.0	LSPNSPTPPLK;YER164W;S1339	0,12	0,39	0,53	2,53	1,10	1,75	0,028	0,39	1,75	4,53	2,18
YBR150C	TBS1	S(12): 100.0	FKDENFDIAVRSR;YBR150C;S184	0,25	0,53	0,34	1,72	0,84	1,50	0,024	0,34	1,50	4,46	2,16
YGL133W	ITC1	S(1): 0.0; S(3): 0.0; S(7): 0.0; S(8): 99.6; S(11): 0.4	SNSANVSSPESEKNKR;YGL133W;S288	0,19	0,43	0,28	1,42	0,62	1,25	0,035	0,28	1,25	4,43	2,15
YLR357W	RSC2	S(3): 100.0; T(11): 0.0	VGSPGAGGPLTVQGLK;YLR357W;S682	0,27	0,41	0,19	1,23	0,86	1,19	0,004	0,27	1,19	4,39	2,13
YKL112W	ABF1	S(1): 0.0; S(3): 100.0; Y(6): 0.0	SNSIDYAK;YKL112W;S467	0,28	0,33	0,19	1,28	0,58	1,23	0,030	0,28	1,23	4,37	2,13
YMR037C	MSN2	S(2): 0.2; S(3): 99.8; S(8): 0.0; T(9): 0.0	RSSVVIESTK;YMR037C;S633	0,20	0,25	0,31	1,18	0,62	1,07	0,016	0,25	1,07	4,33	2,11
YGR056W	RSC1	S(3): 100.0; S(4): 0.0; S(5): 0.0; T(6): 0.0; T(11): 0.0	VNSSSTIRLPTLK;YGR056W;S607	0,23	0,47	0,39	1,68	1,04	1,75	0,009	0,39	1,68	4,32	2,11
YNL039W	BDP1	S(3): 99.7; T(4): 0.3; S(6): 0.0	RLSTISNK;YNL039W;S164	0,21	0,30	0,30	1,18	0,55	1,15	0,029	0,30	1,15	3,89	1,96
YHR177W	YHR177W	S(3): 99.7; T(4): 0.3; Y(15): 0.0	LGSTHDLPLHNVPEYNIFER;YHR177W;S90	0,36	0,36	0,40	1,39	0,99	1,44	0,003	0,36	1,39	3,80	1,93
YMR280C	CAT8	T(1): 0.4; S(3): 99.6; T(5): 0.0; S(8): 0.0; T(9): 0.0; Y(12): 0.0	TASPTPLSTPIYR;YMR280C;S55	0,24	0,48	0,32	1,21	0,75	1,29	0,016	0,32	1,21	3,73	1,90

Protein accession	Gene	Phosphosite confidence (%)	Peptide, protein, p-site	WT batch 1	WT batch 2	WT batch 3	Mas1 mutant batch1	Mas1 mutant batch 2	Mas1 mutant batch 3	T.TEST mutants against its respective wild types	WT average	Mutant average	Mutant divided by its respective wild type	Ratios log2
YLR375W	STP3	S(3): 0.0; S(5): 100.0; T(11): 0.0	GGSVSPNDDDTHEK;YLR375W;S215	0,31	0,65	0,29	1,14	0,74	1,24	0,033	0,31	1,14	3,69	1,88
YPL124W	SPC29	T(6): 100.0	KFQDDTLNR;YPL124W;T18	0,37	0,69	0,36	1,36	0,87	1,48	0,025	0,37	1,36	3,64	1,86
YNL059C	ARP5	T(2): 0.0; S(10): 0.0; Y(12): 0.0; S(16): 100.0; S(24): 0.0; S(25): 0.0	QTPEPFDEQSAYNPQSPIAIDFGSSK;YNL059C;S38	0,31	0,55	0,33	1,25	0,71	1,21	0,025	0,33	1,21	3,63	1,86
YER164W	CHD1	T(5): 0.0; S(7): 100.0; S(9): 0.0; S(14): 0.0	GGLNTKSPSADIGSK;YER164W;S1272	0,17	0,41	0,33	1,57	0,60	1,19	0,049	0,33	1,19	3,62	1,86
YLR357W	RSC2	S(1): 0.0; T(2): 0.6; T(3): 99.4; S(5): 0.0; S(7): 0.0; T(9): 0.0	STTPSHSGTPQPLGPR;YLR357W;T243	0,24	0,60	0,43	1,68	1,01	1,53	0,012	0,43	1,53	3,57	1,84
YOR172W	YRM1	S(2): 0.0; S(8): 100.0; S(10): 0.0; T(13): 0.0	GSLQDRASPSEETVK;YOR172W;S12	0,42	0,59	0,42	1,50	1,09	1,53	0,004	0,42	1,50	3,55	1,83
YAL011W	SWC3	S(4): 0.0; S(6): 0.0; T(7): 0.0; T(11): 0.0; S(13): 100.0; T(15): 0.0; S(16): 0.0; T(18): 0.0	KIVSESTPAATESPTSGTIPLIR;YAL011W;S139	0,30	0,36	0,33	1,39	0,66	1,18	0,026	0,33	1,18	3,53	1,82
YIL036W	CST6	S(1): 0.0; S(6): 0.0; S(8): 100.0; S(11): 0.0; T(13): 0.0	SALRESHSNPSFTPK;YIL036W;S396	0,30	0,46	0,33	1,14	0,71	1,30	0,020	0,33	1,14	3,47	1,79
YNL039W	BDP1	S(7): 100.0; T(18): 0.0; S(25): 0.0	EIEEDNSDNDKGVDENETAIVEKPSLVGER;YNL039W;S49	0,22	0,57	0,34	1,34	0,67	1,16	0,040	0,34	1,16	3,42	1,78
YIL026C	IRR1	S(4): 0.0; S(9): 100.0; T(22): 0.0	LQNSANNNSDDEDVDDEELDITPLFPIDR;YIL026C;S628	0,47	0,59	0,22	1,78	1,07	1,60	0,012	0,47	1,60	3,38	1,76
YLR228C	ECM22	S(3): 100.0; S(4): 0.0; S(5): 0.0; S(6): 0.0	KDSSSSK;YLR228C;S84	0,16	0,31	0,33	1,42	0,65	1,06	0,028	0,31	1,06	3,36	1,75
YLL054C	YLL054C	S(4): 99.7; T(6): 0.3	INKSPTIENAPHR;YLL054C;S54	0,21	0,48	0,37	1,46	0,64	1,23	0,042	0,37	1,23	3,36	1,75
YLR442C	SIR3	S(3): 0.0; T(9): 100.0	IHSMNENPTPEKGNAK;YLR442C;T454	0,31	0,64	0,47	1,51	0,92	1,61	0,021	0,47	1,51	3,22	1,69
YGL133W	ITC1	T(8): 0.3; S(9): 99.7	LKDIVGQTSR;YGL133W;S1256	0,31	0,48	0,22	0,97	0,56	1,17	0,045	0,31	0,97	3,12	1,64
YBR083W	TEC1	S(7): 100.0; T(9): 0.0	RPLEQLSPTELHQGDRPNK;YBR083W;S325	0,27	0,55	0,45	1,48	0,77	1,36	0,030	0,45	1,36	3,01	1,59
YNL216W	RAP1	S(1): 0.0; T(4): 0.0; T(8): 100.0; T(10): 0.0	SLITDEDTPTAIAR;YNL216W;T486	0,27	0,40	0,41	1,19	0,87	1,26	0,005	0,40	1,19	2,94	1,56
YMR021C	MAC1	T(4): 0.0; T(6): 0.0; S(8): 100.0; S(11): 0.0; T(12): 0.0	APATGTISPDSTK;YMR021C;S143	0,36	0,70	0,53	1,67	0,98	1,55	0,021	0,53	1,55	2,93	1,55
YBR081C	SPT7	S(1): 0.0; T(5): 0.0; S(15): 100.0; T(20): 0.0	SFPLTQEEEHHGAVSPAVDTR;YBR081C;S88	0,38	0,51	0,45	1,31	0,84	1,35	0,013	0,45	1,31	2,89	1,53
YOR290C	SNF2	S(5): 100.0	QFEVSDDEKNDK;YOR290C;S1375	0,23	0,51	0,27	0,78	0,71	1,10	0,023	0,27	0,78	2,87	1,52
YKR092C	SRP40	S(4): 100.0; T(12): 0.0	ARESDNEDAKETK;YKR092C;S133	0,32	0,41	0,33	0,92	0,56	1,25	0,049	0,33	0,92	2,76	1,46
YBR114W	RAD16	S(1): 0.0; Y(4): 0.0; S(8): 100.0; T(12): 0.0	SVNYNELSDDDTAVK;YBR114W;S25	0,40	0,42	0,29	1,07	0,65	1,15	0,022	0,40	1,07	2,69	1,43
YDR216W	ADR1	S(3): 100.0	KASPEANVKR;YDR216W;S212	0,33	0,42	0,31	0,89	0,50	0,96	0,043	0,33	0,89	2,67	1,42
YDR458C	HEH2	S(4): 0.0; T(5): 100.0	EQISTDNEAK;YDR458C;T110	0,36	0,83	0,48	1,27	0,92	1,46	0,036	0,48	1,27	2,66	1,41
YFR034C	PHO4	S(1): 100.0; S(2): 0.0	SSGALVDDDKR;YFR034C;S242	0,33	0,62	0,45	1,23	0,69	1,19	0,043	0,45	1,19	2,64	1,40
YJL020C	BBC1	S(2): 50.1; T(3): 50.1; T(4): 99.8; S(11): 0.0	RSTTHDVGEISNNVK;YJL020C;T895	0,27	0,40	0,40	1,03	0,62	1,12	0,025	0,40	1,03	2,59	1,37
YER092W	IES5	T(2): 0.0; Y(6): 0.0; T(9): 0.0; T(11): 100.0	ETPLLYNDTHTP;YER092W;T124	0,33	0,54	0,59	1,42	1,04	1,39	0,006	0,54	1,39	2,58	1,37
YPL124W	SPC29	S(1): 100.0; S(2): 0.0	SSDNINKEGAR;YPL124W;S216	0,38	0,40	0,38	1,02	0,55	0,99	0,036	0,38	0,99	2,57	1,36
YNL027W	CRZ1	S(1): 0.0; S(3): 100.0; S(5): 0.0	SRSISPDEK;YNL027W;S427	0,31	0,34	0,56	0,96	0,75	0,87	0,010	0,34	0,87	2,55	1,35
YER024W	YAT2	T(2): 0.0; S(3): 0.0; S(4): 100.0; S(5): 0.0; S(6): 0.0	KTSSSSQVNLNR;YER024W;S784	0,39	0,41	0,77	1,03	0,96	1,05	0,018	0,41	1,03	2,51	1,33
YIL036W	CST6	S(2): 0.0; S(4): 0.0; S(7): 0.0; T(9): 100.0	ESHSNPSFTPK;YIL036W;T401	0,25	0,63	0,53	1,32	0,89	1,38	0,019	0,53	1,32	2,47	1,31
YPL089C	RLM1	S(3): 100.0; T(5): 0.0; S(9): 0.0	LLSPTALISK;YPL089C;S164	0,20	0,26	0,30	0,55	0,62	0,64	0,001	0,26	0,62	2,43	1,28
YFL021W	GAT1	S(4): 100.0; S(6): 0.0; S(12): 100.0	RNPSPSIVKPGSR;YFL021W;S262; S270;	0,55	0,58	0,47	1,34	0,80	1,30	0,025	0,55	1,30	2,39	1,26
YIL036W	CST6	S(2): 0.0; S(4): 100.0; S(7): 0.0; T(9): 100.0	ESHSNPSFTPK;YIL036W;S396;T401;	0,35	0,55	0,47	1,12	0,72	1,36	0,035	0,47	1,12	2,39	1,26
YDR145W	TAF12	S(3): 100.0; S(4): 0.0; S(5): 0.0; S(7): 0.0; T(8): 0.0; S(12): 0.0; T(14): 0.0	KISSSNSTEIPSVTGPDALK;YDR145W;S286	0,26	0,36	0,62	0,77	0,85	0,95	0,022	0,36	0,85	2,36	1,24
YDL195W	SEC31	S(3): 0.0; T(7): 0.0; S(8): 0.0; S(10): 100.0	VPSLVATSESPR;YDL195W;S999	0,33	0,29	0,29	0,59	0,70	0,68	0,001	0,29	0,68	2,34	1,22
YNL027W	CRZ1	S(1): 0.0; S(3): 100.0	SISPDEK;YNL027W;S429	0,14	0,52	0,32	1,27	0,74	0,75	0,047	0,32	0,75	2,33	1,22
YMR153W	NUP53	T(1): 0.4; S(2): 99.2; S(3): 0.4; T(5): 0.0; S(6): 0.0; S(8): 0.0; S(9): 0.0	TSSQTSLSSK;YMR153W;S368	0,52	0,66	0,37	1,26	0,93	1,21	0,010	0,52	1,21	2,31	1,21
YKR092C	SRP40	S(4): 100.0	ARESDNEDAK;YKR092C;S133	0,44	0,52	0,41	1,00	0,66	1,28	0,044	0,44	1,00	2,28	1,19

12| Supplemental Information

Protein accession	Gene	Phosphosite confidence (%)	Peptide, protein, p-site	WT batch 1	WT batch 2	WT batch 3	Mas1 mutant batch1	Mas1 mutant batch 2	Mas1 mutant batch 3	T.TEST mutants against its respective wild types	WT average	Mutant average	Mutant divided by its respective wild type	Ratios log2
YKL129C	MYO3	S(3): 99.3; Y(5): 0.7; T(15): 0.0	RGSVYHVPLNPVQATAVR;YKL129C;S357	0,41	0,41	0,50	0,68	1,07	0,92	0,018	0,41	0,92	2,23	1,16
YKR031C	SPO14	S(3): 100.0	RPSIPR;YKR031C;S286	0,43	0,43	0,67	0,94	0,73	1,05	0,032	0,43	0,94	2,18	1,12
YML075C	HMG1	S(5): 100.0; T(7): 0.0; S(11): 0.0	LKDGSVTCIKS;YML075C;S1048	0,66	0,62	0,44	1,48	1,13	1,34	0,004	0,62	1,34	2,17	1,12
YNL156C	NSG2	S(1): 0.0; S(3): 0.0; S(6): 99.7; T(7): 0.3; Y(9): 0.0; S(10): 0.0	SVSIDSTKYSR;YNL156C;S52	0,55	0,50	0,38	1,08	1,01	1,18	0,001	0,50	1,08	2,16	1,11
YCL040W	GLK1	S(1): 100.0; T(9): 0.0	SFDDLHKATER;YCL040W;S2	0,39	0,56	0,37	0,96	0,77	0,83	0,008	0,39	0,83	2,14	1,10
YNR008W	LRO1	S(3): 99.7; S(5): 0.3	GISGSAK;YNR008W;S50	0,69	0,67	0,48	1,42	1,31	1,57	0,001	0,67	1,42	2,13	1,09
YCL040W	GLK1	S(1): 100.0	SFDDLHK;YCL040W;S2	0,42	0,58	0,40	0,89	0,61	0,92	0,039	0,42	0,89	2,13	1,09
YGL140C	YGL140C	S(3): 100.0; T(5): 0.0; S(6): 0.0; T(7): 0.0; S(8): 0.0; S(12): 0.0; S(13): 0.0; S(15): 0.0	AFSITSTSGQLSSLSR;YGL140C;S1167	0,38	0,45	0,60	0,81	1,14	0,95	0,013	0,45	0,95	2,11	1,07
YHR056C	RSC30	S(1): 0.0; S(3): 100.0; S(8): 0.0	SDSPDVPSMDQIR;YHR056C;S152	0,44	0,51	0,53	1,07	0,90	1,18	0,003	0,51	1,07	2,09	1,06
YLR260W	LCB5	S(2): 0.0; S(4): 99.7; S(5): 0.3; S(6): 0.0; S(7): 0.0; T(10): 0.0; S(11): 0.0	GSNSSSSLLTSR;YLR260W;S201	0,63	0,61	0,60	1,27	1,14	1,51	0,003	0,61	1,27	2,08	1,06
YKL188C	PXA2	S(2): 0.0; S(8): 100.0; T(10): 0.0	ESNIIRKSETNLNLFEK;YKL188C;S776	0,41	0,50	0,65	1,32	1,03	0,79	0,034	0,50	1,03	2,07	1,05
YAR002W	NUP60	S(3): 100.0; T(5): 0.0; S(8): 0.0; Y(11): 0.0	RASATVPSAPYRK;YAR002W;S10	0,31	0,30	0,40	0,75	0,64	0,63	0,003	0,31	0,64	2,07	1,05
YDL051W	LHP1	S(3): 100.0; T(10): 0.0	RNSFAVIEFTPEVLDR;YDL051W;S19	0,41	0,45	0,62	0,68	1,05	0,94	0,036	0,45	0,94	2,07	1,05
YMR153W	NUP53	T(1): 0.0; S(2): 0.0; S(3): 0.0; T(5): 0.0; S(6): 0.0; S(8): 99.8; S(9): 0.2	TSSQTSLSSK;YMR153W;S374	0,61	0,74	0,45	1,27	0,82	1,28	0,040	0,61	1,27	2,07	1,05
YJL057C	IKS1	S(7): 100.0; T(9): 0.0; S(11): 0.0	KVFNRFSDTESPEER;YJL057C;S295	0,34	0,45	0,32	0,70	0,66	0,88	0,008	0,34	0,70	2,05	1,03
YDL225W	SHS1	T(3): 100.0; Y(4): 0.0; T(5): 0.0; S(9): 0.0; S(12): 0.0	NDTYTDLASIASGRD;YDL225W;T539	0,40	0,45	0,74	0,75	0,98	0,92	0,048	0,45	0,92	2,05	1,03
YBR068C	BAP2	T(3): 0.0; S(4): 0.0; S(7): 0.3; S(9): 99.7	KETSPDSISIR;YBR068C;S21	0,53	0,81	0,78	1,60	1,76	1,45	0,002	0,78	1,60	2,05	1,03
YGL150C	INO80	T(1): 0.0; S(9): 100.0; T(12): 0.0	TIEVGENDSEVTR;YGL150C;S1466	0,33	0,52	0,64	1,24	0,77	1,06	0,034	0,52	1,06	2,04	1,03
YJL165C	HAL5	S(3): 100.0; S(5): 0.0; T(6): 0.0	KNSLSTPR;YJL165C;S233	0,31	0,26	0,44	0,59	0,67	0,64	0,006	0,31	0,64	2,04	1,03
YMR129W	POM152	Y(4): 0.0; S(5): 100.0	RFQYSDDEPAEK;YMR129W;S45	0,72	0,63	0,42	1,28	1,14	1,59	0,009	0,63	1,28	2,04	1,03
YMR212C	EFR3	T(2): 0.3; T(5): 99.7	VTNITFLLNELK;YMR212C;T690	0,29	0,42	0,46	0,82	1,03	0,85	0,004	0,42	0,85	2,03	1,02
YNL156C	NSG2	S(1): 100.0; S(3): 0.0; S(6): 0.0; T(7): 0.0	SVSIDSTK;YNL156C;S47	0,52	0,41	0,51	1,00	1,21	1,02	0,001	0,51	1,02	2,01	1,01
YER105C	NUP157	S(3): 100.0; S(7): 0.0	ANSGELSK;YER105C;S517	0,61	0,70	0,37	1,23	0,83	1,30	0,033	0,61	1,23	2,00	1,00
YIL070C	MAM33	T(2): 0.0; S(6): 99.8; T(7): 0.2; S(8): 0.0; S(11): 0.0	ETLPESTSLDSFNDFLNK;YIL070C;S71	2,14	1,87	1,65	0,92	0,91	0,96	0,003	1,87	0,92	0,49	-1,02
YOL019W	YOL019W-A	S(7): 100.0; S(15): 100.0	FDIDADSEANLRGDSR;YOL019W;S224;S232;	1,10	1,46	1,33	0,61	1,08	0,66	0,048	1,33	0,66	0,49	-1,02
YLR190W	MMR1	S(6): 100.0; S(7): 0.0; S(9): 0.0	LEQLRSSESVAQVQK;YLR190W;S154	1,44	1,69	1,41	0,73	0,64	0,69	0,001	1,44	0,69	0,48	-1,05
YFL014W	HSP12	S(11): 100.0	GKDNAEGQGESLADQAR;YFL014W;S73	0,41	0,70	0,50	0,31	0,24	0,23	0,037	0,50	0,24	0,48	-1,07
YIL140W	AXL2	S(5): 0.3; S(8): 99.7	LVDFSNKSNVNVGQVK;YIL140W;S805	1,04	1,51	1,61	0,70	0,71	0,73	0,018	1,51	0,71	0,47	-1,08
YDR033W	MRH1	S(5): 100.0; T(11): 0.0; S(15): 0.0	APVASPRPAATPNLSKDK;YDR033W;S289	0,37	0,56	0,76	0,26	0,21	0,26	0,047	0,56	0,26	0,46	-1,12
YLR355C	ILV5	T(3): 0.0; T(5): 0.0; S(8): 100.0; S(13): 0.0; Y(17): 0.0	NGTETKRSLEFNSQPDYR;YLR355C;S355	2,88	2,51	2,17	1,14	1,41	1,04	0,005	2,51	1,14	0,45	-1,14
YER020W	GPA2	S(5): 100.0	QQQPSPHNVKDR;YER020W;S61	0,64	1,03	1,11	0,49	0,34	0,46	0,031	1,03	0,46	0,44	-1,17
YLR248W	RCK2	S(1): 0.0; S(2): 0.0; T(4): 0.0; S(10): 0.0; T(13): 0.0; S(14): 0.3; S(15): 99.7	SSGTNNKDVSQITSSPK;YLR248W;S46	0,90	0,97	1,19	0,60	0,40	0,38	0,008	0,97	0,40	0,41	-1,29
YLR332W	MID2	Y(2): 0.0; S(10): 100.0	FYDEQGNELSPR;YLR332W;S372	0,92	1,01	1,16	0,31	0,40	0,46	0,002	1,01	0,40	0,40	-1,32
YPL186C	UIP4	T(1): 0.0; S(4): 99.3; S(8): 0.7	TAISQDGSAFAK;YPL186C;S146	1,27	1,63	1,74	0,65	0,87	0,47	0,009	1,63	0,65	0,40	-1,33
YLR413W	YLR413W	S(7): 100.0	IIEEHESPIDAEKNFAR;YLR413W;S665	1,15	1,44	1,67	0,56	0,51	0,61	0,005	1,44	0,56	0,39	-1,37
YLR248W	RCK2	S(1): 0.0; S(2): 0.0; T(4): 0.0; S(10): 0.0; T(13): 0.0; S(14): 0.0; S(15): 100.0	SSGTNNKDVSQITSSPKK;YLR248W;S46	0,86	1,00	1,17	0,51	0,37	0,34	0,004	1,00	0,37	0,37	-1,42
YPL186C	UIP4	T(4): 0.0; S(7): 100.0	GNVTFPSPK;YPL186C;S140	1,31	1,19	1,37	0,49	0,89	0,37	0,013	1,31	0,49	0,37	-1,43
YPL186C	UIP4	S(3): 100.0; S(7): 0.0; T(11): 0.0	ELSPNFSQEQTENKQDK;YPL186C;S185	1,56	1,24	1,48	0,53	0,76	0,48	0,003	1,48	0,53	0,36	-1,49
YLR019W	PSR2	S(3): 100.0; S(4): 0.0; T(9): 0.0	KHSSNKAQTQGR;YLR019W;S37	1,60	2,18	2,49	0,80	0,43	0,75	0,008	2,18	0,75	0,35	-1,53
YPL186C	UIP4	S(7): 100.0; S(11): 0.0; T(15): 0.0	EENKELSPNFSQEQTENK;YPL186C;S185	1,70	1,45	1,51	0,51	0,73	0,43	0,001	1,51	0,51	0,33	-1,58
YLR413W	YLR413W	S(7): 100.0	IIEEHESPIDAEK;YLR413W;S665	1,53	1,59	2,11	0,42	0,42	0,45	0,002	1,59	0,42	0,27	-1,91

Supplemental Table 13. Up- and down-regulated phosphopeptides from the 2 h time shift yeast MAS1 ChaFRADIC experiment. At least a 2-fold regulation between the mutant and respective wild type was considered as regulation ($p \leq 0.05$). Wild type (WT) and mutant normalized abundance values are displayed. “Phosphosite confidence” indicates percentage of binding confidence of the phosphorylation on the S, T or/and Y amino acid present in the peptide sequence. ”P-site” indicates amino acid and position within the protein.

Protein accession	Gene	Phosphosite confidence (%)	Peptide, protein, p-site	WT batch 1	WT batch 2	WT batch 3	Mas1 mutant batch1	Mas1 mutant batch 2	Mas1 mutant batch 3	T.TEST mutants against its respective wild types	WT average	Mutant average	Mutant divided by its respective wild type	Ratios log2
YER164W	CHD1	S(2): 0.0; S(5): 100.0; T(7): 0.0	LSPNSPTPPLK;YER164W;S1339	0,38	0,81	0,50	1,75	1,77	0,91	0,04	0,50	1,75	3,50	1,81
YLR228C	ECM22	S(3): 100.0; S(4): 0.0; S(5): 0.0; S(6): 0.0	KDSSSSK;YLR228C;S84	0,39	0,59	0,50	2,33	1,61	1,00	0,04	0,50	1,61	3,21	1,68
YDR033W	MRH1	S(5): 100.0; T(11): 100.0; S(15): 0.0	APVASPRPAATPNLSK;YDR033W;S289;T295;	0,35	0,48	0,35	1,17	0,72	1,03	0,01	0,35	1,03	2,97	1,57
YDR033W	MRH1	S(5): 100.0; T(11): 100.0; S(15): 0.0	APVASPRPAATPNLSKDK;YDR033W;S289;T295;	0,37	0,45	0,27	1,22	0,75	1,04	0,01	0,37	1,04	2,80	1,48
YGR008C	STF2	S(5): 100.0; S(9): 0.0	DRRGSNLQSHEQK;YGR008C;S69	0,65	0,52	0,53	0,82	1,54	1,49	0,04	0,53	1,49	2,79	1,48
YDR033W	MRH1	S(5): 0.0; T(11): 100.0; S(15): 0.0	APVASPRPAATPNLSKDK;YDR033W;T295	0,58	0,74	0,49	1,61	1,28	1,51	0,00	0,58	1,51	2,59	1,38
YAR002W	NUP60	S(3): 100.0; T(5): 0.0; S(8): 0.0; Y(11): 0.0	RASATVPSAPYRK;YAR002W;S10	0,54	0,62	0,49	1,39	1,25	1,38	0,00	0,54	1,38	2,57	1,36
YDR348C	YDR348C	S(1): 0.0; T(3): 100.0; S(6): 0.0	SKTVNSPNR;YDR348C;T436	0,80	0,63	0,59	1,49	1,86	1,25	0,01	0,63	1,49	2,38	1,25
YDR145W	TAF12	S(3): 100.0; S(4): 0.0; S(5): 0.0; S(7): 0.0; T(8): 0.0; S(12): 0.0; T(14): 0.0	KISSSNSTEIPSVTGPDALK;YDR145W;S286	0,69	0,62	0,63	2,19	1,48	1,10	0,04	0,63	1,48	2,36	1,24
YDR033W	MRH1	S(5): 0.0; T(11): 99.4; S(15): 0.6	APVASPRPAATPNLSK;YDR033W;T295	0,62	0,82	0,49	1,46	1,25	1,46	0,00	0,62	1,46	2,36	1,24
YCL040W	GLK1	S(1): 100.0	SFDDLHK;YCL040W;S2	0,69	1,17	0,49	1,42	1,71	1,59	0,02	0,69	1,59	2,32	1,22
YMR153W	NUP53	T(1): 0.3; S(2): 49.7; S(3): 49.7; T(5): 1.0; S(6): 99.4; S(8): 0.0; S(9): 0.0	TSSQTSLSSK;YMR153W;S372	0,58	0,83	0,49	1,64	1,29	1,04	0,03	0,58	1,29	2,22	1,15
YLR377C	FBP1	S(3): 100.0; T(4): 0.0; T(9): 0.0; T(13): 0.0	RDSTEGFDTDIITLPR;YLR377C;S12	0,71	0,62	0,63	1,35	1,95	1,41	0,01	0,63	1,41	2,22	1,15
YGL150C	INO80	T(1): 0.0; S(9): 100.0; T(12): 0.0	TIEVGENDSEVTR;YGL150C;S1466	0,63	0,86	0,54	2,02	1,37	1,34	0,02	0,63	1,37	2,17	1,12
YHR117W	TOM71	S(3): 100.0; S(21): 0.0; S(24): 0.0; S(26): 0.0	RQSEAFAGQNEDEADLKDDGSVVSGSNK;YHR117W;S55	0,62	0,63	0,62	1,12	1,26	1,28	0,00	0,62	1,26	2,03	1,02
YJR092W	BUD4	S(2): 0.3; S(3): 0.3; S(4): 99.4	LSSSPLK;YJR092W;S149	1,97	1,75	1,51	0,87	0,89	0,56	0,00	1,75	0,87	0,50	-1,00
YMR212C	EFR3	S(5): 0.0; T(6): 0.0; S(7): 0.0; S(11): 100.0; S(13): 0.0	DNQISTSDLLSDSQVR;YMR212C;S570	1,48	1,44	1,05	0,66	0,71	0,89	0,02	1,44	0,71	0,50	-1,01
YIL105C	SLM1	S(2): 0.0; T(3): 0.0; S(4): 0.0; S(5): 100.0; S(8): 0.0; T(9): 0.0; S(11): 0.0	NSTSSPNSTGSDAK;YIL105C;S533	1,71	1,56	1,29	0,60	0,77	0,86	0,01	1,56	0,77	0,49	-1,03
YER020W	GPA2	S(5): 100.0	QQQPSPHNVKDRK;YER020W;S61	1,76	1,61	1,27	0,79	0,94	0,67	0,01	1,61	0,79	0,49	-1,03
YPL150W	YPL150W	S(1): 0.0; S(3): 0.0; S(9): 100.0	SISFDGKVSPPPIR;YPL150W;S620	1,40	1,56	1,06	0,96	0,64	0,67	0,03	1,40	0,67	0,48	-1,07
YDR475C	JIP4	S(1): 0.0; S(3): 100.0	SRSPQIK;YDR475C;S726	1,83	1,59	1,21	0,74	0,88	0,76	0,01	1,59	0,76	0,47	-1,07
YIL105C	SLM1	S(3): 0.0; T(4): 0.0; S(5): 0.0; S(6): 100.0; S(9): 0.0; T(10): 0.0; S(12): 0.0	KNSTSSPNSTGSDAK;YIL105C;S533	1,66	1,58	1,31	0,62	0,72	0,74	0,00	1,58	0,72	0,46	-1,13
YPL186C	UIP4	S(3): 100.0; S(7): 0.0; T(11): 0.0	ELSPNFSQEQTENKQDK;YPL186C;S185	1,38	1,17	1,54	0,63	0,97	0,48	0,02	1,38	0,63	0,45	-1,14
YER020W	GPA2	S(5): 100.0	QQQPSPHNVK;YER020W;S61	1,75	1,72	1,14	0,76	0,83	0,77	0,02	1,72	0,77	0,45	-1,16
YIL117C	PRM5	S(3): 0.0; S(4): 100.0; S(6): 0.0	IASSPSRK;YIL117C;S268	2,41	1,59	1,83	0,81	1,03	0,59	0,01	1,83	0,81	0,44	-1,18
YLR355C	ILV5	T(3): 0.0; T(5): 0.0; S(8): 100.0; S(13): 0.0; Y(17): 0.0	NGTETKRSLEFNSQPDYR;YLR355C;S355	0,86	0,90	1,03	0,39	0,39	0,58	0,00	0,90	0,39	0,44	-1,19
YER020W	GPA2	S(5): 100.0	QQQPSPHNVKDR;YER020W;S61	1,77	1,76	1,43	0,77	0,81	0,57	0,00	1,76	0,77	0,44	-1,19
YPL186C	UIP4	S(7): 100.0; S(11): 0.0; T(15): 0.0	EENKELSPNFSQEQTENK;YPL186C;S185	1,28	1,11	1,54	0,56	0,87	0,51	0,02	1,28	0,56	0,44	-1,20
YFL014W	HSP12	S(11): 100.0	GKDNAEGQGESLADQAR;YFL014W;S73	1,54	1,59	1,10	0,54	0,75	0,66	0,01	1,54	0,66	0,43	-1,22
YDR475C	JIP4	S(2): 0.0; S(3): 100.0	VSSPLDEEKR;YDR475C;S86	1,98	1,64	1,41	0,77	0,71	0,65	0,00	1,64	0,71	0,43	-1,22

12| Supplemental Information

Protein accession	Gene	Phosphosite confidence (%)	Peptide, protein, p-site	WT batch 1	WT batch 2	WT batch 3	Mas1 mutant batch1	Mas1 mutant batch 2	Mas1 mutant batch 3	T.TEST mutants against its respective wild types	WT average	Mutant average	Mutant divided by its respective wild type	Ratios log2
YDR348C	YDR348C	S(1): 0.0; T(3): 0.0; S(6): 100.0	SKTVNSPNR;YDR348C;S439	1,70	1,31	1,36	0,66	0,55	0,57	0,00	1,36	0,57	0,42	-1,26
YBR069C	TAT1	S(2): 0.0; S(6): 100.0; T(13): 0.0	NSELESQEKNNLTK;YBR069C;S84	1,00	1,02	1,02	0,42	0,47	0,35	0,00	1,02	0,42	0,42	-1,26
YBR069C	TAT1	S(3): 100.0; Y(7): 0.0; S(8): 0.0; S(10): 100.0	EASPAQYSHSLHER;YBR069C;S13; S20;	1,49	1,44	1,23	0,58	0,68	0,49	0,00	1,44	0,58	0,40	-1,32
YBL101C	ECM21	S(7): 100.0; T(9): 0.0	GQPFQPSPTKK;YBL101C;S33	2,05	1,71	1,36	0,66	0,72	0,68	0,01	1,71	0,68	0,40	-1,32
YBR069C	TAT1	S(8): 0.0; S(12): 100.0; T(19): 0.0	QLPPDRNSELESQEKNNLTK;YBR069C;S84	1,04	1,04	0,76	0,42	0,58	0,29	0,01	1,04	0,42	0,40	-1,32
YLR248W	RCK2	S(1): 0.0; S(2): 0.0; T(4): 0.0; S(10): 0.0; T(13): 0.0; S(14): 0.3; S(15): 99.7	SSGTNNKDVSQITSSPK;YLR248W; S46	1,71	1,71	1,62	0,67	0,72	0,59	0,00	1,71	0,67	0,39	-1,35
YDR348C	YDR348C	T(1): 0.0; S(4): 100.0; T(8): 0.0	TVNSPNRTHK;YDR348C;S439	1,71	1,39	1,42	0,72	0,56	0,37	0,00	1,42	0,56	0,39	-1,35
YDL204W	RTN2	Y(3): 0.0; S(6): 100.0; T(13): 0.0	AEYPVSQNENIGTLK;YDL204W;S278	1,94	1,87	1,27	0,72	0,77	0,64	0,01	1,87	0,72	0,39	-1,37
YLR248W	RCK2	S(1): 0.0; S(2): 0.0; T(4): 0.0; S(10): 0.0; T(13): 0.0; S(14): 0.0; S(15): 100.0	SSGTNNKDVSQITSSPKK;YLR248W ;S46	1,81	1,77	1,77	0,68	0,70	0,51	0,00	1,77	0,68	0,38	-1,38
YML059C	NTE1	S(2): 0.0; S(3): 0.0; S(5): 100.0	FSSLSPELR;YML059C;S634	1,81	1,65	1,14	0,80	0,63	0,59	0,02	1,65	0,63	0,38	-1,39
YIL105C	SLM1	S(3): 0.0; T(4): 0.0; S(5): 0.0; S(6): 0.0; S(9): 99.7; T(10): 0.3; S(12): 0.0	KNSTSSPNSTGSDAK;YIL105C;S536	1,78	1,72	1,52	0,58	0,62	0,65	0,00	1,72	0,62	0,36	-1,48
YDL223C	HBT1	T(4): 100.0; T(5): 0.0; S(10): 0.0	RAKTTQDIASDAK;YDL223C;T731	2,21	1,59	1,39	0,49	0,88	0,55	0,02	1,59	0,55	0,34	-1,54
YLR332W	MID2	Y(2): 0.0; S(10): 100.0	FYDEQGNELSPR;YLR332W;S372	1,52	1,73	1,05	0,52	0,49	0,62	0,01	1,52	0,52	0,34	-1,55
YDL223C	HBT1	T(1): 0.0; T(2): 0.4; S(3): 99.6; T(5): 0.0; T(7): 0.0; S(11): 0.0	TTSPTNTHEHSK;YDL223C;S218	2,35	1,89	1,34	0,47	0,54	0,53	0,01	1,89	0,53	0,28	-1,83
YOL130W	ALR1	S(2): 0.0; S(4): 0.0; S(5): 0.0; S(6): 0.0; S(8): 100.0; T(11): 0.0	LSASSSASPITK;YOL130W;S176	2,16	1,92	1,42	0,62	0,53	0,53	0,00	1,92	0,53	0,28	-1,85
YLR019W	PSR2	S(3): 100.0; S(4): 0.0; T(9): 0.0	KHSSNKAQTQGR;YLR019W;S37	1,56	1,54	0,98	0,47	0,42	0,41	0,01	1,54	0,42	0,27	-1,88
YLR413W	YLR413W	S(7): 100.0	IIEEHESPIDAEKNFAR;YLR413W;S665	1,82	1,72	1,33	0,59	0,38	0,43	0,00	1,72	0,43	0,25	-2,00
YLR413W	YLR413W	S(7): 100.0	IIEEHESPIDAEK;YLR413W;S665	2,00	1,92	1,68	0,25	0,33	0,20	0,00	1,92	0,25	0,13	-2,93

Supplemental Table 14. Up- and down-regulated phosphopeptides from the 4 h time shift yeast MAS1 ChaFRADIC experiment. At least a 2-fold regulation between the mutant and respective wild type was considered as regulation ($p \leq 0.05$). Wild type (WT) and mutant normalized abundance values are displayed. "Phosphosite confidence" indicates percentage of binding confidence of the phosphorylation on the S, T or/and Y amino acid present in the peptide sequence. "P-site" indicates amino acid and position within the protein.

Protein accession	Gene	Phosphosite confidence (%)	Peptide, protein, p-site	WT batch 1	WT batch 2	WT batch 3	Mas1 mutant batch1	Mas1 mutant batch 2	Mas1 mutant batch 3	T.TEST mutants against its respective wild types	WT average	Mutant average	Mutant divided by its respective wild type	Ratios log2
YNL039W	BDP1	S(3): 99.7; T(4): 0.3; S(6): 0.0	RLSTISNK;YNL039W;S164	0,63	0,41	0,53	1,48	3,18	2,82	0,02	0,53	2,82	5,31	2,41
YIL126W	STH1	S(4): 100.0	KEDSEPLGR;YIL126W;S1045	0,40	0,44	0,23	1,01	2,10	2,52	0,03	0,40	2,10	5,25	2,39
YKR008W	RSC4	S(1): 0.0; T(2): 0.0; T(3): 0.0; S(4): 100.0	STTSDIEK;YKR008W;S406	0,49	0,43	0,34	0,90	2,25	2,62	0,05	0,43	2,25	5,23	2,39
YMR091C	NPL6	S(9): 100.0; T(15): 0.0	HVDEEEDLSEDKGVTR;YMR091C;S86	0,38	0,46	0,42	0,99	2,06	2,66	0,04	0,42	2,06	4,94	2,30
YMR037C	MSN2	S(2): 0.2; S(3): 99.8; S(8): 0.0; T(9): 0.0	RSSVVIESTK;YMR037C;S633	0,72	0,51	0,51	1,06	2,48	2,83	0,05	0,51	2,48	4,85	2,28
YML065W	ORC1	T(4): 0.0; T(6): 0.0; S(10): 100.0; T(14): 0.0	DKATQTAQISDAETR;YML065W;S237	0,51	0,47	0,49	1,07	2,38	2,69	0,03	0,49	2,38	4,81	2,27
YIL126W	STH1	S(3): 100.0	INSIIDFIK;YIL126W;S329	0,38	0,39	0,29	0,79	1,79	2,03	0,04	0,38	1,79	4,76	2,25
YKL112W	ABF1	S(1): 0.0; S(3): 100.0; Y(6): 0.0	SNSIDYAK;YKL112W;S467	0,58	0,49	0,33	1,25	2,27	3,07	0,03	0,49	2,27	4,64	2,21
YJL081C	ARP4	T(2): 0.0; T(4): 0.0; S(13): 100.0	VTPTEEKEQEAVSK;YJL081C;S349	0,39	0,52	0,27	0,96	1,74	2,36	0,03	0,39	1,74	4,44	2,15
YER169W	RPH1	S(10): 0.0; S(11): 100.0; S(15): 0.0	NDDLDKEQGSSPLNSK;YER169W;S689	0,51	0,55	0,40	0,99	2,24	2,63	0,04	0,51	2,24	4,41	2,14
YDR303C	RSC3	S(3): 100.0; T(8): 0.0; S(18): 0.0	KLSEDGVTDGDGKPIPESER;YDR303C;S236	0,38	0,58	0,48	1,03	2,11	2,47	0,03	0,48	2,11	4,41	2,14
YKR064W	OAF3	S(3): 99.6; T(4): 0.4	KQSTPAER;YKR064W;S73	0,50	0,64	0,40	1,05	2,10	2,66	0,04	0,50	2,10	4,19	2,07
YOR304W	ISW2	T(1): 0.0; S(2): 0.0; T(4): 0.0; T(8): 100.0; S(11): 0.0; S(15): 0.0; T(16): 0.0	TSATREDTPLSQNESTR;YOR304W;T1079	0,54	0,54	0,25	1,03	2,11	2,89	0,05	0,54	2,11	3,91	1,97
YLR228C	ECM22	S(3): 100.0; S(4): 0.0; S(5): 0.0; S(6): 0.0	KDSSSSK;YLR228C;S84	0,34	0,60	0,67	1,35	2,24	2,44	0,01	0,60	2,24	3,70	1,89
YBR114W	RAD16	S(1): 0.0; Y(4): 0.0; S(8): 100.0; T(12): 0.0	SVNYNELSDDDTAVK;YBR114W;S25	0,77	0,60	0,49	1,09	2,22	2,81	0,05	0,60	2,22	3,67	1,88
YNR001C	CIT1	S(11): 99.3; S(13): 0.4; T(14): 0.4	AVGAPIERPKSFSTEK;YNR001C;S462	0,40	0,30	0,47	1,46	1,00	1,50	0,01	0,40	1,46	3,63	1,86
YGL150C	INO80	S(5): 100.0	NANLSDIINEK;YGL150C;S133	0,46	0,67	0,50	1,23	1,80	2,46	0,02	0,50	1,80	3,61	1,85
YNL027W	CRZ1	S(1): 0.0; S(3): 100.0; S(5): 0.0	SRSISPDEK;YNL027W;S427	0,65	0,58	0,78	1,99	2,75	2,35	0,00	0,65	2,35	3,59	1,85
YAL001C	TFC3	S(8): 100.0	GFDELGKSR;YAL001C;S434	0,48	0,61	0,37	0,88	1,70	2,17	0,05	0,48	1,70	3,57	1,84
YBL103C	RTG3	S(3): 100.0; T(6): 0.0	HGSINTPR;YBL103C;S246	0,72	0,78	0,60	1,79	2,51	2,78	0,01	0,72	2,51	3,46	1,79
YDR167W	TAF10	S(8): 100.0; T(18): 0.0	EAVVDDGSENAFGIPEFTRK;YDR167W;S58	0,63	0,60	0,45	1,12	1,97	2,74	0,04	0,60	1,97	3,30	1,72
YFL021W	GAT1	S(3): 99.6; S(4): 0.4; T(5): 0.0; S(6): 0.0; S(9): 0.0; S(10): 0.0; T(12): 0.0; S(15): 0.0; T(17): 0.0; S(18): 0.0; S(19): 0.0	IKSSTSVQSSATPPSNTSSNPDIK;YFL021W;S288	0,61	0,49	0,58	0,98	1,75	2,07	0,03	0,58	1,75	3,02	1,59
YFL021W	GAT1	S(4): 100.0; S(6): 0.0; S(12): 100.0	RNPSPSIVKPGSR;YFL021W;S262;S270;	0,63	0,77	0,57	1,05	1,90	2,30	0,04	0,63	1,90	2,99	1,58
YDR216W	ADR1	S(3): 100.0; S(5): 50.0; S(6): 50.0	KNSASSVK;YDR216W;S180	0,69	0,82	0,48	1,47	2,03	3,38	0,05	0,69	2,03	2,94	1,56
YLR272C	YCS4	S(4): 100.0; T(7): 0.0; T(11): 0.0	KVESQETLNDTIER;YLR272C;S464	0,53	0,66	0,45	1,00	1,55	2,28	0,05	0,53	1,55	2,94	1,56
YOR304W	ISW2	S(1): 0.0; S(3): 0.0; T(6): 100.0	SASKQTPQPK;YOR304W;T774	0,59	0,72	0,61	1,03	1,79	2,34	0,05	0,61	1,79	2,91	1,54
YIL036W	CST6	S(1): 0.0; S(6): 0.0; S(8): 100.0; S(11): 0.0; T(13): 0.0	SALRESHSNPSFTPK;YIL036W;S396	0,55	0,76	0,53	1,05	1,60	2,29	0,05	0,55	1,60	2,91	1,54
YOR374W	ALD4	S(4): 100.0	FVPSKQNK;YOR374W;S56	0,68	0,74	0,77	2,71	1,84	2,15	0,00	0,74	2,15	2,90	1,54
YNL216W	RAP1	S(1): 0.0; T(4): 0.0; T(8): 100.0; T(10): 0.0	SLITDEDTPTAIAR;YNL216W;T486	0,59	0,78	0,58	1,11	1,71	2,35	0,04	0,59	1,71	2,88	1,53
YGR274C	TAF1	S(5): 100.0	DNPASPK;YGR274C;S1064	0,65	0,63	0,41	1,21	1,81	2,59	0,03	0,63	1,81	2,86	1,52
YDR145W	TAF12	S(3): 100.0; S(4): 0.0; S(5): 0.0; S(7): 0.0; T(8): 0.0; S(12): 0.0; T(14): 0.0	KISSSNSTEIPSVTGPDALK;YDR145W;S286	0,67	0,68	0,82	1,42	2,01	1,88	0,00	0,68	1,88	2,78	1,48
YDR033W	MRH1	S(5): 100.0; T(11): 100.0; S(15): 0.0	APVASPRPAATPNLSK;YDR033W;S289;T295;	1,60	1,22	0,78	2,70	3,36	3,48	0,00	1,22	3,36	2,76	1,46
YHR177W	YHR177W	S(3): 99.7; T(4): 0.3; Y(15): 0.0	LGSTHDLPLHNVPEYNIFER;YHR177W;S90	0,49	0,79	0,60	1,20	1,60	2,20	0,03	0,60	1,60	2,68	1,42
YDR033W	MRH1	S(5): 100.0; T(11): 100.0; S(15): 0.0	APVASPRPAATPNLSKDK;YDR033W;S289;T295;	1,49	1,25	0,78	2,71	3,32	3,61	0,00	1,25	3,32	2,66	1,41
YBR114W	RAD16	S(2): 0.0; Y(5): 0.0; S(9): 100.0; T(13): 0.0	KSVNYNELSDDDTAVK;YBR114W;S25	0,72	0,65	0,87	1,14	2,23	1,89	0,04	0,72	1,89	2,64	1,40
YIL036W	CST6	S(2): 0.0; S(4): 100.0; S(7): 0.0; T(9): 100.0	ESHSNPSFTPK;YIL036W;S396;T401;	0,56	0,74	0,59	1,19	1,55	2,09	0,02	0,59	1,55	2,62	1,39
YDR348C	YDR348C	S(1): 0.0; T(3): 100.0; S(6): 0.0	SKTVNSPNR;YDR348C;T436	0,82	0,35	0,69	1,56	1,70	1,87	0,00	0,69	1,70	2,47	1,31
YIL036W	CST6	S(2): 0.0; S(4): 100.0; S(7): 0.0; T(9): 0.0	ESHSNPSFTPK;YIL036W;S396	0,59	0,70	0,56	1,06	1,42	2,01	0,04	0,59	1,42	2,42	1,27

12| Supplemental Information

Protein accession	Gene	Phosphosite confidence (%)	Peptide, protein, p-site	WT batch 1	WT batch 2	WT batch 3	Mas1 mutant batch1	Mas1 mutant batch 2	Mas1 mutant batch 3	T.TEST mutants against its respective wild types	WT average	Mutant average	Mutant divided by its respective wild type	Ratios log2
YML065W	ORC1	T(2): 0.0; T(4): 0.0; S(8): 100.0; T(12): 0.0	ATQTAQISDAETR;YML065W;S237	0,60	0,68	0,85	1,11	1,95	1,64	0,03	0,68	1,64	2,40	1,26
YMR005W	TAF4	S(3): 100.0; T(5): 0.0; T(6): 0.0	NVSPTTNLR;YMR005W;S80	0,68	0,68	0,81	1,14	1,63	2,17	0,04	0,68	1,63	2,38	1,25
YGR008C	STF2	S(5): 100.0; S(9): 0.0	DRRGSNLQSHEQK;YGR008C;S69	1,09	0,83	1,49	2,70	2,57	2,02	0,01	1,09	2,57	2,36	1,24
YMR129W	POM152	Y(4): 0.0; S(5): 100.0	RFQYSDDEPAEK;YMR129W;S45	0,51	0,72	0,49	1,17	1,07	1,97	0,05	0,51	1,17	2,29	1,19
YBR081C	SPT7	S(1): 0.0; T(5): 0.0; S(15): 100.0; T(20): 0.0	SFPLTQEEEHHGAVSPAVDTR;YBR081C;S88	0,68	0,75	0,70	0,99	1,56	1,97	0,05	0,70	1,56	2,25	1,17
YLR357W	RSC2	S(1): 0.0; T(2): 0.6; T(3): 99.4; S(5): 0.0; S(7): 0.0; T(9): 0.0	STTPSHSGTPQPLGPR;YLR357W;T243	0,55	0,67	0,81	0,98	1,51	1,63	0,03	0,67	1,51	2,24	1,16
YOR189W	IES4	T(4): 0.0; S(5): 0.0; S(8): 100.0; S(11): 0.0	IEDTSPPSANSR;YOR189W;S28	0,68	0,83	0,79	1,31	1,75	2,08	0,01	0,79	1,75	2,22	1,15
YHR051W	COX6	Y(2): 0.0; S(3): 100.0; T(10): 0.0; T(15): 0.0	KYSDAHDEETFEEFTAR;YHR051W;S41	1,04	1,27	1,04	2,30	2,15	2,48	0,00	1,04	2,30	2,20	1,14
YIL135C	VHS2	S(6): 100.0	NFHNLSQR;YIL135C;S84	0,74	0,68	0,93	1,78	1,52	1,60	0,00	0,74	1,60	2,15	1,11
YMR153W	NUP53	T(1): 0.0; S(2): 0.3; S(3): 99.7; T(5): 0.0; S(6): 0.0; S(8): 0.0; S(9): 0.0	TSSQTSLSSK;YMR153W;S369	0,60	0,62	0,64	1,22	1,33	2,04	0,02	0,62	1,33	2,14	1,10
YOR043W	WHI2	S(6): 0.0; S(7): 0.5; S(8): 99.5; S(11): 0.0	FFDRPSSSFVSNAK;YOR043W;S131	0,93	0,76	0,80	1,71	1,40	2,26	0,02	0,80	1,71	2,14	1,10
YPL124W	SPC29	T(6): 100.0	KFQDDTLNR;YPL124W;T18	0,49	0,92	0,60	1,07	1,28	1,80	0,05	0,60	1,28	2,12	1,09
YER024W	YAT2	T(2): 0.0; S(3): 0.0; S(4): 100.0; S(5): 0.0; S(6): 0.0	KTSSSSQVNLNR;YER024W;S784	0,67	0,61	0,76	1,55	1,14	1,41	0,01	0,67	1,41	2,12	1,08
YJL165C	HAL5	S(3): 100.0; S(5): 0.0; T(6): 0.0	KNSLSTPR;YJL165C;S233	0,94	0,68	0,90	1,87	1,90	2,23	0,00	0,90	1,90	2,11	1,08
YLR377C	FBP1	S(3): 100.0; T(4): 0.0; T(9): 0.0; T(13): 0.0	RDSTEGFDTDIITLPR;YLR377C;S12	0,47	0,62	0,75	2,11	1,26	1,31	0,03	0,62	1,31	2,11	1,08
YCL040W	GLK1	S(1): 100.0	SFDDLHK;YCL040W;S2	0,83	0,87	0,66	1,76	1,05	1,95	0,05	0,83	1,76	2,11	1,08
YMR075W	RCO1	S(11): 100.0	FLNIENPENQSE;YMR075W;S683	0,61	0,94	0,72	1,50	1,22	2,03	0,03	0,72	1,50	2,08	1,06
YDR186C	YDR186C	S(3): 100.0; S(5): 0.0	NNSNSNLLFEK;YDR186C;S692	0,75	0,74	0,91	1,55	1,38	1,67	0,00	0,75	1,55	2,08	1,06
YER024W	YAT2	T(2): 0.0; S(3): 0.0; S(4): 0.0; S(5): 0.0; S(6): 100.0	KTSSSSQVNLNR;YER024W;S786	0,69	0,48	0,76	1,68	1,16	1,43	0,01	0,69	1,43	2,07	1,05
YGL140C	YGL140C	S(3): 100.0; T(5): 0.0; S(6): 0.0; T(7): 0.0; S(8): 0.0; S(12): 0.0; S(13): 0.0; S(15): 0.0	AFSITSTSGQLSSLSR;YGL140C;S1167	0,79	0,88	0,97	1,82	1,37	2,02	0,01	0,88	1,82	2,07	1,05
YOR324C	FRT1	S(3): 100.0; S(4): 0.0	RASSGDAVK;YOR324C;S34	0,94	0,84	1,29	1,92	1,84	1,93	0,00	0,94	1,92	2,03	1,02
YOR267C	HRK1	S(3): 100.0; S(6): 0.0	AHSIASDNK;YOR267C;S661	0,90	0,82	0,77	1,52	1,67	1,85	0,00	0,82	1,67	2,02	1,02
YLR259C	HSP60	S(3): 100.0	RGSQVAVEK;YLR259C;S141	1,04	1,05	1,06	2,17	1,70	2,11	0,00	1,05	2,11	2,01	1,01
YAR002W	NUP60	S(3): 100.0; T(5): 0.0; S(8): 0.0; Y(11): 0.0	RASATVPSAPYRK;YAR002W;S10	1,06	1,06	0,77	1,95	2,13	2,33	0,00	1,06	2,13	2,00	1,00
YPL186C	UIP4	T(4): 0.0; S(7): 100.0	GNVTFPSPK;YPL186C;S140	1,40	1,19	1,68	0,71	0,70	0,65	0,01	1,40	0,70	0,50	-1,00
YPL186C	UIP4	S(7): 100.0; S(11): 0.0; T(15): 0.0	EENKELSPNFSQEQTENK;YPL186C;S185	1,32	1,15	1,34	0,63	0,69	0,66	0,00	1,32	0,66	0,50	-1,01
YDR475C	JIP4	S(2): 0.0; S(3): 100.0	VSSPLDEEKR;YDR475C;S86	1,64	1,68	1,98	0,84	0,69	0,91	0,00	1,68	0,84	0,50	-1,01
YMR212C	EFR3	S(5): 100.0; T(6): 0.0; S(7): 0.0; S(11): 100.0; S(13): 0.0	DNQISTSDLLSDSQVR;YMR212C;S564;S570;	1,30	1,90	1,69	0,91	0,52	0,83	0,01	1,69	0,83	0,49	-1,02
YGR086C	PIL1	Y(1): 0.0; S(6): 100.0	YKDPQSPKIEVLEQELVR;YGR086C;S163	1,84	2,20	1,99	1,01	0,70	0,98	0,00	1,99	0,98	0,49	-1,03
YDR033W	MRH1	S(5): 0.0; T(11): 0.0; S(15): 100.0	APVASPRPAATPNLSKDKK;YDR033W;S299	1,22	1,50	1,02	0,60	0,46	0,67	0,01	1,22	0,60	0,49	-1,03
YBR260C	RGD1	S(3): 100.0; S(12): 0.0	NKSPPKFAVDPSR;YBR260C;S336	1,22	1,58	1,40	0,68	0,68	0,97	0,01	1,40	0,68	0,49	-1,04
YIL117C	PRM5	S(3): 0.0; S(4): 100.0; S(6): 0.0	IASSPSRK;YIL117C;S268	1,20	1,15	1,57	0,52	0,72	0,58	0,01	1,20	0,58	0,49	-1,04
YOR153W	PDR5	S(1): 0.3; S(5): 99.7; S(8): 0.0; S(9): 0.0; S(19): 0.0; Y(26): 0.0	SDAQSIFSSGVEGVNPIFSDPEAPGYDPK;YOR153W;S70	1,71	1,86	1,08	0,89	0,41	0,83	0,04	1,71	0,83	0,48	-1,05
YML072C	TCB3	S(4): 100.0; S(7): 0.0	EFRSAPSR;YML072C;S128	1,13	1,42	1,59	0,69	0,60	0,69	0,01	1,42	0,69	0,48	-1,05
YPR028W	YOP1	T(4): 0.0; Y(6): 0.0; S(7): 100.0	QFDTKYSGNR;YPR028W;S20	1,60	1,98	1,59	0,77	0,68	1,32	0,03	1,60	0,77	0,48	-1,05
YPL221W	FLC1	S(2): 0.5; S(3): 99.0; S(4): 0.5; S(7): 0.0	ASSSPNSK;YPL221W;S713	1,15	1,23	1,27	0,59	0,49	0,96	0,02	1,23	0,59	0,48	-1,06
YDR348C	YDR348C	S(1): 0.0; T(3): 0.0; S(6): 100.0; T(10): 0.0	SKTVNSPNRTHK;YDR348C;S439	1,18	1,58	1,35	0,51	0,64	0,81	0,01	1,35	0,64	0,48	-1,07
YOL152W	FRE7	T(1): 0.0; T(5): 0.0; T(8): 100.0; S(10): 100.0; S(13): 100.0	TFPQTIDTASDQSDLAK;YOL152W;T517;S519;S522	1,06	1,11	1,01	0,50	0,40	0,82	0,02	1,06	0,50	0,47	-1,08
YPL004C	LSP1	S(9): 0.0; T(12): 100.0; Y(20): 0.0; Y(23): 0.0; S(26): 0.0	ALLELLDDSPVTPGEARPAYDGYEASR;YPL004C;T233	1,63	1,58	1,69	0,90	0,75	0,77	0,00	1,63	0,77	0,47	-1,09

12| Supplemental Information

Protein accession	Gene	Phosphosite confidence (%)	Peptide, protein, p-site	WT batch 1	WT batch 2	WT batch 3	Mas1 mutant batch1	Mas1 mutant batch 2	Mas1 mutant batch 3	T.TEST mutants against its respective wild types	WT average	Mutant average	Mutant divided by its respective wild type	Ratios log2
YER020W	GPA2	S(5): 100.0	QQQPSPHNVK;YER020W;S61	1,80	1,51	1,37	0,71	0,58	1,06	0,02	1,51	0,71	0,47	-1,10
YPL186C	UIP4	T(1): 0.0; S(4): 99.3; S(8): 0.7	TAISQDGSAFAK;YPL186C;S146	1,29	1,12	1,63	0,73	0,47	0,60	0,01	1,29	0,60	0,47	-1,10
YER020W	GPA2	S(5): 100.0	QQQPSPHNVKDRK;YER020W;S61	1,59	1,50	1,53	0,71	0,60	0,90	0,00	1,53	0,71	0,47	-1,10
YML072C	TCB3	S(3): 100.0; S(4): 0.0; S(11): 0.0; S(12): 0.0	KQSSKDIFVASSAQK;YML072C;S88	1,36	1,30	1,98	0,62	0,63	0,84	0,02	1,36	0,63	0,46	-1,11
YPL186C	UIP4	S(3): 100.0; S(7): 0.0; T(11): 0.0	ELSPNFSQEQTENKQDK;YPL186C;S185	1,31	1,08	1,43	0,60	0,78	0,59	0,01	1,31	0,60	0,46	-1,12
YML059C	NTE1	S(2): 0.0; S(3): 0.0; S(5): 100.0	FSSLSPELR;YML059C;S634	1,62	1,70	1,97	0,77	0,74	1,04	0,00	1,70	0,77	0,45	-1,14
YIL105C	SLM1	S(2): 0.0; T(3): 0.0; S(4): 0.0; S(5): 100.0; S(8): 0.0; T(9): 0.0; S(11): 0.0	NSTSSPNSTGSDAK;YIL105C;S533	1,22	1,37	1,16	0,47	0,55	0,80	0,01	1,22	0,55	0,45	-1,15
YER087C-B	SBH1	T(3): 0.0; S(5): 100.0; S(8): 0.0	KNTNSNNSILK;YER087C-B;S35	1,13	1,59	1,60	0,71	0,64	1,05	0,03	1,59	0,71	0,45	-1,16
YBR069C	TAT1	S(8): 0.0; S(12): 100.0; T(19): 0.0	QLPPDRNSELESQEKNNLTK;YBR069C;S84	0,74	0,97	0,70	0,33	0,31	0,39	0,01	0,74	0,33	0,44	-1,19
YFL042C	YFL042C	S(2): 0.0; T(5): 0.0; S(11): 100.0	ISNATIAEIGSPLQQVEKPDEVK;YFL042C;S149	1,72	1,72	2,43	0,52	0,75	0,81	0,01	1,72	0,75	0,44	-1,19
YGR086C	PIL1	Y(1): 0.0; S(6): 100.0	YKDPQSPK;YGR086C;S163	2,06	2,23	1,95	0,99	0,65	0,89	0,00	2,06	0,89	0,43	-1,21
YER020W	GPA2	S(5): 100.0	QQQPSPHNVKDR;YER020W;S61	1,64	1,51	1,63	0,70	0,56	0,80	0,00	1,63	0,70	0,43	-1,23
YMR212C	EFR3	S(5): 0.0; T(6): 0.0; S(7): 0.0; S(11): 100.0; S(13): 0.0	DNQISTSDLLSDSQVR;YMR212C;S570	1,79	1,91	1,82	0,78	0,63	0,76	0,00	1,82	0,76	0,42	-1,26
YBR069C	TAT1	S(2): 0.0; S(6): 100.0; T(13): 0.0	NSELESQEKNNLTK;YBR069C;S84	0,78	0,83	0,74	0,32	0,20	0,38	0,00	0,78	0,32	0,41	-1,29
YDR348C	YDR348C	S(1): 0.0; T(3): 0.0; S(6): 100.0	SKTVNSPNR;YDR348C;S439	1,26	1,54	1,35	0,55	0,46	0,66	0,00	1,35	0,55	0,41	-1,30
YFL014W	HSP12	S(11): 100.0	GKDNAEGQGESLADQAR;YFL014W;S73	2,12	1,87	2,70	1,08	0,85	0,81	0,01	2,12	0,85	0,40	-1,32
YIL105C	SLM1	S(3): 0.0; T(4): 0.0; S(5): 0.0; S(6): 100.0; S(9): 0.0; T(10): 0.0; S(12): 0.0	KNSTSSPNSTGSDAK;YIL105C;S533	1,25	1,44	1,18	0,45	0,50	0,70	0,00	1,25	0,50	0,40	-1,32
YDR348C	YDR348C	T(1): 0.0; S(4): 100.0; T(8): 0.0	TVNSPNRTHK;YDR348C;S439	1,25	1,69	1,55	0,60	0,42	0,61	0,00	1,55	0,60	0,39	-1,36
YBL101C	ECM21	S(7): 100.0; T(9): 0.0	GQPFQPSPTKK;YBL101C;S33	1,44	1,54	1,47	0,55	0,53	0,75	0,00	1,47	0,55	0,38	-1,41
YLR248W	RCK2	S(1): 0.0; S(2): 0.0; T(4): 0.0; S(10): 0.0; T(13): 0.0; S(14): 0.0; S(15): 100.0	SSGTNNKDVSQITSSPKK;YLR248W;S46	1,55	1,58	1,62	0,59	0,58	0,59	0,00	1,58	0,59	0,37	-1,43
YDL204W	RTN2	Y(3): 0.0; S(6): 100.0; T(13): 0.0	AEYPVSQNENIGTLK;YDL204W;S278	1,55	2,01	2,00	0,74	0,50	0,79	0,00	2,00	0,74	0,37	-1,44
YOL130W	ALR1	S(2): 0.0; S(4): 0.0; S(5): 0.0; S(6): 0.0; S(8): 100.0; T(11): 0.0	LSASSSASPITK;YOL130W;S176	1,58	1,51	1,89	0,57	0,45	0,63	0,00	1,58	0,57	0,36	-1,46
YDL223C	HBT1	T(4): 100.0; T(5): 0.0; S(10): 0.0	RAKTTQDIASDAK;YDL223C;T731	1,85	1,84	2,41	0,71	0,58	0,65	0,00	1,85	0,65	0,35	-1,51
YLR248W	RCK2	S(1): 0.0; S(2): 0.0; T(4): 0.0; S(10): 0.0; T(13): 0.0; S(14): 0.3; S(15): 99.7	SSGTNNKDVSQITSSPK;YLR248W;S46	1,48	1,64	1,66	0,63	0,58	0,56	0,00	1,64	0,58	0,35	-1,51
YLR019W	PSR2	S(3): 100.0; S(4): 0.0; T(9): 0.0	KHSSNKAQTQGR;YLR019W;S37	1,12	1,20	0,97	0,46	0,25	0,39	0,00	1,12	0,39	0,35	-1,52
YBR069C	TAT1	S(3): 100.0; Y(7): 0.0; S(8): 0.0; S(10): 100.0	EASPAQYSHSLHER;YBR069C;S13;S20;	1,22	1,33	1,33	0,45	0,40	0,59	0,00	1,33	0,45	0,34	-1,55
YLR332W	MID2	Y(2): 0.0; S(10): 100.0	FYDEQGNELSPR;YLR332W;S372	2,10	1,88	2,00	0,63	0,48	0,70	0,00	2,00	0,63	0,32	-1,66
YIL105C	SLM1	S(3): 0.0; T(4): 0.0; S(5): 0.0; S(6): 0.0; S(9): 99.7; T(10): 0.3; S(12): 0.0	KNSTSSPNSTGSDAK;YIL105C;S536	1,25	1,64	1,18	0,40	0,33	0,54	0,00	1,25	0,40	0,32	-1,66
YLR413W	YLR413W	S(7): 100.0	IIEEHESPIDAEKNFAR;YLR413W;S665	1,31	1,69	1,51	0,57	0,26	0,45	0,00	1,51	0,45	0,30	-1,75
YDL223C	HBT1	T(1): 0.0; T(2): 0.4; S(3): 99.6; T(5): 0.0; T(7): 0.0; S(11): 0.0	TTSPTNTHEHSK;YDL223C;S218	1,84	2,23	2,39	0,54	0,41	0,54	0,00	2,23	0,54	0,24	-2,05
YLR413W	YLR413W	S(7): 100.0	IIEEHESPIDAEK;YLR413W;S665	1,65	1,52	1,38	0,14	0,23	0,18	0,00	1,52	0,18	0,12	-3,07